


**For Reference**

**NOT TO BE TAKEN FROM THIS ROOM**



Ex LIBRIS  
UNIVERSITATIS  
ALBERTAENSIS





Digitized by the Internet Archive  
in 2023 with funding from  
University of Alberta Library

<https://archive.org/details/Logan1982>













THE UNIVERSITY OF ALBERTA

RELEASE FORM

NAME OF AUTHOR ..... *KERRY JANE LOGAN* .....

TITLE OF THESIS ..... *COMPARATIVE BEHAVIOR OF  $^{67}\text{Ga}$ -CITRATE, .....*  
*.....  $^{67}\text{Ga}$ -TRANSFERRIN AND  $^{59}\text{Fe}$ -CITRATE IN HUMANS .....*

DEGREE FOR WHICH THESIS WAS PRESENTED ..... *MSc.* .....

YEAR THIS DEGREE GRANTED ..... *1982* .....

Permission is hereby granted to THE UNIVERSITY OF ALBERTA LIBRARY  
to reproduce single copies of this thesis and to lend or sell copies for private, scholarly  
or scientific research purposes only.

The author reserves other publication rights, and neither the thesis nor  
extensive extracts from it may be printed or otherwise reproduced without the  
author's written permission.







THE UNIVERSITY OF ALBERTA

COMPARATIVE BEHAVIOR OF  $^{67}\text{Ga}$ -CITRATE,  $^{67}\text{Ga}$ -TRANSFERRIN  
AND  $^{59}\text{Fe}$ -CITRATE IN HUMANS

by

KERRY JANE LOGAN



A THESIS

SUBMITTED TO THE FACULTY OF GRADUATE STUDIES AND RESEARCH  
IN PARTIAL FULFILLMENT OF THE REQUIREMENTS FOR THE DEGREE  
OF MASTER OF SCIENCE IN PHARMACEUTICAL SCIENCES (RADIOPHARMACY)

FACULTY OF PHARMACY AND PHARMACEUTICAL SCIENCES

EDMONTON, ALBERTA

SPRING, 1982





THE UNIVERSITY OF ALBERTA

FACULTY OF GRADUATE STUDIES AND RESEARCH

The undersigned certify that they have read, and recommend to the Faculty of Graduate Studies and Research, for acceptance, a thesis entitled

*COMPARATIVE BEHAVIOR OF  $^{67}\text{Ga}$ -CITRATE,  $^{67}\text{Ga}$ -TRANSFERRIN  
AND  $^{59}\text{Fe}$ -CITRATE IN HUMANS*

submitted by KERRY JANE LOGAN in partial fulfillment of the requirements for the degree of MASTER of SCIENCE in PHARMACEUTICAL SCIENCES (Radiopharmacy).





*TO THE MEMORY OF MY FATHER  
AND THE STRENGTH OF MY MOTHER*





## ABSTRACT

An aseptic method for labelling human apo-transferrin with Ga-67 for the purpose of clinical investigation was developed. The  $^{67}\text{Ga}$ -transferrin was prepared by direct incubation of  $^{67}\text{Ga}$ -citrate or highly concentrated  $^{67}\text{GaCl}_3$  with transferrin dissolved in a solution of HEPES buffer and sodium bicarbonate. Separation of the  $^{67}\text{Ga}$ -transferrin from unbound  $^{67}\text{Ga}$  was accomplished by concentrating the incubation mixture in a Minicon B15 macrosolute concentrator. All solutions were sterile and pyrogen-free. An acute toxicity study in mice found transferrin to be nontoxic at a dose 450X that of the desired human dose of 10 mg.

A comparison of the pharmacokinetics and *in vivo* distribution of  $^{67}\text{Ga}$ -citrate,  $^{67}\text{Ga}$ -transferrin, and  $^{59}\text{Fe}$ -citrate was undertaken in four healthy adult males.

Curve stripping analysis of the plasma concentration-time plots by the computer program AUTOAN/NONLIN demonstrated that the plasma disappearance of  $^{67}\text{Ga}$ -citrate and  $^{67}\text{Ga}$ -transferrin was best described by a three-exponential equation. A three-compartment open model with elimination from the central compartment was chosen as the simplest model to describe the data. A significant difference between  $^{67}\text{Ga}$ -citrate and  $^{67}\text{Ga}$ -transferrin was found in the hybrid rate constant describing the second exponential phase of plasma disappearance. However, the overall elimination rate constant was not different for the two complexes of gallium. This suggested that  $^{67}\text{Ga}$ -transferrin was distributed more rapidly from the intravascular compartment to the other body tissues.

The plasma disappearance of  $^{59}\text{Fe}$ -citrate was best described by a two-exponential equation, and a two-compartment open model with elimination from the central compart-





ment was chosen to describe the data. Statistically significant differences between  $^{59}\text{Fe}$ -citrate and  $^{67}\text{Ga}$ -citrate were observed for the overall elimination rate constant, half-life of the terminal phase, volume of distribution, and plasma clearance. A marked difference in red blood cell uptake of these two nuclides was also observed.

The *in vivo* distribution of  $^{67}\text{Ga}$ -citrate,  $^{67}\text{Ga}$ -transferrin, and  $^{59}\text{Fe}$ -citrate was studied using collimated NaI(Tl) crystals and a multichannel analyzer system. Uptake in the regions of the liver, spleen, heart, sacrum, and knee were monitored over ten days. The data was corrected for background, physical decay, and the percent of radioactivity remaining in the whole blood. Day 0 was used as the standard to which subsequent observations were compared. The *in vivo* distribution of  $^{59}\text{Fe}$ -citrate was found to be very different from that of  $^{67}\text{Ga}$  in the regions of interest studied. There were no significant differences observed in the *in vivo* organ uptake of  $^{67}\text{Ga}$ -citrate and  $^{67}\text{Ga}$ -transferrin.



## ACKNOWLEDGEMENTS

My biggest thank-you's must go to Dr. Tony Noujaim and Dr. Brian Lentle for their guidance and participation as subjects in this project.

There were several other key people involved that I would like to thank: Dr. Philip Ng, for his professional expertise; Dr. Uwe Turner and Mr. Colin Welch, as willing subjects; Miss Connie Turner, for her many hours of hard work and moral support; Mr. John Scott, Mr. Ron Schmidt, Dr. Rick Hooper, Mr. Steve McQuarrie, Mr. Chris Ediss, Dr. Jim Coates, Dr. G. Bain, Mr. John Hanson, and the technologists at the Cross Cancer Institute, for their technical assistance.

Thank-you to all my family and friends in Radiopharmacy and Bionucleonics, and at the Foothills Hospital, for their undying faith and endless moral support. Special thank-you's are deserved by David Smith, Anne Jaffe, Donna Ethier, John Mercer, Gilbert Matte, and Marnie Worbets.

Financial support from the Medical Research Council is gratefully acknowledged.





## TABLE OF CONTENTS

ABSTRACT	v
ACKNOWLEDGEMENTS	vii
TABLE OF CONTENTS	viii
LIST OF TABLES	xiv
LIST OF FIGURES	xv
INTRODUCTION	1
SURVEY OF THE LITERATURE	
I. GALLIUM	
A. Properties And Uses	4
B. Chemistry Of Gallium	7
1. Reactions Of Gallium With Oxygen	7
a) Gallium Oxides	7
b) Gallium Hydroxides	8
c) Gallates	10
2. Gallium Chloride	10
3. Gallium Citrate	11
C. Isotopes Of Gallium	12
D. Biological Studies Of Gallium	14
1. Toxicity Of Gallium	14
2. Protein Binding Of Gallium In Serum	16
3. Gross Tissue Distribution	18
a) Early Studies With Stable Ga And $^{72}\text{Ga}$	18
b) Animal Studies With $^{67}\text{Ga}$ -citrate	20
c) Human Studies With $^{67}\text{Ga}$ -citrate	22



d) Factors Affecting the Gross Tissue Distribution Of Gallium	23
4. Excretion Of Gallium	23
E. Subcellular Localization	25
1. Association With Organelles	25
2. Macromolecular Binding	26
F. Tumor Uptake Of Gallium	28
1. General Considerations In Tumor Localization	28
2. The Role Of Transferrin	29
a) <i>In vitro</i> Studies	29
b) <i>In vivo</i> Studies	31
3. Other Proposed Mechanisms	33
G. Clinical Studies With $^{67}\text{Ga}$ -citrate	35
1. The Normal $^{67}\text{Ga}$ Scan	35
2. Clinical Usefulness of $^{67}\text{Ga}$ -citrate In Malignant Diseases	36
a) Lymphatic Malignancies	38
b) Malignant Melanoma	42
c) Hepatoma	43
d) Carcinoma Of The Lung	44
e) Tumors Of The Head And Neck	45
f) Breast Carcinoma	46
g) Bone Tumors	47
h) Genitourinary Tumors	47
i) Gastrointestinal Tumors	48
j) Pediatric Tumors	48
3. $^{67}\text{Ga}$ -citrate Imaging In Inflammatory Conditions	49
a) Mechanisms Of Uptake	49
b) Clinical Applications	51
H. Radiation Dosimetry of $^{67}\text{Ga}$ -citrate	53





<b>II.</b>	<b>IRON</b>	
	A. Iron Metabolism	54
	B. Isotopes Of Iron In Nuclear Medicine	55
	C. Iron Kinetics	56
	D. Radiation Dosimetry of $^{59}\text{Fe}$	56
<b>III.</b>	<b>TRANSFERRIN</b>	
	A. General Description	58
	B. Metal-binding Characteristics	59
	1. Binding Of Iron	59
	2. Binding of Gallium	61
	C. Cell-Surface Receptors	62

## EXPERIMENTAL

<b>I.</b>	<b>MATERIALS</b>	
	A. Preparation Of Solutions	64
	B. Chromatographic Methods	64
	C. Radioisotopes	64
	D. Animals	66
	E. Human Subjects	66
<b>II.</b>	<b>METHODS</b>	
	A. Preparation Of Sterile Reagents	67
	1. Sterilization Of Equipment	67
	2. Preparation Of Sterile Solutions	67
	3. Quality Control	68
	B. Preparation Of $^{67}\text{Ga}$ -transferrin	69
	C. Toxicity Study	70



D. Clinical Study	71
1. Administration Of Radioisotopes	71
2. Blood Sampling	72
a) Collection Of Samples	72
b) Sample-handling Techniques	73
c) Determination Of $^{67}\text{Ga}$ and $^{59}\text{Fe}$ Radioactivities	73
3. Urine Sample Analysis	74
a) Sample Collection and Handling	74
b) Determination of $^{67}\text{Ga}$ and $^{59}\text{Fe}$ Radioactivities	75
4. <i>In vivo</i> Distribution Measurements	75
a) Instrumentation	75
b) Standards	75
c) Collection of Data	76
5. Data Analysis	76
a) Blood Data	76
b) Urine Data	77
c) <i>In vivo</i> Distribution	77

## RESULTS AND DISCUSSION

I. TOXICITY OF TRANSFERRIN IN MICE	80
II. PREPARATION OF $^{67}\text{Ga}$ -TRANSFERRIN	
A. Initial Labelling Experiments With $^{67}\text{Ga}$ -chloride	81
B. Labelling Experiments With $^{67}\text{Ga}$ -citrate	82
1. Initial Labelling Experiments	82
2. Scaled-up Procedure	82
C. Separation Techniques	83





D. Sterile Preparation Of $^{67}\text{Ga}$ -transferrin By The Incubation Method	87
1. Reagents	87
2. Preparation Technique	87
E. Final Experiments With $^{67}\text{Ga}$ -chloride	89
 III. CLINICAL COMPARISON OF $^{67}\text{Ga}$ -CITRATE, $^{67}\text{Ga}$ -TRANSFERRIN, AND $^{59}\text{Fe}$ -CITRATE	
A. Pharmacokinetics	90
1. Pharmacokinetic Methods	90
2. Parameters Of Measurement	100
3. Comparison Of $^{67}\text{Ga}$ -citrate And $^{67}\text{Ga}$ -transferrin Kinetics	102
4. Comparison Of $^{67}\text{Ga}$ -citrate And $^{59}\text{Fe}$ -citrate Kinetics	106
B. Urinary Excretion Of $^{67}\text{Ga}$ -citrate, $^{67}\text{Ga}$ -transferrin, And $^{59}\text{Fe}$ -citrate	107
C. <i>In vivo</i> Distribution Of $^{67}\text{Ga}$ -citrate, $^{67}\text{Ga}$ -transferrin, And $^{59}\text{Fe}$ -citrate	110
 SUMMARY AND CONCLUSIONS	117
 REFERENCES	120
 APPENDIX A. Factors Affecting The Gross Distribution Of $^{67}\text{Ga}$ -citrate	142
APPENDIX B. $^{67}\text{Ga}$ And $^{59}\text{Fe}$ Data Correction Program	150
APPENDIX C. Clinical Study Blood Data	152
APPENDIX D. Blood Biochemistry Data	164



APPENDIX E. Plasma Disappearance Curves And Percent Dose In Compartments Plots	169
APPENDIX F. Pharmacokinetic Parameters For Each Subject	186
APPENDIX G. <i>In vivo</i> Distribution Data	190





## LIST OF TABLES

Table	Description	Page
I	Physical Constants of Gallium.....	5
II	Nuclear Data of $^{67}\text{Ga}$ , $^{68}\text{Ga}$ , and $^{72}\text{Ga}$ .....	13
III	Estimated Absorbed Doses from $^{67}\text{Ga}$ -citrate .....	53
IV	Nuclear Data of $^{59}\text{Fe}$ .....	55
V	Materials Used in the Preparation of Sterile $^{67}\text{Ga}$ -transferrin .....	65
VI	Regression Analysis of the Weight Gain Versus Time in Treated and Control Mice .....	80
VII	The Removal of Unbound $^{67}\text{Ga}$ in Solution by Concentration in the Minicon B15 Macrosolute Concentrator .....	85
VIII	Definitions and Symbols of Pharmacokinetic Parameters .....	101
IX	Pharmacokinetic Parameters of $^{67}\text{Ga}$ -citrate and $^{67}\text{Ga}$ -transferrin in Humans Following I.V. Injection .....	103
X	Microscopic Rate Constants of the Three-Compartment Model Describing $^{67}\text{Ga}$ -citrate and $^{67}\text{Ga}$ -transferrin Kinetics in Humans.....	104
XI	Pharmacokinetic Parameters of $^{67}\text{Ga}$ -citrate and $^{59}\text{Fe}$ -citrate in Humans Following I.V. Injection .....	106
XII	Cumulative Urinary Excretion to 48 Hours Following Administration of $^{67}\text{Ga}$ -citrate, $^{67}\text{Ga}$ -transferrin, and $^{59}\text{Fe}$ -citrate .....	109



## LIST OF FIGURES

Figure	Page
1. Elution Profile of $^{67}\text{Ga}$ -transferrin . . . . .	84
2. Paper Chromatography of $^{67}\text{Ga}$ Solutions . . . . .	88
3. Three-Compartment Open Model for $^{67}\text{Ga}$ -citrate and $^{67}\text{Ga}$ -transferrin in Humans . . . . .	92
4. Two-Compartment Open Model for $^{59}\text{Fe}$ -citrate in Humans . . . . .	93
5. Plasma Disappearance of $^{67}\text{Ga}$ -citrate in One Subject . . . . .	94
6. Plasma Disappearance of $^{67}\text{Ga}$ -transferrin in One Subject . . . . .	95
7. Plasma Disappearance of $^{59}\text{Fe}$ -citrate in One Subject . . . . .	96
8. Percent of the Total Radioactivity in Each Compartment Following Injection of $^{67}\text{Ga}$ -citrate in One Subject . . . . .	97
9. Percent of the Total Radioactivity in Each Compartment Following Administration of $^{67}\text{Ga}$ -transferrin in One Subject . . . . .	98
10. Percent of the Total Radioactivity in Each Compartment Following Administration of $^{59}\text{Fe}$ -citrate in One Subject . . . . .	99
11. Percent of the Injected Dose Present in Red Blood Cells Over Time Following I.V. Injection of $^{59}\text{Fe}$ -citrate and $^{67}\text{Ga}$ -citrate in One Subject . . . . .	108
12. Net Relative Uptake of $^{67}\text{Ga}$ -citrate, $^{67}\text{Ga}$ -transferrin, and $^{59}\text{Fe}$ -citrate in the Sacrum . . . . .	111
13. Net Relative Uptake of $^{67}\text{Ga}$ -citrate, $^{67}\text{Ga}$ -transferrin, and $^{59}\text{Fe}$ -citrate in the Liver . . . . .	112
14. Net Relative Uptake of $^{67}\text{Ga}$ -citrate, $^{67}\text{Ga}$ -transferrin, and $^{59}\text{Fe}$ -citrate in the Heart . . . . .	113



Figure	Page
15.	Net Relative Uptake of $^{67}\text{Ga}$ -citrate, $^{67}\text{Ga}$ -transferrin, and $^{59}\text{Fe}$ -citrate in the Spleen. . . . . 114
16.	Net Relative Uptake of $^{67}\text{Ga}$ -citrate, $^{67}\text{Ga}$ -transferrin, and $^{59}\text{Fe}$ -citrate in the Knee. . . . . 115





## INTRODUCTION

The most important goal in nuclear medicine has always been the earliest possible detection of disease. In particular, the search for a tumor-specific radiopharmaceutical has been the object of intensive investigation.

The unexpected uptake of  $^{67}\text{Ga}$ -citrate in soft tissue tumors observed by Edwards and Hayes (1) in 1969 has led to the widespread use of  $^{67}\text{Ga}$ -citrate in the diagnosis of both malignant and inflammatory diseases, and to the classification of  $^{67}\text{Ga}$ -citrate as a tumor scanning agent. Since that serendipitous discovery there have been several investigations into the factors which influence the distribution and uptake of this radionuclide.

It is known that after intravenous injection  $^{67}\text{Ga}$  is rapidly bound by plasma proteins, notably transferrin (2). Gallium-67 also shows affinity for the iron storage proteins ferritin and lactoferrin (3,4). This affinity of  $^{67}\text{Ga}$  for the proteins involved in the transport and storage of iron suggests that these two nuclides may be handled biologically in an analogous manner.

The factors affecting the binding of iron to transferrin have been studied in detail (5, 6). Due to the common association of gallium and iron with transferrin and since the binding of gallium to transferrin has not been investigated to a great extent, the iron-transferrin studies have been the basis of present labelling techniques of transferrin with gallium (7).

Investigation into the role of transferrin in the tumor uptake of  $^{67}\text{Ga}$ -citrate has been undertaken in recent years. Several *in vitro* experiments employing tissue culture techniques have shown that transferrin stimulates the uptake of gallium, as well as iron,



by tumor cells (7, 8). *In vivo* studies in tumor bearing mice and dogs have indicated that transferrin is involved in the tumor uptake of  $^{67}\text{Ga}$  (9, 10).

The logical step along this route of investigation was the initiation of clinical trials, to study the effect of transferrin on the distribution and uptake of  $^{67}\text{Ga}$  in humans. Thus, the objectives of my research were threefold:

1. To modify the labelling of transferrin with  $^{67}\text{Ga}$  for use in clinical studies.
2. To determine the safety of this preparation for human use.
3. To do a comparative pharmacokinetic study of  $^{67}\text{Ga}$ -transferrin,  $^{67}\text{Ga}$ -citrate and  $^{59}\text{Fe}$ -citrate in healthy human subjects.





## SURVEY OF THE LITERATURE



## I. GALLIUM

### A. Properties And Uses

Much effort was made in the late 1860's to organize the known elements into a suitable classification system. In 1869, the Russian scientist Mendeleev published a detailed system of classification that is the basis for the present day Periodic Chart (11). In 1871, Mendeleev predicted that an element "eka-aluminum" existed which would fill a gap in this table of elements. This prediction was confirmed in 1875 by the French chemist de Boisbourdon, and the element "gallium" was discovered (12, 13).

Gallium is a member of group III of the periodic table, with an atomic number of 31. In nature, gallium occurs with an atomic weight of 69.72 (12, 13), as a result of a mixture of the two stable isotopes  $^{69}\text{Ga}$  (60.1%), and  $^{71}\text{Ga}$  (39.9%) (14). Gallium is a dispersed element, and has a natural occurrence of 15 g/ton (13). It is usually found associated with its closest neighbours in the periodic table; Al, Zn, Ge, and In (13). Gallium and aluminum have similar ionic radii ( $\text{Ga} = 0.62\text{\AA}$  ;  $\text{Al} = 0.57\text{\AA}$ ), and both have a maximum valence of +3 (13). Therefore, gallium is often found in nature as a substitute for aluminum. Most of the gallium used in industry is obtained as a byproduct in the alumina and aluminum industries. It is also found associated with germanium in coal (12, 13). Table I gives the various physical constants associated with gallium.



TABLE I  
PHYSICAL CONSTANTS OF GALLIUM \*

---

Atomic Number	31
Atomic Weight	69.72
Melting Point	29.78°C
Boiling Point	1983 – 2516°C
Density (solid)	5.904 g/cm <sup>3</sup>
Density (liquid)	6.095 g/cm <sup>3</sup>
Ionic Radius	0.62 Å
Interatomic Distances	2.447 Å

---

\* From References 12 and 13



Gallium as a pure metal is soft, silvery-white with a bluish tinge (11, 12). As a liquid, gallium resembles mercury, but unlike mercury, gallium tends to wet glass readily (12). Gallium has several unusual properties. When Ga crystalizes it does so in a lattice of diatomic molecules, which is rare in metals (12, 13). Also, due to the unusually open crystal structure when solid, the density of the solid is less than that of the liquid (11). Gallium is liquid over a wide temperature range, and when of high purity, Ga has a tendency to supercool before crystallization occurs (12, 13).

Although the use of Ga in industry and science is limited by its availability and price, it does have some interesting applications (11, 12, 13):

- 1) The large temperature range at which Ga remains liquid makes it useful in thermometers for measuring high temperatures, safety fuses and fire alarms.
- 2) Gallium is used in lenses and optical mirrors to increase the refractive index.
- 3) The increase in volume upon solidification is useful in creating high pressure in sealed vessels.
- 4) Gallium forms some low melting alloys with some metals which are used for several purposes.
- 5) Gallium is used in the production of some semiconductor compounds, such as GaP and GaS, and is used to add certain electrical properties to Ge and Si.





## B. Chemistry of Gallium

### 1. Reactions of Gallium With Oxygen

#### a. Gallium oxides

Gallium forms three oxides:  $\text{Ga}_2\text{O}$  (suboxide),  $\text{GaO}$  (oxide), and  $\text{Ga}_2\text{O}_3$  (sesquioxide or trioxide) (12, 13).

i) Gallium suboxide:  $\text{Ga}_2\text{O}$  can be produced by a variety of reactions, all of which involve reduction of  $\text{Ga}_2\text{O}_3$  to  $\text{Ga}_2\text{O}$ . In general, these reactions require extreme conditions such as high temperatures. The resulting product sublimes and is deposited on the walls of the reaction vessel. These methods may be used to deposit Ga on the surface of semiconductors. It is difficult to obtain pure  $\text{Ga}_2\text{O}$  as it is not very stable, and gallium oxide,  $\text{GaO}$ , is often a contaminant.  $\text{Ga}_2\text{O}$  is a strong reducing agent (12).

ii) Gallium oxide:  $\text{GaO}$  may be produced by the oxidation of metallic gallium, or by the reduction of  $\text{Ga}_2\text{O}_3$  at high temperatures. This oxide is not stable and decomposes rapidly to  $\text{Ga}_2\text{O}$  and  $\text{Ga}_2\text{O}_3$ . Gallium oxide is also a strong reducing agent (12, 13).

iii) Gallium trioxide:  $\text{Ga}_2\text{O}_3$  is the most stable of all the gallium oxides and is stable even at high temperatures (12, 13). Gallium trioxide exists in five modifications:  $\alpha$ ,  $\beta$ ,  $\gamma$ ,  $\delta$ ,  $\epsilon$ , the  $\beta$  modification being the most stable. Specific reactions produce each of these different modifications, and all can be converted to the  $\beta$ -form by heating at temperatures greater than  $1000^\circ\text{C}$  (12). Gallium trioxide is similar to  $\text{Al}_2\text{O}_3$  in that it is only sparingly soluble in acids and bases (13).  $\text{Ga}_2\text{O}_3$  can be reduced to the lower oxides and if heated to redness will be reduced to Ga metal. Reaction with elemental fluorine, or fusion with  $\text{NH}_4\text{Cl}$  at  $250^\circ\text{C}$ , will produce  $\text{GaF}_3$  and  $\text{GaCl}_3$  respectively. Optical glasses prepared from calcium and gallium oxides (containing 59 – 69%  $\text{Ga}_2\text{O}_3$ ) are good transmitters for infrared rays (12).



b) Gallium Hydroxides:

Gallium also forms several hydroxides:  $\text{GaOH}$ ,  $\text{GaO(OH)}$ ,  $\text{Ga}_2\text{O(OH)}_4$ , and  $\text{Ga(OH)}_3$  (12, 13).

i)  $\text{GaOH}$ : This hydroxide of gallium has only been shown by spectroscopic methods, and has not been isolated in a pure state (12).

ii)  $\text{GaO(OH)}$ : This compound is the metahydroxide of trivalent gallium, and can be produced by a variety of reactions which include dehydration of  $\text{Ga(OH)}_3$ , and slow precipitation from either alkaline or acid solutions (12, 13). This compound is stable between  $110^\circ\text{C}$  and  $300^\circ\text{C}$ ; below  $100^\circ\text{C}$   $\text{Ga(OH)}_3$  is produced (12).

iii)  $\text{Ga}_2\text{O(OH)}_4$ : This hydroxide of gallium is produced by mixing hot solutions of gallium bicarbonate and gallium nitrate with subsequent drying of the precipitate. If the temperature is increased above  $70^\circ\text{C}$ ,  $\text{Ga(OH)}_3$  will also be produced (12).

iv)  $\text{Ga(OH)}_3$ : Gallium hydroxide is produced either by the action of bases on gallium salts, or by the neutralization of gallates by acids (12, 13). The precipitate contains variable amounts of water and tends to dehydrate with time (13). Also, the method of precipitation may affect the crystal structure (12).

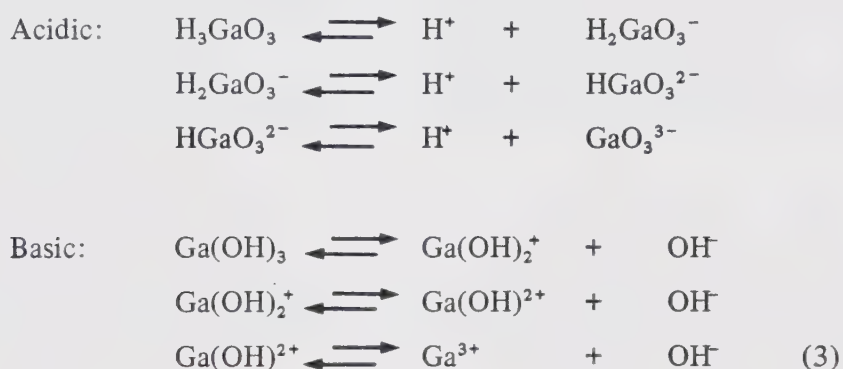
The pH at which precipitation of  $\text{Ga(OH)}_3$  occurs depends on several factors. The nature of the anion of the gallium salt affects the amount of base required to initiate precipitation (12, 13). For example, the precipitation of  $\text{Ga(OH)}_3$  from  $\text{Ga}_2(\text{SO}_4)_3$  is incipient at a molar ratio of  $\text{NaOH/Ga}$  of 0.2, whereas with  $\text{GaCl}_3$  incipient precipitation occurs at a molar ratio of 2.6 (13). The required pH for precipitation of  $\text{Ga(OH)}_3$  decreases as the concentration of gallium in solution increases, as the temperature of the solution increases, or in the presence of aliphatic polyhydric alcohols such as glycerol



and mannitol (12, 13).

Gallium hydroxide tends to age with time. This aging process is increased at high temperatures, in the presence of some cations, or if there is an excess amount of base present in solution. Aging has a negative effect on the solubility of  $\text{Ga}(\text{OH})_3$ , particularly in ammonia (12, 13).

Gallium hydroxide demonstrates amphoteric properties, with its acidic properties slightly more pronounced than its basic properties (12, 13, 15). Thus,  $\text{Ga}(\text{OH})_3$  is soluble in both acids and bases. The acidic properties of  $\text{Ga}(\text{OH})_3$  are more pronounced than those of  $\text{Al}_2\text{O}_3$ , which precipitates at a higher pH (13). The acidic and basic dissociation of  $\text{Ga}(\text{OH})_3$  can be described in a simplified manner as follows:



The ionic species of gallium present in acidic solution is  $\text{Ga}^{3+}$  (13) which is thought to exist as octahedral ions of the structure  $[\text{Ga}(\text{H}_2\text{O})_6]^{3+}$  (15, 16). These ions are moderately acidic (15). The reaction of  $\text{Ga}(\text{OH})_3$  with alkali produces ionic species which have been described as follows: anhydrous gallate ions ( $\text{GaO}_2^-$ ), hydrated 4-coordinate gallate ions ( $\text{Ga}(\text{OH})_4^-$ ), dimerized hydrated gallate ions ( $\text{Ga}_2(\text{OH})_8^{2-}$ ), sodium gallate dissociating to  $\text{GaO}_3^-$ , and possibly gallates with higher coordination numbers, for example  $[\text{Ga}(\text{OH})_4(\text{H}_2\text{O})_2]^-$  (12, 13, 15).





c) Gallates:

Gallium forms gallates with the majority of metals from Groups I and II of the periodic table (12, 13). These gallates vary in their lattice parameters and coordination numbers (12). Gallates with metals from Groups III, VII, and VIII are also known (12).

## 2. Gallium Chloride

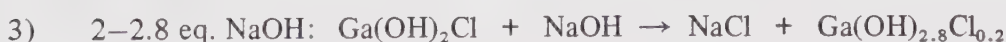
Trivalent gallium chloride,  $\text{GaCl}_3$ , may be prepared by a variety of methods (12).  $\text{GaCl}_3$  prefers a coordination of 4, and thus exists as a dimeric structure (12, 15).  $\text{GaCl}_3$  is hygroscopic and over a period of time converts from long white crystals to a gelatinous mass (12, 13).

Gallium chloride is soluble in water, but is stable only at pH less than 3.4 (12, 13, 15). If concentrated aqueous solutions are diluted, or if the pH is raised, hydrolysis occurs with the formation of  $\text{Ga}(\text{OH})_3$ .  $\text{GaCl}_3$  is also soluble in ethers and can be extracted from other compounds with ethyl ether, isopropyl ether, isobutyl ether, or butylacetate (12, 13).

In an excess of acid (2N – 5.5N HCl),  $\text{GaCl}_3$  exists as the anion  $\text{GaCl}_4^-$  (12). The titration of  $\text{GaCl}_3$  with a strong base occurs in distinct stages. When equivalents of NaOH are added stepwise to a solution of  $\text{GaCl}_3$  the following reactions occur (12, 16):



Both  $\text{Ga}(\text{OH})\text{Cl}_2$  and  $\text{Ga}(\text{OH})_2\text{Cl}$  are soluble basic salts which dissociate in solution.



At this point precipitation is initiated. A colloidal solution also exists at this stage; the exact composition is unknown, but is possibly:





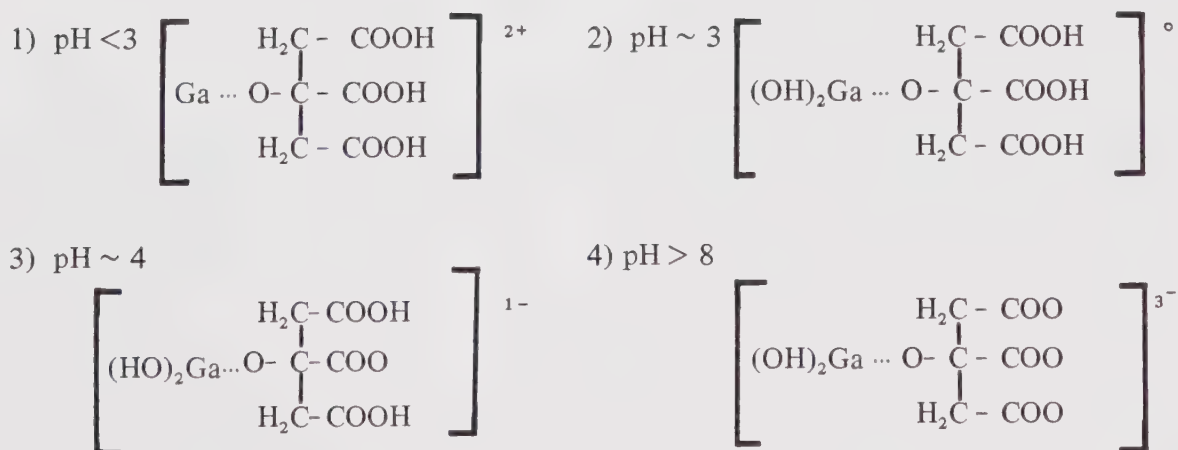
- 4) 2.8 – 3.0 eq. NaOH:  $\text{Ga}(\text{OH})_3$  is precipitated
- 5) >3 eq. NaOH:  $\text{Ga}(\text{OH})_3$  is dissolved in the excess base forming gallates, as discussed previously.

Gallium chloride will react with some inorganic chlorides, for example ammonium chloride and iodine monochloride, forming complex compounds (12, 13). Gallium chloride also forms complexes with some organic compounds containing nitrogen, oxygen, or sulfur. In the case of N-containing compounds, aromatic complexes are generally more stable than aliphatic complexes; the ammoniate complexes are unstable in water and decompose (13).

### 3. Gallium Citrate

Gallium salts form complex ions with citric acid or sodium citrate (12). Although most gallium complexes have a strong tendency to hydrolyze, Ga-citrate is a stable complex between pH 3 and 7.5 (12, 13, 17, 18). It is also stable upon prolonged heating (16).

The form in which Ga-citrate exists is dependent upon pH (13, 16, 18). The addition of alkali to an acidic solution of Ga-citrate results in the following sequence of reactions (13):





There is also evidence for the existence of polynuclear species of Ga-citrate (16, 18). At low pH, with Ga-to-citrate ratios of 1:1, only low molecular weight complexes are detectable (16). From approximately pH 2 to 4 a complex is formed with the possible empirical formula  $[\text{Ga}_3^{3+}(\text{OH})_4\text{C}_3\text{H}_4\text{OH}(\text{COO})_3^-]_n$  (16, 18). Maximum poly-complexation occurs at approximately pH 5 (18). As neutral pH is approached the complex begins to break down into smaller gallium complexes (16, 18). The pH at which dissociation occurs appears to decrease as the concentration of Ga-citrate in solution increases (18). The degree of poly-complexation is minimal at pH of approximately 9 – 10 and at pH  $\geq 12$  there is a complete breakdown of the complex into free citrate and gallate ions (16 – 18).

The effective chelation of carrier-free  $^{67}\text{Ga}$  or  $^{68}\text{Ga}$  was found to be dependent upon both citrate concentration and pH (19). Experiments at neutral pH showed that at low sodium citrate concentrations (0.2 mg/ml), 60% of the  $^{67}\text{Ga}$  existed as gallium hydroxide, 32% as gallate, and only 8% was present as gallium citrate. Effective chelation (greater than 90%) was found to occur only at sodium citrate concentrations of 10 mg/ml or greater. This corresponded to a molar ratio of citrate to carrier-free  $^{67}\text{Ga}$  or  $^{68}\text{Ga}$  of greater than  $10^6$ . When the sodium citrate concentration was held constant at 2 mg/ml it was found that effective chelation only occurred at pH less than 6. These experiments suggested existence of competition between citrate and hydroxyl ions for gallium.

### C. Isotopes of Gallium

There are several isotopes of gallium, ranging in atomic weight from  $^{63}\text{Ga}$  to  $^{76}\text{Ga}$  (14). Of these, only two isotopes are stable,  $^{69}\text{Ga}$  and  $^{71}\text{Ga}$  (14). The radioactive isotopes of gallium that are of interest in Nuclear Medicine are  $^{67}\text{Ga}$ ,  $^{68}\text{Ga}$ , and from a historical interest,  $^{72}\text{Ga}$  (20). The decay characteristics and methods of production of these isotopes are summarized in Table II.



TABLE II

NUCLEAR DATA OF  $^{67}\text{Ga}$ ,  $^{68}\text{Ga}$ ,  $^{72}\text{Ga}$  \*

Isotope	Half Life	Type of Decay	Principal Photon Energies (Mev)	Photons Emitted	Principal Means of Production
$^{67}\text{Ga}$	78.26 h	electron capture	0.093	38.3%	$^{66}\text{Zn}(\text{d}, \text{n})$
			0.185	20.9%	$^{65}\text{Cu}(\alpha, 2\text{n})$
			0.300	16.8%	
			0.394	4.7%	
			others	<3% each	
$^{68}\text{Ga}$	68.33 m	positron ( $\beta^+$ )	0.511 (annihilation)	176%	daughter of $^{68}\text{Ge}$
			1.078	3.0%	
			others	<1% each	
$^{72}\text{Ga}$	14.12 h	beta ( $\beta^-$ )	0.630	24.9%	$^{71}\text{Ga}(\text{n}, \gamma)$
			0.834	95.9%	
			0.894	9.9%	
			1.051	6.9%	
			1.861	5.3%	
			2.202	26.0%	
			2.491	7.7%	
			2.508	12.8%	
			others	< 5% each	

\* From References 14 and 21





## D. Biological Studies Of Gallium

### 1. Toxicity Of Gallium

The first extensive biological studies on gallium were initiated in the late 1940's, when gallium was being investigated as a possible nuclear reactor coolant (20).

The toxicity of stable gallium as gallium chloride and gallium lactate was reported by Dudley and Levine in 1949 (22). Oral administration of both forms of gallium in rats resulted in no more than trace amounts of gallium in the liver, spleen and kidney. Gallium lactate in oral doses up to 1g Ga/kg of food resulted in bone uptake of only 1 – 3  $\mu$ g/kg bone. These results suggested that neither gallium chloride nor gallium lactate were absorbed in appreciable quantities from the gastrointestinal tract (GIT), as the alkalinity of the GIT was likely sufficient to produce insoluble complexes of gallium. It was later reported that stable gallium citrate was also not absorbed from the GIT when administered orally (23). The intravenous or subcutaneous injection of gallium lactate into rats and rabbits resulted in the following acute toxic doses ( $LD_{50}$ , ten days) (22):

In rats:        intravenous 47 mg Ga/kg  
                  subcutaneous 121 mg Ga/kg

In rabbits:    intravenous 43 mg Ga/kg  
                  subcutaneous 97 mg Ga/kg

The following symptoms resulting from lethal or nonlethal doses of gallium lactate were observed: hyperexcitability during the first 24 hours followed by limited activity and sluggishness; decreased food intake and a marked drop in body weight; in some cases, photophobia and blindness; and terminal flaccid paralysis. Pathological investigation indicated that the cause of death at the earlier times after administration was likely due to acute respiratory failure; renal failure was implicated in deaths occurring later than three days after injection. (22).



The toxicity of stable gallium citrate was investigated by Dudley *et al.* (23). Acute toxic doses ( $LD_{50}$ , 10 days) of gallium citrate administered subcutaneously were:

mice	600 mg Ga/kg
rats ( 50–100g)	220 – 240 mg Ga/kg
rats (200–300g)	100 mg Ga/kg
rabbits	45 mg Ga/kg
dogs and goats	10 – 15 mg Ga/kg

This investigation demonstrated the species variability in gallium toxicity. The larger species of animals were more susceptible to the toxic action of gallium citrate than were the smaller species. There was also a trend towards greater susceptibility with increased age and body weight. The symptoms of gallium citrate poisoning were similar to those reported for gallium lactate. Blood analysis after subcutaneous injection of 30 mg Ga/kg in rabbits revealed no significant changes in hemoglobin, cellular fractions, Ca, Mg, or total protein. However, there was a 15% increase in non-protein nitrogen 48-72 hours after injection.

Bruner, Cooper and Rehbock (24) also studied the toxicity of gallium citrate administered intravenously in dogs and rats. They reported similar values for acute toxic doses, and similar adverse effects. It was noted that the liver, pancreas, heart, intestine and bone marrow were unaffected by toxic doses; chronic administration of the drug produced similar results but to a lesser degree. Both Dudley *et al.* (23) and Bruner *et al.* (24) noted an immediate response of acute respiratory depression in some animals upon injection of gallium citrate. Dudley attributed this effect to the speed of injection, whereas Bruner presumed that it was a result of acute hypocalcemia induced by the citrate. Administration of prophylactic doses of calcium gluconate prevented this acute response (24).

Perkinson and co-workers (25) investigated the effect of  $^{72}\text{Ga}$  on the consumption



of oxygen by rat liver slices. A dose of 8 – 10 mg Ga/kg was found to inhibit oxygen consumption for approximately 6-12 hours. Stable gallium plus  $^{72}\text{Ga}$  (63 MBq/kg) produced a greater degree of inhibition, indicating that the radiation dose delivered to the liver by  $^{72}\text{Ga}$  had an added effect on liver metabolism. No histologic damage was apparent.

Adverse effects upon the administration of 0.37 – 3.7 GBq of  $^{72}\text{Ga}$ -citrate (15 – 70 mg Ga/kg) in humans for the investigation and treatment of terminal bone cancer were reported by Andrews *et al.* (26). The toxic symptoms fell into three categories: 1) bone marrow depression as a result of radiation damage; 2) metal toxicity producing a metallic taste in the mouth and some prominent dermatological changes; and 3) GIT symptoms such as anorexia, nausea, and vomiting, due to a combination of both radiation and metal toxicity.

In comparison, the toxicities of sodium lactate and sodium citrate in mice were found to be 520 g/kg body weight and 115 mg/kg respectively (27).

Recently gallium nitrate has been introduced as a possible anticancer drug (28). Toxic symptoms in animals included weight loss, pneumonitis, renal tubular damage and liver damage. Renal precipitates have been found to be composed of gallium, calcium, and phosphate (29). In clinical toxicologic studies, Ga-nitrate was consistently nephrotoxic and also produced anemia (30).

The wide species variation in toxicity makes it difficult to predict the toxic dose of gallium in man. Bruner *et al.* (24) estimated the  $\text{LD}_{10}$  for man to be approximately 20 mg Ga/kg body weight. Commercially supplied  $^{67}\text{Ga}$ -citrate is essentially carrier-free, and contains only 4.5 ng Ga per 37 MBq.

## 2. Protein Binding Of Gallium In Serum

The association of gallium with plasma proteins was first demonstrated by Hartman and Hayes (31). Employing the techniques of ultrafiltration, gel filtration, and equilibrium



dialysis, it was established that gallium was bound by a high molecular weight component of rabbit serum which absorbed ultraviolet light at 280 nm. Thus, it was suggested that it was plasma proteins which bound  $^{67}\text{Ga}$  *in vivo*. Ultrafiltration showed that approximately 80% of the Ga was retained on the membrane, whereas measurements using equilibrium dialysis showed that gallium binding to serum was approximately 97%. The percentage of gallium bound decreased when the concentration of gallium exceeded  $3.6 \times 10^{-2}$  mol/10 ml serum. Binding of gallium was decreased at pH values less than 6.5 but remained relatively unchanged above pH 6.5.

The concentration of citrate was found to have only a slight effect on gallium binding, as binding was still 55% at citrate-to-gallium ratios of 1000:1. This decrease in protein binding with increasing citrate concentration was also observed in *in vitro* experiments by Hnatowich *et al.* (19). However, administration of large amounts of Na-citrate (3g) had no effect on the *in vivo* protein binding of  $^{68}\text{Ga}$  in dogs (19).

A study by Gunasekera *et al.* (32) showed that the ultrafiltration of human serum after intravenous administration of  $^{67}\text{Ga}$ -citrate demonstrated strong binding of gallium to serum proteins. At three hours after administration, 85% of the radioactivity remaining in the serum was bound and at 24 and 48 hours, binding was 97% and 99% respectively. All the serum samples retained only 30% of their initial activity after exhaustive dialysis or zone electrophoresis, suggesting that 70% of the bound  $^{67}\text{Ga}$  was only loosely associated with albumin and some globulins. Immuno-electrophoresis autoradiography demonstrated association of  $^{67}\text{Ga}$  with two distinct peaks, identified as transferrin (Tf) and haptoglobin. Electrophoresis of dialyzed samples showed that all radioactivity was in the  $\beta$ -fraction containing Tf, suggesting specific binding to this protein (32).

Slightly differing results were reported by Clausen *et al.* (2). Using a similar electrophoresis-autoradiographic technique,  $^{67}\text{Ga}$ , after incubation with normal serum,





was found to be virtually 100% associated with Tf. In contrast to these results, Hara (33), using electrophoretic techniques, determined that most of the  $^{67}\text{Ga}$  in serum existed freely and was only partially associated with Tf. However, a recent report by Vallabhajosula *et al.* (34) indicated that the electric field in electrophoresis affected the distribution of  $^{67}\text{Ga}$  radioactivity between the serum proteins. As time increased from 15-60 minutes, the radioactivity associated with Tf decreased and free  $^{67}\text{Ga}$  radioactivity increased. On the other hand, ultrafiltration experiments showed that 97% of the  $^{67}\text{Ga}$  in serum was bound to Tf. Thus, it was concluded that Tf is the transport protein for  $^{67}\text{Ga}$  *in vivo*. The same group later reported similar findings employing the techniques of ultrafiltration, gel chromatography, and affinity chromatography (35). Very little  $^{67}\text{Ga}$  was associated with albumin; all  $^{67}\text{Ga}$  in plasma was associated with Tf (35).

### 3. Gross Tissue Distribution

#### a) Early Studies With Stable Gallium And $^{72}\text{Ga}$

The effect of time and route of administration on the distribution of gallium lactate was reported by Dudley, Maddox and LaRue (36). Subcutaneous injection of 100 mg Ga/kg into rats showed rapid bone uptake with appreciable retention of gallium in bone for greater than 90 days. Most of the gallium found in the bone was associated with the bone matrix, not the bone marrow. The liver and kidney shared moderate uptake, with most gallium removed by 30 days. Greater than 85% of the injected dose was retained in the whole body after ten days. All gallium in blood was found in plasma.

The demonstration of bone uptake of gallium prompted an autoradiographic study of the skeletal accumulation of  $^{72}\text{Ga}$ -citrate in rabbits and dogs (37). Administration 18.5 MBq/kg of  $^{72}\text{Ga}$ -citrate (total Ga = 8 mg/kg) demonstrated the rapid deposition and significant accumulation of radio-gallium in the epiphyseal junction, particularly in younger animals. Thus,  $^{72}\text{Ga}$ -citrate was found to accumulate in areas of greatest



osteogenic activity (37). The subcutaneous injection of  $^{72}\text{Ga}$ -citrate in rabbits was shown to result in bone uptake of 30 – 48% of the injected radioactivity within 16 hours of administration, which was at least eight times greater than uptake observed in the liver, intestine, lungs or whole blood (38). This study also demonstrated the faster clearance of gallium citrate from the soft tissues than gallium lactate.

Bruner *et al.* (39) compared the distribution of  $^{72}\text{Ga}$ -chloride and  $^{72}\text{Ga}$ -citrate in rats. Injection of  $^{72}\text{GaCl}_3$  intravenously at pH 2 resulted in a diffuse distribution, with no rapid or sufficient differential uptake by any particular tissue. A molar ratio of citrate-to-gallium of 5:1 demonstrated high uptake in the bone, liver and spleen, but the bone absorption ratio was lower compared to that of the molar ratio of citrate-to-gallium of 1.2:1. At this concentration, the differential absorption ratio of the femur-to-liver and spleen was four times at 24 hours and 14 times by 96 hours.

The first clinical study with  $^{72}\text{Ga}$ , performed by Mulry and Dudley (40), was the administration of 11 – 15 MBq of  $^{72}\text{Ga}$ -citrate, containing 3.8 – 5.0 mg carrier gallium, for use as a possible diagnostic agent in bone tumors. The  $^{72}\text{Ga}$ -citrate was administered as an infusion drip, and the deposition of  $^{72}\text{Ga}$  was measured by placing a collimated Geiger-Mueller counting assembly on the skin surface. The  $^{72}\text{Ga}$  was found to selectively concentrate in bone tumors, both osteolytic and osteogenic, with tumor-to-bone ratios of 20:1 observed.

The distribution of  $^{72}\text{Ga}$ -citrate in humans was further investigated while testing the possible therapeutic effects of  $^{72}\text{Ga}$  in terminal bone cancer (26). Patterns of localization were determined by Geiger-techniques, as well as biopsies, when possible. In normal bone, the gallium was found just below the outer covering of the bone, and as was observed in animal studies, there was marked deposition at the epiphyseal junctions in growing bones. In diseased bone, the  $^{72}\text{Ga}$  was often found to be associated around areas of calcification.



Liver, spleen, and bone marrow were observed to accumulate some  $^{72}\text{Ga}$  and fairly high levels were also seen in the kidney and endocrine glands. Although there was highly selective bone uptake of  $^{72}\text{Ga}$ -citrate, there was little clinical improvement observed.

Thus,  $^{72}\text{Ga}$ -citrate was found to have little diagnostic or therapeutic value in the treatment of malignant bone disease. The interest in gallium was revived in the early 1960's with the development of the  $^{68}\text{Ge}$ — $^{68}\text{Ga}$  generator, but the clinical usefulness of  $^{68}\text{Ga}$ -radiopharmaceuticals was not found to be superior to that of existing techniques (20). Active interest was again renewed after the observation by Edwards and Hayes (1) that  $^{67}\text{Ga}$  accumulated in soft tissue tumors. Since that time there have been several investigations into the distribution of  $^{67}\text{Ga}$ -citrate and the factors which influence this distribution.

#### b) Animal Studies With $^{67}\text{Ga}$ -citrate

The preliminary study with carrier-free  $^{67}\text{Ga}$ -citrate in rats by Bruner, Hayes, and Perkinson (41) was the first to recognize the importance of the effect of carrier gallium on the relative distribution and excretion of gallium citrate. With carrier amounts in excess of 0.25 mg Ga/kg the distribution was almost identical to that previously observed with  $^{72}\text{Ga}$ -citrate. However, a reversal of distribution occurred at carrier levels of less than 0.25 mg/kg. Blood clearance was slower and a much greater accumulation of gallium was observed in soft tissues such as liver and spleen relative to uptake in the femur, due to a greater retention of activity by the soft tissues.

A comparative study of the kinetics of  $^{67}\text{Ga}$ -citrate,  $^{67}\text{Ga}$ -lactate,  $^{67}\text{Ga}$ -chloride, and  $^{67}\text{Ga}$ -iron-DTPA in tumor-bearing mice was reported by Konikowski *et al.* (27). The tumor uptake of the first three complexes were similar; that of the DTPA was considerably lower. The liver uptake of  $^{67}\text{Ga}$ -chloride at 30 minutes after injection was about three times that observed for the citrate and lactate.  $^{67}\text{Ga}$ -iron-DTPA had the lowest liver uptake. The highest tumor-to-background ratios were achieved after 24 hours. Kidney uptake was less than 1% for all four gallium complexes and some skin uptake was observed.



A detailed analysis of the kinetics of gross distribution of  $^{67}\text{Ga}$ -citrate in rats was performed by Glaubitt *et al.* (42). The amount of  $^{67}\text{Ga}$ -radioactivity in various organs was measured for 30 days after injection; the whole skeleton was found to retain 46% of the total dose; liver uptake was 15%, skeletal muscle 25%, and other organs each accounted for 1 – 2% of the injected radioactivity when extrapolated back to the time of injection. Whole body scans in rats after administration of 7.4 MBq demonstrated the following characteristics:

- 1) the heart was visible at one hour and five hours after administration, due to blood activity,
- 2) The highest uptake was observed in the liver and spleen, especially during the first 24 hours; although the skeleton took up most of the injected radioactivity, the liver and spleen had a greater concentration of  $^{67}\text{Ga}$  due to their smaller mass,
- 3) there was definite accumulation in the skeleton after five hours which reached a peak at approximately 15 hours,
- 4) maximum accumulation in the kidneys occurred at 11 hours,
- 5) small and large intestines showed uptake from at least five hours to 24 hours after injection,
- 6) uptake in testicles occurred during the first 12 hours, and
- 7) uptake in the head occurred after the first 12 hours.

Sephton *et al.* (43) demonstrated in mice that normal tissue distribution of  $^{67}\text{Ga}$ -citrate was essentially completed by one hour after administration. The clearance of radioactivity from the plasma was gradual, but by 24 hours had reached low levels. Uptake in liver, spleen, kidney and intestine was measured at 3 – 5% of the injected radioactivity; other soft tissues such as lung and muscle were approximately ten times lower. The radioactivity in the joint was approximately twice that of the activity in the bone shaft. There was considerably greater bone uptake observed in younger animals.





In the same investigation, tumor-bearing mice displayed similar tissue distribution to the normal animals (43). The accumulation of  $^{67}\text{Ga}$  in the tumor occurred as early as 30 minutes after injection, and was several times greater than that of the other soft tissues. An investigation by Ito *et al.* (44) demonstrated by whole body scans of tumor-bearing rabbits that the tumor was visible on the first day of the experiment. The tumor-to-blood ratios increased with time, and by three days after administration the tumor could be clearly delineated.

### c) Human Studies With $^{67}\text{Ga}$ -citrate

An early study of  $^{67}\text{Ga}$ -citrate scanning by Edwards and Hayes (45) noted the distribution of gallium to the liver, spleen and skeleton, particularly in instances where there was no tumor or the tumor was small. Uptake in the liver was homogenous, with no preferential localization in the Kupffer cells.

Autopsies of patients who died from three hours to 23 days after intravenous administration of  $^{67}\text{Ga}$ -citrate revealed a considerable variation in organ uptake, particularly in the spleen and adrenals (46). The highest average concentration of  $^{67}\text{Ga}$  was observed in the spleen (4.1% of the administered dose/kg), with the lowest concentration observed in the brain and spinal fluid (0 – 0.7%/kg). Relatively high, but variable, uptake was observed in the kidney (2.7%/kg), adrenals (3.8%/kg), bone marrow (3.6%/kg), liver (2.8%/kg) and bone (2.6%/kg). Uptake was greater in the renal cortex than medulla. Other organs with appreciable  $^{67}\text{Ga}$  uptake included lymph nodes, bowel, and lung. Other soft tissues took up less than 1% of administered dose/kg. During the first week after  $^{67}\text{Ga}$ -citrate administration the highest tissue concentration was initially observed in the kidney, then shifted from the kidney to the lymph nodes, adrenals, or bone. After the first week, liver and spleen exhibited the highest tissue concentration other than tumor.

The concentration of  $^{67}\text{Ga}$  within tumors was also variable, with uptake ranging from 0.2%/kg (glioblastoma multiforme) to 41.0%/kg (adenocarcinoma of the breast) (46).



Often there was variation in  $^{67}\text{Ga}$  uptake between different samples of the same tumor. This variation of uptake between tumor types, and even similar histologic types, was also observed by Edwards and Hayes (47). Tumor accumulation of  $^{67}\text{Ga}$  ranged from 1.6% to 68% of the injected dose per kg of tumor. Tumor viability was thought to be involved in uptake, as necrotic or fibrotic tumors generally accumulated less radioactivity than viable tumors. If the tumor contained less than 5% of the injected dose/kg, it was difficult to detect on the scan.

#### d) Factors Affecting The Gross Tissue Distribution Of Gallium

There are several factors that have been found to affect the tissue distribution of gallium. These are presented in Appendix A.

#### 4. Excretion Of Gallium

Subcutaneous injection of stable gallium or  $^{72}\text{Ga}$ -citrate into rabbits resulted in 0.1 – 1.0% of the total dose excreted into stomach contents (12-18 hours after injection), 0.8 – 1.3% in intestinal contents, 0.3 – 1.1% in feces (16 hours after injection), with the largest fraction excreted in the urine, 30 – 55% (average 45%) (38). High initial urinary excretion of  $^{72}\text{Ga}$  up to 24 hours followed by decreasing amounts was also observed in dogs, and man (40, 48). The amount of gallium excreted was found to vary widely between patients, and polyuria was observed to increase the amount excreted (85, 40).

From a study of the urinary excretion of  $^{72}\text{Ga}$  in man, the following conclusions were drawn: 1) higher doses resulted in greater urinary excretion; 2) although there was a greater percentage of the injected dose excreted with increasing amounts of  $^{72}\text{Ga}$ , the absolute retention of  $^{72}\text{Ga}$  was increased; 3) the retention of  $^{72}\text{Ga}$  varied widely between patients and no correlation was found between retention and presence of disease; 4) multiple dosing had no effect on amount of gallium excreted; 5) there was no evidence of kidney damage (86).



The dependence of excretion patterns on the amount of gallium administered was observed in studies with both  $^{72}\text{Ga}$  and  $^{67}\text{Ga}$  (39, 41). Excretion of  $^{72}\text{Ga}$ -citrate in rat urine was increased, as well as the ratio of urinary-to-fecal excretion, with increasing amounts of gallium administered (39). The preliminary study with  $^{67}\text{Ga}$ -citrate in rats demonstrated that low levels of carrier gallium (0.25 mg/kg) resulted in initial high urinary excretion of  $^{67}\text{Ga}$  (more than twice that of fecal excretion during the first 24 hours), followed by greater fecal excretion during subsequent measurements (1.5 – 3.0 fold that of urinary excretion). However, at carrier levels of gallium greater than 0.25 mg/kg, the ratio of urinary-to-fecal excretion increased, reaching 10.5 at 25 mg Ga/kg (41).

Konikowski *et al.* (27) measured the average whole blood and plasma renal clearances of different complexes of  $^{67}\text{Ga}$ :

	<u>Whole Blood Renal Clearance</u>	<u>Plasma Renal Clearance</u>
$^{67}\text{Ga}$ -citrate	0.7 ml/min	0.4 ml/min
$^{67}\text{Ga}$ -lactate	3.8 ml/min	2.3 ml/min
$^{67}\text{GaCl}_3$	6.1 ml/min	3.5 ml/min
$^{67}\text{Ga-Fe-DTPA}$	33.8 ml/min	19.7 ml/min

This demonstrated that the renal clearance of  $^{67}\text{Ga-Fe-DTPA}$  was considerably faster than the other  $^{67}\text{Ga}$  complexes, with  $^{67}\text{Ga}$ -citrate being cleared through the kidneys the slowest.

Clinical studies with  $^{67}\text{Ga}$ -citrate have demonstrated that 20 – 30% of the injected dose was excreted in the urine (45 – 47). The most rapid excretion was during the first 24 hours (0 – 15%), with the remaining 10 – 15% being excreted over the next five days (47). The whole body retention of  $^{67}\text{Ga}$  after one week has been reported to average 65%, ranging from 35 – 81% (45 – 47). Whole body retention has been found to have two exponential components, with half-lives of 30 hours and 613 hours consecutively (52).



The form in which  $^{67}\text{Ga}$  is excreted in urine after intravenous administration of  $^{67}\text{Ga}$ -citrate was investigated by Zivanovic *et al.* (87). Ultrafiltration experiments demonstrated the association of  $^{67}\text{Ga}$  with a low molecular weight compound. Gel filtration studies showed the elution of  $^{67}\text{Ga}$  at an elution volume similar to that of  $^{14}\text{C}$ -citric acid, suggesting that  $^{67}\text{Ga}$  was present in urine bound to citrate. However, paper chromatography experiments with urine at pH 6 – 8 revealed the presence of two  $^{67}\text{Ga}$  peaks, corresponding possibly to  $\text{Ga}(\text{OH})_3$  and  $\text{Ga}(\text{OH})_4^-$ .

The measurement of urinary excretion of  $^{67}\text{Ga}$  after administration of  $^{67}\text{Ga}$ -citrate to patients with neoplastic disease indicated no correlation between urinary excretion and: sex, age, plasma protein binding of  $^{67}\text{Ga}$ , the site and size of uptake into tumor, current chemotherapy or radiotherapy, protein or citrate urinary concentration, abnormal protein in serum or urine, or any histologic abnormalities (88).

The excretion of  $^{67}\text{Ga}$ -citrate in rats by the GIT was investigated by Chen *et al.* (89). Most of the gallium was found in the contents of the GIT, rather than in the mucosal cells. The majority of the  $^{67}\text{Ga}$  that was secreted into the GIT was found in the small intestine (60%), with significant amounts also found in the bile (20%), large intestine (10%), and esophagus and stomach (10%). By 24 hours, 9% of the injected dose had been secreted into the contents of the GIT. The saturation of iron binding sites on transferrin by prior treatment with iron dextran was found to reduce the GI excretion of  $^{67}\text{Ga}$ -citrate, suggesting that: 1) Tf may play a role in the bowel excretion of gallium, or: 2) enhanced urinary excretion may decrease bowel excretion.

## E. Subcellular Localization

### 1. Association With Organelles

The nature of the subcellular localization of  $^{67}\text{Ga}$  was first reported by Swartzendruber *et al.* (90), who demonstrated by scanning electron microscope autoradio-





graphy the association of  $^{67}\text{Ga}$  with lysosome-like granules. The uptake of  $^{67}\text{Ga}$  by lysosomes in normal liver and several tumor models 24 to 48 hours after administration of  $^{67}\text{Ga}$ -citrate was confirmed by several subsequent studies using ultracentrifugation techniques along with lysosomal enzyme activity markers (91 – 94).

Others reported a relatively large percentage of  $^{67}\text{Ga}$  in tissue homogenates associated with the soluble fraction (44, 95), or nucleic fraction (4, 96). However, these results have been contradicted (48, 97). The high activity of  $^{67}\text{Ga}$  observed in the soluble fraction of some tumor homogenates has been attributed to the fragility of the  $^{67}\text{Ga}$ -binding organelles (48). With respect to  $^{67}\text{Ga}$  in the nucleic fraction, it was reported by Brown *et al.* (97) that by using a refined procedure for subcellular fractionation with removal of mucilaginous debris from the tissue homogenates prior to centrifugation, the trapping of  $^{67}\text{Ga}$  within the nucleic fraction was prevented, and at least 90% of  $^{67}\text{Ga}$  radioactivity from tissue homogenates was recoverable.

In addition to lysosomes, a smaller lysosome-like granule was found to concentrate  $^{67}\text{Ga}$  (48, 97). Whereas  $^{67}\text{Ga}$  preferentially localized in the lysosomal fraction in normal liver tissue, these microvesicles of the microsomal fraction were the primary binding component of  $^{67}\text{Ga}$  in hepatoma. The authors speculated that this difference in the site of localization between normal liver tissue and hepatoma may be the basis for observed differences in normal and tumor  $^{67}\text{Ga}$  uptake (97). Recently, Samezima and Orie (98) reported the association of  $^{67}\text{Ga}$  in the rough endoplasmic reticulum and implicated heavy microsomes in the cellular accumulation of  $^{67}\text{Ga}$ . Peroxisomes have also been reported to accumulate gallium (99).

## 2. Macromolecular Binding

There have been several investigations into the localizations of  $^{67}\text{Ga}$  at the macromolecular level. Samezima and Orie (98) reported the presence of an unidentified



component in the supernatant of homogenized rat liver that was found to bind  $^{67}\text{Ga}$  at early times after intravenous administration; Tf was implicated as one of the intracellular binding proteins of  $^{67}\text{Ga}$  by Aulbert *et al.* (100).

A glycoprotein, with protein content of approximately 51% and a molecular weight between 45,000–55,000, was found to be associated with  $^{67}\text{Ga}$  in normal liver and various tumor homogenates by Hayes and Carlton (101), and was later isolated and characterized by Lawless *et al.* (102). A quantitative difference between normal and tumor tissue in the amount of  $^{67}\text{Ga}$  associated with this component was observed, with greater amounts of  $^{67}\text{Ga}$  bound to this glycoprotein in tumor tissue (101). Small amounts of stable gallium saturated the binding sites of this species, suggesting its presence in both normal and tumor tissues in minute quantities only. This glycoprotein was found to be partially sensitive to heating at 60°C and alkaline pH.

Larson *et al.* (103) observed after hypotonic shock of tumor cells that most  $^{67}\text{Ga}$  found in the tumor lysate was protein bound. At early times after intravenous administration of  $^{67}\text{Ga}$ , immunoprecipitation techniques demonstrated most of the  $^{67}\text{Ga}$  bound to Tf. However, with time a shift in binding from Tf to a component of molecular weight 45,000, as well as to higher molecular weight components, was observed. By 24 hours, the amount of  $^{67}\text{Ga}$  associated with the 45,000 MW component was still increasing as the  $^{67}\text{Ga}$  associated with Tf decreased.

Other proteins have been implicated in the intracellular binding of  $^{67}\text{Ga}$ . Ferritin, the iron storage protein, is found in high concentrations in the liver, spleen and bone marrow, and in lesser amounts in other soft tissues (104, 105). Increased serum ferritin levels have been demonstrated in the presence of various malignant diseases and inflammatory conditions (105 – 108). Although it is not known where this excess ferritin arises, it has been postulated that it is the result of increased ferritin synthesis observed in some



cancers (107). The binding of  $^{67}\text{Ga}$  by ferritin intracellularly has been reported in rabbit hepatocytes by Hegge *et al.* (3), and in tumor cell homogenates by Clausen *et al.* (2). On the other hand, Orii *et al.* (109) reported that ferritin was not involved in the *in vivo* transport of gallium. Lentle *et al.* (110) found a statistically significant difference in the serum ferritin levels of patients with or without positive  $^{67}\text{Ga}$ -citrate tumor uptake. Those patients with positive  $^{67}\text{Ga}$ -citrate tumor uptake had significantly greater serum ferritin levels, suggesting that this protein may play a role in the binding of gallium.

Another iron-binding protein, lactoferrin, has been reported to bind  $^{67}\text{Ga}$  more avidly than Tf (4). Lactoferrin can remove the  $^{67}\text{Ga}$  bound to Tf, and retain the  $^{67}\text{Ga}$  activity, under both physiological and acidic (pH 6.2) conditions (111). Lactoferrin is found in many organs with secretory functions (for example: breast, upper GIT, bronchial glands), and in external secretions including genital and nasal secretions, milk, tears, and saliva (104). It is also found in the cytoplasm of polymorphonuclear leukocytes (112). Hoffer *et al.* (4), demonstrated the association of  $^{67}\text{Ga}$  with lactoferrin in the breast secretions of a patient with a history of galactorrhea and suffering from acute myelogenous leukemia. Analysis of tumor tissue from patients with Hodgkin's disease and Burkitt's lymphoma demonstrated high levels of lactoferrin which were correlated with  $^{67}\text{Ga}$  uptake observed in these lesions (113). The binding of  $^{67}\text{Ga}$  by lactoferrin may be involved in the normal distribution patterns observed with  $^{67}\text{Ga}$  and uptake in inflammatory lesions and tumors (4, 111).

## F. Tumor Uptake Of Gallium

### 1. General Considerations In Tumor Localization

The localization of radiopharmaceuticals in tumors is a function of the altered physiology of tumor tissue compared to normal tissue. Neoplasms, as well as areas of inflammation and some phases of tissue infarction, are characterized by altered microvasculature. There is increased permeability of the capillary beds to macromolecules, due in part to neovascularization which results in large intercapillary pores. Also, there is an



increase in the total perfusion of tumor tissue compared to normal tissue. A decrease in lymphatic drainage is observed, due to a delay in new lymphatic vessel growth, which has the effect of increasing the residence time of macromolecules in the vicinity of the tumor. The increased macrophage activity associated with tissue necrosis may result in the ingestion of labelled macromolecules by macrophages. Pinocytosis by other cells in the area of the lesion may occur. Some labelled macromolecules may have specific receptor sites on the cell membrane which may lead to fixation of the label on the cell surface or intracellularly with translocation of the label. The altered cell membrane permeability observed in tumors is also a possible factor in the localization of radiopharmaceuticals (114).

## 2. The Role Of Transferrin

### a) *In vitro* Studies:

Although Gams *et al.* (115) reported that Tf was one of several serum components that inhibited the uptake of  $^{67}\text{Ga}$ -citrate into leukemic cells, several investigators have since shown that Tf is important in the cellular accumulation of gallium. Sephton and Harris (116) reported that the uptake of  $^{67}\text{Ga}$ -citrate by several mouse tumor lines was stimulated by the addition of sera to the cell medium; mouse, rabbit, horse, and human sera were effective, and Tf was determined to be the active serum factor involved. The same investigators later published a study of the dose – response relationship between Tf concentration and mouse myeloma cell uptake of both  $^{67}\text{Ga}$  and  $^{59}\text{Fe}$  (117). Very low concentrations of human Tf (as low as  $2\text{ }\mu\text{g/ml}$ ) stimulated the uptake of both isotopes by the cells, except when the Tf was pre-saturated with cold iron, whereby there was decreased cell uptake of both isotopes. However, differences were observed between the  $^{67}\text{Ga}$  and  $^{59}\text{Fe}$  dose – response relationships to Tf. Whereas  $^{59}\text{Fe}$  uptake started to decline at Tf levels of  $20\text{ }\mu\text{g/ml}$ ,  $^{67}\text{Ga}$  uptake continued to rise, reaching a maximum at  $200\text{ }\mu\text{g/ml}$ . This difference was attributed to the different binding affinities of Tf for gallium and iron. A similar study with human lymphoblastoid cells gave comparable results, with maximum  $^{67}\text{Ga}$  uptake occurring at  $160\text{ }\mu\text{g Tf/ml}$ , and maximum  $^{59}\text{Fe}$  uptake between  $20$  and  $40\text{ }\mu\text{g Tf/ml}$  (118).







Noujaim *et al.* (119) suggested that the tumor cell uptake of  $^{67}\text{Ga}$  was mediated by the binding of  $^{67}\text{Ga}$ -labelled Tf to tumor cell membrane receptors, with the subsequent release and incorporation of  $^{67}\text{Ga}$  into the cell. Human melanoma cells were incubated with either  $^{67}\text{Ga}$ -citrate, a mixture of  $^{67}\text{Ga}$ -citrate and apo-Tf,  $^{67}\text{Ga}$ -Tf, or iodinated ( $^{125}\text{I}$ )  $^{67}\text{Ga}$ -Tf. Greatest cellular uptake of  $^{67}\text{Ga}$  was achieved with the prelabelled  $^{67}\text{Ga}$ -Tf preparation, as compared to pre-incubation with either apo-Tf or  $^{67}\text{Ga}$ -citrate before addition of  $^{67}\text{Ga}$ -citrate or apo-Tf, respectively. Upon incubation of the cells with  $^{125}\text{I}$ -Tf- $^{67}\text{Ga}$  it was found that the association of  $^{125}\text{I}$  with melanoma cells was constant after 15 minutes, while the  $^{67}\text{Ga}$  radioactivity continued to increase, suggesting a rapid turnover of Tf at a finite number of receptor sites on the cell membrane. A similar study by Turner *et al.* (7) gave comparable results for  $^{125}\text{I}$ -Tf- $^{67}\text{Ga}$  and  $^{125}\text{I}$ -Tf- $^{59}\text{Fe}$ , providing more evidence for an active uptake mechanism. Also, when a mixture of  $^{67}\text{Ga}$ -citrate and  $^{67}\text{Ga}$ -Tf (or  $^{59}\text{Fe}$ -citrate and  $^{59}\text{Fe}$ -Tf) was incubated with the melanoma cells, a greater accumulation of isotope in the cells was observed than when either tracer was incubated alone. The authors attributed this to a potentiation effect whereby a Tf molecule that had donated its ion to the cell was free to bind another  $^{67}\text{Ga}$  or  $^{59}\text{Fe}$  that was present in the medium in an unbound form. The addition of iron, and increasing phosphate concentration, were both found to have a negative effect on the uptake of  $^{67}\text{Ga}$ -Tf and  $^{59}\text{Fe}$ -Tf by the melanoma cells.

Larson *et al.* (120) also supported the concept of membrane receptor sites for Tf on EMT-6 sarcoma cell membranes and have determined the number of receptors to be  $5 \times 10^6$  per cell. However, they proposed adsorptive endocytosis of the  $^{67}\text{Ga}$ -Tf complex as the mechanism of  $^{67}\text{Ga}$  uptake. Potentiation of  $^{67}\text{Ga}$  uptake by the cells reached a maximum at  $250 \mu\text{g}$  Tf/ml of serum; the decline in uptake of  $^{67}\text{Ga}$  at higher Tf concentrations was attributed to saturation of the cell surface receptors. Larson and co-workers (8) later published a comparison of  $^{67}\text{Ga}$ -citrate and  $^{59}\text{Fe}$ -uptake by the EMT-6 sarcoma. The



cellular uptake of both isotopes was proportional to the binding of the Tf-iron complex to the Tf receptors. Again, it was demonstrated that Tf stimulated the uptake of both isotopes, although maximum uptake occurred at different concentrations of Tf, as observed earlier by Harris and Sephton (117) and Sephton and Kraft (118).

The effect of membrane composition on the uptake of  $^{67}\text{Ga}$ -citrate and  $^{67}\text{Ga}$ -Tf was investigated by Rogers and Noujaim (121), using multiple bilayer liposomes as artificial model membranes. Both complexes of gallium showed affinity for negatively charged sites on the surface of the liposomes, but differences were observed in the ability to partition between the lipid and aqueous phases. The partition of  $^{67}\text{Ga}$ -citrate was influenced by the nature of the lipid phase; similarly  $^{67}\text{Ga}$ -Tf was also affected and was thought to extend through the bilayer. Most of the incorporated activity was found associated with the lipid phase.

The effect of the tumorigenicity of transformed cells on the cellular uptake of Fe has shown that as tumorigenicity increased the binding of  $^{125}\text{I}$ -Tf and the transport of Fe from Tf into the cell both decreased (122). Less specific uptake mechanisms appeared to be more important in Fe uptake. The author suggested that  $^{67}\text{Ga}$  uptake may likewise be affected by cell tumorigenicity, and that the role of Tf is only one of many possible molecular mechanisms which may exist depending on cell type and environment.

#### b) *In vivo* Studies:

The similarities between iron and gallium uptake observed in the *in vitro* tumor cell models have not been apparent in published *in vivo* studies. Sephton *et al.* (123) found striking differences between the *in vivo* distributions of  $^{67}\text{Ga}$ -citrate and  $^{59}\text{Fe}$ -citrate in mice.  $^{67}\text{Ga}$ -citrate had a high affinity for tumor tissue and low affinity for hematopoietic tissues; the reverse was observed with  $^{59}\text{Fe}$ -citrate. The authors suggested that factors other than the Tf effect must be involved.



Administration of mouse serum incubated with  $^{67}\text{Ga}$ -citrate to mice bearing EMT-6 sarcoma produced greater  $^{67}\text{Ga}$  radioactivity in the tumor than administration of  $^{67}\text{Ga}$ -citrate (9). However, blood radioactivity was also increased, thus resulting in little change in tumor:blood ratios.

A comparison of the uptake of  $^{67}\text{Ga}$ -Tf and  $^{68}\text{Ga}$ -citrate in a canine transmissible venereal tumor (TVT) was reported by Wong *et al.* (10). At early times after injection the association of  $^{67}\text{Ga}$ -Tf with the tumor was much greater than that observed with  $^{68}\text{Ga}$ -citrate. By approximately two hours after injection,  $^{68}\text{Ga}$  activity in the tumor paralleled  $^{67}\text{Ga}$  activity, in the tumor. Additionally, the tumor:blood ratios were found to be higher for  $^{67}\text{Ga}$ -Tf. Rapid uptake of  $^{68}\text{Ga}$  was observed in the upper thigh, possibly reflecting uptake of the citrate complex by bone and muscle. The fate of Tf *in vivo* was determined by administration of dual-labelled Tf ( $^{125}\text{I}$ -Tf- $^{67}\text{Ga}$ ). The  $^{125}\text{I}$  radioactivity associated with tumor increased rapidly in the first few minutes and then remained constant after ten minutes from injection, while the  $^{67}\text{Ga}$  radioactivity continued to rise throughout the course of the experiment. These results were similar to the findings of the tissue culture experiments by the same group described previously (7, 119), thus substantiating evidence for the existence of a finite number of Tf-receptor sites on the cells of the TVT tumor. The constant  $^{125}\text{I}$  radioactivity was thought to represent the greater affinity of  $^{67}\text{Ga}$ -Tf for the cell membrane than Tf that had donated its  $^{67}\text{Ga}$  ion, thus resulting in a rapid turnover of Tf at the cell membrane (10).

Using the same tumor model, Turner *et al.* (124) have demonstrated the dependence of the composition of the  $^{67}\text{Ga}$ -Tf complex on the TVT uptake of  $^{67}\text{Ga}$ . Differences in the anionic component resulted in different uptakes of  $^{67}\text{Ga}$  by the tumor : nitrilotriacetate and maleate complexes showed a similar high uptake of  $^{67}\text{Ga}$ , whereas malonate and oxalate complexes had much lower tumor uptake. The authors speculate that this could imply either differing tumor Tf-receptor affinities or different rates of release at the cell membrane.



### 3. Other Proposed Mechanisms:

Other mechanisms which have been proposed to play a role in the tumor uptake of  $^{67}\text{Ga}$  include:

- 1) viability of tumor: Greater uptake of  $^{67}\text{Ga}$  was reported to occur in viable, rather than nonviable tumor (45, 125, 126). Contrary to these findings Ito *et al.* (44) found that less accumulation of  $^{67}\text{Ga}$  occurred in the capsular, viable areas of an epidermoid carcinoma than in the necrotic mass. The dependence of  $^{67}\text{Ga}$  uptake by nonviable tumor on the time after injection was reported by Hagan *et al.* (127). Uptake in viable rat hepatoma was greater than nonviable tumor uptake at earlier times, but by 72-96 hours after injection more  $^{67}\text{Ga}$  was found associated with nonviable tumor.
- 2) vascularity of tumor: Ito *et al.* (44) suggested that the increased vascularity occurring secondarily to both neoplastic and inflammatory processes was important in the accumulation of  $^{67}\text{Ga}$ . A comparison of liver tumor uptake of  $^{67}\text{Ga}$  with selective arteriography by Suzuki *et al.* (128) demonstrated a correlation between higher  $^{67}\text{Ga}$  radioactivity and highly vascular tumors. Yeh *et al.* (129) also observed less uptake of  $^{67}\text{Ga}$  in a less vascular tumor model.
- 3) hyperpermeability: The extravasation of  $^{67}\text{Ga}$  into the tumor due to increased permeability of either capillaries or tumor cell membranes has been proposed as a possible mechanism of  $^{67}\text{Ga}$  tumor uptake by several investigators (44, 64, 130, 131). Increased capillary permeability stimulated by histamine was found to increase the accumulation of  $^{67}\text{Ga}$ -citrate, but not  $^{67}\text{Ga}$ -Tf, suggesting that  $^{67}\text{Ga}$ -Tf does not diffuse readily across capillary membranes (130). Driedger *et al.* (131) proposed hypoxia as one factor which could induce hyperpermeability of tumor cell membranes and thereby increase  $^{67}\text{Ga}$  accumulation.





- 4) differentiation: Nash *et al.* (126) found a positive correlation between the uptake of  $^{67}\text{Ga}$ -citrate in colonic and rectal tumors and the degree of differentiation of the tumor. Poorly-differentiated tumors accumulated more radioactivity than well-differentiated tumors.
- 5) rate of growth: The rate of growth of both normal and tumor cells was proposed by Bichel and Hansen (96) to play a role, either directly or indirectly, in the incorporation of  $^{67}\text{Ga}$ ; Orie (95) found no such correlation. Hammersley *et al.* (132) reported a positive correlation between  $^{67}\text{Ga}$  uptake in both normal and regenerating rat liver and the rate of protein synthesis, particularly aryl sulfatase. Uptake was found to be unrelated to DNA synthesis. Hammersley and Taylor (133) later reported similar findings in mouse tumors as well and proposed that the increased lysosomal activity (measured by total aryl sulfatase activity) observed in rapidly growing tissues in the primary factor is the apparent relationship between  $^{67}\text{Ga}$  accumulation and rate of cellular proliferation.
- 6) pH: Winchel *et al.* (134) proposed that decreased pH in the vicinity of the tumor, due to increased anaerobic glycolysis, caused the dissociation of  $^{67}\text{Ga}$ -citrate with subsequent cellular uptake and binding of the free  $^{67}\text{Ga}$ . Vallabhajosula *et al.* (135) found the uptake of  $^{67}\text{Ga}$ -Tf by tumor cells in tissue culture was increased at low pH. Orie *et al.* (136) suggested that the polymerization of  $^{67}\text{Ga}$ -citrate at low pH, as demonstrated by Glickson *et al.* (16), resulted in cellular uptake of  $^{67}\text{Ga}$  due to adsorption of the  $^{67}\text{Ga}$ -polymer of the cell surface.
- 7) exchange with calcium: Anghileri (137 – 139) found that gallium could replace or compete with calcium: a) chemically in some insoluble complexes; b) in binding to membrane phospholipids and; c) in cellular metabolism. Also, Anghileri and Heidbreder (140) reported the competition of  $\text{Ga}^{+3}$  with  $\text{Mg}^{+2}$  as well as  $\text{Ca}^{+2}$  binding sites, and proposed that there may be fewer  $\text{Ca}^{+2}$  and  $\text{Mg}^{+2}$  binding sites in normal than malignant tissues, accounting for the differ-



ential  $^{67}\text{Ga}$  uptakes.

- 8) increased residence time: Muranaka *et al.* (141) found that although the rate of uptake of  $^{67}\text{Ga}$  by normal and tumor tissue was similar, the excretion of  $^{67}\text{Ga}$  from normal tissue was more rapid, thereby increasing the residence time of  $^{67}\text{Ga}$  in tumor tissue relative to normal tissue.

## G. Clinical Studies With $^{67}\text{Ga}$

### 1. The Normal $^{67}\text{Ga}$ Scan

The normal gallium scan is a function of the biodistribution of  $^{67}\text{Ga}$ -citrate. The relatively slow blood clearance is reflected in the initial high activity observed in the soft tissues at early scan times (6 and 24 hours).

Due to renal excretion during the first 24 hours, and the relatively slow establishment of equilibrium between the blood and other tissues, scanning is usually delayed for 48-72 hours after administration (142).

The  $^{67}\text{Ga}$ -citrate image is complicated by several variations of the normal pattern which may occur. The following are features of a normal  $^{67}\text{Ga}$ -citrate scan:

- 1) The greatest uptake is observed in the liver and skeleton (142, 143). However, liver uptake may be reduced when there is a large tumor mass elsewhere that is concentrating the gallium (143).
- 2) Head and neck: Uptake is normally observed in both the bony structures and marrow cavity of the skull, and in the soft tissues of the scalp and neck (144). The greatest activity is seen in the region of the nasopharynx and the occiput (144). The lacrimal glands usually accumulate  $^{67}\text{Ga}$ , and may be pronounced (142, 144). Uptake in the salivary glands may be observed, especially after irradiation of the neck (142).
- 3) Thorax: The rib cage, spine, and scapulae are usually visualized, and uptake in



the sternum may be prominent. Uptake in the breast may be observed when under physiological stimulus (142, 144). Lung activity may be observed on early images but fades by 48 hours (142).

- 4) Abdomen: Activity in the kidneys may be observed at 24 hours, but is usually not detectable at later scanning times (142, 144). Liver uptake is always prominent 48 and 72 hours after injection; splenic accumulation is variable, and is usually demonstrated as a diffuse background (142). Activity in the colon is often detected due to bowel excretion of gallium, which complicates scan interpretation of the abdomen (142, 144). Although laxatives and enemas are usually administered, prominent uptake may still occur (142). One study found no significant difference between bowel preparation with laxatives and no preparation on the observed bowel uptake of  $^{67}\text{Ga}$  (145). On posterior views the sacrum and spine are visualized (144).
- 5) Extremities: Gallium is normally concentrated in the epiphyseal region of the long bones, and is observed in the shoulders, elbows, hips, and knees (142, 144).
- 6) In children, normal distribution is altered somewhat. There is less colonic activity, and greater bone uptake, especially in areas of bone growth (142, 146). Uptake in the thymus and spleen may be increased (146).

## 2. Clinical Usefulness Of $^{67}\text{Ga}$ -citrate In Malignant Diseases

A comprehensive analysis of all published clinical studies involving  $^{67}\text{Ga}$ -citrate is beyond the scope of this thesis. A general overview of the usefulness of  $^{67}\text{Ga}$ -citrate imaging in various types of malignant diseases will be given, with representative studies cited.

In general, the major clinical indications for  $^{67}\text{Ga}$ -citrate imaging in malignant disease are: 1) as an adjunctive procedure in staging; 2) as a method to measure the



response to treatment, and; 3) as a method for the early detection of recurrent disease. Since the gallium scan is nonspecific, a positive result should be confirmed by other techniques. Also, the sensitivity of  $^{67}\text{Ga}$  imaging in the detection of different malignancies is variable. Thus, a negative result is not necessarily indicative of the absence of disease (147).

The actual sensitivity of  $^{67}\text{Ga}$ -citrate imaging may in fact be underestimated as a result of the methods used to confirm or deny the presence of disease. For example, the  $^{67}\text{Ga}$ -citrate scan may detect lymphomatous lesions in the mediastinum that are not detected by conventional x-rays, or lesions in the abdomen that are not detected by lymphangiography. In these cases, the  $^{67}\text{Ga}$  scan results will erroneously be classified as false-positive (148, 149).

Older clinical investigations of  $^{67}\text{Ga}$ -citrate imaging were limited by low count densities due to less efficient detectors (for example, dual 5" crystal rectilinear scanners with a single pulse height analyzer) and low doses of  $^{67}\text{Ga}$ -citrate (150). Improvement of scan quality can be accomplished with increasing the count density (by bracketing three photopeaks and using larger doses of  $^{67}\text{Ga}$ -citrate), and by using instruments with better spatial resolution, such as the Anger tomoscanner or large field of view gamma camera (148, 150).

The terms sensitivity (the percentage of true abnormal sites that are classified as positive on the scan) and specificity (the percentage of true normal sites that are negative on the scan) are widely used to describe the accuracy of  $^{67}\text{Ga}$ -citrate imaging. However, the predictive value of a positive or a negative test is a more meaningful term. The predictive value of a positive test describes the probability that the presence of disease will be observed on the scan as a positive result; the predictive value of a negative test describes the probability that the absence of disease will produce a negative scan. These values are calculated knowing the values of the true positive rate, true negative rate, and the





probability that disease is present based on prior knowledge (148).

#### a. Lymphatic Malignancies:

The sensitivity of  $^{67}\text{Ga}$ -citrate imaging in the detection of sites of involvement in lymphatic malignancies varies with the type of lymphoma and the anatomic location of the lesion. In general, Hodgkin's disease and histiocytic lymphomas are the most accurately detected histologic types. A lesion present within or close to an area that normally accumulates  $^{67}\text{Ga}$ -citrate, such as the liver or colon, may be difficult to detect. Also, superficial lesions are more likely to be detected than the deeper abdominal nodes (148, 149).

##### i) Hodgkin's Disease

One of the largest studies on the utility of  $^{67}\text{Ga}$ -citrate scanning in Hodgkin's disease, involving 668 patients, was reported by Johnston *et al.* (151). Positive uptake in one or more lesions occurred in 69% of the total number of patients. Lesions were detected more readily in untreated patients (88%) than in treated patients (56%). Both radiation therapy and chemotherapy decreased the sensitivity of detection; radiotherapy had a greater effect. In both the treated and nontreated groups, the lymphocyte predominant type showed a lower incidence of detection than the other histologic types (nodular sclerosing, mixed cellular, and lymphocyte depleted). The detectability of lesions was dependent on both size and location. Tumors less than 1 cm in diameter were not detected due to the limitations of instrument resolution. From 1 cm to 5 cm, the detectability increased linearly. Lesions greater than 5 cm in diameter were detected less efficiently, due perhaps to a poor blood supply. Lesions in the neck and thorax (mediastinum) were most accurately detected while those of the axilla, abdomen, and inguinal regions were not demonstrated as well.

Lymphangiography and  $^{67}\text{Ga}$ -citrate imaging in Hodgkin's disease were



comparable in the detection of untreated disease sites. However, the results of the two techniques did not always coincide, and when combined, more lesions were detected but a higher false positive rate was observed (151). Martin and Sephton (152) found  $^{67}\text{Ga}$ -citrate imaging to be complementary to lymphangiography. Although nodal involvement of Hodgkin's disease was detected by lymphangiography with greater sensitivity, the  $^{67}\text{Ga}$  scan was valuable in the detection of extranodal lesions not observed on radiographs.

Mediastinal involvement in Hodgkin's disease is detected with probably the greatest sensitivity and specificity by  $^{67}\text{Ga}$ -citrate imaging. For evaluation of superficial node involvement, the  $^{67}\text{Ga}$ -citrate scan does not replace the physical examination. Lymphangiography, computed tomography and possibly ultrasound are more accurate in the evaluation of the para-aortic lymph nodes (150).

Yeh *et al.* (143) evaluated the usefulness of  $^{67}\text{Ga}$ -citrate imaging in recurrent Hodgkin's disease in children. The  $^{67}\text{Ga}$  scan was found to be a sensitive technique in the early detection of recurrence and in the detection of obscure sites of involvement. The value of a positive scan was greater than that of a negative scan, in that it was strongly indicative of treatment failure, whereas the negative scan could not be considered as strong evidence against the possibility of recurrence.

## ii) Non-Hodgkin's Lymphoma

In a large cooperative study involving 296 untreated and 394 treated patients, Andrews *et al.* (154) reported that 65% of the total number of patients had positive gallium uptake in one or more sites. As observed with Hodgkin's disease, the untreated group had a higher detection rate than the treated group (76% versus 57%). However, chemotherapy was more effective than radiation therapy in decreasing the sensitivity of detection. When compared to the results of the Hodgkin's disease study by Johnston *et al.* (151), the non-Hodgkin's lymphomas had a lower detection rate, and greater variability



with histologic type. Histiocytic lymphoma was detected more accurately than the mixed-cell or poorly-differentiated lymphocytic types. The dependence of lesion detectability on size and location was similar to that observed for Hodgkin's disease, although the decrease in detectability of lesions greater than 5 cm in diameter was not observed.

Brown *et al.* (155) found a lower overall detection rate of nodal involvement, 45%, in 174 scans of patients with non-Hodgkin's lymphoma proven by biopsy. The overall detection rate of extranodal sites was 77%. The rate of detection of involved sites was reported to increase after treatment.

A recent study by Longo *et al.* (156) analyzed the value of  $^{67}\text{Ga}$ -citrate imaging in the staging of 122 untreated patients with non-Hodgkin's lymphoma. The overall patient true positive rate was 52%, the false negative rate was 34%, and the false positive rate was 13%. The false positive scan findings were not confined to any particular anatomical area. The results of  $^{67}\text{Ga}$  imaging changed the status of tumor staging in only one patient. When the scans were analyzed site by site, the overall sensitivity of the  $^{67}\text{Ga}$  image was only 18.5%. The greatest accumulation of  $^{67}\text{Ga}$  occurred in the diffuse histiocytic, diffuse mixed, and diffuse undifferentiated types; nodular histiocytic, and nodular and diffuse poorly differentiated lymphocytic varieties had the least  $^{67}\text{Ga}$  uptake.

Gallium-67 imaging was found to be much less sensitive than lymphangiography in the evaluation of involvement in the abdominal-pelvic region (154, 156, 157). Rudders *et al.* (157) reported that, although the false negative rate of  $^{67}\text{Ga}$ -citrate imaging was higher than lymphangiography, the false positive rate was lower, and thus, the two techniques were comparable. However, Longo *et al.* (156) found a high false positive rate with  $^{67}\text{Ga}$  imaging. Also, the  $^{67}\text{Ga}$  scan did not detect any lesions that were not visible on the lymphangiogram. From these results, the authors concluded that the routine use of



of  $^{67}\text{Ga}$ -citrate imaging in the staging of non-Hodgkin's lymphomas is unwarranted due to the nonsensitivity and high false positive rate. However,  $^{67}\text{Ga}$ -citrate imaging may be useful to monitor the effectiveness of treatment and to screen for possible recurrences on an individual patient basis (158).

### iii) Burkitt's Lymphoma

Only one relatively small study on Burkitt's Lymphoma has been reported. Richman *et al.* (159) evaluated 14 patients with  $^{67}\text{Ga}$  imaging: nine patients for initial evaluation and five with relapse. Positive gallium uptake was observed in all tumor sites that were proven, apparent, or suspected. Occult disease was also detected in two patients. Seven patients with complete remission had normal gallium scans. Gallium-67 was considered to be very useful in both the initial evaluation and subsequent follow-up of these patients.

### iv) Leukemia

The accumulation of  $^{67}\text{Ga}$ -citrate in the sites of leukemic involvement, both in bone marrow and extramedullary sites, has been observed in acute lymphocytic, acute myelocytic, and chronic granulocytic leukemia, but not chronic lymphocytic leukemia (160, 161). *In vitro* and *in vivo* studies in chronic leukemic patients demonstrated that  $^{67}\text{Ga}$ -citrate had high affinity for granulocytes but little affinity for lymphocytes (161). Thus, patients with chronic granulocytic leukemia had prolonged whole body retention of  $^{67}\text{Ga}$ -citrate, whereas those with chronic lymphocytic leukemia did not.

Milder *et al.* (160) observed both diffuse and focal accumulation of  $^{67}\text{Ga}$ -citrate in involved leukemic sites, and found highly positive uptakes in both abscesses and osteomyelitis in these patients. As the number of leukemic cells regressed with therapy, the uptake of  $^{67}\text{Ga}$ -citrate in involved areas also decreased. Although in this study the abnormal bone uptake correlated with the bone marrow status of the patient, another





study involving acute nonlymphocytic leukemic patients found no such correlation (162).

The major usefulness of  $^{67}\text{Ga}$ -citrate imaging is in the detection of inflammatory lesions that are often associated with acute leukemias (163).

#### b. Malignant Melanoma

Milder *et al.* (164) reported that  $^{67}\text{Ga}$ -citrate imaging detected 54% of evident or biopsy proven sites, and 52% of suspected sites in patients with malignant melanoma. The false positive rate was very low (2%) and the false negative rate was 47%. The sensitivity of detection was influenced by the size of the lesion and the location. *In vitro* studies demonstrated high affinity of  $^{67}\text{Ga}$ -citrate for the melanoma masses, yet lesions less than 2 cm in diameter were not reliably detected. Bone lesions were the most accurately detected, 100%; lymph nodes, lung, brain, and liver, approximately 60%; skin and subcutaneous tissues, less than 50%; and, GIT, kidneys, adrenals, and other organs about 45%.

Jackson *et al.* (165) found 69% of proven metastatic melanoma sites positive on the  $^{67}\text{Ga}$ -citrate scintigraph, with a false positive rate of 5.7%. It was observed that patients with abnormal scans at any time had a shorter life expectancy than those patients with normal images.

On both studies the positive  $^{67}\text{Ga}$  scan was felt to have great clinical significance. Although the sensitivity for detection of metastatic sites is fairly low, the value of  $^{67}\text{Ga}$  imaging lies in the detection of unsuspected metastases (150).

As an evaluation of pre-operative staging of malignant melanoma,  $^{67}\text{Ga}$ -citrate imaging was reported to be more specific but much less sensitive than a physical examination (166). The predictive value of both techniques was determined to be approximately 95%. Thus,  $^{67}\text{Ga}$ -citrate imaging was felt to serve no useful purpose in the pre-operative



screening of patients with malignant melanoma.

### c. Hepatoma

Hepatoma is not commonly found as a primary tumor in North America, and the diagnosis of this malignancy is often obscured by the existence of other hepatic diseases such as cirrhosis (163). The usefulness of  $^{67}\text{Ga}$ -citrate imaging in conjunction with conventional colloid liver scans has been reported by several investigators (128, 167 – 170).

The key to the diagnosis is in the uptake of  $^{67}\text{Ga}$ -citrate relative to the defects observed on the colloid scan, rather than in greater uptake by a lesion compared to normal liver activity (150, 163, 171). The  $^{67}\text{Ga}$  scan is particularly useful in differentiating hepatoma from the pseudotumors of cirrhosis, as about 90% of hepatomas accumulate  $^{67}\text{Ga}$ -citrate, and less than 10% of cirrhotic defects are gallium avid (171). However, hepatoma cannot be differentiated from other  $^{67}\text{Ga}$ -avid lesions such as most hepatic abscesses and some metastases from other organs (150, 163).

The determination of serum alphafetoprotein is also a specific indicator for hepatoma, but is not particularly sensitive (163). Suzuki *et al.* (169) found that  $^{67}\text{Ga}$ -citrate detected 26 hepatomas in 27 patients, of which only 17 had positive alphafetoprotein tests. Gallium imaging was therefore considered to be valuable in detecting hepatomas not detectable by alphafetoprotein tests. Waxman *et al.* (172) found no correlation between alphafetoprotein and  $^{67}\text{Ga}$ -citrate uptake. Conversely, Levin *et al.* (170) found that the uptake of  $^{67}\text{Ga}$ -citrate in hepatoma was positively correlated with the presence of alphafetoprotein, although the group of patients was too small to draw conclusions.

Suzuki *et al.* (128) also reported that significant gallium uptake was observed in hypervascular lesions, and less in hypovascular lesions. In a comparison of  $^{67}\text{Ga}$ -citrate uptake in hepatoma with contrast angiography, Waxman *et al.* (172) also found that



avascular lesions did not accumulate  $^{67}\text{Ga}$ -citrate, but that moderately vascular lesions concentrated relatively more activity than hypervascular lesions.

#### d. Carcinoma of the Lung

Gallium-67 citrate imaging is a highly sensitive technique for the detection of primary bronchogenic carcinoma. Detection rates of at least 80%, and most greater than 90%, have been reported (173 – 178). Slight differences in the affinity of the different histologic varieties of lung carcinoma for  $^{67}\text{Ga}$ -citrate have been observed, but all histologies are detected with high sensitivity (173, 174, 179, 180). Higashi *et al.* (180) found that those tumors with the greatest  $^{67}\text{Ga}$  uptake were the most responsive to radiation therapy, and suggested that  $^{67}\text{Ga}$ -citrate imaging may be a useful technique to estimate the radiation sensitivity of lung tumors.

However, the nonspecificity of  $^{67}\text{Ga}$ -citrate uptake in pulmonary lesions limits the contribution of a positive  $^{67}\text{Ga}$  scan to a differential diagnosis (176). The smallest detectable lesion, as reported by DeLand *et al.* (173) and DeMeester *et al.* (174) is about 1.5 cm in diameter, which is no better than the resolution capabilities of the conventional chest radiograph (181). The chest radiograph still remains the method of choice for the detection of primary lung neoplasms (150).

Gallium-67 imaging has been shown to be a sensitive technique for the detection of mediastinal or hilar sites of metastases, with reported sensitivities ranging from 75% to 100% in some of the larger studies (173 – 175, 177, 178, 182, 183). The accuracy of detecting mediastinal involvement is greater when the primary tumor is peripheral rather than paramediastinal (178). The occurrence of false positive uptake decreases the specificity of gallium imaging, and may be a result of confusion with normal uptake, the blending of normal activity in the sternum and spine with a medially situated primary tumor, or by the overlapping of the primary tumor with the hilum (181). Gallium imaging is more sensitive than other noninvasive techniques such as chest x-rays and mediastinal tomography in the



delineation of mediastinal involvement (150, 177, 183). It is comparable to, and complementary with, the more invasive procedure of mediastinoscopy, but does not replace this technique. A positive gallium scan in the mediastinum is considered to be an indication for mediastinoscopy (176, 177).

A major point of controversy in the routine use of  $^{67}\text{Ga}$ -citrate imaging for the staging of bronchogenic carcinoma is in the detection of extrathoracic metastases. Brereton *et al.* (175) investigated the utility of  $^{67}\text{Ga}$  scanning in the staging of small cell carcinoma, and reported that of 27 extrathoracic metastases found by other organ specific methods, only two were demonstrated on the gallium scan. Thus, the organ specific techniques were felt to be of greater value in staging than the gallium scan. Contrary to this view, DeMeester *et al.* (178) considered the gallium scan to be valuable in the initial assessment of remote sites of metastases, and specific organ studies secondary. The overall sensitivity of gallium scanning for the detection of extrathoracic metastases was 75%, and of particular value was the demonstration of 11 sites of occult disease that were not detected by other techniques.

#### e. Tumors of the Head and Neck

Gallium-67 imaging has not proven to be valuable in the staging of head and neck tumors (184, 185). Higashi *et al.* (186, 187) reported that  $^{67}\text{Ga}$  imaging may be useful in differentiating malignant tumors of the maxillary sinus from chronic sinusitis, for predicting the sensitivity of a tumor to treatment, and in assessing the response to therapy. Silberstein (184) found that all lesions detected by  $^{67}\text{Ga}$ -citrate could be detected by other methods.

Although  $^{67}\text{Ga}$ -citrate is highly sensitive in the detection of both primary and metastatic brain tumors, the uptake is not more specific than other currently used methods such as  $^{99}\text{Tc}^{\text{m}}$ -pertechnetate scans and computed tomography (150, 188). However,  $^{67}\text{Ga}$ -citrate does detect skull metastases missed by the pertechnetate scan, and may be





useful in detecting persistent or recurrent tumors post-operatively, as gallium accumulates less in the craniotomy site than does  $^{99}\text{Tc}^{\text{m}}$ -pertechnetate (188).

In a recent report of a cooperative study on the value of  $^{67}\text{Ga}$ -citrate imaging in the detection of head and neck tumors, excluding central nervous system, thyroid and lymphomatous lesions, Teates *et al.* (185) reported an overall detection accuracy of 59%. There were no significant differences in the accuracy of detection of treated versus untreated lesions, or in the sensitivity of detection of primary versus metastatic lesions. Tumors less than 3 cm in diameter were not detected as accurately as larger tumors. The authors suggested that a positive scan in a patient with known cancer indicated the presence of a lesion, but that a negative scan was inconclusive.

The uptake of  $^{67}\text{Ga}$ -citrate by thyroid lesions is neither very sensitive nor specific. The overall patient true positive rate in thyroid carcinoma is only approximately 40% (150). Although anaplastic carcinoma more frequently shows positive uptake, it is an uncommon variety of thyroid tumor. Also, thyroiditis and other benign inflammatory lesions may accumulate  $^{67}\text{Ga}$ -citrate (150, 188). Therefore,  $^{67}\text{Ga}$  imaging is not routinely used to evaluate thyroid nodules which do not accumulate either  $^{131}\text{I}$  or  $^{99}\text{Tc}^{\text{m}}$ -pertechnetate (188).

#### f. Breast Carcinoma

In a study of  $^{67}\text{Ga}$ -citrate imaging in 125 patients with primary and metastatic breast carcinoma, Richman *et al.* (189) reported an overall detection rate of 54%. Primary lesions were detected with an accuracy of only 52%. Metastases to other organ systems were more efficiently detected by techniques specific for those systems. The value of  $^{67}\text{Ga}$ -citrate imaging was felt to be in the high sensitivity of detection of mediastinal involvement.

The normal variation observed in breast uptake limits the usefulness of  $^{67}\text{Ga}$ -citrate



imaging in the early detection of breast carcinoma (188).

#### g. Bone Tumors

The sensitivity of  $^{67}\text{Ga}$ -citrate imaging in detecting primary bone tumors is high (190). In an investigation of  $^{67}\text{Ga}$ -citrate imaging in Ewing's sarcoma, the gallium scan was found to be less sensitive than the bone scan in detecting primary tumors, and skeletal and extraskkeletal metastases were detected with greater sensitivity by bone scans and radiographs, respectively (191). The value of  $^{67}\text{Ga}$ -citrate imaging was that it detected greater extension of the tumor than was indicated by the x-ray or the bone scan.

#### h. Genitourinary Tumors

In general, it is felt that the detection of renal, urethral, bladder, ovarian, uterine, cervical, and prostate primary lesions and their metastases by  $^{67}\text{Ga}$ -citrate imaging is not sensitive enough to justify its routine use (150, 188). The sensitivity of detection for most genitourinary tumors is 50% or less (190).

A cooperative study of  $^{67}\text{Ga}$ -citrate imaging in genitourinary tumors found that primary tumors were detected poorly (192). Metastases, particularly those to soft tissues, were detected more accurately. The low success rate in visualizing the primary tumors was felt to be related to the location of the tumor and possibly small tumor size. The highest detection rate was found for soft tissue metastases from kidney primaries.

The usefulness of  $^{67}\text{Ga}$  imaging in detecting primary renal neoplasms is limited by poor avidity and variability in uptake by the tumor (171). It is not abnormal to faintly visualize the kidneys on the 48 hour scan. If the activity is intense, focal, or asymmetric the scan may be considered abnormal, but is nonspecific as it could be a result of several different disease processes.

The most useful application of  $^{67}\text{Ga}$  imaging in genitourinary tumors has been in



the staging and follow up of patients with testicular neoplasms. Although primary tumors are not accurately detected,  $^{67}\text{Ga}$ -citrate has been shown to be sensitive in detecting metastatic spread (193 – 196). The best results appear to occur with the seminoma and embryonal cell varieties, with the poorest sensitivity in teratomas (192 – 194).

#### i. Gastrointestinal Tumors

Gallium-67 citrate imaging has not proven to be useful in either the detection or staging of most gastrointestinal malignancies, as the sensitivity of detection is generally less than 50% (150, 188, 197). The poor results observed in the abdominal area may be a result of the difficulty in distinguishing abnormal from normal uptake (188).

Although both the sensitivity and specificity of gallium imaging is low in most GIT malignancies, it does have importance in certain clinical situations: suspected lymphomas or carcinomas, detection of recurrence, metastases, or onset of malignancy in suspected patients; evaluation of therapy; and, an alternative to conventional radiography techniques (197). Lentle *et al.* (198) reported an accuracy of 83% in the detection of pelvic recurrence of rectal carcinoma after excision of the primary tumor.

Relatively good results have been reported for esophageal carcinoma (199). Although the sensitivity of detection of the primary tumor and lymph node metastases was low (39% and 27% respectively), extramural extension was detected with a sensitivity of 67% and a specificity of 100%. Gallium-67 imaging was considered to be valuable as a noninvasive technique.

#### j. Pediatric Tumors

In a study of the usefulness of  $^{67}\text{Ga}$ -citrate imaging in solid tumors in children Lepanto *et al.* (200) observed only a 34% overall true positive rate. The highest true positive rate occurred in Hodgkin's disease. Bekerman *et al.* (201) also found a high sensitivity of detection in juvenile Hodgkin's disease, particularly in the detection of



mediastinal lymph node involvement. Abdominal lymph node sites were also accurately detected. Since lymphangiography is difficult to perform in small children,  $^{67}\text{Ga}$  imaging is particularly useful in the detection of involved abdominal and pelvic lymph nodes (202).

Edeling (203) reported a sensitivity of 78% and specificity of 79% in the diagnosis of malignant disease in children, and concluded that gallium imaging was useful in the detection and follow-up of pediatric malignancies. Handmaker and O'Mara (146) suggested that gallium imaging was comparable to other techniques for the detection and staging of pediatric tumors. However, the nonspecificity and variability of  $^{67}\text{Ga}$  accumulation in malignant lesions required cautious interpretation of  $^{67}\text{Ga}$ -citrate images.

Although  $^{67}\text{Ga}$ -citrate imaging was sensitive in detecting sites of soft tissue sarcomas, chest x-rays were more sensitive in the detection of lung metastases (201). Gallium-67 imaging is not considered to be useful in the detection or staging of neuroblastoma, Wilm's tumor, and rare pediatric tumors (200 – 202). A correlation of persistent or recurrent positive  $^{67}\text{Ga}$  images with poor prognosis in various childhood malignancies was found by Yang *et al.* (204).

### 3. $^{67}\text{Ga}$ -citrate Imaging in Inflammatory Conditions

#### a. Mechanisms of Uptake

Lavender *et al.* (205) first reported the observation that  $^{67}\text{Ga}$ -citrate accumulated in inflammatory lesions. Littenberg *et al.* (206) subsequently emphasized the clinical value of  $^{67}\text{Ga}$  imaging in inflammatory conditions by demonstrating the accumulation of  $^{67}\text{Ga}$ -citrate in focal sources of sepsis in several patients.

The exact mechanism by which  $^{67}\text{Ga}$ -citrate accumulates in inflammatory lesions is not known, but several theories have been proposed. Excellent reviews on this subject have been presented by Hoffer (207, 208). The increased permeability of blood vessels at





sites of inflammation is probably important as an indirect method of accumulation of  $^{67}\text{Ga}$ -citrate, by increasing the availability of free and protein-bound  $^{67}\text{Ga}$  (130). More direct factors which have been postulated as mechanisms of uptake include: 1) the binding of  $^{67}\text{Ga}$  to leukocytes; 2) binding of  $^{67}\text{Ga}$  to lactoferrin at the site of inflammation, and; 3) direct bacterial uptake (207, 208).

Burleson *et al.* (209) demonstrated the binding of  $^{67}\text{Ga}$ -citrate to rabbit leukocytes both *in vitro* and *in vivo*. A subsequent study using human autologous  $^{67}\text{Ga}$ -labelled leukocytes demonstrated the migration of these leukocytes to proven sites of inflammation (210). The uptake of  $^{67}\text{Ga}$ -citrate has been suggested to depend upon the presence of leukocytes that will infiltrate the site of inflammation (58, 211). Although Hammersley and Taylor (211) found a correlation between  $^{67}\text{Ga}$  uptake into abscesses and the lysosomal enzyme activity of the infiltrating leukocytes, others have reported that  $^{67}\text{Ga}$  is preferentially associated with nonviable and hypoxic leukocytes (212 – 214). Also, the largest amount of  $^{67}\text{Ga}$  in the inflammatory exudates of abscesses, in both normal and agranulocytic rabbits, has been found associated with a soluble, noncellular fraction (215). Thus, it appears that leukocytes are not exclusively involved in the uptake of  $^{67}\text{Ga}$  in inflammatory lesions. This has been demonstrated in patients with  $^{67}\text{Ga}$ -citrate accumulation in inflammatory lesions in the absence of circulating leukocytes (216).

The leukocytes may be important with respect to the large concentrations of lactoferrin that are contained within the secondary granule. When the leukocytes have infiltrated the area of inflammation, lactoferrin may be secreted into the surrounding fluid, and bind the  $^{67}\text{Ga}$  that has leaked into the area. The gallium may also be bound by lactoferrin that is produced locally by the involved organ. Other proteins may also be involved in the binding of  $^{67}\text{Ga}$  at the inflammatory site, such as ferritin (207, 208).

Gallium-67 citrate may be directly taken up by bacteria, probably by a siderophore-mediated mechanism (207, 208). However,  $^{67}\text{Ga}$ -citrate will also accumulate in sterile



inflammations (215).

Terner *et al.* (217) reported that  $^{68}\text{Ga}$ -citrate and  $^{67}\text{Ga}$ -Tf demonstrated identical uptake into experimentally induced sterile abscesses in dogs. However, the ratio of gallium to Tf (labelled with  $^{125}\text{I}$ ) remained constant, unlike results observed in tumors where the Ga-to-Tf ratio increased with time (indicating a specific mechanism). Thus, the uptake of Ga-citrate or Ga-Tf by abscesses was a nonspecific process, possibly simple cellular diffusion.

#### b. Clinical Applications

Excellent reviews of the clinical indications and advantages and disadvantages of  $^{67}\text{Ga}$ -citrate imaging have been presented by Henkin (218), Staab and McCartney (219), and Hoffer (208, 220). The value of gallium imaging in the search of occult infections is that it has a whole body application. The sensitivity and specificity for the detection of abscesses is approximately 90% (218). One advantage of gallium scanning over other techniques for detection of abscesses, such as ultrasound and computed tomography, is that  $^{67}\text{Ga}$ -citrate does not detect only formed lesions, but may also localize in sites of inflammation before the formation of the abscess. A disadvantage of gallium imaging is the necessary time lag between injection and scanning. Often patients are too ill to wait the usual 48 to 72 hours before imaging. Thus, severely ill patients should be imaged at earlier times, 6 – 8 hours after injection of  $^{67}\text{Ga}$ -citrate. However, the diagnosis cannot always be made on the basis of the six-hour image alone, and 24-hour scans are advisable. Imaging at later times, 48 and 72 hours, is performed if necessary. Although  $^{67}\text{Ga}$ -citrate does accumulate in sites of recent surgery, this uptake is recognizable and usually does not provide much interference in scan interpretation (207, 218, 220).

The anatomical locations in which  $^{67}\text{Ga}$ -citrate imaging has been most useful are:

- 1) Abdominal infections:  $^{67}\text{Ga}$ -citrate imaging is useful in the detection of focal



infections, such as abscesses, and diffuse infections such as cellulitis and peritonitis (208, 220). It is indicated as a primary test in suspected abdominal inflammation as it is a sensitive technique and usually identifies lesions within 24 hours (218). Ultrasound and computed tomography should be performed as complementary techniques to increase the specificity of diagnosis. Persistent bowel activity may be suspicious of an inflammatory bowel condition (218).

- 2) Lung:  $^{67}\text{Ga}$ -citrate has been shown to accumulate in most primary or secondary inflammatory lung lesions, including abscesses, sarcoidosis, pneumoconiosis, active idiopathic fibrosis, and infections by opportunistic organisms. However, pulmonary infarcts do not accumulate gallium (208, 220). The chest radiograph is still the method of choice for the detection of pulmonary inflammatory conditions (218).
- 3) Bone and Joint: Although the bone scan is the preferred method for detection of inflammation of bone (eg. osteomyelitis),  $^{67}\text{Ga}$  imaging is useful as an adjunctive procedure in symptomatic patients with negative bone scans (208, 220). Gallium imaging is useful in neonates, and in assessing active inflammatory processes in patients with chronic inflammatory bone lesions. It is a useful technique for evaluating the response to treatment, as the bone scan tends to remain positive (219).
- 4) Renal: Gallium imaging is useful in the detection of renal and perirenal abscesses, infected renal cysts, and acute interstitial pyelonephritis (208, 220).
- 5) Others: Other inflammatory conditions which have been observed to result in abnormal  $^{67}\text{Ga}$ -citrate distribution includes thyroiditis, Duchenne muscular dystrophy, and renal amyloidosis (220). Any organ system with an acute inflammatory lesion will accumulate  $^{67}\text{Ga}$  in at least 90% of cases (208).



### H. Radation Dosimetry Of $^{67}\text{Ga}$ -citrate

The absorbed organ and whole body doses from a single intravenous injection of  $^{67}\text{Ga}$ -citrate are presented in Table III. The critical organ in  $^{67}\text{Ga}$ -citrate imaging is the lower large intestine, with an absorbed radiation dose of 0.24 mGy/MBq (221).

**TABLE III**

**ESTIMATED ABSORBED DOSES FROM  $^{67}\text{Ga}$ -CITRATE \***

<u>Tissue</u>	<u>mGy/MBq</u>
Stomach	0.06
Small Intestine	0.10
Upper Large Intestine	0.15
Lower Large Intestine	0.24
Ovaries	0.08
Testes	0.06
Kidneys	0.11
Liver	0.12
Marrow	0.16
Skeleton	0.12
Spleen	0.14
Total Body	0.07

\* From Reference 221.





## II. IRON

### A. Iron Metabolism

The ability of iron to exist in more than one stable oxidation state, and its ability to form several complexes, makes iron an important metal in biology. Several iron-containing proteins exist, including hemoglobin, myoglobin, the cytochromes, iron-sulfur proteins, transferrin, lactoferrin, ferritin, and hemosiderin. The greatest concentration of iron is found in the liver and spleen. Other organs that contain appreciable quantities of iron include the kidney, heart, skeletal muscle, pancreas and brain (222).

Iron is ingested in both organic and inorganic forms. By the action of gastric secretions, and reducing agents in other digestive secretions, inorganic and protein-bound iron is released from conjugation and reduced to the ferrous state for effective absorption by the mucosal cells of the duodenum and proximal jejunum. Iron that is contained in heme-compounds is directly absorbed in that state (222).

The daily intake of iron in a well-balanced diet is about 15 mg. However, of this amount only 1 mg of iron is absorbed per day. This balances the normal daily loss of 1 mg iron per day by gastrointestinal bleeding, sloughing of renal and intestinal mucosal cells and desquamation of skin (223).

An excellent summary of the metabolism of iron in humans was presented by Pollycove and Tono (223). After absorption by the intestinal mucosal cells, the iron is released into the plasma where it is tightly bound to transferrin in the ferric state. Transferrin-bound iron in the plasma is in equilibrium with the labile pool of the erythroid series, comprised of immature red blood cells and bone marrow iron. Equilibrium with ferritin, hemosiderin, heme enzymes and extracellular fluid is also maintained in normal individuals.



Approximately 27 mg of iron is transported to the labile erythroid pool per day. Iron is incorporated into hemoglobin in the ferrous state, and once bound by the red blood cell is no longer in equilibrium with the plasma. Normally, the heme-iron does not re-enter the plasma until the red blood cell dies and is sequestered by the reticuloendothelial cells. Erythrophagocytosis does not normally occur for at least 105 days after formation of the cell. The release of iron by the reticuloendothelial cells is the most significant source of iron entering the plasma.

The exchange of plasma iron with iron stores is dependent upon the degree of saturation of the total iron-binding capacity of Tf. The amount of iron exchange at normal Tf saturation (approximately one-third) is quite small, only 1 – 2 mg per day. However, this amount can become quite large to compensate for abnormal changes in the degree of Tf saturation (223).

#### B. Isotopes Of Iron In Nuclear Medicine

There are several isotopes of iron, ranging in atomic weight from  $^{49}\text{Fe}$  to  $^{62}\text{Fe}$ . The stable isotopes of iron include:  $^{54}\text{Fe}$  (5.89%),  $^{56}\text{Fe}$  (91.8%),  $^{57}\text{Fe}$  (2.15%), and  $^{58}\text{Fe}$  (0.29%) (14). The only isotope of iron that is commonly used in Nuclear Medicine is  $^{59}\text{Fe}$ . The nuclear data for  $^{59}\text{Fe}$  is presented in Table IV.

TABLE IV

#### NUCLEAR DATA OF $^{59}\text{Fe}$ \*

$t_{1/2}$	Mode Of Decay	Major $\beta^-$ radiations (Mev)	Major $\gamma$ radiations (Mev)	Principal Method of Production
44.6 d	$\beta^-$	1.573 (0.30%)	0.143 (0.9%)	$^{58}\text{Fe}$ (n, $\gamma$ )
		0.475 (51.2%)	0.192 (2.7%)	$^{59}\text{Co}$ (n, p)
		0.273 (48.5%)	1.099 (56.5%)	
			1.292 (43.5%)	

\* From Reference 14.



### C. Iron Kinetics

The injection of tracer amounts of  $^{59}\text{Fe}$ , either as the citrate or bound to Tf by pre-incubation, results in an initially rapid, exponential decline of plasma radioiron (223, 224). For the first 60 to 90 minutes after intravenous injection the plasma radioiron disappearance approximates a single exponential. Beyond this time the plasma radioactivity decreases more slowly and begins to deviate from the single exponential (224). The decrease in plasma  $^{59}\text{Fe}$  measured over several days is actually the sum of three exponential components, describing the rapid uptake of  $^{59}\text{Fe}$  by immature red cells in bone marrow, the incorporation of  $^{59}\text{Fe}$  into ferritin, and the daily fixation of  $^{59}\text{Fe}$  into hemoglobin (223). However, the second component describing ferritin incorporation is generally very small in relation to the erythropoietic component.

After six to eight hours, there is feedback of radioiron into the plasma (223, 224). One source of this refluxed radioiron is the return of Tf-bound  $^{59}\text{Fe}$  from the extracellular fluid. Another major source of refluxed iron is from the death of malformed immature red cells, or ineffective erythropoiesis (224).

The uptake of  $^{59}\text{Fe}$  by the sacrum, measured by external organ monitoring, corresponds to the rapid exponential decrease in plasma radioiron (223). The  $^{59}\text{Fe}$  appears in the circulating red cells after one day. Normally, the incorporation of radioiron in the red cells reaches a maximum of 85 – 100% of the injected radioactivity. The liver and spleen normally accumulate little radioiron. The radioactivity measured in these organs is usually a reflection of the radioactivity in the blood: initially plasma radioiron, and later,  $^{59}\text{Fe}$  incorporated into the circulating red cells.

### D. Radiation Dosimetry Of $^{59}\text{Fe}$

The estimated absorbed doses to the various organs were calculated on the assumption that 90% of the injected iron is incorporated into the red blood cells within eight to ten days of injection in normal patients. The mean dose estimates (mGy/kBq) from  $^{59}\text{Fe}$



incorporated into red blood cells are: whole body: 0.23; blood: 0.77; bone marrow: 0.65; liver: 0.27; and spleen: 0.57 (225).





### III. TRANSFERRIN

#### A. General Description

Transferrin is a glycoprotein which consists of two identical branched carbohydrate chains (comprising about 6% of the total weight), attached to a single polypeptide chain. Each of the carbohydrate branches terminates in a sialic acid (N-acetyl-neuraminic acid) residue (22, 227). Although Tf is a globular protein it deviates from a symmetrical spherical conformation, particularly in the apo-state (227). When iron is bound to Tf, the molecule becomes more compact, more spherical, and more stable (226, 227).

The major physiologic role of Tf is the transport of iron from sites of absorption and storage to areas of utilization, such as immature erythrocytes for the synthesis of hemoglobin, and to other cells for the synthesis of other iron-containing proteins and enzymes. There are two sites contained within the transferrin molecule that are capable of selectively binding iron. Other metal ions may also bind to Tf, including gallium (226, 227).

The synthesis of Tf in adult humans occurs predominantly in the hepatocytes, at a rate of 12 – 14 mg per day. Iron deficiency anemia is the only condition that has been shown to increase the synthesis of Tf. Other conditions that may result in increased plasma levels of Tf include pregnancy, acute hypoxia, and administration of estrogen or cortisol. In rats, decreased synthesis has been observed in conditions of fasting and protein malnutrition, and with the administration of alcohol (226, 227).

Transferrin is distributed throughout the extracellular space, 50 – 60% of which is extravascular. Transferrin has been observed in lymph, cerebrospinal fluid, interstitial fluid, edema fluid, and urine. The total body Tf pool is approximately 230 mg/kg, and is circulated from the plasma into the interstitial fluid, and back to the plasma via the



lymphatic system. The amount of Tf circulating through the lymphatic system daily has been estimated to be 70 – 100% of the plasma Tf pool (226, 227). Immunohistological staining techniques have demonstrated the presence of Tf in hepatocytes, some epithelial cells, including gastrointestinal mucosa, and in myoepithelial cells in some tissues (104).

Approximately 15% of the plasma Tf pool is catabolized per day (226). Catabolism does not occur in any tissue preferentially, and is most likely the result of the intracellular uptake and enzymatic degradation of Tf by several tissues. Loss of Tf into the stomach and intestine may also occur. Increased catabolism of Tf has been observed in infections, nephrosis, and hemolytic anemias (226, 227).

## **B. Metal-Binding Characteristics**

### **1. Binding of Iron**

There are two binding sites for iron on Tf, situated in separate domains at least 4.3 nm apart, at the C-terminal (A-site) and N-terminal (B-site) of the polypeptide chain (228, 229). Each site binds one iron atom, and the concomitant binding of a synergistic anion is required for specific binding to occur (230). The ligands involved at the binding sites have been identified as the hydroxyl groups of two or three tyrosine residues, and the imidazole nitrogen of one or two histidine residues. At least one water molecule is bound as well (227).

Under physiologic conditions, the anion bound by Tf along with iron is derived from carbonic acid; whether it is carbonate or bicarbonate is unclear. The distance between the metal-binding site and the anion-binding site is less than 0.9 nm, which indicates that the anion is either bound to the iron atom itself, or is in close proximity (6). An “interlocking site” hypothesis describing the binding of the anion and iron to Tf was proposed by Schlabach and Bates (5), in which the protein interacts with the carboxyl group of the anion, and the iron atom is bound to the proximal functional group of the anion. Other anions may also be synergistically bound to Tf, such as oxalate, malonate, and nitrilo-



triacetate (NTA) (5, 6). Citrate is not a synergistic anion (5, 230), although according to Aisen *et al.* (232)  $^{59}\text{Fe}$ -citrate is preferentially directed to the B-site.

The two binding sites of Tf are not totally independent of one another (6, 231, 232). It has been observed that the binding of an iron atom to one site causes a perturbation in the domain of the other site (231). The binding constants are affected: when one of either site is occupied, the binding constant for the other site is decreased (232).

The two binding sites of Tf are not equivalent in their binding characteristics. It is well established that the binding of iron to Tf is pH dependent (232, 235). At lower pH values (<7), the binding of iron preferentially occurs at the A-site, and at less than 50% iron saturation, essentially only this monoferric form exists (234, 235). The binding at the A-site is much stronger than the binding at the B-site, and if binding at the B-site does occur, it is sequential to the binding of the A-site (232). At physiological pH, the difference in binding strengths is not as great but the A-site is still labelled preferentially (232, 235). Thus, at the normal *in vivo* iron saturation of about 30%, it could be expected that most iron is bound to the A-site of Tf (235).

The sites also differ in their accessibility to different complexes of iron. When complexed to NTA, iron is preferentially bound to A-site. Ferric citrate, oxalate, ammonium sulfate, and chloride initially bind to the B-site, but will eventually be transferred to the A-site if there is an iron-complexing agent present to mediate the exchange (232). If ferric chloride is added to a neutral or alkaline solution of transferrin, the degree of specific binding is low, due to the formation of large polymeric complexes (236).

Citrate is able to mediate the exchange of iron between the two sites of iron, although the time required for this distribution is relatively long (232). There is little scrambling of iron observed at physiological (millimolar) concentration of citrate (235, 237).



The mechanisms involved in the release of iron from transferrin *in vivo* are poorly understood. Factors which could be involved include protonation, removal of the anion, reduction of iron, or a conformational change in the protein (226). Removal of iron by reduction would require the presence of a powerful reducing agent *in vivo*, as most reducing agents are unable to remove iron from Tf at physiological pH (238). Pyrophosphate compounds, notably ATP, have been shown to cause the release of iron from transferrin, and to stimulate the uptake of iron by isolated rat liver mitochondria. (239, 240).

The differences observed between the two binding sites of Tf has raised the question of possible differences in the physiological role of each site (227). Results of experiments on the ability of each site to donate iron to reticulocytes appear to differ with the species tested. Functional heterogeneity of the two sites has been demonstrated in *in vivo* experiments in rats, where one site preferentially donated iron to erythroid receptors, and the other preferentially donated iron to the liver and small intestine (241). Harris and Aisen (242) found that the two sites of human Tf were not equivalent in their donation of rabbit reticulocytes, but no difference was observed when rabbit Tf was tested with rabbit reticulocytes. Harris (243) later reported that the two sites of human Tf donated iron equally to human reticulocytes.

## 2. Binding of Gallium

Although it has been firmly established that gallium is bound to Tf *in vivo*, there has been little investigation into the biochemical aspects of this association. Clausen *et al.* (2) estimated the presence of 14 binding sites for gallium on each molecule of Tf, with an intrinsic relative association constant,  $K$ , of 1.772 l/mol. However, this data was obtained using fairly large quantities of gallium nitrate. Thermodynamic studies suggested that carrier-free  $^{67}\text{Ga}$ -citrate was bound to Tf in a colloidal form. Tomimatsu and Donovan (244) reported that two atoms of gallium are bound sequentially to one molecule of Tf, and that the second gallium atom is bound more weakly than the first. Larson *et al.* (245)





recently reported a value for  $K$  of  $2.5 \times 10^5$  l/mol to describe the binding of carrier-free  $^{67}\text{Ga}$ -citrate to human Tf.

### C. Cell-Surface Receptors

The interaction of Tf and cells has been studied most extensively using rabbit reticulocytes. The existence of a Tf-receptor on the cell membrane of reticulocytes has been proven by several investigators (247 – 251). Transferrin receptors on rat hepatocyte membranes have also been isolated (252, 253). Larson *et al.* (253) have recently isolated a Tf binding macromolecular component from the stroma of EMT-6 sarcoma cells.

The number of binding sites on the cell surface has been estimated to be approximately  $1 - 8 \times 10^5$  (246, 247, 250, 254). However, efforts to isolate the Tf-receptors from the reticulocyte cell membrane have produced conflicting results. Several different values of the molecular weight of the receptor have been reported, ranging from 108,000 to 350,000 (247 – 251).

The mechanisms involved in the cellular uptake of iron are not clearly understood. The first step involved is the adsorption of the iron-Tf to the cell surface receptors, followed by firmer bonding (227). Whether or not the iron-Tf complex actually enters the cell by endocytosis has not been proven, although there is supporting evidence for this theory (255). It has also been proposed that Tf releases the iron at the cell membrane whereupon it is transported by intracellular intermediates to sites of heme synthesis (246). Ferritin may be involved in iron uptake and intracellular iron transport (254, 256).



## EXPERIMENTAL



## I. MATERIALS

### A. Preparation Of Solutions

All chemicals and solvents used for the preliminary non-sterile experiments were of analytical grade. Deionized and glass distilled water was used to prepare all solutions.

The reagents and materials used in the preparation of  $^{67}\text{Ga}$ -transferrin for the clinical study are listed in Table V.

### B. Chromatographic Methods

The following chromatographic materials were used:

- 1) Dowex 1-X4, 100 – 200 mesh (Bio-Rad Laboratories, Richmond, California). The resin was allowed to swell overnight in distilled water, then washed and rinsed to remove any fine particles. The resin was resuspended in 8N HCl and was poured into a 0.7 x 2.5 cm column. The resin was packed and equilibrated by rinsing several times with 8N HCl.
- 2) Sephadex G-50, fine grade (Pharmacia Canada Ltd., Dorval, Quebec). The Sephadex gel was hydrated by boiling in distilled water for one hour. The gel was poured into a 0.9 x 17 cm column and packed by running several volumes of distilled water through the column. The gel was then equilibrated by running several volumes of the appropriate buffer through the column.

### C. Radioisotopes

- 1)  $^{67}\text{Ga}$ -citrate: New England Nuclear, North Billerica, Mass.; supplied in vials containing 122 MBq on assay date (1.65 ml).
- 2)  $^{59}\text{Fe}$ -citrate: Charles E. Frosst and Co., Montreal, Quebec; supplied in vials containing 1.85 MBq per 1.0 ml on assay date.
- 3)  $^{67}\text{Ga Cl}_3$ : Charles E. Frosst and Co., Montreal, Quebec, provided in a 0.1N solution of HCl with a specific activity of 111 – 222 MBq per 10-15  $\mu\text{l}$  of solution.



**TABLE V**  
**MATERIALS USED IN THE PREPARATION OF STERILE  $^{67}\text{Ga}$ -TRANSFERRIN**

Material or Reagent	Manufacturer	Specifications
Human apo-transferrin	Sigma Chemical Co. St. Louis, Missouri	Lot No. 96C-0107
HEPES* Buffer	Sigma Chemical Co. St. Louis, Missouri	Lot No. 107C-5060
Sodium Hydroxide (1N)	Anachemia Chemicals Ltd. Montreal, Quebec	Lot No. 750403
Sodium Bicarbonate	J.T. Baker Chemical Co., Phillipsburg, New Jersey	Lot No. 6137922
Water for Injection	Baxter Laboratories of Canada Malton, Ontario	Sterile, pyrogen-free Lot No. AP 13242
Sterile Saline	New England Nuclear North Billerica, Massachusetts	NEN Generator eluant vials
Millipore filters	Millipore Corporation Bedford, Massachusetts	0.22 $\mu$ , disposable
Minicon B15 Macrosolute Concentrators	Amicon Canada Ltd. Oakville, Ontario	5 ml capacity; 15,000 MW cut-off
Plastic Incubation vials	Beckman Instruments Fullerton, California	Poly QII 20 ml liquid scintillation vials
Sterile Vials	New England Nuclear North Billerica, Mass.	NEN generator eluate collection vials
Vacuum Blood Collection Tubes	Terumo Medical Corp. Elkton, Maryland	Red Top (plain) and green top (with heparin)
Needles and Syringes	Becton, Dickinson & Co. Mississauga, Ontario	

\* HEPES = N-2-hydroxyethylpiperazine – N<sup>1</sup>-2-ethane sulfonic acid





#### D. Animals

Ten male ICR mice each weighing approximately 20 g were used for the toxicity study. They were housed in two groups of five mice per cage, and were allowed free access to food (Purina Laboratory Animal Chow) and water throughout the course of the study.

#### E. Human Subjects

Ethics approval was requested and obtained from the Cross Cancer Institute to administer  $^{67}\text{Ga-Tf}$  to human volunteers. All volunteers were required to give informed consent to the study. Subjects chosen for the clinical study were four healthy adult males, aged 39 – 59 years and weighing 66 – 105 kg.



## II. METHODS

### A. Preparation Of Sterile Reagents

#### 1. Sterilization of Equipment

Glassware used for the aseptic preparation of reagents was prepared by washing twice in an automatic dishwasher, once with soap, and once without soap. The clean glassware was carefully rinsed with sterile, pyrogen-free water, covered immediately with aluminum foil, and oven-heated at 260° for one hour.

The plastic incubation vials were also washed twice, in a similar manner, followed by rinsing with sterile, pyrogen-free water. The vials were then autoclaved immediately for one hour at 121°C. The four inch stainless steel needles used to remove the concentrated solution from the Minicon macrosolute concentrators were sterilized by the same method.

#### 2. Preparation of Sterile Solutions

All manipulations other than weighing and pH adjustment were done in a laminar flow hood. After their preparation, all solutions were stored at 4°C until the results of sterility and pyrogen tests were known.

##### a. Preparation of 0.1M HEPES Buffer

- 1) HEPES buffer, 5.96 g, was weighed into a sterile 400 ml beaker.
- 2) Sterile, pyrogen-free water, 200 ml, was added.
- 3) The pH was adjusted to 7.4 with concentrated NaOH.
- 4) The solution volume was then adjusted to 250 ml with sterile, pyrogen-free water.
- 5) 5 ml aliquots of the solution were filtered through a 0.22  $\mu$  millipore filter into sterile, evacuated single dose containers.



#### b) Preparation of 0.1M NaHCO<sub>3</sub>

- 1) Sodium bicarbonate, 0.84 g, was weighed into a sterile 150 ml beaker.
- 2) Sterile, pyrogen-free water was added to a volume of 100 ml.
- 3) 2 ml aliquots of the solution were filtered through a 0.22  $\mu$  millipore filter into sterile, evacuated, single dose containers.

### 3. Quality Control

#### a. Sterility Tests

A total of eight "cold" preparations of Tf were made with sterile saline replacing the <sup>67</sup>Ga-citrate. Samples of each of the test solutions, and one vial each of the 0.1M HEPES buffer and 0.1M NaHCO<sub>3</sub> were sent to the Department of Microbiology, University of Alberta Hospital for sterility tests, using thioglycollate and soybean-casein digest. Samples were also sent to the Provincial Laboratory of Public Health for mycological studies.

#### b. Pyrogen Tests

Samples from the first four cold runs were pooled together (0.5 ml each) as were samples from the other four cold runs. These pooled samples, plus a 1.0 ml sample each of the 0.1M HEPES buffer and 0.1M NaHCO<sub>3</sub> solution, were sent to the Vancouver General Hospital for pyrogen testing.

#### c. Hepatitis B Antigen Test

A sample of Tf dissolved in HEPES buffer was sent to the Provincial Laboratory of Public Health to check for the presence of Hepatitis B surface antigen on the Tf.

#### d. Radionuclidic Purity

Confirmation of radionuclidic purity of the radioisotope solutions was established by analysis of the gamma-ray spectrums obtained from a NaI (Tl) detector and multi-channel analyzer.



## B. Preparation Of $^{67}\text{Ga}$ -transferrin

The following method of preparation of  $^{67}\text{Ga}$ -Tf was developed for clinical use, and was administered to the first three volunteer subjects.

- 1) Human apo-transferrin (13 mg) was dissolved in 3.0 ml of 0.1M HEPES buffer, and was allowed to hydrate for 30 minutes.
- 2) To remove any undissolved or colloidal impurities, the Tf solution was passed through a  $0.22\ \mu$  millipore filter into a sterile incubation vial.
- 3) 0.1M  $\text{NaHCO}_3$  (0.2 ml), and approximately 111 MBq of  $^{67}\text{Ga}$ -citrate ( $\sim 1.6$  ml), were added to the Tf solution, and the mixture was incubated for one hour at room temperature.
- 4) To remove unbound  $^{67}\text{Ga}$  from the  $^{67}\text{Ga}$ -Tf, the sample was placed in a chamber of a Minicon macrosolute concentrator, and concentrated to approximately 0.05 – 0.10 ml.
- 5) The  $^{67}\text{Ga}$ -Tf was recovered from the concentrator with 1.0 ml of sterile saline for final filtration. To prevent loss of labelled Tf onto the millipore filter, a pretreated filter was used for the final sterilization of the  $^{67}\text{Ga}$ -Tf. To pretreat the filter, 5 mg of Tf dissolved in 2.0 ml of sterile saline was passed through a  $0.22\ \mu$  millipore filter followed by 2 – 3 ml of sterile saline. The  $^{67}\text{Ga}$ -Tf solution was then passed through this filter into a sterile single dose container. The filter was rinsed with a further 2 ml of saline, giving a final volume of 3 ml of  $^{67}\text{Ga}$ -Tf in sterile saline for injection.

The  $^{67}\text{Ga}$ -Tf administered to the fourth subject was prepared by a modified procedure as follows:

- 1) The human apo-transferrin (13 mg), was dissolved in 3.0 ml of HEPES buffer, and filtered as previously described.
- 2) 0.1M  $\text{NaHCO}_3$  (0.2 ml), and approximately 88 MBq of  $^{67}\text{GaCl}_3$  ( $\sim 10\ \mu\text{l}$ ), was added to the Tf solution, and the mixture was incubated overnight. ( $\sim 18$  hours) at  $4^\circ\text{C}$ .
- 3) The sample was concentrated, recovered, and sterilized by filtration through a  $0.22\ \mu$  pretreated millipore filter as previously described.





### C. Toxicity Study

The addition of  $^{67}\text{Ga}$ -citrate to the transferrin solution was not felt to be a requirement in the acute toxicity study, as the safety of diagnostic doses of this radiopharmaceutical in humans has been well established.

The amount of Tf that would be administered to human subjects was not more than 10 mg. Thus, assuming a 50 kg patient, the usual adult dose would be approximately 0.2 mg/kg body weight. For the toxicity study performed on mice, a dose of 400 – 500 times that of the usual patient dose was desired. Therefore, a dose of 80 to 100 mg/kg, or 1.6 to 2.0 mg/20 g mouse, was required.

Transferrin (25 mg) was dissolved in 5 ml of 0.1M HEPES buffer and 0.5 ml of 0.1M  $\text{NaHCO}_3$ , and the mixture was incubated overnight at 4°C. The solution was concentrated to approximately 0.25 ml and collected from the concentrator with 1 ml of sterile saline. The Tf solution was passed through a 0.22  $\mu$  millipore filter, which was then rinsed with 1.5 ml of sterile saline. The final protein concentration was measured by UV absorption, and was determined to be 7.2 mg Tf/ml. Thus, the loss of Tf onto the millipore filter was 7 mg.

Each of five mice was injected with 0.25 ml of the Tf solution (1.8 mg of Tf), via a tail vein. The other five mice were injected with the same volume of sterile saline to act as a control. The test mice and control mice were housed separately, and were assigned different tail markings for ready identification.

The mice were observed for approximately 30 minutes for any initial adverse reactions to the injection. For the next three weeks the mice were weighed every one or two days and observed for any obvious physical or behavioral changes.



After the three week test period two mice from the test group and one mouse from the control group were sacrificed by cervical dislocation. The lungs, liver, and kidneys were removed, and sections of these tissues were preserved in a 10% formalin solution and sent to the Department of Pathology, Faculty of Medicine, for pathological examination. The weight-gain data was analyzed by a statistician at the Cross Cancer Institute.

#### D. Clinical Study

##### 1. Administration of Radioisotopes

The  $^{67}\text{Ga}$ -citrate,  $^{67}\text{Ga}$ -Tf and  $^{59}\text{Fe}$ -citrate were administered in the following sequence:

Subject 1 (U.T.):  $^{67}\text{Ga}$ -Tf (3.7 MBq) and  $^{59}\text{Fe}$ -citrate (185 KBq), followed by  $^{67}\text{Ga}$ -citrate (7.4 MBq) one month later.

Subject 2 (C.W.):  $^{67}\text{Ga}$ -Tf (7.4 MBq), followed by  $^{67}\text{Ga}$ -citrate (69 MBq) and  $^{59}\text{Fe}$ -citrate (185 KBq) one month later.

Subject 3 (B.L.):  $^{67}\text{Ga}$ -citrate (7.4 MBq); followed by  $^{67}\text{Ga}$ -Tf (7.4 MBq) and  $^{59}\text{Fe}$ -citrate (185 KBq) two months later.

Subject 4 (A.N.):  $^{67}\text{Ga}$ -citrate (7.4 MBq); followed by  $^{67}\text{Ga}$ -Tf (7.4 MBq) two months later.

Thus, each subject acted as his own control. The initial protocol called for the administration of 3.7 MBq of  $^{67}\text{Ga}$ . However, this was increased to 7.4 MBq after analysis of the results of the first experiment, due to the low count rates obtained. Subject C.W. was injected with a much larger dose of  $^{67}\text{Ga}$ -citrate than desired due to an error in dose calculation. There is no data for  $^{59}\text{Fe}$ -citrate in Subject A.N. due to the interstitial injection of this radioisotope. Another injection was not attempted because of the radiation dose provided by  $^{59}\text{Fe}$ -citrate.

An interval of at least one month between the administration of  $^{67}\text{Ga}$ -citrate and  $^{67}\text{Ga}$ -Tf was desired to minimize the possibility of residual  $^{67}\text{Ga}$  background radioactivity.



Subjects B.L. and A.N. had longer intervals between the administration of  $^{67}\text{Ga}$ -citrate and  $^{67}\text{Ga}$ -Tf because of other obligations.

A “butterfly”, or intermittent, infusion set was inserted into a vein in the antecubital fossa of the subject’s right arm for the administration of the radioisotopes. Another intermittent infusion set was inserted into a vein in the left arm for blood sample collection on the first day of the experiment. The  $^{59}\text{Fe}$ -citrate was injected first, followed by the  $^{67}\text{Ga}$ -citrate or  $^{67}\text{Ga}$ -Tf. The apparatus was then flushed with 5 ml of sterile saline to ensure that all the radioactivity had been administered. The exact time of administration was recorded.

## 2. Blood Sampling

### a. Collection of Samples:

A 10 ml sample of blood was collected in a red-topped vacutainer tube (no anticoagulant), before the administration of the radioisotopes, and then daily for the next nine days, for the determination of serum iron, transferrin, total iron-binding capacity (TIBC), and ferritin. These determinations were made by the Department of Laboratories at the University of Alberta Hospital.

For the initial experiments, blood samples were collected in green-topped vacutainer tubes (containing heparin) for the measurement of  $^{59}\text{Fe}$  and  $^{67}\text{Ga}$  radioactivity in whole blood, plasma, and RBC, at the following intervals: 0 – 2, 5, 10, 20, 30, 45, 60 and 90 minutes; 2, 4, 6, 9, and 14 hours after injection on the first day of the experiment. One sample was collected daily for the next nine days. Analysis of the early experiments showed that fewer early samples were required, and in the subsequent experiments, the first sample was collected 15 minutes after injection. The exact time of sample collection was recorded. The infusion set was flushed with a dilute solution of heparin in sterile saline after each sample was taken to prevent the formation of blood clots in the assembly.



b. Sample— Handling Techniques:

Immediately upon collection of the blood sample in the green-topped vacutainer tube, hematocrits were determined in quadruplicate, on an Adams Autocrit Centrifuge. Only one sample was used for hematocrit determination on the first day of the experiment.

A 2 ml aliquot of whole blood was transferred into a counting tube, with a sterile, disposable pipette, and the remainder of the sample was centrifuged (Beckman Model TJ-6 Centrifuge) at 2200 rpm for ten minutes. The plasma was carefully removed, the volume noted, and 2 ml was transferred into a counting tube. A volume of sterile saline equal to the volume of plasma removed was added to the sample to wash the red blood cells (RBC). The sample was inverted gently a few times and re-centrifuged. Two ml aliquots of the wash and RBC were transferred into counting tubes.

The blood in the red-topped vacutainer tube was allowed to clot, then centrifuged at approximately 2500 rpm for 25 – 30 minutes. The serum was transferred to another sterile vacutainer tube and stored at -20°C until sent to the University Hospital for analysis.

c. Determination of  $^{67}\text{Ga}$  and  $^{59}\text{Fe}$  Radioactivities:

i) Standards:

Dilutions of the injected solutions were made for the determination of the injected dose (in the units of counts per minute injected), and for the determination of  $^{59}\text{Fe}$  crossover into the  $^{67}\text{Ga}$  channel on the gamma spectrometer. A 0.1 ml aliquot of the injected solution was diluted to 1.0 ml with normal saline. Triplicate 0.010 ml samples were taken, and were diluted to 2.0 ml to preserve the counting geometry.

The injected dose (in cpm) was determined from the dilution factor of the standard, and the volume injected into the subject.





The standards, and all samples, were counted on a Picker-Pace 1 Dual Isotope multisample, well-crystal gamma spectrometer. To determine the contribution of  $^{59}\text{Fe}$  energy to the  $^{67}\text{Ga}$  counting window, Channel A was set to measure  $^{67}\text{Ga}$ , using a wide window for maximum count rate (1 mev range: 50 – 500 unit window), and Channel B was set to measure  $^{59}\text{Fe}$  (2 mev range: 250 – 750 unit window). Each set of standards was counted in each channel, corrected for background, and the ratio of  $^{59}\text{Fe}$  counts in Channel A to Channel B was calculated. There was no crossover of  $^{67}\text{Ga}$  counts into the  $^{59}\text{Fe}$  channel.

ii) Samples:

For the measurement of  $^{67}\text{Ga}$  radioactivity in the blood samples, one minute counts were collected in Channel A (50 – 500 kev). In the experiments that included  $^{59}\text{Fe}$ -citrate, the windows were set as for the crossover determination. Each set of samples prepared daily were counted on that day, along with the standards and background tubes. Each sample was counted twice. The time at which the samples were counted was recorded to allow decay corrections on the data; the time of the midpoint in sample counting was used to correct for physical decay.

For the measurement of  $^{59}\text{Fe}$  radioactivity in the blood samples, 15 minute counts were collected in Channel A (500 – 1500 kev window). Since the half-life of  $^{59}\text{Fe}$  is much longer than the time required to count the samples, all samples were counted at once.

### 3. Urine Sample Analysis

#### a. Sample Collection and Handling:

The subjects were requested to collect all urine up to 48 hours after the administration of the radioisotope(s). Plastic containers were provided for this purpose. The time of collection, and the volume of urine, were recorded. Aliquots of 2 ml were pipetted in duplicate into counting tubes.



b. Determination of  $^{67}\text{Ga}$  and  $^{59}\text{Fe}$  Radioactivities:

The urine samples were counted along with the blood samples. Thus, the same counting parameters were applied.

4. In Vivo Distribution Measurements

a. Instrumentation:

Two multichannel analyzer systems and three collimated 3" x 3" NaI(Tl) crystals were used initially. Later in the study the third probe (Probe C) was eliminated due to technical problems and only one multichannel analyzer system was required. The systems were calibrated for the detection and measurement of  $^{67}\text{Ga}$  and  $^{59}\text{Fe}$ , and were frequently recalibrated throughout the study.

To determine the crossover of  $^{59}\text{Fe}$  energy into the  $^{67}\text{Ga}$  channel, and vice versa, two large plastic bottles were filled with water and about 10 KBq of  $^{59}\text{Fe}$ -citrate was added to one bottle; about 10 KBq of  $^{67}\text{Ga}$ -citrate was similarly added to the other bottle. Counts per 20 second channel were collected in the time-scale mode for several minutes with each isotope for all probes. Background counts were also collected. The ratio of  $^{59}\text{Fe}$  counts in the  $^{67}\text{Ga}$  channel to the counts in the  $^{59}\text{Fe}$  channel were calculated. Gallium-67 did not contribute any counts to the  $^{59}\text{Fe}$  channel.

b. Standards:

A standard was prepared on the first day of each experiment to correct for the physical decay of the radioisotopes and instrumental drift. A strip of chromatographic paper was taped to a block of wood upon which was outlined the shape of the probe in order to maintain geometry. The paper was spotted with a drop of the radioactive solution(s) that were being injected, and was allowed to dry in air. The standard was counted daily for five minutes under each probe. Background counts were also recorded daily.



### c. Collection of Data:

The subject was positioned in the supine position on the stretcher approximately 45 minutes after injection. Probe A was positioned over the area of the liver, and Probe B was positioned over the area of the heart. The position of the probes on the patient's skin was marked with a felt-tipped marking pen to preserve the geometry of counting in the daily measurements. Counts per 20 second channel were collected for each isotope with both probes for ten minutes. The subject was then positioned in the prone position, with Probe A placed over the area of the spleen and Probe B over the area of the sacrum. When Probe C was operational, it was placed over the knee cap when the subject was in the supine position, and counts were collected for ten minutes. Later in the study, Probe A was used to measure the radioactivity over the knee cap, before the spleen and sacrum measurements were made.

The collection of counts over the various organs was performed daily for ten consecutive days.

## 5. Data Analysis

### a. Blood Data:

The values of whole blood volume, plasma volume, and red blood cell volume for each subject was calculated on the basis of height and weight (263). All standard counts and blood sample counts (whole blood, plasma plus wash, and RBC) were corrected for background, crossover of  $^{59}\text{Fe}$  into the  $^{67}\text{Ga}$  channel (when applicable), and physical decay of  $^{67}\text{Ga}$  and  $^{59}\text{Fe}$ , by a computer program on a digital PDP-8L mini-computer (see Appendix B).

The mean count rate of the standards was multiplied by the dilution factor to determine the exact amount of radioactivity injected into the subject. The count rate for each 2 ml of whole blood was calculated to determine the fraction of injected dose present in the whole blood in each sample.



The concentration-time curves of  $^{67}\text{Ga}$ -citrate,  $^{67}\text{Ga}$ -Tf and  $^{59}\text{Fe}$ -citrate in the whole blood and plasma were subjected to curve-fitting using the computer programs AUTOAN and NONLIN, which were made available and analyzed by a pharmacokinetics expert. AUTOAN is a curve-stripping program that fits the data to the best estimate of the number of exponential components, giving the number of data points in each phase and the initial estimates of the model parameters. The NONLIN program requires the original data, plus the initial estimates of the parameters from the AUTOAN program. The NONLIN program gives a better estimate of the parameters of the concentration-time curve, by minimizing the sum of squared weighted deviations and the randomness of the data points. \*

On the basis of the number of exponentials that best fit the concentration-time curves, the simplest pharmacokinetic model was chosen to compare  $^{67}\text{Ga}$ -citrate,  $^{67}\text{Ga}$ -Tf, and  $^{59}\text{Fe}$ -citrate. A programmable Hewlett-Packard calculator was used to compute the various pharmacokinetic parameters for each of the three radiopharmaceuticals tested.

#### b. Urine Data:

The urine samples were corrected for background, crossover of  $^{59}\text{Fe}$  into the  $^{67}\text{Ga}$  channel (when applicable), and physical decay by the same computer program used for the blood samples. The fraction of the injected dose in each urine sample for  $^{67}\text{Ga}$ -citrate,  $^{67}\text{Ga}$ -Tf, and  $^{59}\text{Fe}$ -citrate, was calculated by multiplying the corrected count rate per unit volume of the sample by the total volume of urine voided at that time, and dividing it by the activity of the injected dose.

#### c. *In Vivo* Distribution:

The data for the *in vivo* distribution of  $^{67}\text{Ga}$ -citrate,  $^{67}\text{Ga}$ -Tf, and  $^{59}\text{Fe}$ -citrate was

\* Dr. P.K. Ng, Faculty of Pharmacy and Pharmaceutical Sciences, The University of Alberta, Edmonton, Alberta: personal communication





subjected to the following calculations:

- 1) The  $^{67}\text{Ga}$  and  $^{59}\text{Fe}$  counts per 20-second channel were averaged for the background, standard, and organ region of interest measurements.
- 2) The average counts collected over the liver, heart, spleen, sacrum and knee were corrected for background, as were the standard counts.
- 3) When applicable, crossover corrections were made as follows:  $^{67}\text{Ga}$  counts in  $^{67}\text{Ga}$  channel – ( $^{59}\text{Fe}$  counts in  $^{59}\text{Fe}$  channel x crossover of  $^{59}\text{Fe}$  counts into  $^{67}\text{Ga}$  channel as calculated earlier).
- 4) “Correction factors” were calculated for each probe from the standard probe counts for each isotope according to the following equation:

$$\text{Correction Factor} = \frac{\text{Standard Probe Counts on Day 0}}{\text{Standard Probe Counts on Subsequent Days.}}$$

- 5) Each of the organ count rates were multiplied by the correction factor of the probe used for that organ to correct for physical decay and instrumental drift.
- 6) The data of Day 0 was arbitrarily chosen to be 100%, and subsequent observations were corrected accordingly.
- 7) Finally, the relative radioactivity present in each organ was corrected for the radioactivity present in the whole blood at the time of the probe count collection. This was done to minimize the factor of organ vascularity in the determination of tissue uptake. The radioactivity in the whole blood at the time of the probe-count collection on the first day of the experiment was taken as 100%, and the radioactivity present on subsequent days was compared to this value.



## RESULTS AND DISCUSSION



## I. TOXICITY OF TRANSFERRIN IN MICE

No initial adverse reactions to the administration of the Tf solution or sterile saline were noted. For the duration of the study all animals appeared healthy and alert.

Regression analysis of the observed data revealed no significant difference between the test and control mice in the slopes of the weight gain curves, as given in Table VI. Pathological analysis of lung, liver and kidney tissues revealed no significant abnormalities by light microscopy in either group.

The administration of a single dose of 90 mg Tf/kg in mice, approximately 450 times the desired human dose of apo-transferrin, was found to be non-toxic in this study. Therefore, it was decided that the Tf could be used in humans with precautions taken to avoid possible anaphylactic reactions to the protein.

TABLE VI

### REGRESSION ANALYSIS OF THE WEIGHT GAIN VERSUS TIME IN TREATED AND CONTROL MICE

	Treated Group	Control Group
Intercept	18.754	20.279
Slope	0.5681	0.6024
Degrees of Freedom	13	13

$t = 0.2415$  with 26 D.F.

$p < 0.05$  when  $t = 2.16$



## II. PREPARATION OF $^{67}\text{Ga}$ -TRANSFERRIN

### A. Initial Labelling Experiments With $^{67}\text{Ga}$ -chloride

It was desirable to develop a method of preparation of  $^{67}\text{Ga}$ -Tf for use in clinical investigations that involved a minimum number of reagents and steps: 1) to reduce the possibility of bacterial or pyrogenic contamination, and; 2) to reduce the time involved in manipulation of radioactive material, thereby maintaining minimal radiation exposure.

Several attempts were made to prepare  $^{67}\text{Ga}$ -Tf by the method described by Noujaim and co-workers (119). This technique employed the use of nitrilotriacetic acid to direct the  $^{67}\text{Ga}$  to the specific metal-binding sites of Tf, particularly to the C-terminal site (A-site) as described by Aisen and co-workers (232) for the labelling of Tf with iron.

The  $^{67}\text{Ga}$ -citrate (7.4 – 18.5 MBq) was acidified with a three-fold volume of 8N HCl. This solution was applied to a 0.7 x 2.5 cm Dowex 1–X4 ion-exchange resin previously equilibrated with 8N HCl, which bound the gallium as  $^{67}\text{GaCl}_4^-$ . The column was rinsed with 2 – 3 ml of 8N HCl to remove any free citrate. The  $^{67}\text{Ga}$  was eluted from the column as  $^{67}\text{GaCl}_3$  with approximately 3 ml of 0.1N HCl. The first 1.1 ml of the eluate contained no radioactivity and was discarded. The  $^{67}\text{GaCl}_3$  solution was incubated with 25  $\mu\text{l}$  of 1  $\mu\text{M}$  NTA solution (a 2 – 3 times molar excess of NTA-to- $^{67}\text{Ga}$ ) for approximately 30 minutes to complex the  $^{67}\text{Ga}$  to the NTA. The pH was adjusted to pH 2 with concentrated NaOH, and then to  $\sim$  pH 7 with 0.1N NaOH. The Tf solution, containing 2 – 5 mg of protein in 1.0 ml of 0.05 M HEPES/0.1M KCl buffer, was added when the pH of the  $^{67}\text{Ga}$  solution was greater than 5, as at low pH Tf does not bind metal ions (233). The choice of HEPES buffer was based on the report by Glickson and co-workers (258), which demonstrated the lack of complex formation between this buffer and  $^{67}\text{Ga}$ . The desired pH of 7.4 was achieved by addition of 0.2 – 0.3 ml of 0.1M  $\text{NaHCO}_3$ , and more 0.1N NaOH if required. The  $^{67}\text{Ga}$ -Tf was allowed to incubate overnight (approximately 18





hours) at 4°C. The separation of free  $^{67}\text{Ga}$  from  $^{67}\text{Ga-Tf}$  was done by Sephadex G-50 chromatography.

By this method the usual percentage of  $^{67}\text{Ga}$  bound to the Tf was approximately 25%, ( $n = 20$ ), which was unacceptable for the proposed clinical studies. The major problem encountered with this labelling technique was the pH adjustment. It was easy to overshoot the desired pH of 7.4 when adding the concentrated and 0.1N NaOH, which resulted in a poorly labelled product. This was possibly due to the formation of some  $^{67}\text{Ga}$ -hydroxides or gallates, thereby rendering the  $^{67}\text{Ga}$  unavailable for binding to the Tf.

## **B. Labelling Experiments With $^{67}\text{Ga}$ -citrate**

### **1. Initial Labelling Experiments**

The direct incubation approach was tried whereby the desired activity of  $^{67}\text{Ga}$ -citrate (7.4 – 18.5 MBq) was mixed with 100  $\mu\text{l}$  of 0.1M  $\text{NaHCO}_3$  and 2 – 5 mg of Tf dissolved in 1.0 ml of 0.05 M HEPES/0.1M KCl buffer. This solution was incubated for approximately 18 hours at 4°C, and the  $^{67}\text{Ga-Tf}$  was separated from unbound  $^{67}\text{Ga}$  by Sephadex G-50 chromatography. With this method the amount of  $^{67}\text{Ga}$  bound to Tf was greater than 50%, ranging between 50% and 70% ( $n = 9$ ).

### **2. Scaled-up Procedure**

The desired objective was to label 10 mg of Tf with 111 MBq of  $^{67}\text{Ga}$ , the usual adult dose of  $^{67}\text{Ga}$ -citrate. Since the total amount of Tf in a normal adult is 200 – 400 mg/100 ml of blood (257), the administration of only 10 mg of Tf allowed a great margin of safety.

The scaled-up labelling procedure was attempted as follows: 111 MBq of  $^{67}\text{Ga}$ -citrate (in 1.65 ml) was mixed with 0.2 ml of 0.1M  $\text{NaHCO}_3$  and 10 mg of Tf dissolved in 2.0 ml of 0.05 M HEPES/0.1M KCl buffer (pH 7.4), and was allowed to incubate for approximately 18 hours at 4°C. The labelling yield (between 40 – 60%,  $n = 6$ ) of the scaled-up



method was consistently lower than previously obtained with smaller amounts of  $^{67}\text{Ga}$ -citrate.

An attempt was made to improve the labelling yield by increasing the buffer strength. Increasing the concentration of HEPES buffer to 0.1 molar, and deleting the KCl, slightly increased the percentage of  $^{67}\text{Ga}$  bound to Tf when small amounts of  $^{67}\text{Ga}$ -citrate were used ( $n = 4$ ). However, when more than 37 MBq of  $^{67}\text{Ga}$ -citrate was used there was no observable difference in the amount of  $^{67}\text{Ga}$  bound by Tf in either 0.05M HEPES/0.1 KCl or 0.1M HEPES buffers. Thus, in order to simplify the preparation of sterile  $^{67}\text{Ga}$ -Tf, the 0.1M HEPES buffer, pH 7.4 was used.

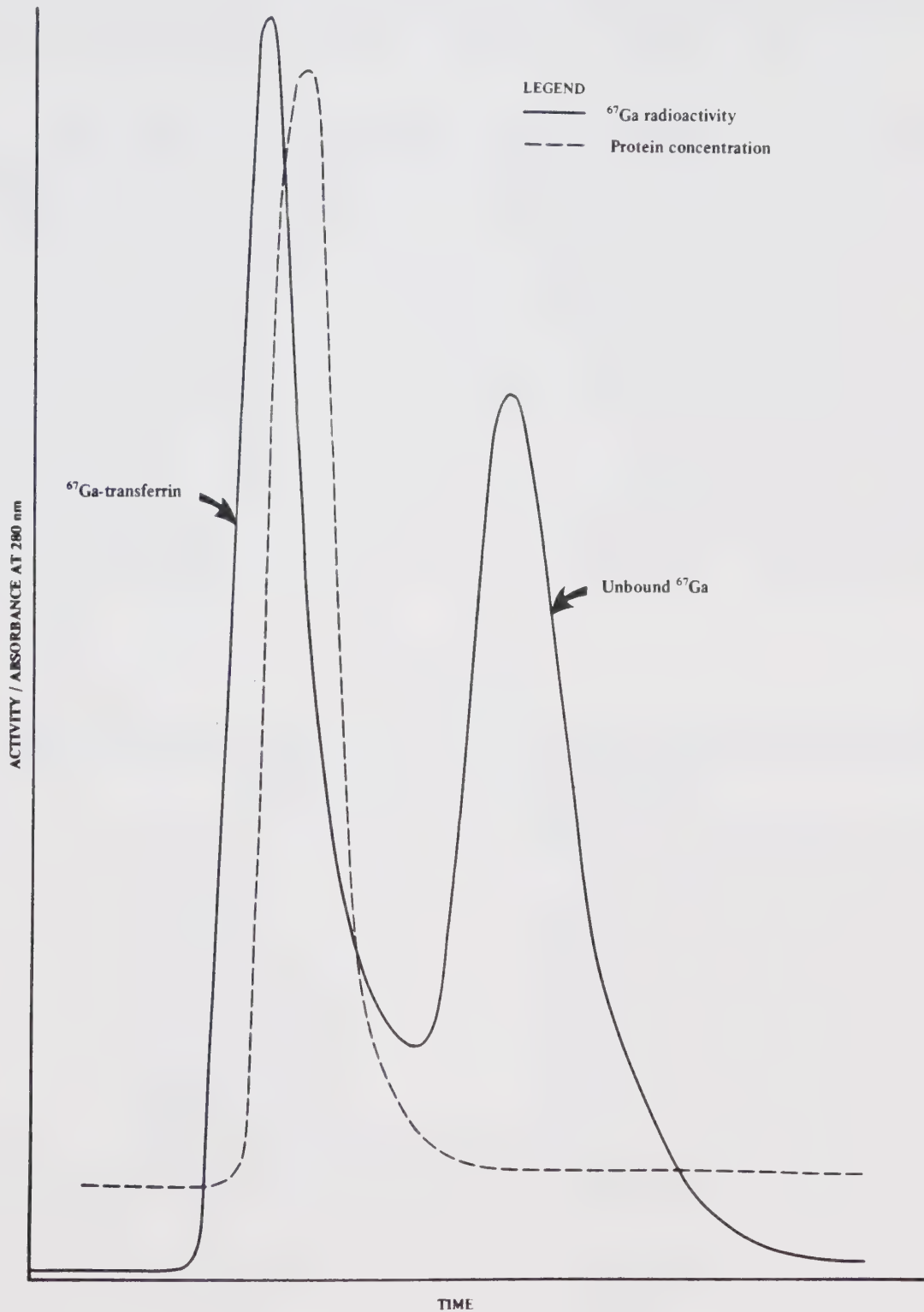
The effects of incubation time and temperature were studied. There was no difference in labelling yield when the  $^{67}\text{Ga}$ -Tf solution was incubated at  $4^{\circ}\text{C}$  or  $20^{\circ}\text{C}$  for 18 hours ( $n = 2$ ). An incubation time of one hour at  $20^{\circ}\text{C}$  was found to result in a labelling yield (approximately 65%) similar to that of the overnight incubation method ( $n = 2$ ). Therefore the most convenient method, incubation for one hour at room temperature, was adopted.

### C. Separation Techniques

Initially, gel chromatography was used to separate the  $^{67}\text{Ga}$  bound to Tf from any free  $^{67}\text{Ga}$  remaining in the incubation mixture. The preparation of the column was described previously. The eluate from the column was passed through a UV detector (Duo-monitor) and in front of a shielded sodium iodide detector. The output signal of both was connected to a dual-pen recorder. By this method, both protein concentration and  $^{67}\text{Ga}$  radioactivity were monitored almost simultaneously. The column had a void volume of approximately 5 ml. The  $^{67}\text{Ga}$ -Tf was eluted from the column first, with an elution time of about six minutes. Free  $^{67}\text{Ga}$  appeared in the eluate at about 14 minutes. Figure 1. shows an example of the elution profile.

The gel chromatography procedure was satisfactory for the separation of the bound



FIGURE 1: Elution profile of  $^{67}\text{Ga}$ -transferrin

The separation of  $^{67}\text{Ga}$ -Tf and unbound  $^{67}\text{Ga}$  by Sephadex G-50 chromatography, monitored by a NaI detector and U.V. monitor.



and free  $^{67}\text{Ga}$  for samples of small volume (between 50 – 70% recovery of  $^{67}\text{Ga-Tf}$ ). However, when the labelling procedure was scaled up, the incubation mixture was too large a volume for a good separation (between 40 – 60% recovery of  $^{67}\text{Ga-Tf}$ ). Also, the elution volume was greater than 5 ml which was undesirable for an injectable product.

The removal of unbound  $^{67}\text{Ga}$  from  $^{67}\text{Ga-Tf}$  was accomplished by concentrating the incubation mixture in a Minicon B15 Macrosolute Concentrator. The concentrator consisted of ten separate chambers. One wall of the chamber was made of clear plastic so that the concentration process could be easily monitored. The back of the chamber was a membrane filter with a molecular weight cut-off of 15,000 MW, which was backed with an absorbent layer. Concentration was achieved by a strictly physical process whereby the solvent and any compounds with a molecular weight of less than 15,000 were drawn into the absorbent layer, leaving the  $^{67}\text{Ga-Tf}$  in the chamber. Experiments using  $^{67}\text{Ga-citrate}$  in HEPES buffer (no protein added) showed that the amount of radioactivity removed from the chamber was indeed a function of the degree of concentration, as shown in Table VII.

**TABLE VII**  
**THE REMOVAL OF  $^{67}\text{Ga}$  IN SOLUTION BY CONCENTRATION IN THE MINICON**  
**B15 MACROSOLUTE CONCENTRATOR**

	Run 1	Run 2
Initial Volume	1.0 ml	1.0 ml
Final Volume	0.03 ml	0.05 ml
Degree of Concentration	<u>33X</u>	<u>20X</u>
Initial Radioactivity	4.6 MBq	3.5 MBq
Final Radioactivity	0.13 MBq	0.15 MBq
Degree of Concentration	<u>36X</u>	<u>24X</u>





Measurements of protein concentration by ultraviolet spectroscopy (Unicam SP 1800 Ultraviolet Spectrophotometer) before and after concentration of 10 mg of Tf revealed that essentially no protein was lost in the concentration chamber ( $n = 2$ ).

Experiments comparing the separation of bound  $^{67}\text{Ga}$ -Tf from free  $^{67}\text{Ga}$  using Sephadex G-50 chromatography and the Minicon concentrators showed that the two systems gave similar results: Sephadex G-50,  $61.5 \pm 12.3\%$  recovery; Minicon concentrators,  $62.7 \pm 10.6\%$  recovery ( $n = 6$ ). The advantages of the Minicon concentrators were: 1) simplicity of use; 2) volumes of up to 5 ml could be placed in the chamber, which could be concentrated to 50  $\mu\text{l}$  or less; 3) the final  $^{67}\text{Ga}$ -Tf concentrate could be diluted to the volume desired.

An experiment employing ascending paper chromatography, based on the report by Kulprathipanja and Hnatowich (17), was undertaken to evaluate the binding of  $^{67}\text{Ga}$  to Tf and the effectiveness of the Minicon concentrators in removing unbound  $^{67}\text{Ga}$ . The solvent system for the chromatography was a pyridine: ethanol: water (1:2:4) mixture, with the pH adjusted to 6.8 with 1N HCl. Whatman No. 1 paper chromatography strips (2.5 cm x 15 cm) were spotted 1 cm from the bottom with: 1) pre-concentrated  $^{67}\text{Ga}$ -Tf Solution; 2) post-concentrated  $^{67}\text{Ga}$ -Tf solution; 3)  $^{67}\text{Ga}$ -citrate; and, 4)  $^{67}\text{Ga}$ -citrate in HEPES buffer. The strips were developed in the solvent, then dried and cut into 1 cm strips starting  $\frac{1}{2}$  cm below the origin. The samples were measured for  $^{67}\text{Ga}$  radioactivity in a multisample well-type gamma spectrometer (Nuclear Chicago 1185, 50 – 120 kev, one minute counts).

Using this solvent system, the Tf stayed at the origin. The  $^{67}\text{Ga}$ -citrate appeared at an Rf value of 0.7, although there was also a small amount of  $^{67}\text{Ga}$  that remained at the origin. In HEPES buffer, the  $^{67}\text{Ga}$ -citrate was smeared from the origin to Rf 0.7. Before concentration of the incubation mixture, there was a large proportion of the radioactivity that corresponded to free  $^{67}\text{Ga}$ -citrate. After concentration, all the  $^{67}\text{Ga}$  radioactivity was observed at the origin, presumably associated with the Tf. The chromatograms are depicted



graphically in Figure 2.

Thus, due to effective separation of bound  $^{67}\text{Ga}$  from unbound  $^{67}\text{Ga}$  by the Minicon concentrators, this method was chosen for the separation of  $^{67}\text{Ga}$ -Tf for the clinical study.

#### D. Sterile Preparation of $^{67}\text{Ga}$ -transferrin by the Incubation Method

##### 1. Reagents

Both the 0.1M HEPES buffer and 0.1M  $\text{NaHCO}_3$  solutions were reported to be sterile and pyrogen-free. Samples of “cold” runs were also found to be sterile and free of pyrogens. The Tf was found to be negative for Hepatitis B antigen. The commercially obtained  $^{67}\text{Ga}$ -citrate was obtained sterile and pyrogen-free.

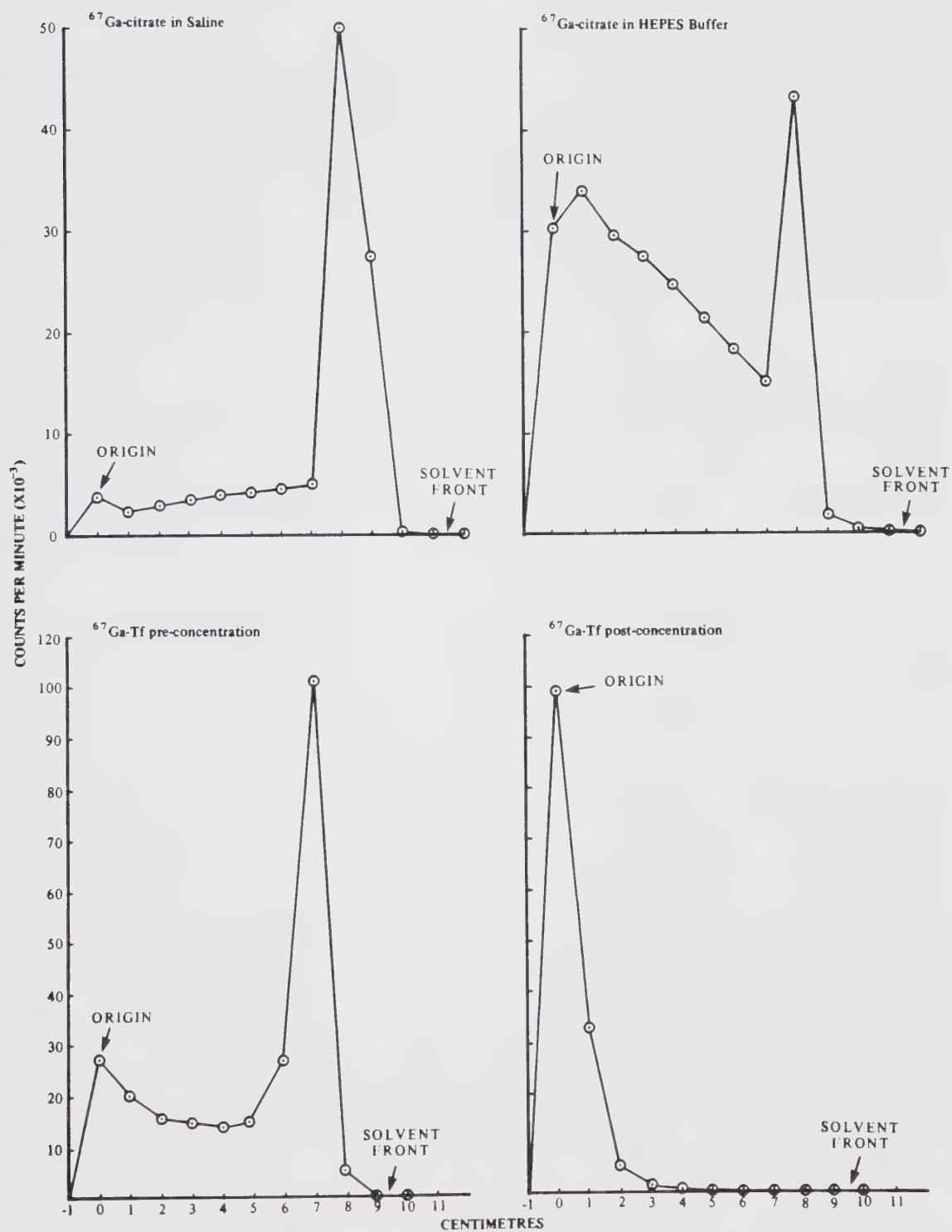
##### 2. Preparation Technique

A detailed discussion of the preparation of  $^{67}\text{Ga}$ -Tf used in the clinical investigation was described previously under “Methods”. The Tf was incubated with the buffer for 20 – 30 minutes before addition of the  $^{67}\text{Ga}$ -citrate to allow hydration of the protein. To ensure that there was no undissolved material or colloidal impurities in the incubation mixture, the Tf solution was passed through a  $0.22\ \mu$  millipore filter into a sterile incubation vial. Measurements of protein concentration by UV spectrometry before and after filtration revealed that a significant amount of Tf (from 10 – 30%) was lost by adsorption onto the millipore filter. Thus, to obtain a filtrate containing approximately 10 mg of Tf in 2 ml of buffer, the initial Tf solution consisted of 13 mg of Tf in 3.0 ml of 0.1M HEPES buffer. The filter was not rinsed. The sterile 0.1M  $\text{NaHCO}_3$  (0.2 ml) and  $^{67}\text{Ga}$ -citrate (111 MBq) were added to the sterile Tf solution, and the mixture was incubated for one hour at room temperature. The  $^{67}\text{Ga}$ -Tf was separated from the free  $^{67}\text{Ga}$  as previously described.

To ensure sterility of the labelled product, a final step of cold sterilization by



FIGURE 2: Paper chromatography of  $^{67}\text{Ga}$  solutions in pyridine:ethanol:water (1:2:4), pH6.8





filtration through a 0.22  $\mu$  millipore filter was added. The filter was “pretreated” by passing a 2 ml solution of unlabelled Tf (5 mg) in sterile saline through the filter, followed by rinsing with sterile saline. Using this technique, the loss of  $^{67}\text{Ga}$ -Tf on the filter was less than 10%.

#### **E. Final Experiments With $^{67}\text{Ga}$ -chloride**

Near the conclusion of the clinical study, no-carrier-added  $^{67}\text{GaCl}_3$  became available commercially from Charles E. Frosst and Company. Between 111 and 222 MBq of  $^{67}\text{GaCl}_3$  were received in 10 – 15  $\mu\text{l}$  of 0.1N HCl. Trial labelling experiments using 7.4 MBq of  $^{67}\text{GaCl}_3$  with 2 mg of Tf in 1 ml of buffer and 0.1 ml of 0.1M  $\text{NaHCO}_3$  showed consistent labelling of the Tf with  $^{67}\text{Ga}$  of greater than 90% ( $93.4 \pm 2.3\%$ ,  $n = 5$ ).

When the reaction was scaled up to 90 MBq and 13 mg of Tf, using the incubation method described for  $^{67}\text{Ga}$ -citrate, the percentage of  $^{67}\text{Ga}$  bound by the Tf was approximately 90%. Thus, the final clinical experiment with  $^{67}\text{Ga}$ -Tf was performed using the  $^{67}\text{GaCl}_3$  method.





### III. CLINICAL COMPARISON OF $^{67}\text{Ga}$ -CITRATE, $^{67}\text{Ga}$ -TRANSFERRIN, AND $^{59}\text{Fe}$ -CITRATE

#### A. Pharmacokinetics

##### 1. Pharmacokinetic Methods

The amounts of  $^{67}\text{Ga}$ -citrate,  $^{67}\text{Ga}$ -Tf, and  $^{59}\text{Fe}$ -citrate radioactivity in the plasma, red blood cells and whole blood versus time after intravenous injection for each subject are presented in Appendix C. Blood biochemistry data (serum iron, total iron binding capacity, transferrin and ferritin levels) for each subject are presented in Appendix D.

Analysis of the plasma radioactivity data by AUTOAN and NONLIN showed that the plasma concentration-time data for  $^{67}\text{Ga}$ -citrate and  $^{67}\text{Ga}$ -Tf were best described by a three exponential equation:

$$C_p = A_1 e^{-\lambda_1 t} + A_2 e^{-\lambda_2 t} + A_3 e^{-\lambda_3 t}$$

where  $C_p$  is plasma concentration;  $A_1$ ,  $A_2$  and  $A_3$  are pre-exponential coefficients,  $\lambda_1$ ,  $\lambda_2$  and  $\lambda_3$  are exponential coefficients, and  $t$  is time after intravenous injection. Similar results were reported by Larson (259) and Clausen and co-workers (2) for  $^{67}\text{Ga}$ -citrate.

The plasma concentration-time curves for  $^{59}\text{Fe}$ -citrate were best described by a two-exponential equation:

$$C_p = A_1 e^{-\lambda_1 t} + A_2 e^{-\lambda_2 t}$$

Plasma radioiron disappearance has been described as a three-exponential function when plasma radioactivity was measured up to 14 days after administration of  $^{59}\text{Fe}$ -citrate (223, 224). However, in this study the plasma  $^{59}\text{Fe}$  radioactivity was close to background activity



within 12 hours after injection and therefore the fluctuating count rates were subject to large statistical errors. The fluctuation of  $^{59}\text{Fe}$  radioactivity in the plasma samples past 12 hours after injection was possibly due to the small amount of iron that is recirculated into the plasma from Tf in the extracellular fluid, and from the destruction of red blood cells containing  $^{59}\text{Fe}$  (224). Even slight hemolysis of blood samples would add significant error into the plasma  $^{59}\text{Fe}$  measurements.

Conventionally, if a biexponential equation describes the plasma disappearance curve, a two-compartment model is chosen to describe the distribution of the drug; if a triexponential equation describes the curve, a three-compartment model is chosen (260). The compartments cannot be designated to any particular anatomical or physiological component, but rather describe areas of the body that appear to have similar rates of equilibration (260, 261). In cases where the disposition of a drug is not known extensively it is recommended to use the simplest model to describe the observed data (262). For example, elimination may occur from the peripheral compartments, the central compartments, or both. Usually, it is not possible to determine where elimination is occurring from plasma-concentration data. However, because most drugs are metabolized and excreted by the liver and kidney and these organs are highly perfused, it is generally assumed that elimination is occurring from the central compartment (260). Thus, the model chosen to describe the plasma concentration-time data of  $^{67}\text{Ga}$ -citrate and  $^{67}\text{Ga}$ -Tf is a three-compartment open model with elimination occurring from the central compartment (Fig. 3). A two-compartment open model with elimination from the central compartment was chosen to describe  $^{59}\text{Fe}$ -citrate plasma concentration as a function of time (Fig. 4).

Figures 5, 6 and 7 show the typical concentration-time plots of the plasma  $^{67}\text{Ga}$  and  $^{59}\text{Fe}$  radioactivity following an intravenous injection of  $^{67}\text{Ga}$ -citrate,  $^{67}\text{Ga}$ -transferrin, and  $^{59}\text{Fe}$ -citrate, respectively, in one subject (C.W.). The percent of the total dose of  $^{67}\text{Ga}$  and  $^{59}\text{Fe}$  in each compartment after administration of  $^{67}\text{Ga}$ -citrate,  $^{67}\text{Ga}$ -Tf, and  $^{59}\text{Fe}$ -citrate in the same subject as a function of time is shown in Figures 8, 9 and 10 respectively.



FIGURE 3: Three-compartment open model for  $^{67}\text{Ga}$ -citrate and  $^{67}\text{Ga}$ -transferrin in humans

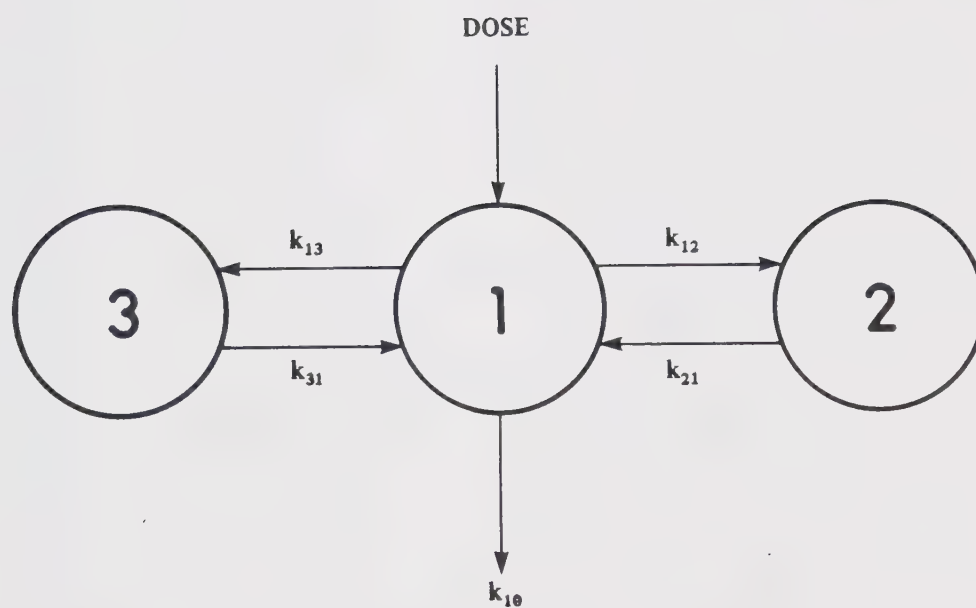




FIGURE 4: Two-compartment open model for  $^{59}\text{Fe}$ -citrate in humans

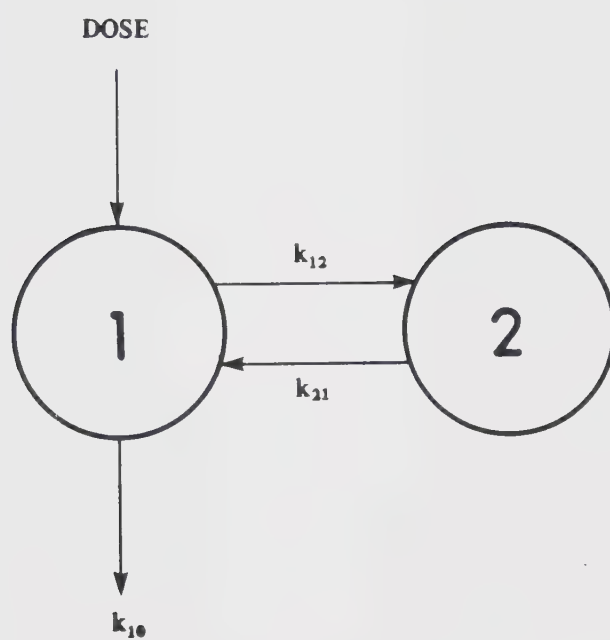






FIGURE 5: Plasma disappearance of  $^{67}\text{Ga}$ -citrate in one subject





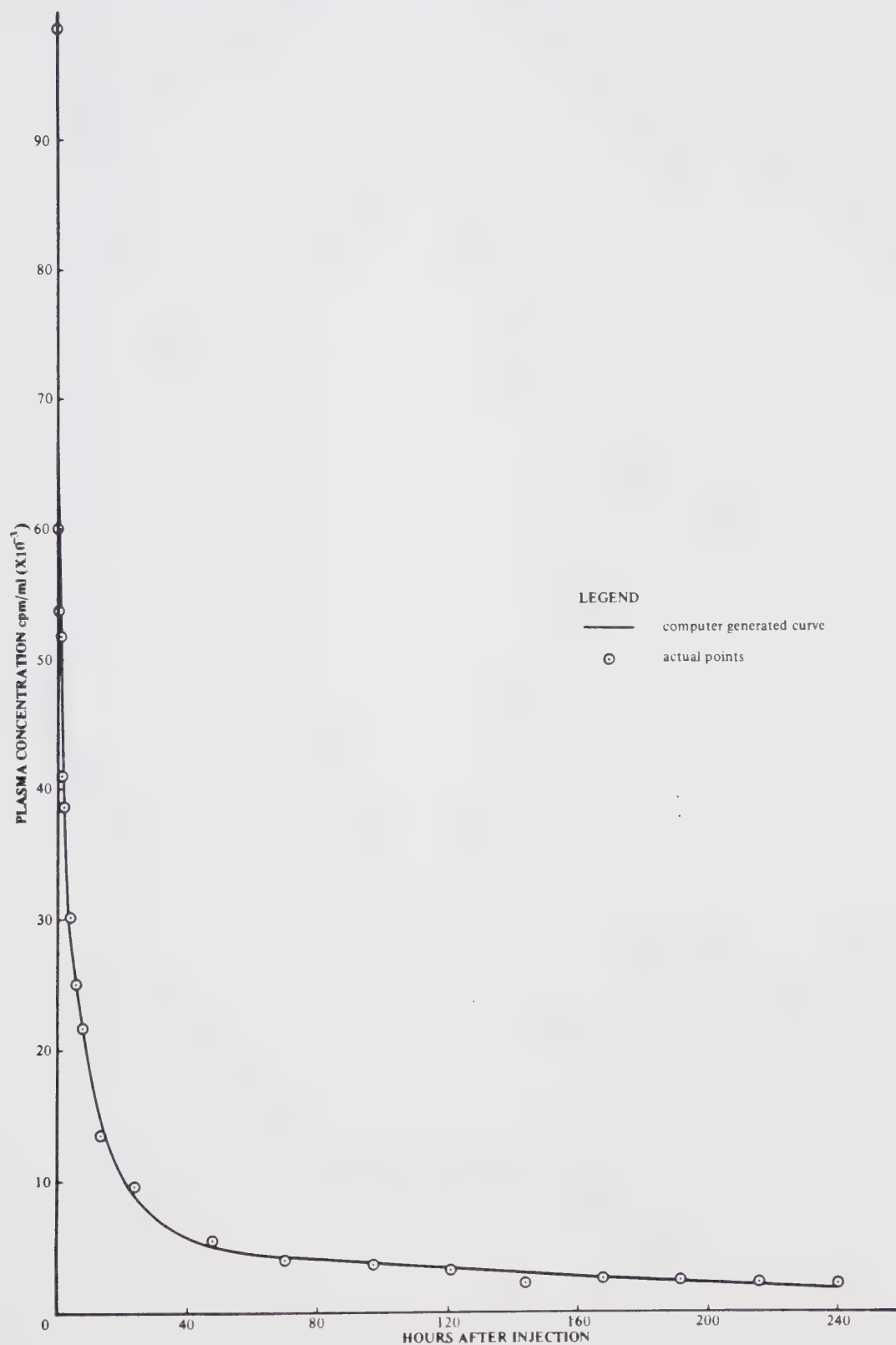
FIGURE 6: Plasma disappearance of  $^{67}\text{Ga}$ -transferrin in one subject



FIGURE 7: Plasma disappearance of  $^{59}\text{Fe}$ -citrate in one subject

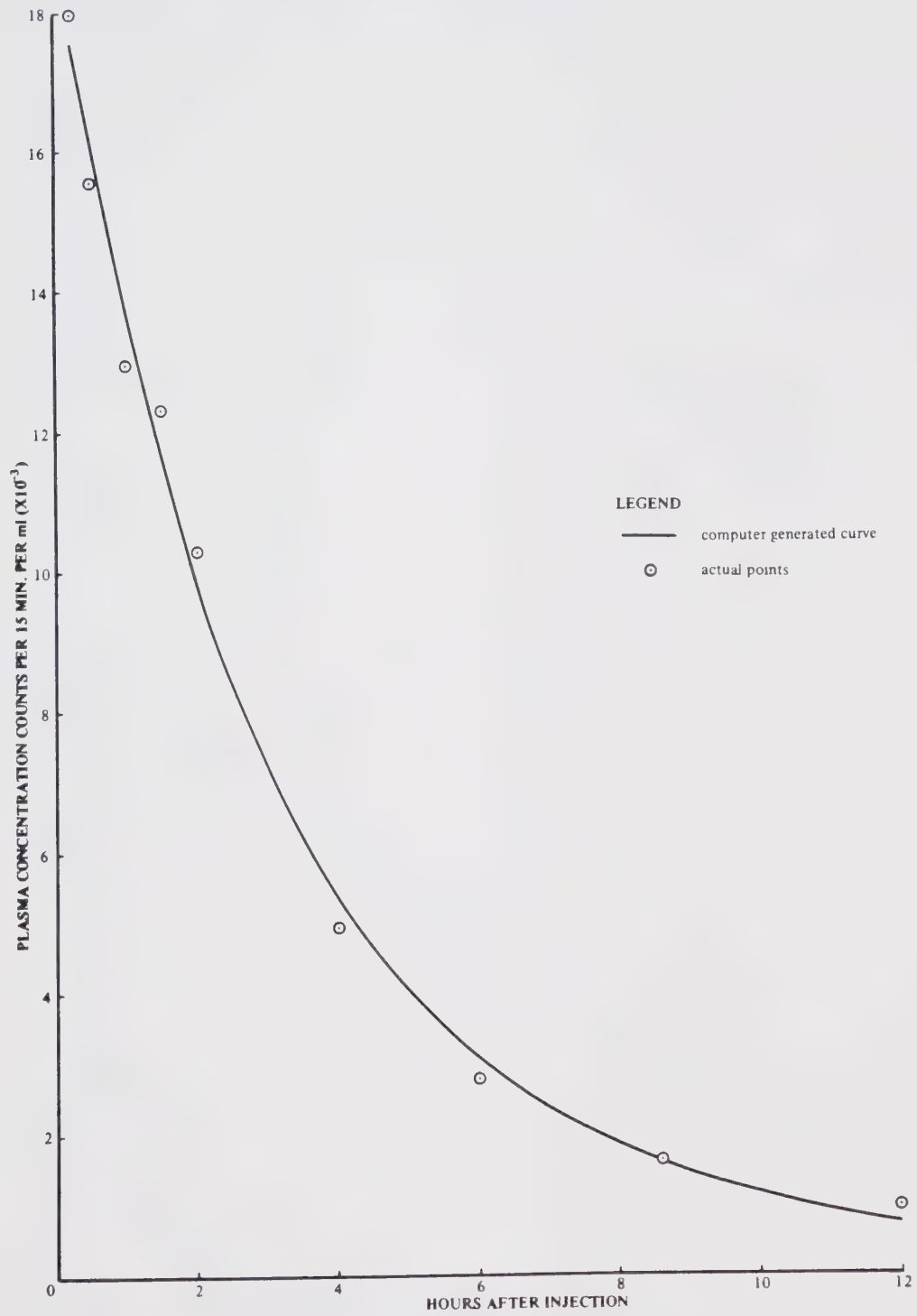




FIGURE 8: Percent of the total radioactivity in each compartment following I.V. injection of  $^{67}\text{Ga}$ -citrate in one subject

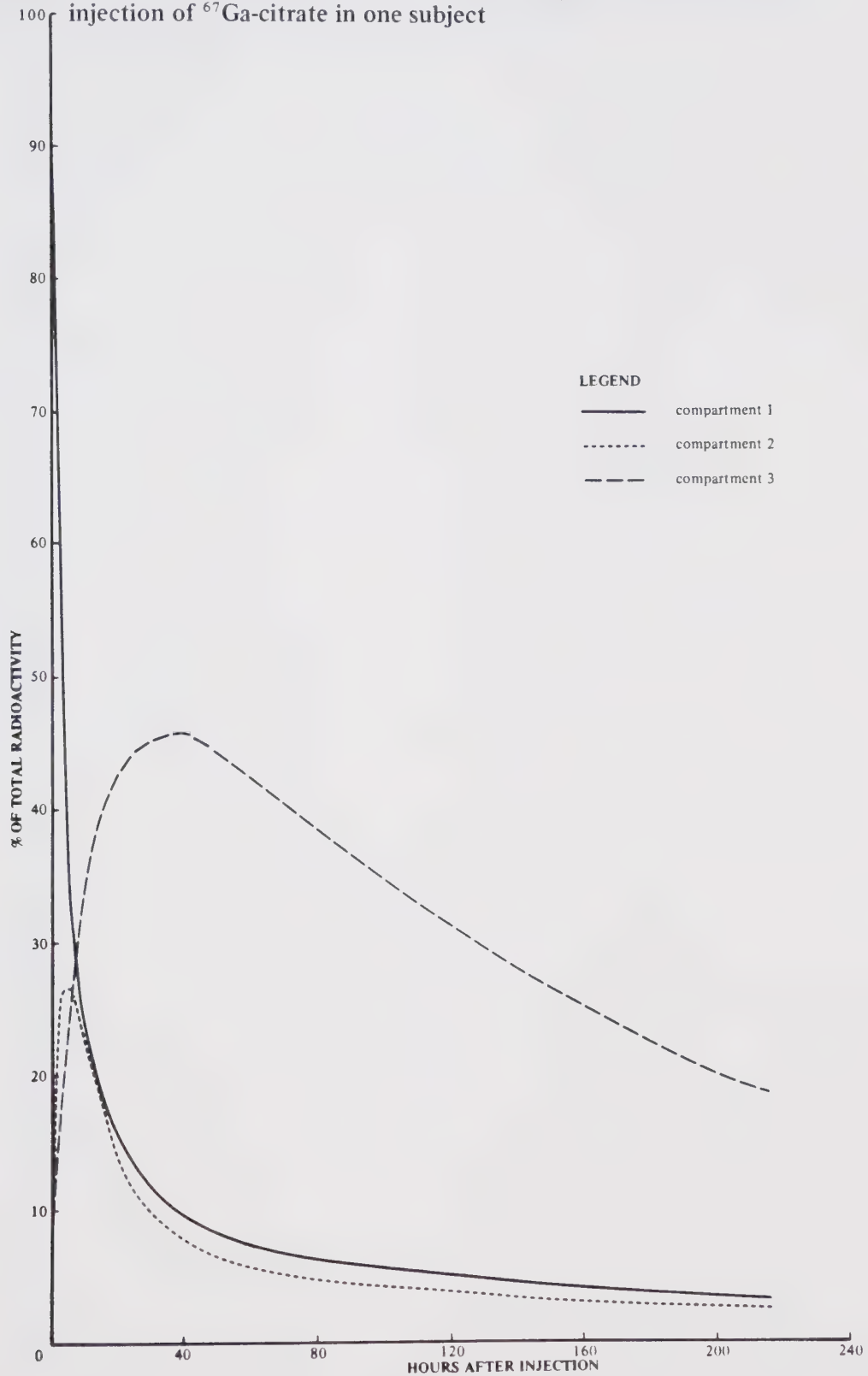






FIGURE 9: Percent of the total radioactivity in each compartment following I.V. injection of  $^{67}\text{Ga}$ -transferrin in one subject

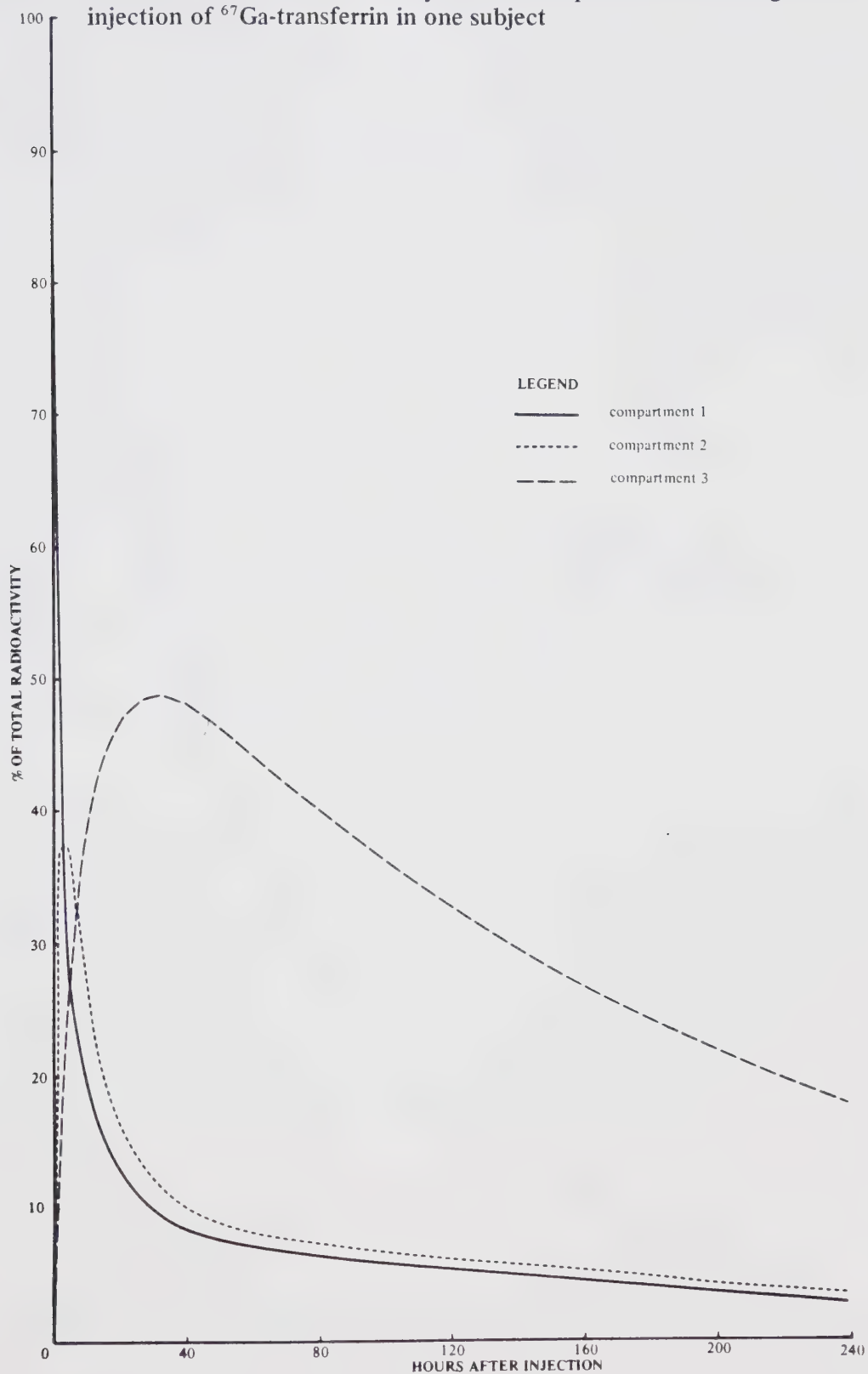
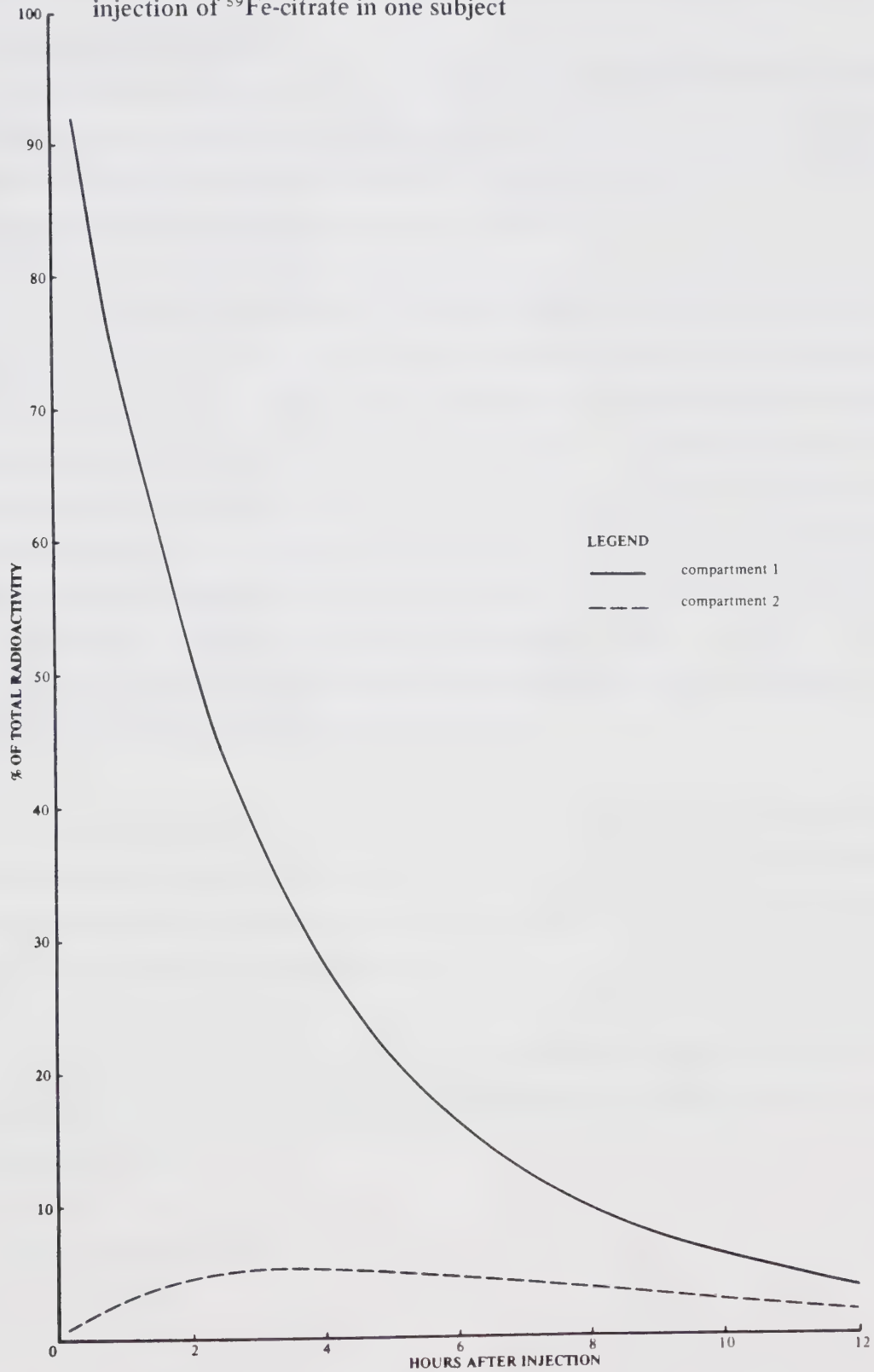




FIGURE 10: Percent of the total radioactivity in each compartment following I.V. injection of  $^{59}\text{Fe}$ -citrate in one subject





Similar plots were obtained for all subjects, and are presented in Appendix E.

## 2. Parameters of Measurement

The pharmacokinetic parameters for each subject receiving  $^{67}\text{Ga}$ -citrate,  $^{67}\text{Ga}$ -Tf and  $^{59}\text{Fe}$ -citrate were calculated by model-independent methods using the coefficients and exponents of the polyexponential equation.\* The equations used for such calculations and the definitions of the symbols are presented in Table VIII.

The exponential coefficients,  $\lambda_i$ , are also referred to as hybrid rate constants. The smallest rate constant,  $\beta$  ( $\lambda_3$  for  $^{67}\text{Ga}$ -citrate and  $^{67}\text{Ga}$ -Tf, and  $\lambda_2$  for  $^{59}\text{Fe}$ -citrate), is the overall elimination rate constant, and thus describes the elimination of the radiopharmaceutical from the plasma. The largest rate constant,  $\lambda_1$ , indicates the rate of initial distribution and elimination from the plasma to other body tissues. This rate constant is not only governed by the physical and chemical properties of the agent, but may also be dependent upon physiological factors such as blood flow. In a three-compartment model, the middle rate constant,  $\lambda_2$ , describes distribution of the agent from the central compartment. The values of the pre-exponential coefficients,  $A_i$ , are dependent upon the injected dose and the corresponding rate constants.

The microscopic rate constants are hypothetical constants based upon the hypothetical model chosen, and are calculated from the hybrid rate constants. (The hybrid rate constants may be calculated from the microscopic rate constants as well.) The microscopic rate constants are model-dependent.

The half-life of the terminal phase,  $t_{1/2}$ , describes the elimination of the drug from the plasma.  $V_p$  is the volume of central compartment, and should be equal to or greater than plasma volume.

\* programs supplied by Dr. P.K. Ng.



TABLE VIII

## DEFINITIONS AND SYMBOLS OF PHARMACOKINETIC PARAMETERS

<u>TERM</u>	<u>DEFINITION</u>
$C_p$	Plasma concentration (cpm/ml) following I.V. bolus injection
	$= \sum_{i=1}^n A_i e^{-\lambda_i t}$
$n$	number of exponentials
$A_i$	pre-exponential coefficients, $A_1, A_2, \dots, A_n$
$\lambda_i$	exponential coefficients $\lambda_1, \lambda_2, \dots, \lambda_n$
$t$	time after I.V. bolus injection
$t_{1/2}$	half-life of terminal exponential = $\frac{0.693}{\lambda_n}$
$D$	injected amount of radioactivity
$AUC$	area under the curve (0 to $\infty$ ) following I.V. bolus injection.
	$= \sum_{i=1}^n A_i / \lambda_i$
$Cl_p$	Plasma clearance = $D/AUC$
$V_{d \text{ area}}$	Volume of distribution = $D/AUC \cdot \lambda_n$
$V_p$	volume of central compartment = $D / \sum_{i=1}^n A_i$





The apparent volume of distribution,  $V_{d \text{ area}}$ , is a proportionality constant describing the relationship between the total amount of drug in the body and the plasma concentration at a given time. In essence,  $V_{d \text{ area}}$  describes the extent to which a drug penetrates the peripheral compartments from the central compartment.

### 3. Comparison of $^{67}\text{Ga}$ -citrate and $^{67}\text{Ga}$ -transferrin Kinetics

Table IX presents the mean pharmacokinetic parameter estimates of  $^{67}\text{Ga}$ -citrate and  $^{67}\text{Ga}$ -Tf in the four subjects. The microscopic rate constants are listed in Table X. The values of all the pharmacokinetic parameters for each subject are presented in Appendix F.

Of all the measured parameters, a statistically significant difference ( $p < 0.05$ , paired t-test) was observed for the values of  $\lambda_2$ , the distribution rate constant, and the microscopic rate constants  $k_{13}$ , and  $k_{10}$ . Since no difference was found in the overall elimination rate constant,  $\lambda_3$ , for the citrate and Tf complexes of  $^{67}\text{Ga}$ , the larger values of  $\lambda_2$ ,  $k_{13}$ , and  $k_{10}$  obtained after  $^{67}\text{Ga}$ -Tf injection were probably due to a faster distribution and uptake of the latter complex from the intravascular compartment of other tissues of the body. It is interesting to note that the subject with the largest rate constants for  $^{67}\text{Ga}$ -citrate and  $^{67}\text{Ga}$ -Tf (A.N.) had approximately a ten-fold increase in ferritin levels over the other three subjects.

Edwards and Hayes observed that the elimination of  $^{67}\text{Ga}$ -citrate from the blood was a slow process, reporting that after 40 hours there was approximately 5% of the initial activity in the blood, and 2% still remaining after five days (47). The half-life of the terminal phase of gallium-67 clearance from the plasma in the subjects of our study ranged from 70 to 139 hours, thus supporting the previous authors' findings. Slightly lower results were observed for gallium nitrate in humans, 10.5 to 50.4 hours (28). Larson (259) and Clausen and co-workers (2) found lower values for the terminal half-life of  $^{67}\text{Ga}$ -citrate plasma disappearance (about 38 hours, and 48 hours respectively).



TABLE IX

PHARMACOKINETIC PARAMETERS OF  $^{67}\text{Ga}$ -CITRATE AND  $^{67}\text{Ga}$ -TRANSFERRIN  
IN HUMANS FOLLOWING I.V. INJECTION

Terms	Units	X $\pm$ S.D. *	
		Ga-67 citrate	Ga-67 transferrin
$\lambda_1$	hr $^{-1}$	0.883 $\pm$ 0.845	1.575 $\pm$ 1.643
$\lambda_2$	hr $^{-1}$	0.072 $\pm$ 0.035	0.102 $\pm$ 0.039
$\lambda_3$	hr $^{-1}$	0.007 $\pm$ 0.002	0.008 $\pm$ 0.002
$t_{1/2}$	hr	109 $\pm$ 30	92 $\pm$ 32
$\text{Cl}_p$	ml/hr	142 $\pm$ 17	175 $\pm$ 43
$V_{d \text{ area}}$	L	22.4 $\pm$ 6.4	22.5 $\pm$ 6.9
$V_p$	L	3.17 $\pm$ 0.52	3.34 $\pm$ 1.27

\* Mean  $\pm$  standard deviation



TABLE X

MICROSCOPIC RATE CONSTANTS OF THE THREE-COMPARTMENT MODEL  
DESCRIBING  $^{67}\text{Ga}$ -CITRATE AND  $^{67}\text{Ga}$ -TRANSFERRIN KINETICS IN HUMANS

Rate Constants ( $\text{hr}^{-1}$ )	X $\pm$ S.D. *	
	Ga-67 Citrate	Ga-67 Transferrin
$k_{10}$	$0.046 \pm 0.014$	$0.056 \pm 0.019$
$k_{12}$	$0.353 \pm 0.359$	$0.676 \pm 0.773$
$k_{21}$	$0.474 \pm 0.473$	$0.824 \pm 0.827$
$k_{13}$	$0.068 \pm 0.038$	$0.102 \pm 0.052$
$k_{31}$	$0.020 \pm 0.008$	$0.028 \pm 0.008$

\* Mean  $\pm$  Standard Deviation



Since the calculated volume of the central compartment ( $V_p$ ) was similar to that of the plasma volume calculated on the basis of height and weight (263), this suggested that the central compartment was composed mainly of the intravascular compartment. Because  $V_p$  was only 15% of the total volume of distribution ( $V_{d \text{ area}}$ ), it appears that most of the  $^{67}\text{Ga}$  was found in the peripheral compartments after equilibration.

The mean ratio between  $k_{31}$  and  $k_{13}$  was 0.29, implying slow establishment of equilibrium between compartments one and three. In this study, it took from 12 to 48 hours following injection for equilibrium between the previous two compartments to be reached. Also, analysis of the data points in each exponential phase indicated that the distribution phase (phase 2) was generally more rapid for  $^{67}\text{Ga-Tf}$  than for  $^{67}\text{Ga-citrate}$ .

Uptake of both  $^{67}\text{Ga-citrate}$  and  $^{67}\text{Ga-Tf}$  in the red blood cells was negligible.





#### 4. Comparison of $^{67}\text{Ga}$ -citrate and $^{59}\text{Fe}$ -citrate Kinetics

The  $^{67}\text{Ga}$ -citrate data for the fourth subject (A.N.) was excluded from this comparison, as he did not receive  $^{59}\text{Fe}$ -citrate. Table XI presents the mean pharmacokinetic parameter estimates of  $^{67}\text{Ga}$ -citrate and  $^{59}\text{Fe}$ -citrate in the remaining three subjects.

TABLE XI

#### PHARMACOKINETIC PARAMETERS OF $^{67}\text{GA}$ -CITRATE AND $^{59}\text{FE}$ -CITRATE IN HUMANS FOLLOWING I.V. BOLUS INJECTION

Terms	Units	$\bar{X} \pm \text{S.D.}^\dagger$	
		$^{67}\text{Ga}$ -citrate	$^{59}\text{Fe}$ -citrate
$\lambda_1$	$\text{hr}^{-1}$	$0.465 \pm 0.149$	$2.821 \pm 4.027$
$\lambda_2^*$	$\text{hr}^{-1}$	$0.006 \pm 0.002$	$0.303 \pm 0.127$
$t_{1/2}$	hr	$118 \pm 30$	$2.613 \pm 1.209$
$\text{Cl}_p$	ml/hr	$136 \pm 15$	$1155 \pm 384$
$V_d \text{ area}$	L	$23.4 \pm 7.4$	$3.99 \pm 0.87$

\*  $\lambda_2$  of  $^{59}\text{Fe}$ -citrate corresponds to  $\lambda_3$  of  $^{67}\text{Ga}$ -citrate.

† Mean  $\pm$  standard deviation.

The overall elimination rate constant for  $^{67}\text{Ga}$ -citrate ( $\lambda_3$ ) was found to be approximately 50 times slower than that of  $^{59}\text{Fe}$ -citrate ( $\lambda_2$ ). This indicates that  $^{59}\text{Fe}$  was cleared from the plasma at a faster rate than  $^{67}\text{Ga}$ . There was also a significant difference in the biological half-lives in plasma ( $t_{1/2}$ ) and plasma clearance ( $\text{Cl}_p$ ) of  $^{67}\text{Ga}$ -citrate and  $^{59}\text{Fe}$ -



citrate ( $p < 0.05$ ).

The volume of distribution ( $V_{d \text{ area}}$ ) of  $^{67}\text{Ga}$ -citrate was approximately six times that of  $^{59}\text{Fe}$ -citrate suggesting that  $^{67}\text{Ga}$ -citrate was more widely distributed in the other body tissues than  $^{59}\text{Fe}$ -citrate. This is not surprising, as  $^{59}\text{Fe}$  is generally confined to the hematopoietic system (223), whereas  $^{67}\text{Ga}$ -citrate is more diffusely distributed in tissues (142). Sephton and co-workers (43) had observed this difference in mice.

The difference between  $^{59}\text{Fe}$ -citrate and  $^{67}\text{Ga}$ -citrate uptake in red blood cells is demonstrated in Figure 11.  $^{67}\text{Ga}$  present in red blood cells remained little above background throughout the experiment, whereas  $^{59}\text{Fe}$  uptake followed the sigmoid curve previously reported (223). This fact clearly reveals a fundamental difference in the biological handling of iron and gallium.

#### **B. Urinary Excretion Of $^{67}\text{Ga}$ -citrate, $^{67}\text{Ga}$ -transferrin And $^{59}\text{Fe}$ -citrate**

The cumulative urinary excretion of  $^{67}\text{Ga}$ -citrate,  $^{67}\text{Ga}$ -transferrin, and  $^{59}\text{Fe}$ -citrate is presented in Table XII. Due to the lack of subject compliance, complete quantitative data is not available. However, the data does show little, if any, difference between the amount of  $^{67}\text{Ga}$ -citrate and  $^{67}\text{Ga}$ -Tf excreted in the urine. Very little  $^{59}\text{Fe}$ -citrate, (between 0 and 3.1%) was excreted in the urine.



FIGURE 11: Percent of injected dose in red blood cells over time following I.V. injection of  $^{59}\text{Fe}$ -citrate and  $^{67}\text{Ga}$ -citrate in one subject

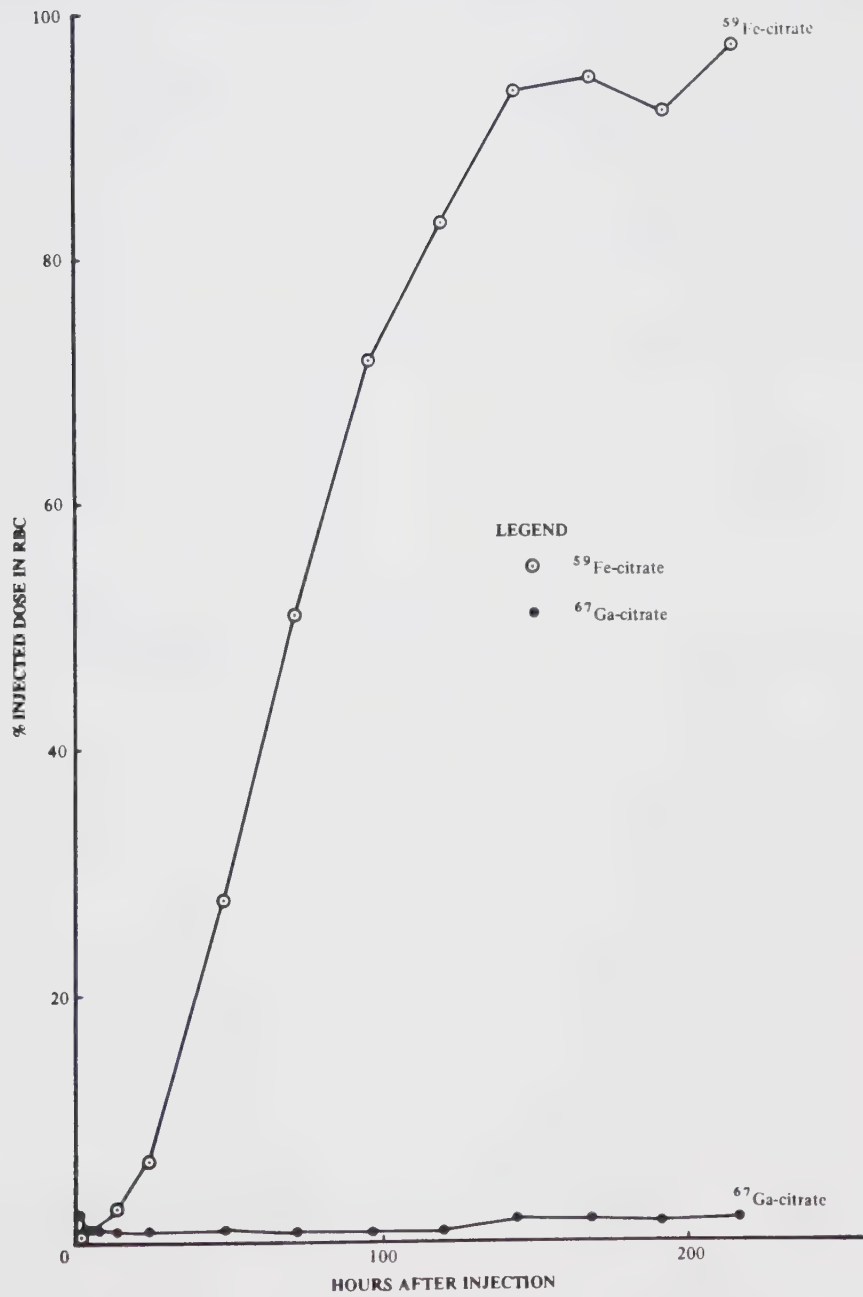




TABLE XII

CUMULATIVE URINARY EXCRETION TO 48 HOURS AFTER INTRAVENOUS  
INJECTION OF  $^{67}\text{Ga}$ -CITRATE,  $^{67}\text{Ga}$ -TRANSFERRIN, AND  $^{59}\text{Fe}$ -CITRATE

Subject	% of dose excreted		
	$^{67}\text{Ga}$ -citrate	$^{67}\text{Ga}$ -Tf	$^{59}\text{Fe}$ -citrate
UT	18.9 *	12.5	0
CW	12.2	12.9	3.1
BL	16.3 †	16.0	1.3
AN	22.7	19.3	—
$\bar{X} \pm \text{S.D.}$	$18.4 \pm 4.44$	$15.2 \pm 3.16$	—

\* One sample was missed between 32.8 and 39.7 hours after administration.

† The first urine sample after administration was not collected.





### C. *In Vivo* Distribution Of $^{67}\text{Ga}$ -citrate, $^{67}\text{Ga}$ -Tf, and $^{59}\text{Fe}$ -citrate

The net relative uptake of  $^{67}\text{Ga}$ -citrate,  $^{67}\text{Ga}$ -Tf, and  $^{59}\text{Fe}$ -citrate in the regions of the sacrum, liver, heart, spleen and knee of all subjects is shown in Figures 12 – 16, respectively.

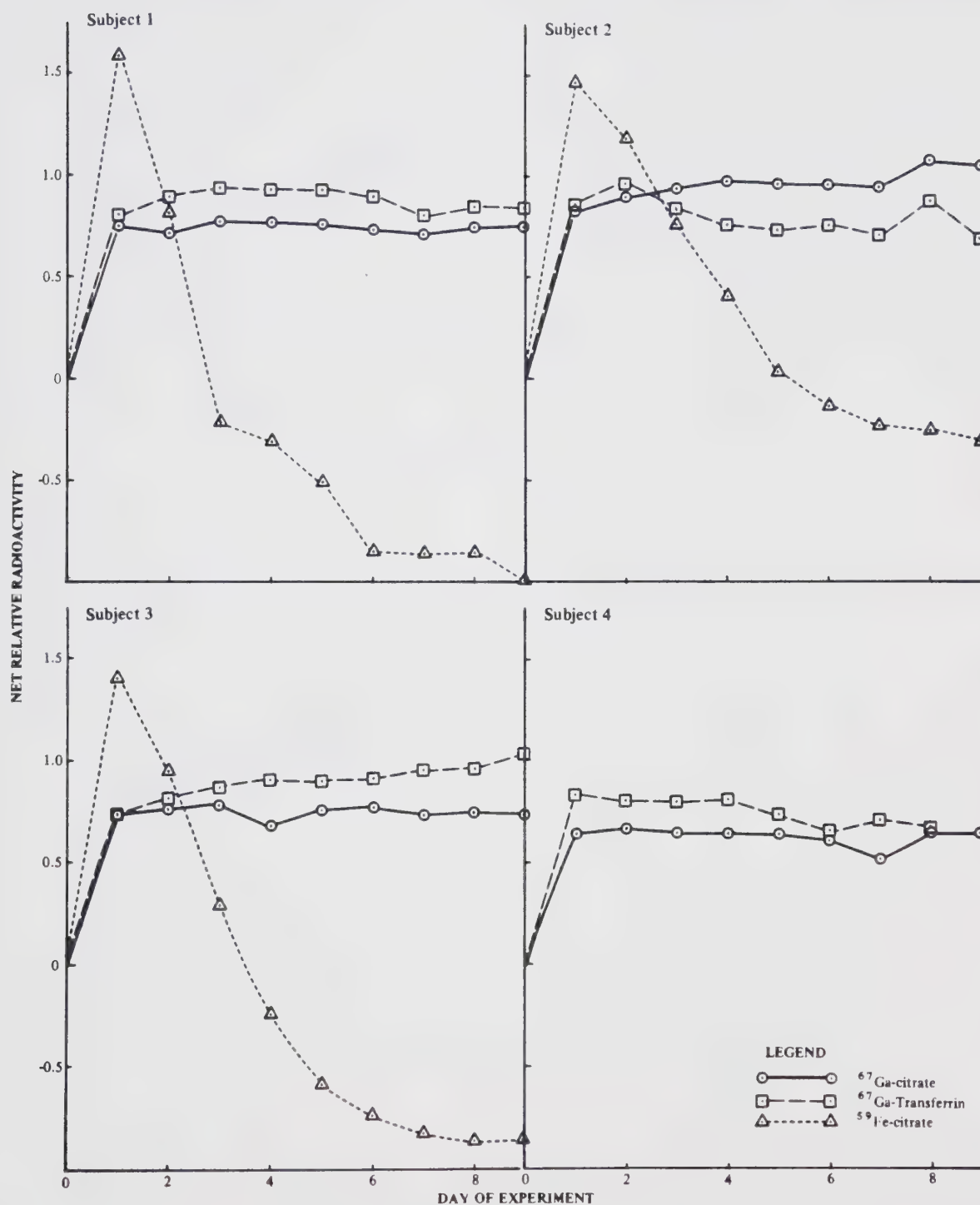
The activity of  $^{59}\text{Fe}$  in the sacrum behaved according to classical iron kinetics (223), with rapid uptake during the first 24 hours followed by a steady decline. On the other hand, uptake of  $^{67}\text{Ga}$ -citrate and  $^{67}\text{Ga}$ -Tf in the sacrum was essentially complete 24 hours after injection and then remained constant for up to ten days. No differences were observed between the handling of the two complexes of gallium.

The uptake of  $^{59}\text{Fe}$  in the liver, heart, and spleen was similar to that in the sacrum. This peak of activity at 24 hours may reflect either the equilibration of plasma  $^{59}\text{Fe}$  with the extracellular fluids in these organs, or specific tissue uptake. The accumulation of  $^{67}\text{Ga}$ -citrate and  $^{67}\text{Ga}$ -Tf in the liver, heart and spleen was markedly different from that of  $^{59}\text{Fe}$ . The uptake of both  $^{67}\text{Ga}$ -citrate and  $^{67}\text{Ga}$ -Tf in the liver increased rapidly up to 24 hours, then gradually increased over the following nine days. The similarity in the rate of uptake in the liver suggests that accumulation of these two complexes of  $^{67}\text{Ga}$  was not different. The activities of  $^{67}\text{Ga}$ -citrate and  $^{67}\text{Ga}$ -Tf in the heart and spleen were greatest at 24 hours and then remained largely unchanged. Normal accumulation of  $^{67}\text{Ga}$  in the spleen has been reported to be erratic (142) and this was evident in these probe studies. No difference was detected in the rate of uptake of  $^{67}\text{Ga}$ -citrate and  $^{67}\text{Ga}$ -Tf in either the heart or spleen.

The uptake of  $^{67}\text{Ga}$ -citrate and  $^{67}\text{Ga}$ -Tf in the knee was small in comparison to uptake in the other tissues. Both  $^{67}\text{Ga}$  complexes appear to be incorporated into the bone, as the radioactivity associated with the knee did not follow the blood curve but remained fairly constant after Day 1 of the experiment. There was very little uptake of  $^{59}\text{Fe}$ -citrate in the knee. Due to problems with instrumentation there was no data for knee uptake in Subject C.W.



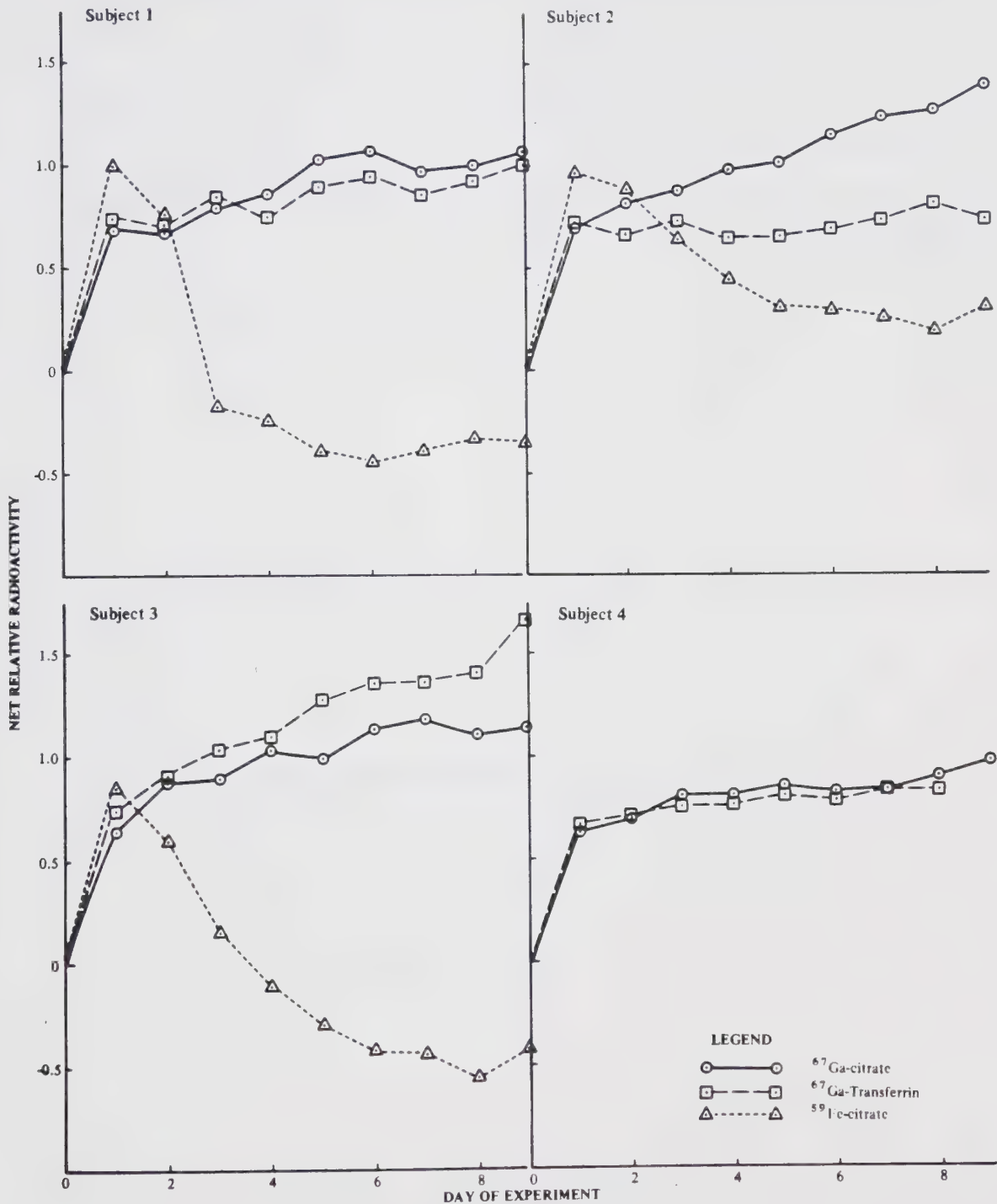
FIGURE 12: Net relative uptake of  $^{67}\text{Ga}$ -citrate,  $^{67}\text{Ga}$ -transferrin and  $^{59}\text{Fe}$ -citrate in the Sacrum



Net relative uptake of  $^{67}\text{Ga}$ -citrate,  $^{67}\text{Ga}$ -Tf, and  $^{59}\text{Fe}$ -citrate in the sacrum. Data was corrected for background, physical decay, and percent of radioactivity remaining in the whole blood. All data was compared to data obtained on Day 0.



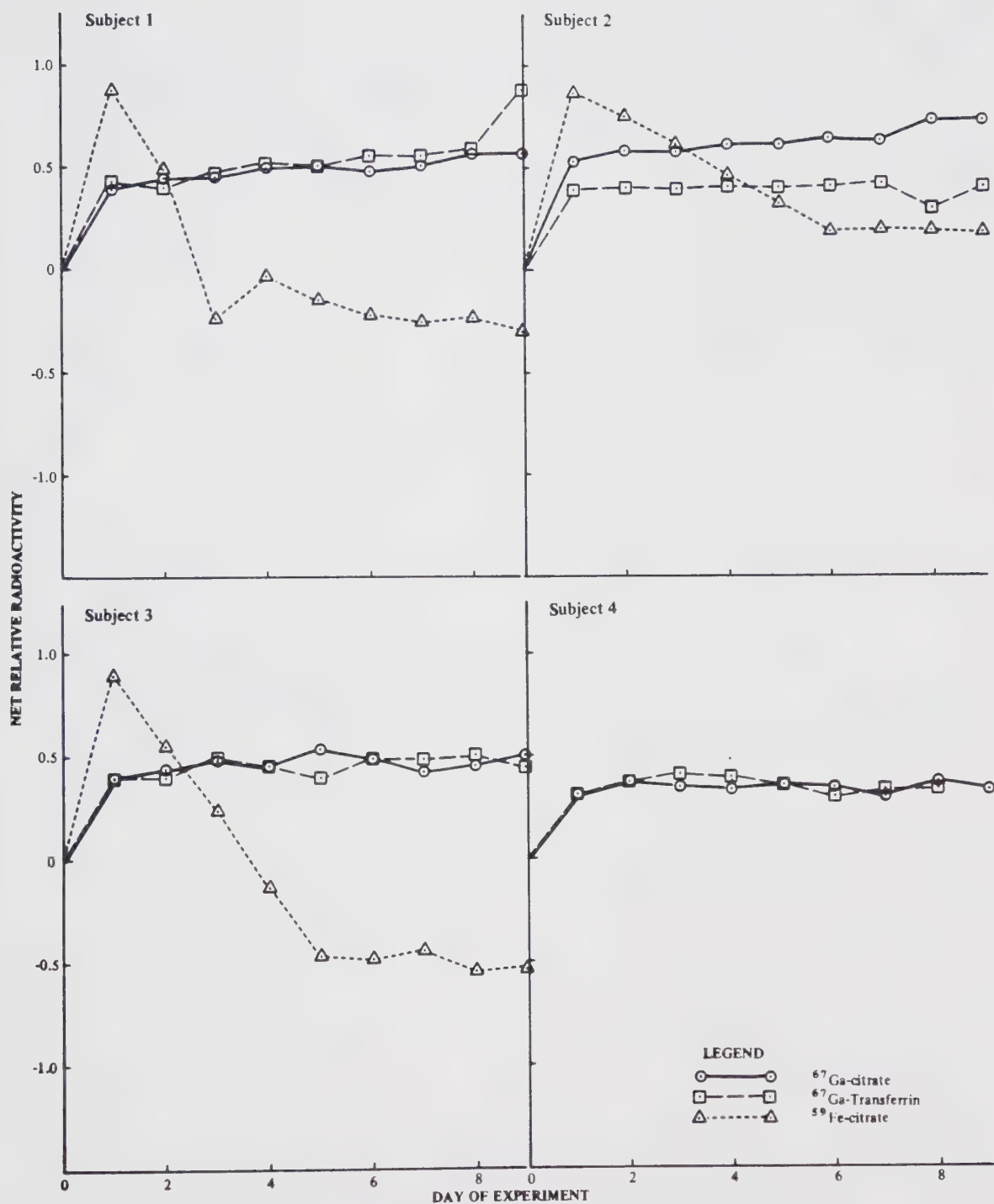
FIGURE 13: Net relative uptake of  $^{67}\text{Ga}$ -citrate,  $^{67}\text{Ga}$ -transferrin and  $^{59}\text{Fe}$ -citrate in the Liver



Net relative uptake of  $^{67}\text{Ga}$ -citrate,  $^{67}\text{Ga}$ -Tf, and  $^{59}\text{Fe}$ -citrate in the liver. Data was corrected for background, physical decay, and percent of radioactivity remaining in the whole blood. All data was compared to data obtained on Day 0.



FIGURE 14: Net relative uptake of  $^{67}\text{Ga}$ -citrate,  $^{67}\text{Ga}$ -transferrin and  $^{59}\text{Fe}$ -citrate in the Heart

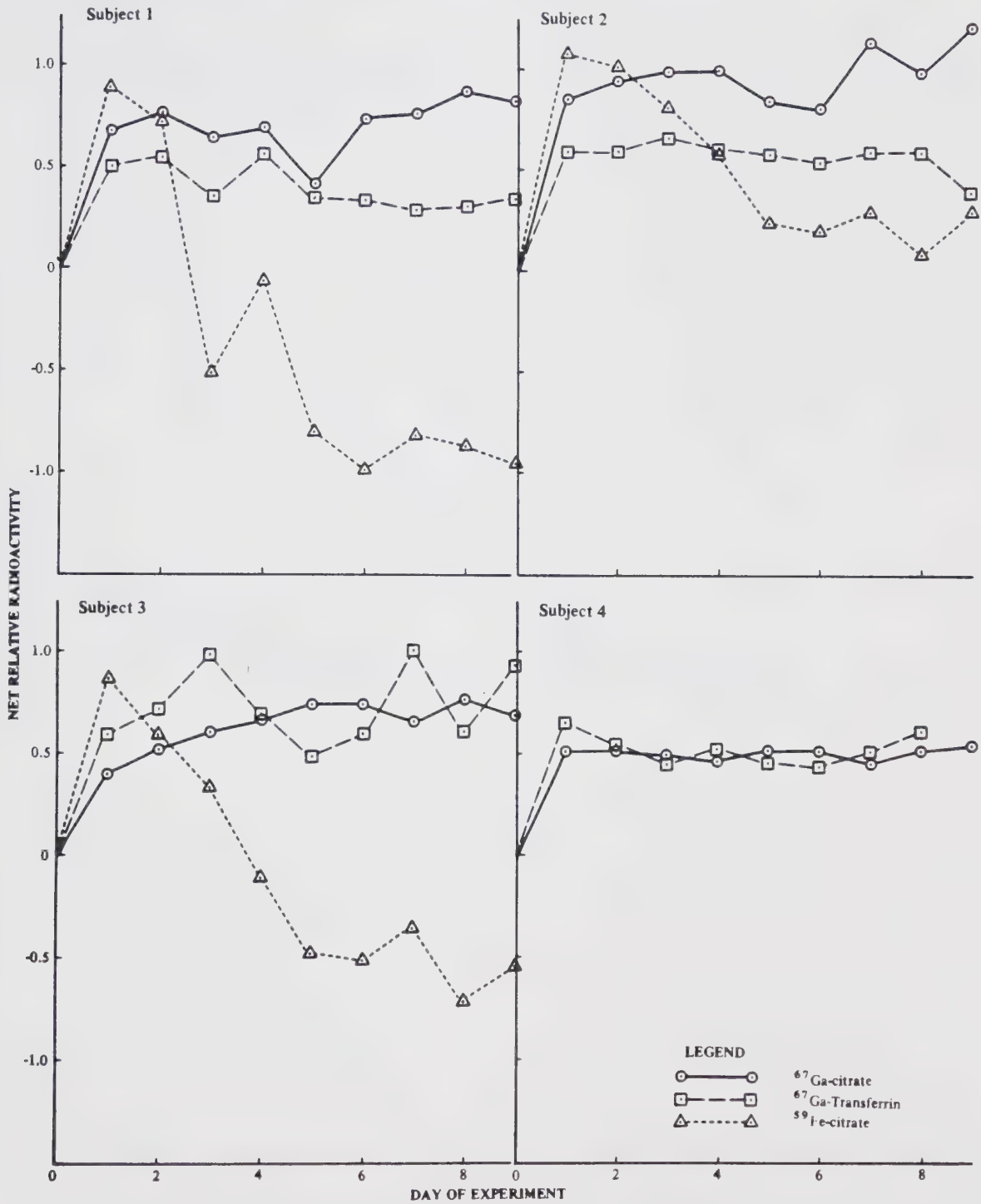


Net relative uptake of  $^{67}\text{Ga}$ -citrate,  $^{67}\text{Ga}$ -Tf, and  $^{59}\text{Fe}$ -citrate in the heart. Data was corrected for background, physical decay, and percent of radioactivity remaining in the whole blood. All data was compared to data obtained on Day 0.





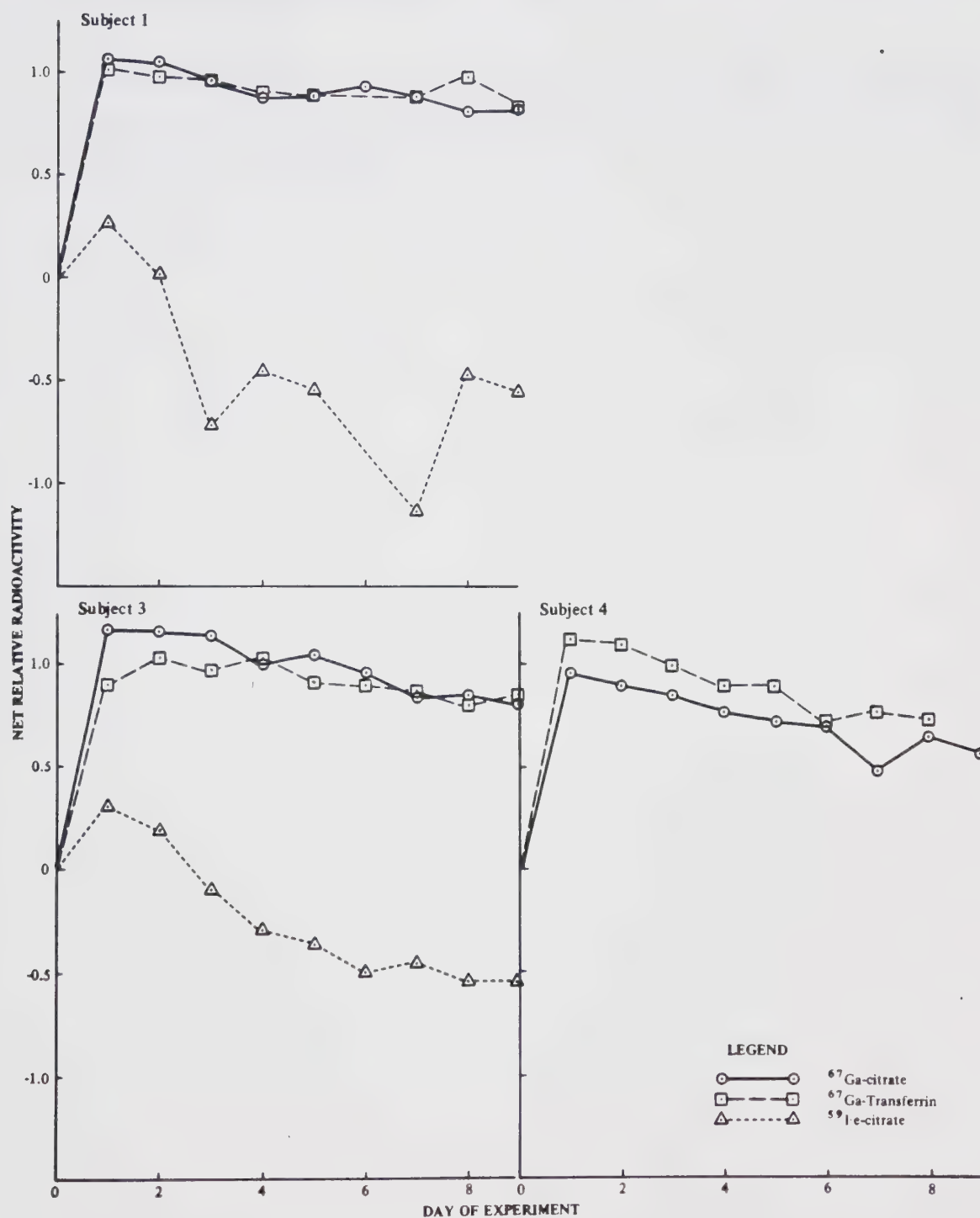
FIGURE 15: Net relative uptake of  $^{67}\text{Ga}$ -citrate,  $^{67}\text{Ga}$ -transferrin and  $^{59}\text{Fe}$ -citrate in the Spleen



Net relative uptake of  $^{67}\text{Ga}$ -citrate,  $^{67}\text{Ga}$ -Tf, and  $^{59}\text{Fe}$ -citrate in the spleen. Data was corrected for background, physical decay, and percent of radioactivity remaining in the whole blood. All data was compared to data obtained on Day 0.



FIGURE 16: Net relative uptake of  $^{67}\text{Ga}$ -citrate,  $^{67}\text{Ga}$ -transferrin and  $^{59}\text{Fe}$ -citrate in the Knee



Net relative uptake of  $^{67}\text{Ga}$ -citrate,  $^{67}\text{Ga}$ -Tf, and  $^{59}\text{Fe}$ -citrate in the knee. Data was corrected for background, physical decay, and percent of radioactivity remaining in the whole blood. All data was compared to data obtained on Day 0.



The lack of observable differences in this *in vivo* distribution comparison between  $^{67}\text{Ga}$ -citrate and  $^{67}\text{Ga}$ -Tf in healthy subjects does not preclude possible differences in the uptake of these agents in sites of disease.

Thus, the disposition of  $^{67}\text{Ga}$  and  $^{59}\text{Fe}$  in human subjects was not similar despite their common association with Tf. Other factors must be involved in the uptake of these radionuclides by the various body tissues.



## SUMMARY AND CONCLUSIONS





1)  $^{67}\text{Ga-Tf}$  was aseptically prepared by the direct incubation method, using either  $^{67}\text{Ga-citrate}$  or  $^{67}\text{GaCl}_3$ . The  $^{67}\text{GaCl}_3$  method resulted in a product with higher specific activity (i.e. greater % labelling). No adverse effects were observed in either mice or humans.

2) The plasma disappearances of  $^{67}\text{Ga-citrate}$  and  $^{67}\text{Ga-Tf}$  were both best described by a three exponential equation. A three-compartment open model with elimination occurring from the central compartment was the simplest model chosen to describe the distribution of these two  $^{67}\text{Ga}$  complexes.

3) A statistically significant difference was observed between  $^{67}\text{Ga-citrate}$  and  $^{67}\text{Ga-Tf}$  in the distribution rate constant,  $\lambda_2$  and the microscopic rate constants  $k_{13}$  and  $k_{10}$ , which indicated that  $^{67}\text{Ga-Tf}$  left the plasma for the peripheral compartments at a faster rate than  $^{67}\text{Ga-citrate}$ .

4) The plasma disappearance of  $^{59}\text{Fe-citrate}$  was best described by a two exponential equation, and a two-compartment model with elimination from the central compartment was chosen to describe  $^{59}\text{Fe-citrate}$  pharmacokinetics.

5) There were significant differences between  $^{67}\text{Ga-citrate}$  and  $^{59}\text{Fe-citrate}$  in the overall elimination rate constant, biological half-life, plasma clearance, volume of distribution, and red blood cell uptake, revealing fundamental differences in the biological handling of iron and gallium.

6) There was no observable difference in the amount of  $^{67}\text{Ga-citrate}$  and  $^{67}\text{Ga-Tf}$  excreted in the urine. Essentially no  $^{59}\text{Fe-citrate}$  was found in the urine.

7) The uptake of  $^{67}\text{Ga-citrate}$  and  $^{67}\text{Ga-Tf}$  in the regions of the sacrum, liver, heart, spleen and knee did not appear to be significantly different. The *in vivo* distribution



$^{59}\text{Fe}$ -citrate was strikingly different than that observed with the  $^{67}\text{Ga}$  complexes and appeared to follow classical iron kinetics, especially with respect to uptake in the sacrum.

8) Other factors beside a common association with Tf must be involved in the tissue uptake of  $^{67}\text{Ga}$ -citrate and  $^{59}\text{Fe}$ -citrate.



## REFERENCES



1. Edwards, C.L., Hayes, R.L., Tumor scanning with 67-gallium citrate. *J. Nucl. Med.* 10: 103–105, 1969.
2. Clausen, J., Edeling, C.J., Fogh, J.,  $^{67}\text{Ga}$  binding to human serum proteins and tumor components. *Cancer Res.* 34:1931-1937, 1974.
3. Hegge, F.N., Mahler, D.J., Larson, S.M., The incorporation of Ga-67 into the ferritin fraction of rabbit hepatocytes *in vivo*, *J. Nucl. Med.* 18:937-939, 1977.
4. Hoffer, P.B., Huberty, J., Khayam-Bashi, H., The association of Ga-67 and lactoferrin, *J. Nucl. Med.* 18:713-717, 1977.
5. Schlabach, M.R., Bates, G.W., The synergistic binding of anions and  $\text{Fe}^{3+}$  by transferrin. Implications for the interlocking sites hypothesis. *J. Biol. Chem.* 250:2182-2188, 1975.
6. Harris, D.C., Gray, G.A., Aisen, P.,  $^{13}\text{C}$  Nuclear magnetic resonance study of the spatial relation of the metal- and anion- binding sites of human transferrin. *J. Biol. Chem.* 249:5261-5264, 1974.
7. Terner, U.K., Wong, H., Noujaim, A.A., et al.,  $^{67}\text{Ga}$  and  $^{59}\text{Fe}$  uptake in human melanoma cells. *Int. J. Nucl. Med. Biol.* 6:23-28, 1979.
8. Larson, S.M., Rasey, J.S., Allen, D.R., et al., Common pathway for tumor cell uptake of gallium -67 and iron-59 via a transferrin receptor. *J. N. C. I.* 64:41-53, 1980.
9. Larson, S.M., Rasey, J.S., Allen, D.R., et al., A transferrin-mediated uptake of gallium-67 by EMT-6 sarcoma. II. Studies *in vivo* (BALB/c mice). *J. Nucl. Med.* 20:843-846, 1979.
10. Wong, H., Terner, U.K., English, D., et al., The role of transferrin in the *in vivo* uptake of gallium-67 in a canine tumor. *Int. J. Nucl. Med. Biol.* 7:9-16, 1980.
11. Hagg, G., "General and Inorganic Chemistry", John Wiley and Sons, New York, 1969, pp. 86, 646.
12. Sheka, I.A., Chaus, I.S., Mityureva, T.T., "The Chemistry of Gallium", Elsevier Publishing Company, Amsterdam, 1966, pp. 1-20, 28-57.
13. Dymov, A.M., Savostin, A.P., "Analytical Chemistry of Gallium", A.N. Ermakov, ed., Ann Arbor Science Publishers, London, 1970, pp. 1-22.
14. "Table of Isotopes", 7th edition, C.M. Lederer, V.S. Shirley, eds., John Wiley and Sons, New York, 1978, pp. 213, 216, 233-234, 173.





15. Cotton, F.A., Wilkinson, G., "Advanced Inorganic Chemistry", John Wiley and Sons, London, 1962, pp. 332-344.
16. Glickson, J.D., Pitner, T.P., Webb, J., et al., Hydrogen-1 and gallium-71 nuclear magnetic resonance of gallium citrate in aqueous solution. *J. Am. Chem. Soc.* 97:1679-1683, 1975.
17. Kulprathipanja, S., Hnatowich, D.J., A method for determining the pH stability of gallium radiopharmaceuticals. *Int. J. Appl. Rad. Isot.* 28:229-233, 1977.
18. Harris, W.R., Martell, A.E., Aqueous complexes of gallium (III). *Inorganic Chem.* 15:713-720, 1976.
19. Hnatowich, D.J., Kulprathipanja, S., Beh, R., The importance of pH and citrate concentration on the *in vitro* and *in vivo* behavior of radiogallium. *Int. J. Appl. Radiat. Isot.* 28:925-931, 1977.
20. Hayes, R.L., The medical use of gallium radionuclides: a brief history with some comments. *Semin. Nucl. Med.* 8:183-191, 1978.
21. Nass, H.W., Accepted gallium-67 decay data. *J. Nucl. Med.* 21:704, 1980.
22. Dudley, H.C., Levine, M.D., Studies of the toxic action of gallium. *J. Pharmacol. Exp. Ther.* 95:487-493, 1949.
23. Dudley, H.C., Henry, K.E., Lindsley, B.F., Studies of the toxic action of gallium. II. *J. Pharmacol. Exp. Ther.* 98:409-417, 1950.
24. Bruner, H.D., Cooper, B.M., Rehbock, D.J., Toxicity of gallium citrate in dogs and rats. *Radiology* 61:550-555, 1953.
25. Perkinson Jr., J.D., Ingols, R.S., Effect of internal radiation on respiration of rat liver slices. *Radiology* 61:545-550, 1953.
26. Andrews, G.A., Root, S.W., Kerman, H.D., Clinical studies with gallium-72. *Radiology* 61:570-588, 1953.
27. Konikowski, T., Glenn, N.J., Haynie, T.P., Kinetics of  $^{67}\text{Ga}$  compounds in brain sarcomas and kidneys of mice. *J. Nucl. Med.* 14:164-171, 1973.
28. Hall, S.W., Yeung, K., Benjamin, R.S., et al., Kinetics of gallium nitrate, a new anticancer agent. *Clin. Pharmacol. Ther.* 25:82-87, 1979.
29. Newman, R.A., Brody, A.R., Krakoff, I.H., Gallium nitrate (NSC-15200) induced toxicity in the rat. *Cancer* 44:1728-1740, 1979.



30. Krakoff, I.H., Newman, R.A., Goldberg, R.S., Clinical toxicologic and pharmacologic studies of gallium nitrate. *Cancer* 44:1722-1727, 1979.
31. Hartman, R.E., Hayes, R.L., The binding of gallium by blood serum. *J. Pharmacol. Exp. Ther.* 168:193-198, 1969.
32. Gunasekera, S.W., King, L.J., Lavender, P.J., The behavior of tracer gallium-67 towards serum proteins. *Clin. Chim. Acta.* 39:401-406, 1972.
33. Hara, T., On the binding of gallium to transferrin. *J. Nucl. Med. Biol.* 1:152-154, 1974.
34. Vallabhajosula, S.R., Harwig, J.F., Siemsen, J.K., et al., Behavior of gallium-67 in the blood: the role of transferrin. *J. Labelled Compds. Radio.* 16:112-114, 1979.
35. Vallabhajosula, S.R., Harwig, J.F., Siemsen, J.K., et al., Radiogallium localization in tumors: blood binding and transport and the role of transferrin. *J. Nucl. Med.* 21:650-656, 1980.
36. Dudley, H.C., Maddox, G.E., LaRue, H.C., Studies of the metabolism of gallium. *J. Pharmacol. Exp. Ther.* 96:135-138, 1949.
37. Dudley, H.C., Maddox, G.E., Deposition of radiogallium ( $^{72}\text{Ga}$ ) in skeletal tissues. *J. Pharmacol. Exp. Ther.* 96:224-227, 1949.
38. Dudley, H.C., Munn, J.I., Henry, K.E., Studies of the metabolism of gallium II. *J. Pharmacol. Exp. Ther.* 98:105-110, 1950.
39. Bruner, H.D., Perkinson Jr., J.D., King, E.R., et al., Distribution studies of gallium $^{72}$  in rats. *Radiology* 61:555-570, 1953.
40. Mulry, W.C., Dudley, H.C., Studies on radiogallium as a diagnostic agent in bone tumors. *J. Lab. Clin. Med.* 37:239-252, 1951.
41. Bruner, H.D., Hayes, R.L., Perkinson Jr., J.D., Preliminary data on gallium $^{67}$ . *Radiology* 61:602-613, 1953.
42. Glaubitt, D., Kaul, A., Koeppe, P., et al., Kinetic studies in rats for the determination of the radiation dose by  $^{67}\text{Ga}$ , in "Proceedings of the Second Congress of the European Association of Radiology", Excerpta Medica, Amsterdam, 1971, pp. 535-541.
43. Sephton, R.G., Hodgson, G.S., DeAbrew, S., et al., Ga-67 and Fe-59 distributions in mice. *J. Nucl. Med.* 19:930-935, 1978.



44. Ito, Y., Okuyama, S., Sato, K., et al.,  $^{67}\text{Ga}$  tumor scanning and its mechanism studied in rabbits. *Radiology* 100:357-362, 1971.
45. Edwards, C.L., Hayes, R.L., Scanning malignant neoplasms with gallium-67. *J.A.M.A.* 212:1182-1190, 1970.
46. Nelson, B., Hayes, R.L., Edwards, C.L., et al., Distribution of gallium in human tissues after intravenous administration. *J. Nucl. Med.* 13:92-100, 1972.
47. Edwards, C.L., Hayes, R.L., Localization of tumors with radioisotopes, in "Clinical Uses of Radionuclides: Critical Comparison with Other Techniques", F.A. Goswitz, G.A. Andrews, M. Viamonte, eds., U.S. Atomic Energy Commission Office of Information Services, Springfield, 1972, pp. 618-639.
48. Hayes, R.L., Brown, D.H., Biokinetics of radiogallium, in "Nuklearmedizin, Fortschritte der Nuklearmedizin in Klinischer und Technologischer Sicht", H.W. Pabst, G. Hor, H.A.E. Schmidt, eds., Schattauer Verlag, New York, 1975, pp. 837-848.
49. Hammersley, P.A.G., Taylor, D.M., The effect of the administration of iron on gallium 67 citrate uptake in tumors. *Br. J. Radiol.* 53:563-571, 1980.
50. Halpern, S.E., Hagan, P.L., Chauncey, D., et al., The effect of certain variables on the tumor and tissue distribution of tracers. Part 1: Carrier. *Invest. Rad.* 14:482-492, 1979.
51. Heidenreich, P., Kreigel, H., Hor, G., Biologische untersuchungen zur verteilung von  $^{67}\text{Ga}$ -Zitrat an ratten in abhangigkeit von geschlecht und applikationsart. *Int. J. Appl. Radiat. Isot.* 25:557-565, 1974.
52. Watson, E.E., Cloutier, R.J., Gibbs, W.B., Whole body retention of  $^{67}\text{Ga}$  citrate. *J. Nucl. Med.* 14:840-842, 1973.
53. Hayes, R.L., Szymendera, J.J., Byrd, B.L., Effect of food intake on the tissue distribution of gallium-67. *J. Nucl. Med.* 20:938-940, 1979.
54. Otten, J.A., Tyndall, R.L., Estes, P.C., et al., Localization of gallium-67 during embryogenesis. *Proc. Soc. Expl. Biol.* 142:92-95, 1973.
55. Newman, R.A., Gallagher, J.G., Clements, J.P., et al., Demonstration of Ga-67 localization in human placenta. *J. Nucl. Med.* 19:504-506, 1978.
56. Fogh, J.,  $^{67}\text{Ga}$ - accumulation in malignant tumors and in the prelactating or lactating breast. *Proc. Soc. Exp. Biol.* 138:1086-1090, 1971.



57. Kim, Y.C., Brown, M.L., Thrall, J.H., Scintigraphic patterns of gallium-67 uptake in the breast. *Radiology* 124:169-175, 1977.
58. Gelrud, L.G., Arseneau, J.C., Milder, M.S., et al., The kinetics of  $^{67}\text{Ga}$  incorporation into inflammatory lesions: experimental and clinical studies. *J. Lab. Clin. Med.* 83:489-495, 1974.
59. Lentle, B.C., Scott, J.R., Noujaim, A.A., et al., Iatrogenic alterations in radionuclide distributions. *Semin. Nucl. Med.* 9:131-143, 1979.
60. Lentle, B.C., Mallet-Paret, S., Shysh, A., et al., Influence of cutaneous BCG on biodistribution of radiogallium. *Ann. Roy. Coll. Phys. Surg. Canada* 12:69, 1979.
61. Bilgi, C., Brown, N.E., McPherson, T.A., et al., Pulmonary manifestations in patients with malignant melanoma during BCG immunotherapy. A preliminary report. *Chest* 75:685-687, 1979.
62. Fletcher, J.W., Herbig, F.K., Donati, R.M.,  $^{67}\text{Ga}$  citrate distribution following whole-body irradiation or chemotherapy. *Radiology* 117:709-712, 1975.
63. Ito, Y., Okuyama, S., Awano, T., et al., Diagnostic evaluation of  $^{67}\text{Ga}$  scanning of lung cancer and other diseases. *Radiology* 101: 355-362, 1971.
64. Higasi, T., Nakayama, Y., Murata, A., et al., Clinical evaluation of  $^{67}\text{Ga}$  citrate scanning. *J. Nucl. Med.* 13:196-201, 1972.
65. Kondo, M., Hashimoto, S., Kubo, A., et al.,  $^{67}\text{Ga}$  scanning in the evaluation of esophageal carcinoma. *Radiology* 131:723-726, 1979.
66. Swartzendruber, D.C., Hubner, K.F., Effect of external whole-body X-irradiation on gallium-67 retention in mouse tissues. *Rad. Res.* 55:457-468, 1973.
67. Bradley, W.P., Alderson, P.O., Eckelman, W.C., et al., Decreased tumor uptake of gallium-67 by animals after whole-body irradiation. *J. Nucl. Med.* 19:204-209, 1978.
68. Hayes, R.L., Byrd, B.L., Rafter, J.J., et al., The effect of scandium on the tissue distribution in normal tumor-bearing rodents. *J. Nucl. Med.* 21:361-365, 1980.
69. Hill, J.H., Merz, T., Wagner Jr., H.N., Iron-induced enhancement of  $^{67}\text{Ga}$  uptake in a model human leukocyte culture system. *J. Nucl. Med.* 16:1183-1186, 1975.
70. Oster, Z.H., Larson, S.M., Wagner Jr., H.N., Possible enhancement of  $^{67}\text{Ga}$  citrate imaging by iron dextran. *J. Nucl. Med.* 17:356-358, 1976.





71. Larson, S.M., Rasey, J.S., Grumbaum, Z., et al., Pharmacologic enhancement of gallium-67 tumor-to-blood ratios for EMT-6 sarcoma (BALB/c mice). *Radiology* 130:241-244, 1979.
72. Bradley, W.P., Alderson, P.O., Weiss, J.F., Effect of iron deficiency on the bio-distribution and tumor uptake of Ga-67 in animals. *J. Nucl. Med.* 20:243-247, 1979.
73. Sephton, R., Martin, J.J., Modification of distribution of gallium 67 in man by administration of iron. *Br. J. Radiol.* 53:572-575, 1980.
74. Sephton, R., Martin, J.,  $^{67}\text{Ga}$  imaging incorporating administration of iron. *Int. J. Nucl. Med. Biol.*, in press.
75. Smith, F.W., Dendy, P.P., Pocklington, T., et al., A preliminary investigation of  $^{67}\text{Ga}$  citrate distribution in hyperferraemic patients. *Eur. J. Nucl. Med.* 5:327-332, 1980.
76. Oster, Z.H., The effect of deferoxamine-mesylate (Desferal) on the biodistribution of gallium-67 citrate. *J. Nucl. Med.* 19:732, 1978. (Abstract)
77. Oster, Z.H., Som, P., Sacker, D.F., et al., The effect of deferoxamine mesylate on gallium-67 distribution in normal and abcess-bearing animals. *J. Nucl. Med.* 21:421-425, 1980.
78. Hoffer, P.B., Samuel, A., Bushberg, T., et al., Effect of desferoxamine on tissue and tumor retention of gallium-67. *J. Nucl. Med.* 20:248-251, 1979.
79. Hoffer, P.B., Samuel, A., Bushberg, T., et al., Desferoxamine mesylate (Desferal): A contrast-enhancing agent for gallium-67 imaging. *Radiology* 131:775-779, 1979.
80. Hayes, R.L., Radioisotopes of gallium, in "Radioactive Pharmaceuticals", G.A. Andrews, R.M. Knisely, H.N. Wagner Jr., eds., U.S. Atomic Energy Commission, Oak Ridge, 1966, pp. 603-618.
81. Anghileri, L.J., Prpic, B., A new colloidal  $\text{Ga}^{68}$ -compound for liver scanning. *Int. J. Appl. Radiat. Isot.* 18:734-735, 1967.
82. Anghileri, L.J., A new  $^{68}\text{Ga}$ -compound for kidney scanning. *Int. J. Appl. Rad. Isot.* 19:421-422, 1968.
83. Goulet, R.T., Shysh, A., Noujaim, A.A., Investigation of  $^{68}\text{Ga}$ -tripolyphosphate as a potential bone-scanning agent. *Int. J. Appl. Radiat. Isot.* 26:195-199, 1975.



84. Hnatowich, D.J., Clancy, B., Investigations of a new, highly negative liposome with improved biodistribution for imaging. *J. Nucl. Med.* 21:662-669, 1980.
85. Munn, J.I., Walters, N.H., Dudley, H.C., Urinary excretion of gallium by man and animals. *J. Lab. Clin. Med.* 37:676-682, 1951.
86. Bruner, H.D., Gray, J., Root, S.W., Studies of the urinary excretion of gallium<sup>72</sup> in man. *Radiology* 61:588-590, 1953.
87. Zivanovic, M.A., Taylor, D.M., McCready, V.R., The chemical form of gallium-67 in urine. *Int. J. Nucl. Med. Biol.* 5:97-100, 1978.
88. Zivanovic, M.A., McCready, V.R., Taylor, D.M., The urinary excretion of gallium-67 citrate in patients with neoplastic disease. *Eur. J. Nucl. Med.* 4:277-282, 1979.
89. Chen, D.C., Scheffel, U., Camargo, E.E., et al., The source of gallium-67 in gastrointestinal contents. *J. Nucl. Med.* 21:1146-1150, 1980.
90. Swartzendruber, D.C., Nelson, B., Hayes, R.L., Gallium-67 localization in lysosomal-like granules of leukemic and non-leukemic murine tissues. *J. Natl. Cancer Inst.* 46:941-952, 1971.
91. Brown, D.H., Swartzendruber, D.C., Carlton, J.E., et al., The isolation and characterization of gallium-binding granules from soft tissue tumors. *Cancer Res.* 33:2063-2067, 1973.
92. Aulbert, E., Haubold, U., Isolation of the <sup>67</sup>Ga accumulating fraction in normal rat liver. *Nuklearmedizin* 13:72-84, 1974.
93. Takeda, S., Uchida, T., Matsuzawa, T., A comparative study on lysosomal accumulation of gallium-67 and indium-111 in Morris hepatoma 7316A. *J. Nucl. Med.* 18:835-839, 1977.
94. Takeda, S., Okuyama, S., Takusagawa, K., et al., Lysosomal accumulation of gallium-67 in Morris hepatoma-7316A and Shionogi mammary carcinoma-115. *Gann* 69:267-271, 1978.
95. Orij, H., Tumor scanning with gallium (<sup>67</sup>Ga) and its mechanisms studied in rats. *Strahlentherapie* 144:192-200, 1972.
96. Bichel, P., Hansen, H.H., The incorporation of <sup>67</sup>Ga in normal and malignant cells and its dependence on growth rate. *Br. J. Radiol.* 45:182-184, 1972.



97. Brown, D.H., Byrd, B.L., Carlton, J.E., et al. A quantitative study of the sub-cellular localization of  $^{67}\text{Ga}$ . *Cancer Res.* 36:956-963, 1976.
98. Samezima, K., Orii, H., *In vivo* localization of Ga-citrate in rat liver as determined by cell fractionation with isopycnic rate-zonal centrifugation. *Eur. J. Nucl. Med.* 5:281-288, 1980.
99. Pierrez, J., Bertrand, A., The fixation of gallium. *J. Nucl. Med.* 20:456-457, 1979.
100. Aulbert, E., Gebhardt, A., Schulz, E., et al., Mechanism of  $^{67}\text{Ga}$  accumulation in normal rat liver lysosomes. *Nuklearmedizin* 15:185-194, 1976.
101. Hayes, R.L., Carlton, J.E., A study of the macromolecular binding of  $^{67}\text{Ga}$  in normal and malignant animal tissues. *Cancer Res.* 33:3265-3272, 1973.
102. Lawless, D., Brown, D.H., Hubner, K.F., et al., Isolation and partial characterization of a  $^{67}\text{Ga}$ -binding glycoprotein from Morris 5123C rat hepatoma. *Cancer Res.* 38:4440-4444, 1978.
103. Larson, S., Role of transferrin in gallium uptake. *Int. J. Nucl. Med. Biol.*, in press.
104. Mason, D.Y., Taylor, C.R., Distribution of transferrin, ferritin, and lactoferrin in human tissues. *J. Clin. Pathol.* 31:316-327, 1978.
105. Giler, S., Moroz, C., The significance of ferritin in malignant diseases. *Biomedicine* 28:203-206, 1978.
106. Siimes, M.A., Wang, W.C., Dallman, P.R., Elevated serum ferritin in children with malignancies. *Scand. J. Haematol.* 19:153-158, 1978.
107. Hazard, J.T., Drysdale, J.W., Ferritinaemia in cancer. *Nature* 265:755-756, 1977.
108. Birgegard, G., Hallgren, R., Killander, A., et al., Serum ferritin during infection. *Scand. J. Haematol.* 21:333-340, 1978.
109. Orii, H., Samezima, K., Nakamura, K., Gallium localization in liver cells: lysosomal uptake of Ga-67 and the negative role of ferritin in *in vivo* gallium transport. *Int. J. Nucl. Med. Biol.* in press.
110. Lentle, B.C., Garrecht, B., Schmidt, R., et al., A difference between patients with and without tumor uptake of radiogallium. *Int. J. Nucl. Med. Biol.*, in press.
111. Weiner, R., Schreiber, G., Hoffer, P.B., et al., The relative stabilities of Ga-67 complexes of lactoferrin and transferrin at various pH's. *Int. J. Nucl. Med. Biol.*, in press.



112. deVet, B.J.C.M., tenHooften, C.H., Lactoferrin in human neutrophilic polymorphonuclear leukocytes in relation to iron metabolism. *Acta. Med. Scand.* 203:197-203, 1978.
113. Hoffer, P.B., Miller-Catchpole, R., Turner, D.A., Demonstration of lactoferrin in tumor tissue from patients with positive gallium scans. *J. Nucl. Med.* 20:424-427, 1979.
114. Winchell, H.S., Mechanisms for localization of radiopharmaceuticals in neoplasms. *Semin. Nucl. Med.* 6:371-378, 1976.
115. Gams, R.A., Webb, J., Glickson, J.D., Serum inhibition of *in vitro*  $^{67}\text{Ga}$  binding by L1210 leukemic cells. *Cancer Res.* 35:1422-1426, 1975.
116. Sephton, R.G., Harris, A.W., Gallium-67 citrate uptake by cultured tumor cells, stimulated by serum transferrin. *J.N.C.I.* 54:1263-1266, 1975.
117. Harris, A.W., Sephton, R.G., Transferrin promotion of  $^{67}\text{Ga}$  and  $^{59}\text{Fe}$  uptake by cultured mouse myeloma cells. *Cancer Res.* 37:3634-3638, 1977.
118. Sephton, R.G., Kraft, N.,  $^{67}\text{Ga}$  and  $^{59}\text{Fe}$  uptakes by cultured human lymphoblasts and lymphocytes. *Cancer Res.* 38:1213-1216, 1978.
119. Noujaim, A.A., Lentle, B.C., Hill, J.R., et al., On the role of transferrin in the uptake of gallium by tumor cells. *Int. J. Nucl. Med. Biol.* 6:193-199, 1979.
120. Larson, S.M., Rasey, J.S., Allen, D.R., et al., A transferrin-mediated uptake of gallium-67 by EMT-6 sarcoma. I. Studies in tissue culture. *J. Nucl. Med.* 20:837-842, 1979.
121. Rogers, J.A., Noujaim, A.A., Gallium-67 transport across artificial biological membranes. *Int. J. Nucl. Med. Biol.*, in press.
122. Fernandez-Pol, J.A., Peptide and protein complexes of transition metals as modulators of cellular replication. *Int. J. Nucl. Med. Biol.*, in press.
123. Sephton, R.G., Hodgson, G.S., DeAbrew, S., et al., Ga-67 and Fe-59 distributions in mice. *J. Nucl. Med.* 19:930-935, 1978.
124. Turner, U.K., Noujaim, A.A., Lentle, B.C., et al., The effects of differing gallium-transferrin-anion complexes on the tumor uptake of gallium-67. *Int. J. Nucl. Med. Biol.*, in press.
125. Hayes, R.L., Nelson, B., Swartzendruber, D.C., et al., Gallium-67 localization in rat and mouse tumors. *Science* 167:289-290, 1970.





126. Nash, A.G., Dance, D.R., McCready, V.R., et al., Uptake of gallium-67 in colonic and rectal tumors. *Br. Med. J.* 3:508-510, 1972.
127. Hagan, P.L., Chauncey, D.M., Halpern, S.E., et al., Comparison of viable and non-viable tumor uptake of Sc-46, Mn-54, Zn-65, In-111, and Au-195 with Ga-67 citrate in a hepatoma model. *Eur. J. Nucl. Med.* 2:225-230, 1977.
128. Suzuki, T., Honjo, I., Hamamoto, K., et al., Positive scintiphotography of cancer of the liver with  $^{67}\text{Ga}$  citrate. *Am. J. Roentgenol. Radium Ther. Nucl. Med.* 113:92-103, 1971.
129. Yeh, S.D., Helson, L., Grando, R., Tumor-localizing radionuclides in hetero-transplanted human tumors in nude mice. *Int. J. Nucl. Med. Biol.* 6:169-173, 1979.
130. Tzen, K.-Y., Oster, Z.H., Wagner, H.N., et al., Role of iron-binding proteins and enhanced capillary permeability on the accumulation of gallium-67. *J. Nucl. Med.* 21:31-35, 1980.
131. Driedger, A.A., Sutherland, R.M., Stroude, E., et al., Concentration of gallium-67 by V-79 multicellular spheroids. *Int. J. Nucl. Med. Biol.*, in press.
132. Hammersley, P.A.G., Cauchi, M.N., Taylor, D.M., Uptake of  $^{67}\text{Ga}$  in the regenerating rat liver and its relationship to lysosomal enzyme activity. *Cancer Res.* 35:1154-1158, 1975.
133. Hammersley, P.A.G., Taylor, D.M., The role of lysosomal enzyme activity in the localization of  $^{67}\text{Ga}$  citrate. *Eur. J. Nucl. Med.* 4:261-270, 1979.
134. Winchell, W.S., Sanchez, P.D., Watanabe, C.K., et al., Visualization of tumors in humans using  $^{67}\text{Ga}$  citrate and the Anger whole-body scanner, scintillation camera, and tomographic scanner. *J. Nucl. Med.* 11:459-466, 1970.
135. Vallabhajosula, S.R., Harwig, J.F., Wolf, W., The mechanism of tumor localization of gallium-67 citrate: the role of transferrin binding and the effect of tumor pH. *Int. J. Nucl. Med. Biol.*, in press.
136. Orii, H., Nakamura, K., The mechanism of adsorption of Ga-67 citrate to cultured cells. *Eur. J. Nucl. Med.* 5:155-158, 1980.
137. Anghileri, L.J., Studies on the accumulation mechanisms of radioisotopes used in tumor diagnostic. *Strahlentherapie* 142:456-462, 1971.
138. Anghileri, L.J., Role of the tumor phospholipids in the accumulation of  $^{67}\text{Ga}$  citrate. *J. Nucl. Biol. Med.* 16:21-23, 1972.



139. Anghileri, L.J., The effects of gallium ( $\text{Ga}^{3+}$ ) on radiocalcium metabolism in tumors. *J. Nucl. Biol. Med.* 17:1-4, 1973.
140. Anghileri, L.J., Heidbreder, M., On the mechanism of accumulation of  $^{67}\text{Ga}$  by tumors. *Oncology* 34:74-77, 1977.
141. Muranaka, A., Ito, Y., Hashimoto, M., et al., Uptake and excretion of  $^{67}\text{Ga}$ -citrate in malignant tumors and normal cells. *Eur. J. Nucl. Med.* 5:31-37, 1980.
142. Larson, S.M., Hoffer, P.B., Normal patterns of localization, in "Gallium-67 Imaging", P.B. Hoffer, C. Bekerman, R.E. Henkin, eds., John Wiley and Sons, New York, 1978, pp. 24-38.
143. Pinskey, S.M., Henkin, R.E., Gallium-67 tumor scanning. *Semin. Nucl. Med.* 6:397-409, 1976.
144. Camargo, E.E., Johnston, G.S., Larson, S.M., et al., Tumors, in "Textbook of Nuclear Medicine: Clinical Applications", A.F.G. Rocha, J.C. Harbert, eds., Lea and Febiger, Philadelphia, 1979, pp. 440-455.
145. Zeman, R.K., Ryerson, T.W., The value of bowel preparation in Ga-67 citrate scanning. *J. Nucl. Med.* 18:886-889, 1977.
146. Handmaker, H., O'Mara, R.E., Gallium imaging in pediatrics.. *J. Nucl. Med.* 18:1057-1063, 1977.
147. Hoffer, P.B., The utility of gallium-67 in tumor imaging: a comment on the final reports of the cooperative study group. *J. Nucl. Med.* 19:1082-1084, 1978.
148. Turner, D.A., Fordham, E.W., Slayton, R.E., Malignant lymphoma, in "Gallium-67 Imaging", P.B. Hoffer, C. Bekerman, R.E. Henkin, eds., John Wiley and Sons, New York, 1978, pp. 95-112.
149. Turner, D.A., Fordham, E.W., Ali, A., et al., Gallium-67 imaging in the management of Hodgkin's disease and other malignant lymphomas. *Semin. Nucl. Med.* 8:205-219, 1978.
150. Hoffer, P.B., Status of gallium-67 in tumor detection. *J. Nucl. Med.* 21:394-398, 1980.
151. Johnston, G.S., Go, M.F., Benua, R.S., et al., Gallium-67 citrate imaging in Hodgkin's disease: final report of a cooperative group. *J. Nucl. Med.* 18:692-698, 1977.
152. Martin, J.J., Sephton, R.G., Gallium-67 scanning in the malignant lymphomas. *Aust. Radiol.* 22:340-346, 1978.



153. Yeh, S.D.J., Benua, R.S., Tan, C.T.C., Gallium scan in recurrent Hodgkin's disease in children. *Clin. Nucl. Med.* 4:359-367, 1979.
154. Andrews, G.A., Hubner, K.F., Greenlaw, R.H., Ga-67 citrate imaging in malignant lymphoma: final report of a cooperative group. *J. Nucl. Med.* 19:1013-1019, 1978.
155. Brown, M.L., O'Donnell, J.B., Thrall, J.H., et al., Gallium-67 scintigraphy in untreated and treated non-Hodgkin's lymphomas. *J. Nucl. Med.* 19:875-879, 1978.
156. Longo, D.L., Schilsky, R.L., Blei, L., et al., Gallium-67 scanning: limited usefulness in staging patients with non-Hodgkin's lymphoma. *A.J. Med.* 68:695-700, 1980.
157. Rudders, R.A., McCaffrey, J.A., Kahn, P.C., The relative roles of gallium-67-citrate scanning and lymphangiography in the current management of non-Hodgkin's lymphoma. *Cancer* 40:1439-1443, 1977.
158. Johnston, G.S., Clinical applications of gallium in oncology. *Int. J. Nucl. Med. Biol.*, in press.
159. Richman, S.D., Appelbaum, F., Levenson, S.M., et al., <sup>67</sup>Ga radionuclide imaging in Burkitt's lymphoma. *Radiology* 117:639-645, 1975.
160. Milder, M.S., Glick, J.H., Henderson, E.S., et al., <sup>67</sup>Ga scintigraphy in acute leukemia. *Cancer* 32:803-808, 1973.
161. Arseneau, J.C., Aamodt, R., Johnston, G.S., et al., Evidence for granulocytic incorporation of <sup>67</sup>gallium in chronic granulocytic leukemia. *J. Lab. Clin. Med.* 83:496-503, 1974.
162. Hoppin, E.C., Lewis, J.P., DeNardo, S.J., Bone marrow scintigraphy in the evaluation of acute nonlymphocytic leukemia. *Clin. Nucl. Med.* 4:296-301, 1979.
163. Bekerman, C., Hoffer, P.B., Other malignancies in which gallium-67 is useful: hepatoma, melanoma, and leukemia, in "Gallium-67 Imaging", P.B. Hoffer, C. Bekerman, R.E. Henkin, eds., John Wiley and Sons, New York, 1978, pp. 153-160.
164. Milder, M.S., Frankel, R.S., Bulkly, G.B., et al., Gallium-67 scintigraphy in malignant melanoma. *Cancer* 32:1350-1356, 1973.
165. Jackson, F.I., McPherson, T.A., Lentle, B.C., Gallium-67 scintigraphy in multi-system malignant melanoma. *Radiology* 122:163-167, 1977.



166. Romolo, J.L., Gross Fisher, S., Gallium<sup>67</sup> scanning compared with physical examination in the preoperative staging of malignant melanoma. *Cancer* 44:468-472, 1979.
167. Lomas, F., Dibos, P.E., Wagner Jr., H.N., Increased specificity of liver scanning with the use of <sup>67</sup>Ga-citrate. *N. Eng. J. Med.* 286:1323-1329, 1972.
168. Hamamoto, K., Torizuka, K., Mukai, T., et al., Usefulness of computer scintigraphy for detecting liver tumor with <sup>67</sup>Ga-citrate and the scintillation camera. *J. Nucl. Med.* 13:667-672, 1972.
169. Suzuki, T., Matsumoto, Y., Manabe, T., et al., Serum alpha-fetoprotein and Ga<sup>67</sup> citrate uptake in hepatoma. *Am. J. Roentgen. Rad. Ther. Nucl. Med.* 120:627-633, 1974.
170. Levin, J., Kew, M.C., Gallium-67 citrate scanning in primary cancer of the liver: diagnostic value in the presence of cirrhosis and relation to alpha-fetoprotein. *J. Nucl. Med.* 16:949-951, 1975.
171. Hauser, M.F., Alderson, P.O., Gallium-67 imaging in abdominal disease. *Semin. Nucl. Med.* 8:251-270, 1978.
172. Waxman, A.D., Richmond, R., Juttner, H., et al., Correlation of contrast angiography and histologic pattern with gallium uptake in primary liver-cell carcinoma: noncorrelation with alpha-fetoprotein. *J. Nucl. Med.* 21:324-327, 1980.
173. DeLand, F.H., Sauerbrunn, B.J.L., Boyd, C., et al., <sup>67</sup>Ga citrate imaging in untreated primary lung cancer: preliminary report of a cooperative group. *J. Nucl. Med.* 15:408-411, 1974.
174. DeMeester, T.R., Bekerman, C., Joseph, J.G., et al., Gallium-67 scanning for carcinoma of the lung. *J. Thorac. Cardiovasc. Surg.* 72:699-708, 1976.
175. Brereton, H.D., Line, B.R., Londer, H.N., et al., Gallium scans for staging small cell lung cancer. *JAMA* 240:666-667, 1978.
176. Siemsen, J.K., Grebe, S.F., Waxman, A.D., The use of gallium-67 in pulmonary disorders. *Semin. Nucl. Med.* 8:235-249, 1978.
177. Alazraki, N.P., Ramsdell, J.W., Taylor, A., et al., Reliability of gallium scan chest radiography compared to mediastinoscopy for evaluating mediastinal spread in lung cancer. *Am. Rev. Resp. Dis.* 117:415-420, 1978.
178. DeMeester, T.R., Golomb, H.M., Kirchner, P., et al., The role of gallium-67 scanning in the clinical staging and preoperative evaluation of patients with carcinoma of the lung. *Ann. Thorac. Surg.* 28:451-464, 1979.





179. Thesingh, C.W., Driessen, O.M.J., Daems, W.Th., et al., Accumulation and localization of gallium-67 in various types of primary lung carcinoma. *J. Nucl. Med.* 19:28-30, 1978.
180. Higashi, T., Wakao, H., Nakamura, K., et al., Quantitative gallium-67 scanning for predictive value in primary lung carcinoma. *J. Nucl. Med.* 21:628-632, 1980.
181. Bekerman, C., Lung carcinoma, in "Gallium-67 Imaging", P.B. Hoffer, C. Bekerman, R.E. Henkin, eds., John Wiley and Sons, New York, 1978, pp. 113-133.
182. Lesk, D.M., Wood, T.E., Carroll, S.E., et al., The application of  $^{67}\text{Ga}$  scanning in determining the operability of bronchogenic carcinoma. *Radiology* 128:707-709, 1978.
183. Fosburg, R.G., Hopkins, G.B., Kan, M.K., Evaluation of the mediastinum by gallium-67 scintigraphy in lung cancer. *J. Thorac. Cardiovasc. Surg.* 77:76-82, 1979.
184. Silberstein, E.B., Kornblut, A., Shumrick, D.A., et al.,  $^{67}\text{Ga}$  as a diagnostic agent for the detection of head and neck tumors and lymphoma. *Radiology* 110:605-608, 1974.
185. Teates, C.D., Preston, D.F., Boyd, C.M., Gallium-67 citrate imaging in head and neck tumors: report of cooperative group. *J. Nucl. Med.* 21:622-627, 1980.
186. Higashi, T., Aoyama, W., Mori, Y., et al., Gallium-67 scanning in the differentiation of maxillary sinus carcinoma from chronic maxillary sinusitis. *Radiology* 123:117-122, 1977.
187. Higashi, T., Kashima, I., Shimura, K., et al., Gallium-67 scanning in the evaluation of therapy of malignant tumors of the head and neck. *J. Nucl. Med.* 18:243-249, 1977.
188. Hoffer, P.B., Pinskey, S.M., Organ systems in which gallium-67 is of limited utility, in "Gallium-67 Imaging", P.B. Hoffer, C. Bekerman, R.E. Henkin, eds., John Wiley and Sons, New York, 1978, pp. 161-167.
189. Richman, S.D., Ingle, J.N., Levenson, S.M., et al., Usefulness of gallium scintigraphy in primary and metastatic breast carcinoma. *J. Nucl. Med.* 16:996-1001, 1975.
190. Teates, C.D., Bray, S.T., Williamson, B.R.J., Tumor detection with  $^{67}\text{Ga}$ -citrate: a literature survey (1970-1978). *Clin. Nucl. Med.* 3:456-460, 1978.



191. Frankel, R.S., Jones, A.E., Cohen, J.A., et al., Clinical correlations of  $^{67}\text{Ga}$  and skeletal whole body radionuclide studies with radiography in Ewing's sarcoma. *Radiology* 110:597-603, 1974.
192. Sauerbrunn, B.J.L., Andrews, G.A., Hubner, K.F., Ga-67 citrate imaging in tumors of the genito-urinary tract: report of cooperative study. *J. Nucl. Med.* 19:470-475, 1978.
193. Bailey, T.B., Pinskey, S.M., Mittemeyer, B.T., et al., A new adjunct in testis tumor staging: gallium-67 citrate. *J. Urol.* 110:307-310, 1973.
194. Paterson, A.H.G., Peckham, M.J., McCready, V.R., Value of gallium scanning in seminoma of the testis. *Br. Med. J.* 1:1118-1121, 1976.
195. Bloomfield, R.D., Wilfrido, M.Sy., Yoon, T., et al., The use of  $^{67}\text{Ga}$  citrate in gynecologic malignancies. *Gynecol. Oncol.* 6:130-137, 1978.
196. Jackson, F.I., Dierich, H.C., Lentle, B.C., Gallium-67 citrate scintiscanning in testicular neoplasia. *J. Can. Assoc. Radiol.* 27:84-88, 1976.
197. Douds, H.N., Berens, S.V., Long, R.F., et al.,  $^{67}\text{Ga}$ -citrate scanning in gastrointestinal malignancies. *Clin. Nucl. Med.* 3:179-183, 1978.
198. Lentle, B.C., Dierich, H.C., Castor, W.R.,  $^{67}\text{Ga}$ -citrate in detecting recurrent rectal carcinoma after abdomino-perineal resection. *J. Can. Assoc. Radiol.* 30:165-166, 1979.
199. Kondo, M., Hashimoto, S., Kubo, A., et al.,  $^{67}\text{Ga}$  scanning in the evaluation of esophageal carcinoma. *Radiology* 131:723-726, 1979.
200. Lepanto, P.B., Rosenstock, J., Littman, P., et al., Gallium-67 scans in children with solid tumors. *A.J.R.* 126:179-186, 1976.
201. Bekerman, C., Port, R.B., Pang, E., et al., Scintigraphic evaluation of childhood malignancies by  $^{67}\text{Ga}$ -citrate. *Radiology* 127:719-725, 1978.
202. Bekerman, C., Childhood malignancies, in "Gallium-67 Imaging", P.B. Hoffer, C. Bekerman, R.E. Henkin, eds., John Wiley and Sons, New York, 1978, pp. 139-152.
203. Edeling, C.J., Tumor visualization using  $^{67}\text{Ga}$  gallium scintigraphy in children. *Radiology* 127:727-731, 1978.
204. Yang, S.L., Alderson, P.O., Kaizer, H.A., et al., Serial Ga-67 citrate imaging in children with neoplastic disease. *J. Nucl. Med.* 20:210-214, 1979.



205. Lavender, J.P., Lowe, J., Barker, J.R., et al., Gallium-67 citrate scanning in neoplastic disease. *Br. J. Radiol.* 44:361-366, 1971.
206. Littenberg, R.L., Takeda, R.M., Alazraki, N.P. et al., Gallium-67 for localization of septic lesions. *Ann. Intern. Med.* 79:403-406, 1973.
207. Hoffer, P.B., Gallium: mechanisms. *J. Nucl. Med.* 21:282-285, 1980.
208. Hoffer, P.B., Use of gallium-67 for detection of inflammatory diseases: a brief review of mechanisms and clinical applications. *Int. J. Nucl. Med. Biol.*, in press.
209. Burleson, R.L., Johnson, M.C., Head, H., *In vitro* and *in vivo* labelling of rabbit blood leukocytes with  $^{67}\text{Ga}$ -citrate. *J. Nucl. Med.* 15:98-101, 1974.
210. Burleson, R.L., Holman, B.L., Tow, D.E., Scintigraphic demonstration of abscesses with radioactive labelled leukocytes. *Surg. Gynecol. Obstet.* 141:379-382, 1975.
211. Hammersley, P.A.G., Taylor, D.M., The mechanism of the localization of  $^{67}\text{Ga}$  citrate in experimental abscesses. *Eur. J. Nucl. Med.* 4: 271-275, 1979.
212. Tsan, M.-F., Chen, W.Y., Scheffel, U., et al., Studies on gallium accumulation in inflammatory lesions: I. Gallium uptake by human polymorphonuclear leukocytes. *J. Nucl. Med.* 19:36-43, 1978.
213. Camargo, E.E., Wagner Jr., H.N., Tsan, M.-F., Studies of gallium accumulation in inflammatory lesions. IV. Kinetics of accumulation and role of polymorphonuclear leukocytes in the distribution of gallium in experimental inflammatory lesions. *Nucl. Med.* 18:147-150, 1979.
214. Ostroy, F., Johnston, R.B., Gams, R.A., Effect of hypoxia on  $^{67}\text{Ga}$  incorporation into human granulocytes. *Cancer Res.* 39:4971-4974, 1979.
215. Tsan, M.-F., Studies on gallium accumulation in inflammatory lesions. II. Roles of polymorphonuclear leukocytes and bacteria. *J. Nucl. Med.* 19:492-495, 1978.
216. Dhawan, V.M., Sziklas, J.J., Spencer, R.P., Localization of Ga-67 in inflammations in the absence of circulating polymorphonuclear leukocytes. *J. Nucl. Med.* 19:292-294, 1978.
217. Turner, U.K., Wong, H., Noujaim, A., et al., Differential uptake of  $^{67}\text{Ga}$  in canine tumors and abscesses, in "Radiopharmaceuticals II: Proceedings of the Second International Symposium on Radiopharmaceuticals", V.J. Sodd, D.R. Allen, D.R. Hoogland, R.D. Ice, eds., Society of Nuclear Medicine, New York, 1979, pp. 309-319.



218. Henkin, R.E., Gallium-67 in the diagnosis of inflammatory disease, in "Gallium-67 Imaging", P.B. Hoffer, C. Bekerman, R.E. Henkin, eds., John Wiley and Sons, New York, 1978, pp. 65-92.
219. Staab, E.V., McCartney, W.H., Role of gallium-67 in inflammatory disease. *Semin. Nucl. Med.* 8:219-234, 1978.
220. Hoffer, P.B., Gallium and infection. *J. Nucl. Med.* 21:484-488, 1980.
221. Cloutier, R.J., Watson, E.E., Hayes, R.L., et al., MIRD/Dose estimate report no. 2. Summary of current radiation dose estimates to humans from  $^{66}\text{Ga}$ ,  $^{67}\text{Ga}$ ,  $^{68}\text{Ga}$ , and  $^{72}\text{Ga}$ -citrate, *J. Nucl. Med.* 14:755-756, 1973.
222. Prasad, A.S., in "Trace Elements and Iron in Human Metabolism", M.M. Wintrobe, ed., Plenum Publishing Co., New York, 1978, pp. 84-89.
223. Pollycove, M., Tono, M., Studies of the erythron. *Semin. Nucl. Med.* 5:11-61, 1975.
224. Ricketts, C., Cavill, I., Ferrokinetics: methods and interpretation. *Clin. Nucl. Med.* 3:159-164, 1978.
225. Cloutier, R.J., Watson, E.E., Radioation dose from radioisotopes in the blood, in "Medical Radionuclides: Radiation Dose and Effects", R.J. Cloutier, C.L. Edwards, W.S. Snyder, eds., U.S. Atomic Energy Commission, Oak Ridge, 1970, pp. 337-341.
226. Morgan, E.H., Transferrin and transferrin iron, in "Iron in Biochemistry and Medicine", A. Jacobs, M. Worwood, eds., Academic Press, London, 1974, pp. 29-71.
227. Aisen, P., Brown, E.B., The iron-binding function of transferrin in iron metabolism. *Semin. Hematol.* 14:31-53, 1977.
228. Luk, C.K., Study of the nature of the metal-binding sites and estimate of the distance between the metal-binding sites in transferrin using trivalent lanthanide ions as fluorescent probes. *Biochemistry* 10:2838-2843, 1971.
229. Frieden, E., Aisen, P., Forms of iron transferrin. *TIBS* 5:11, 1980.
230. Bates, G.W., Schlabach, M.R., The nonspecific binding of  $\text{Fe}^{3+}$  to transferrin in the absence of synergistic anions. *J. Biol. Chem.* 250:2177-2181, 1975.
231. Donovan, J.W., Differences between ovotransferrin and human serum transferrin in structural and metal-binding cooperativity, in "Proteins of Iron Metabolism", E.B. Brown, ed., Grune and Stratton, New York, 1977, pp. 179-186.





232. Aisen, P., Leibman, A., Zweier, J., Stoichiometric and site characteristics of the binding of iron to human transferrin. *J. Biol. Chem.* 253:1930-1937, 1978.
233. Princiotto, J.V., Zapolski, E.J., Difference between the two iron-binding sites of transferrin. *Nature* 255:87-88, 1975.
234. Lestas, A.N., The effect of pH upon human transferrin: selective labelling of the two iron-binding sites. *Br. J. Haematol.* 32:341-350, 1976.
235. Harris, D.C., Different metal binding properties of the two sites of human transferrin. *Biochemistry* 16:560-564, 1977.
236. Bates, G.W., Schlabach, M.R., The reaction of ferric salts with transferrin. *J. Biol. Chem.* 248:3228-3232, 1973.
237. Okada, S., Rossman, M.D., Brown, E.B., The effect of acid pH and citrate on the release and exchange of iron on rat transferrin. *Biochim. Biophys. Acta.* 543:72-81, 1978.
238. Harris, D.C., Haroutunian, P.V., Gutman, S.M., Equivalence of the two sites of human transferrin upon reduction with dithionite. *Br. J. Haematol.* 37:302-303, 1977.
239. Carver, F.J., Frieden, E., Factors affecting the adenosine triphosphate induced release of iron from transferrin. *Biochemistry* 17:167-172, 1978.
240. Konopka, K., Differential effects of metal-binding agents on the uptake of iron from transferrin by isolated rat liver mitochondria. *FEBS Letters* 92:308-312, 1978.
241. Awai, M., Chipman, B., Brown, E.B., *In vivo* evidence for the functional heterogeneity of transferrin-bound iron. I. Studies in normal rats. *J. Lab Clin. Med.* 85:769-784, 1975.
242. Harris, D.C., Aisen, P., Iron-donating properties of transferrin. *Biochemistry* 14:262-268, 1975.
243. Harris, D.C., Functional equivalence of iron bound to transferrin at low pH or high pH. *Biochim. Biophys. Acta.* 496:563-565, 1977.
244. Tomimatsu, Y., Donovan, J.W., Spectrophotometric and differential scanning calorimetric measurements of Zn(II), Al(III) and Ga(III) binding to ovo- and human transferrin, in "Proteins of Iron Metabolism", E.B. Brown, ed., Grune and Stratton, New York, 1977, pp. 221-226.



245. Larson, S.M., Allen, D.R., Rasey, J.S., et al., Kinetics of binding of carrier-free Ga-67 to human transferrin. *J. Nucl. Med.* 19:1245-1249, 1978.
246. Verhoef, N.J., Noordeloos, P.J., Binding of transferrin and uptake of iron by rat erythroid cells *in vitro*. *Clin. Sci. Molec. Med.* 52:87-96, 1977.
247. van Bockxmeer, F.M., Morgan, E.H., Identification of transferrin receptors in reticulocytes. *Biochim. Biophys. Acta.* 468:437-450, 1977.
248. Leibman, A., Aisen, P., Transferrin receptor of the rabbit reticulocyte. *Biochemistry* 16:1268-1272, 1977.
249. Sly, D.A., Grohlich, D., Bezkorovainy, A., Transferrin receptor from rabbit reticulocyte membranes, in "Cell Surface Carbohydrate Chemistry", Academic Press, New York, 1978, pp. 255-268.
250. Witt, D.P., Woodworth, R.C., Identification of the transferrin receptor of the rabbit reticulocyte. *Biochemistry* 17:3913-3917, 1978.
251. van der Huel, C., Kroos, M.J., van Eijk, H.C., Binding sites of iron transferrin on rat reticulocytes. Inhibition by specific antibodies. *Biochim. Biophys. Acta.* 511:430-441, 1978.
252. Grohlich, D., Morley, C.G.D., Miller, R.J., et al., Iron incorporation into isolated rat hepatocytes. *Biochem. Biophys. Res. Commun.* 76:682-690, 1977.
253. Larson, S.M., Grunbaum, Z., Rasey, J.S., et al., A transferrin binding macromolecular component of EMT-6 sarcoma (BALB/c mice). *J. Nucl. Med.* 20:672, 1979.
254. Glass, J., Nunez, M.T., Fischer, S., et al., Transferrin receptors, iron transport and ferritin metabolism in Friend erythroleukemic cells. *Biochim. Biophys. Acta.* 542:154-162, 1978.
255. Hemmaplardh, D., Morgan, E.H., The role of endocytosis in transferrin uptake by reticulocytes and bone marrow cells. *Br. J. Haematol.* 36:85-96, 1977.
256. Nunez, M.T., Glass, J., Robinson, S.H., Mobilization of iron from the plasma membrane of the murine reticulocyte. The role of ferritin. *Biochim. Biophys. Acta.* 509:170-180, 1978.
257. Wallach, J., "Interpretation of Diagnostic Tests", 3rd edition, Little, Brown, and Co., Boston, 1978, pp. 9-10.
258. Glickson, J.D., Webb, J., Gams, R.A., Effects of buffers and pH on *in vitro* binding of <sup>67</sup>Ga by L1210 leukemic cells. *Cancer Res.* 34:2957-2960, 1974.



- 259. Larson, S.M., Mechanisms of localization of gallium-67 in tumors, *Semin. Nucl. Med.* 8:193-203, 1978.
- 260. Gibaldi, M., Perrier, D., "Pharmacokinetics", J. Swarbrick, ed., Marcel Dekker, Inc., New York, 1975, pp. 1-96.
- 261. Niazi, S., "Textbook of Biopharmaceutics and Clinical Pharmacokinetics", Appleton-Century-Crofts, New York, 1979, pp. 97-112, 141-151.
- 262. Wagner, J.G., "Biopharmaceutics and Relevant Pharmacokinetics", 1st edition, Drug Intelligence Publications, Hamilton, 1971, p. 271.
- 263. Wennesland, R., Brown, E., Hopper, J., et al., Red cell, plasma and blood volume in healthy men measured by radiochromium ( $\text{Cr}^{51}$ ) cell tagging and hematocrit: influence of age, somatotype and habits of physical activity on the variance after regression of volumes to height and weight combined. *J. Clin. Invest.* 38:1065-1077, 1959.



## APPENDICES





**APPENDIX A**  
**FACTORS AFFECTING THE GROSS DISTRIBUTION OF GALLIUM**



## APPENDIX A

FACTOR	MODEL	COMMENT *	REFERENCE
Time after administration	rats	1	48
	mice, rats	2	49
	rats	3	50
	autopsies of humans	4	46
Age	rats	5	48
	autopsies of humans	6	46
Gender	various rat species	7	48, 51
	autopsies of humans	8	46
	humans-whole body retention	9	52
Nutritional status	rats	10	53
	autopsies of humans	11	46
Pregnancy	mice	12	54
	human	13	55
Lactation	human	14	56, 57
Presence of tumor or inflammation	humans	15	45
	rabbits	16	58
	autopsies of humans	17	46
Chemotherapy:			
	General	18	45
	Cis-Platinum	18	59
	BCG immunotherapy	20	60
		21	61
Vincristine sulfate and mechlorethamine	rats	22	62
Antibiotic therapy	rabbits	23	44



## APPENDIX A . . . continued

FACTOR	MODEL	COMMENT *	REFERENCE
Exposure to ionizing radiation	humans	24	45,63-65
	mice	25	66
	rats	26	67
Carrier gallium	rats	27	41, 50
Alteration of protein binding (contrast enhancement)			
1. Scandium	mice and rats	28	48,49,68
2. Iron	human leukocytes	29	69
	rabbits	30	70
	mice	31	71
	mice and rats	32	49
	rats	33	72
	humans	34	73, 74
	humans	35	75
3. Desferioxamine mesylate (Desferal <sup>R</sup> )	rabbits	36	76, 77
	mice and rabbits	37	78, 79
	mice	38	71
Chemical Form:			
<sup>68</sup> Ga-EDTA	rats	39	80
<sup>68</sup> Ga-hydrous ferric oxide	rabbits	40	80
<sup>68</sup> Ga-chromic phosphate	rats	41	81
<sup>68</sup> Ga-polymetaphosphate-Mg-polymetaphosphate	rats	42	82
<sup>68</sup> Ga-tripolyphosphate	mice and rabbits	43	83
<sup>68</sup> Ga-oxine; Liposomes	mice	44	84

\* Comments made by the authors of the referenced literature.



## COMMENTS

1. A time-course study of  $^{67}\text{Ga}$ -citrate distribution in tumor-bearing rats demonstrated that the concentration of  $^{67}\text{Ga}$  in tumor, soft tissues, and bone did not vary significantly over 24 hours. However, blood activity continued to decline (48).
2. Tissue bound  $^{67}\text{Ga}$  was exchangeable with cold Ga six hours after administration, but was fixed by 24 hours (49).
3. Gallium-67 was fixed within both normal and malignant tissue by 19 hours after administration (50).
4. Many organ systems, the kidney in particular, but also bone marrow and bone, showed an initial high accumulation of  $^{67}\text{Ga}$ -citrate with a rapid decline followed by a slower decrease over several days (46).
5. Younger animals generally demonstrated increased uptake of  $^{67}\text{Ga}$ -citrate in bone, with a corresponding decreased uptake in soft tissues (48).
6. Autoradiograms of skeletal tissue from adolescent humans after administration of  $^{67}\text{Ga}$ -citrate demonstrated high accumulation of  $^{67}\text{Ga}$  in areas of bone growth, but no differences were observed in soft tissue distribution (46).
7. Difference in the gender of various species of rats influenced the gross distribution of  $^{67}\text{Ga}$ -citrate. Females tended to have decreased activity in the spleen, bone marrow, and muscle, and increased activity in the blood, liver and kidney (48, 51).
8. The effect of gender on tissue distribution was not apparent in autopsies of patients receiving  $^{67}\text{Ga}$ -citrate (46).
9. Whole-body retention, measured by a whole-body counter, was found to be significantly greater in human females than in males (52).
10. The degree of food intake was found to be a factor in the distribution of  $^{67}\text{Ga}$ -citrate in rats. Fasted animals showed a significantly increased uptake in liver, spleen, kidney, bone marrow and blood (53).
11. The nutritional status of patients had no apparent effect on  $^{67}\text{Ga}$ -citrate distribution, even in cases of emaciation (46).
12. The uptake of  $^{67}\text{Ga}$ -citrate in the spleen and liver of pregnant mice was not significantly different from that of virgin mice. Autoradiography revealed the localization of  $^{67}\text{Ga}$  in fetal tissues, which was related to the time of gestation (54).
13. The localization of  $^{67}\text{Ga}$ -citrate in human placenta was observed (55).





14. Intense uptake of  $^{67}\text{Ga}$ -citrate in the mammary gland was observed in both pathologic and nonpathologic cases (56, 57). Normal uptake occurred in 12% of all female patients, and was usually due to physiological changes relating to hormone status (56). Activity in the lactating breast was especially high (56).
15. High uptake in tumor was accompanied by a decrease in normal tissue accumulation (45).
16. The presence of an inflammatory process in rabbits resulted in decreased  $^{67}\text{Ga}$ -citrate in the blood and increased uptake in the liver, spleen and bone marrow, relative to control animals (58).
17. There was no decrease in the concentration of  $^{67}\text{Ga}$ -citrate in normal tissues in cases of high tumor uptake (46).
18. Chemotherapy decreased the uptake of  $^{67}\text{Ga}$ -citrate in tumors (45).
19. Concomitant therapy with cis-platinum or previous therapy within two weeks of the  $^{67}\text{Ga}$  scan resulted in abnormal  $^{67}\text{Ga}$ -citrate images. High blood radioactivity and greatly decreased liver accumulation was observed in all 14 patients. Increased uptake in bone, kidney and stomach were also observed in some patients. Although the patients were also taking other chemotherapeutic agents, these bizarre effects have not been observed for those drugs (bleomycin, vinblastine, or adriamycin) (59).
20. The intradermal injection of Bacillus Calmette-Guerin (BCG) in mice resulted in increased  $^{67}\text{Ga}$ -citrate accumulation in liver, spleen, kidney, alimentary tract, and injection sites, that could be correlated with the presence of BCG granulomata (60).
21. The diffuse bilateral uptake of  $^{67}\text{Ga}$ -citrate was observed in cases of BCG-induced pneumonitis (61).
22. There was a significant decrease in whole body retention upon administration of vincristine sulfate or mechlorethamine, accompanied by a significant decrease in soft tissue distribution, and increased urinary excretion (62).
23. Intensive antibiotic therapy decreased the accumulation of  $^{67}\text{Ga}$ -citrate in abscesses (44).
24. The radiotherapy of known tumor sites has been reported to significantly decrease the uptake of  $^{67}\text{Ga}$ -citrate by these tumors (45, 63-65).
25. Whole body irradiation of mice resulted in increased uptake in the femur, a transitory decreased retention of  $^{67}\text{Ga}$  in soft tissues, and a lower activity in blood. The distribution was most affected when  $^{67}\text{Ga}$ -citrate was administered 24 hours after irradiation (66).



26. Decreased tumor uptake was observed in rats subjected to whole body irradiation; irradiation of the whole body excluding the tumor-bearing limb produced similar results. However, irradiation of the tumor alone showed no difference in tumor uptake of  $^{67}\text{Ga}$ -citrate from the control group (67).
27. The effect of stable gallium on the *in vivo* distribution of  $^{67}\text{Ga}$ -citrate was first observed by Bruner *et al.* (41). A detailed study of the effect of 22 mg Ga/kg on the tissue distribution of  $^{67}\text{Ga}$ -citrate in hepatoma-bearing rats was recently reported by Halpern *et al.* (50). The following observations were made:
  - a) The distribution of  $^{67}\text{Ga}$  four hours after administration was significantly different in the carrier-treated animals. Decreased activity was observed in the blood, liver, spleen, heart, skeletal muscle, and both viable and nonviable tumor. Uptake in the bone and kidney was increased. The greatest effect was observed when the stable gallium was administered simultaneously with  $^{67}\text{Ga}$ -citrate. However, when carrier gallium was administered two hours after  $^{67}\text{Ga}$ -citrate, less activity was lost from viable and nonviable tumor compared to the decreased activity observed in the muscle and blood, resulting in increased tumor-to-blood and tumor-to-muscle ratios.
  - b) Administration of carrier gallium 19 to 23 hours after  $^{67}\text{Ga}$ -citrate did not produce significant changes in either soft tissue or bone accumulation of  $^{67}\text{Ga}$ -citrate compared to the control group. However, decreased blood levels resulted in higher tumor-to-blood ratios.
  - c) Bowel excretion of  $^{67}\text{Ga}$  remained relatively unchanged but renal excretion was increased significantly.
28. The administration of 0.5 mg Sc/kg as early as four hours before  $^{67}\text{Ga}$ -citrate has been shown to enhance relative  $^{67}\text{Ga}$ -citrate tumor uptake in rats (68). Similar to the effect of stable gallium, scandium resulted in decreased soft tissue accumulation accompanied by increased bone uptake and urinary excretion (48, 68). The uptake of  $^{67}\text{Ga}$  by the tumor was not affected, thereby increasing tumor-to-background ratios (48, 68). There was no uptake of scandium ( $^{46}\text{Sc}$ ) in the tumor (68). Similar results in tumor-bearing rats were reported by Hammersley *et al.* (49). However, they found that scandium decreased tumor uptake to a greater extent than uptake in normal tissues in tumor-bearing mice.
29. The previous addition of iron chloride or iron dextran to human leukocyte cell cultures increased the cellular accumulation of  $^{67}\text{Ga}$ -citrate (69).
30. Iron dextran decreased the whole-body retention of  $^{67}\text{Ga}$ -citrate in normal and abscess-bearing rabbits when it was administered 24 hours before, 24 hours after, or simultaneously with  $^{67}\text{Ga}$ -citrate. The highest abscess-to-muscle ratio was achieved by administration of iron dextran 24 hours after administration of  $^{67}\text{Ga}$ -citrate. (70).



31. Significant decreases in blood  $^{67}\text{Ga}$  radioactivity, and increased tumor-to-blood ratios, were observed upon injection of iron dextran at two, four, or 24 hours after  $^{67}\text{Ga}$ -citrate in mice. The greatest changes in biodistribution were observed when iron dextran was injected soon after the  $^{67}\text{Ga}$ -citrate. Liver uptake appeared to be increased (71).
32. Ferric ammonium citrate decreased the tumor and soft tissue uptake of  $^{67}\text{Ga}$ -citrate in mice and rats. The greatest effect was observed when the iron was administered prior to  $^{67}\text{Ga}$ -citrate. Administration of ferric ammonium citrate 24 hours after  $^{67}\text{Ga}$ -citrate did not decrease either tumor or soft tissue uptake of  $^{67}\text{Ga}$  (49).
33. Iron deficiency in rats resulted in increased  $^{67}\text{Ga}$ -citrate uptake in liver and spleen, increased urinary excretion and lower blood levels of  $^{67}\text{Ga}$ . Although there was no difference between iron-deficient and normal rats in the tumor uptake of  $^{67}\text{Ga}$ , the lower blood levels of  $^{67}\text{Ga}$  in the anemic animals resulted in higher tumor-to-blood ratios. The variable uptake in liver and spleen observed clinically may be related to serum iron levels and unsaturated iron-binding capacity (72).
34. Preliminary clinical studies on the effect of 50 – 100 mg of iron sorbitol administered intramuscularly three hours after  $^{67}\text{Ga}$ -citrate showed that of 14 patients, seven had early (six hr)  $^{67}\text{Ga}$ -citrate images that were comparable to 48 hour images, and less bowel activity was observed (73). Further investigation involving 64 patients, demonstrated that temporarily decreasing the unsaturated iron binding capacity by iron sorbitol did not increase the overall sensitivity of  $^{67}\text{Ga}$  imaging, but did decrease the time scale of the investigation in some patients (74).
35. The administration of 100 mg of iron sorbitol two hours prior to injection of  $^{67}\text{Ga}$ -citrate resulted in decreased activity in the abdomen on the 24 hour scan, with increased uptake in the skeleton. Overall, the rate of lesion detection at earlier times was high (75).
36. The administration of desferrioxamine to abscess-bearing rabbits 20 minutes after injection of  $^{67}\text{Ga}$ -citrate decreased the soft tissue uptake of  $^{67}\text{Ga}$  within five to eight minutes. No effect on abscess uptake occurred; thus, the abscess-to-background ratio was increased (76). The optimal target-to-nontarget ratio was achieved by administration of desferrioxamine between eight and 24 hours after  $^{67}\text{Ga}$ -citrate (77).
37. The simultaneous administration of desferrioxamine with  $^{67}\text{Ga}$ -citrate in mice decreased the uptake of  $^{67}\text{Ga}$  by most tissues (including tumor) to less than 1% of control values. Administration of desferrioxamine three hours after  $^{67}\text{Ga}$ -citrate resulted in  $^{67}\text{Ga}$  uptake values in most tissues of 10 – 20% of control values and tumor uptake 20% of the control value. Tumor-to-blood ratios were increased from 11:1 to 19:1, and marked increases in urinary excretion of  $^{67}\text{Ga}$  as a  $^{67}\text{Ga}$ -desferrioxamine mesylate complex was observed (78). In tumor-bearing mice, the





optimal time for the administration of desferrioxamine (intramuscularly) was 16 hours after  $^{67}\text{Ga}$ -citrate, as tumor-to-blood ratios were increased with only a slight decrease in the concentration of  $^{67}\text{Ga}$  (79). Similar results were observed in abscess-bearing rabbits. The blood clearance and whole body clearance of  $^{67}\text{Ga}$ -citrate decreased nonlinearly as the dose of desferrioxamine increased. The effect on blood clearance was greater than the effect on whole body retention (79).

38. The intravenous or intramuscular administration of desferrioxamine to mice caused the rapid clearance of  $^{67}\text{Ga}$ -citrate from the blood and increased tumor-to-blood ratios. The greatest effect was achieved by administration of desferrioxamine 24 hours after  $^{67}\text{Ga}$ -citrate (71).
39. When complexed to EDTA,  $^{68}\text{Ga}$  was rapidly removed from the blood with a half-life of about ten minutes. The complex was rapidly excreted in the urine and did not deposit in bone. At one-half hour after injection, the percent of injected dose per gram of tissue in the kidney was 1.12%; liver 0.10%; spleen 0.16%; lung 0.14%; and blood 0.19% (80).
40. Hydrous ferric oxide colloid labelled with  $^{68}\text{Ga}$  localized rapidly in the reticuloendothelial system, with high uptake in liver, spleen and bone marrow one hour after injection. There was little observed uptake in bone (80).
41. Chromic phosphate colloid labelled with  $^{68}\text{Ga}$  localized preferentially in the liver (greater than 90% of the injected radioactivity). Less than 1% of the injected dose was observed in the lung, bone and blood at one hour after administration (81).
42.  $^{68}\text{Ga}$ -polymetaphosphate-Mg-polymetaphosphate localized preferentially in the kidney one hour after administration, 40% of the injected dose was in the kidney, 3% in the liver, 29% in the blood and 0.2% in the femur (82).
43.  $^{68}\text{Ga}$ -tripolyphosphate localized preferentially in bone. In mice, there was about 50% of the injected dose in bone at six hours after administration. The addition of carrier gallium to the labelled phosphate decreased the activity in the lung and blood, and maximum bone uptake occurred at one hour. Images in rabbits showed both compounds were taken up into bone to a significant degree within 2 – 2.5 hours after injection. (83).
44. The biodistribution of  $^{67}\text{Ga}$ -oxine incorporated into the lipid phase of liposomes was affected by the liposome composition. The injection of  $^{67}\text{Ga}$ -oxine into mice resulted in high blood levels at two hours and high uptake in lung tissue. Gallium-67 lecithin liposomes were distributed to a great extent to the liver and spleen, with significant uptake in the lung, and high blood levels. Gallium-67 cardiolipin liposomes, which have a higher negative charge, demonstrated at least five times less uptake in the liver, and 20 times less uptake in the spleen, than the lecithin liposomes. Uptake in the blood, lung, and kidney were decreased and uptake in the kidney and muscle were increased (84).





## **APPENDIX B**

### **GALLIUM-67 / IRON-59 DATA CORRECTION PROGRAM**



## APPENDIX B

X?00.00

\*E A

\*C-FOCAL,69CE

\*

\*01.01 E

\*01.05 T !!!" GALLIUM-IRON DATA CORRECTION"!!!

\*01.07 A "SAMPLE ID",X

\*01.10 A !!"NO. OF DATA", N;A"" BKGD". BG,BR

\*01.13 A !"TIME TO START (HRS)", T;A"" COUNTING TIME (MIN)"TC

\*01.15 A !"CROSSOVER",C

\*01.17 T !"START TAPE"

\*01.20 F I=1,N;D 2

\*01.22 T !!!

\*01.25 Q

\*

\*02.10 P;A G;A R;S G=G-BG;S R=R-BR;P

\*02.12 I (G-O)2.5

\*02.13 I (R-O)2.7

\*02.16 S RS=R\*C;S G=G-RS;I (G-O)2.55

\*02.20 S G=G\*FEXP(.693147\*T/77.9)

\*02.22 S R=R\*FEXP(.693147\*T/1094.4)

\*02.27 I (I-2)2.8

\*02.30 G 2.85

\*02.50 S G=O;G 2.13

\*02.55 S G=O;G 2.22

\*02.70 S R=O;G 2.20

\*02.80 T !!!"SAMPLE GALLIUM IRON"

\*02.85 T !,%3.00,I"" ,%7.00,G,"",R

\*02.87 S G=O;S R=o

\*02.90 R

\*\*



**APPENDIX C**  
**CLINICAL STUDY BLOOD DATA**



## APPENDIX C

## SUBJECT U.T.

	Experiment A <sup>67</sup> Ga-Tf and <sup>59</sup> Fe-citrate	Experiment B <sup>67</sup> Ga-citrate
height	186 cm	186 cm
weight	105.5 kg	105.5 kg
Ht	0.50	0.49
whole blood volume	5800 ml	5800 ml
red blood cell volume	2900 ml	2840 ml
plasma volume	2900 ml	2960 ml

SUBJECT U.T. – <sup>67</sup>Ga-citrate Blood Data

Injected dose =  $256156 \times 10^3$  counts per minute (cpm)

time after administration (hr)	plasma + wash cpm/2 ml	RBC cpm/2 ml	whole blood cpm/2 ml
0.20	161951	4502	76382
0.33	140396	3880	67729
0.52	127972	3320	61029
0.77	131710	3943	59718
1.02	124087	2770	54235
1.50	97232	1974	47184
2.00	106382	4190	45260
3.78	76323	2215	35192
5.73	60120	2014	29488
8.28	49728	2098	23272
13.8	39573	1819	18598
24.8	28446	1790	12942
48.7	18420	1966	9288
72.9	12489	1385	6496
96.6	9010	1614	5320
120	7008	1916	4519
144	6019	3226	4689
169	4545	3168	4058
193	4972	2969	3836
216	3676	3643	3634





**SUBJECT U.T.:  $^{67}\text{Ga}$ -Transferrin Blood Data**

Injected does =  $85405.11 \times 10^3$  counts per 5 minutes (cp5m)

time after administration (hr)	plasma + wash cp5m/ml	RBC cp5m/ml	whole blood cp5m/2ml
0.33	15448	748	17012
0.50	13848	847	15400
0.75	12718	689	13823
1.0	12028	556	12868
1.5	10548	464	11652
2.0	10559	370	11186
4.0	7671	340	8092
6.0	6020	186	6482
9.0	5066	164	5495
13.8	4408	240	4629
24.6	2651	169	3008
48.2	2389	464	5756
72.5	1204	102	1811
96.0	839	200	1146
121	788	168	766
145	575	82	616
169	637	300	786
193	499	26	546
217	355	145	688



SUBJECT U.T.:  $^{59}\text{Fe}$ -citrate Blood Data

Injected dose =  $452174 \times 10^2$  counts per 30 minutes (cp30m)

time after administration (hr)	plasma + wash cp30m/ml	RBC cp30m/ml	whole blood cp30m/ml
0.07	12314	889	12953
0.17	12218	489	13411
0.33	10607	260	11718
0.50	9817	387	11333
0.75	8557	232	9352
1.0	7864	45	8301
1.5	6163	204	7269
2.0	5465	112	5730
4.0	2111	106	2475
6.0	753	126	1111
9.0	236	126	495
13.8	44	443	614
24.6	0	1031	1161
48.2	15	4343	4375
72.5	4	7955	11681
96.0	18	11193	11335
121	12	12973	13106
145	107	14669	14626
169	105	14857	14339
193	112	14405	14210
217	24	15245	15062



## SUBJECT C.W.

	Experiment A <sup>67</sup> Ga-Tf	Experiment B <sup>67</sup> Ga-citrate + <sup>59</sup> Fe-citrate
height	171 cm	171 cm
weight	66.4 kg	67.7 kg
Ht	0.427	0.426
whole blood volume	4200 ml	4200 ml
red blood cell volume	1800 ml	1800 ml
plasma volume	2400 ml	2400 ml

SUBJECT C.W.: <sup>67</sup>Ga-citrate Blood Data

Injected dose = 2190489.5 x 10<sup>3</sup> counts per minute (cpm)

time after administration (hr)	plasma + wash cpm/2 ml	RBC cpm/2 ml	whole blood cpm/2ml
0.25	1200808	27096	618992
0.50	1040498	25216	578010
1.0	889242	20914	484196
1.5	873400	22820	441302
2.0	774013	23894	390722
4.0	510068	10320	276906
6.1	391486	9962	214764
8.6	337609	8498	175996
12.0	270701	7656	149912
23.6	163214	6619	87204
47.6	107243	4884	58909
71.7	80996	4002	42905
96.5	67343	3470	37525
121	60271	3155	33201
144	52585	3290	28802
168	46635	3085	25637
192	42117	2899	22750
216	37973	2700	21549



SUBJECT C.W.:  $^{67}\text{Ga}$ -transferrin Blood Data

Injected dose =  $236660 \times 10^3$  counts per minute (cpm)

time after administration (hr)	plasma + wash cpm/2 ml	RBC cpm/2 ml	whole blood cpm/2 ml
0.33	132339	2678	70506
0.50	119663	2276	62591
0.75	107546	2356	56932
1.0	103427	2135	52558
1.75	81839	1652	—
2.0	77239	1498	39116
4.0	60625	1423	29540
5.72	50106	1225	24744
8.20	43158	1152	21082
13.7	27258	1050	14734
23.7	19158	813	9374
48.2	10980	919	5866
72.0	8213	391	4499
96.7	7313	343	3898
121	6397	309	3486
144	4268	238	2428
168	4911	374	2621
192	4807	261	2500
216	4167	380	2225
240	4148	285	2303





SUBJECT C.W.:  $^{59}\text{Fe}$ -citrate Blood Data

Injected dose =  $556542 \times 10^2$  counts per 15 minutes (cp15m)

time after administration (hr)	plasma + wash cp15m/ml	RBC cp15m/ml	whole blood cp15m/ml
0.25	35936	778	17982
0.50	31191	752	16892
1.0	25901	572	13554
1.5	24604	508	12048
2.0	20598	646	9937
4.0	9844	155	5155
6.1	5583	161	2930
8.6	3350	202	1693
12.0	1945	200	1135
23.6	1077	803	1015
47.6	587	5148	2946
71.7	424	12142	6384
96.5	250	19970	10045
120.7	289	27305	13319
144	149	28809	14420
168	187	33158	15276
192	161	32172	15605
216	116	33552	15556



## SUBJECT B.L.

	Experiment A <sup>67</sup> Ga-citrate	Experiment B <sup>67</sup> Ga-Tf + <sup>59</sup> Fe-citrate
height	180 cm	180 cm
weight	84.1 kg	82 kg
Ht	0.449	0.454
whole blood volume	5000 ml	4900 ml
red blood cell volume	2200 ml	2200 ml
plasma volume	2800 ml	2700 ml

SUBJECT B.L.: <sup>67</sup>Ga-citrate Blood Data

Injected dose =  $259806 \times 10^3$  counts per minute (cpm)

time after administration (hr)	plasma + wash cpm/2 ml	RBC cpm/2 ml	whole blood cpm/2 ml
0.18	172957	2849	86628
0.37	146258	2112	73446
0.50	135732	1732	71128
0.75	128036	1822	65764
1.0	120119	5231	60954
1.5	114155	1516	55510
2.0	100896	1493	50052
4.0	79856	1580	41278
6.0	69586	1400	35105
8.1	64954	1412	31282
13.4	46851	2350	24558
23.9	34227	1289	16886
48.0	21378	744	10640
71.9	14356	767	7392
96.2	11663	480	6198
121	9297	402	5124
144	7810	595	4191
168	6258	552	3481
192	5639	391	3179
216	4650	360	2586



SUBJECT B.L.:  $^{67}\text{Ga}$ -transferrin Blood Data

Injected dose =  $246751.5 \times 10^3$  counts per minute (cpm)

time after administration (hr)	plasma + wash cpm/2 ml	RBC cpm/2 ml	whole blood cpm/2 ml
0.25	149132	3041	74849
0.50	127066	2050	64810
0.76	133640	1759	57923
1.0	110808	1911	54051
1.55	97724	1209	48481
2.05	90112	2315	45513
3.0	76032	1274	45794
4.0	71438	1469	34679
6.0	57520	953	28461
8.4	48222	944	24217
12.0	39114	845	20094
24.1	28436	874	13908
48.4	17718	824	9126
72.5	13204	486	6511
97.1	9968	351	4875
120	7763	282	4207
144	7031	338	3462
168	5383	281	2811
192	4947	297	2660
216	3922	219	2273



SUBJECT B.L.:  $^{59}\text{Fe}$ -citrate Blood Data

Injected dose =  $220359 \times 10^2$  counts per 15 minutes (cp15m)

time after administration (hr)	plasma + wash cp15m/2 ml	RBC cp15m/2 ml	whole blood cp15m/2 ml
0.25	14450	385	7083
0.50	12549	228	6406
0.76	11275	175	5765
1.0	10920	140	5210
1.55	8966	120	4222
2.05	7339	232	3815
3.0	5074	75	3040
4.0	3627	86	1784
6.0	1778	76	972
8.38	897	76	536
12.1	395	273	370
24.1	180	827	537
48.4	213	2658	2259
72.5	67	6751	4271
97.1	119	9270	6071
120	93	12101	7273
144	37	13044	7797
168	65	12149	7778
192	87	14523	8153
216	17	15251	7936





## SUBJECT A.N.

	Experiment A <sup>67</sup> Ga-citrate	Experiment B <sup>67</sup> Ga-Tf
height	179 cm	179 cm
weight	101 kg	101 kg
Ht	0.493	0.490
whole blood volume	5500 ml	5500 ml
red blood cell volume	2700 ml	2700 ml
plasma volume	2800 ml	2800 ml

SUBJECT A.N.: <sup>67</sup>Ga-citrate Blood Data

Injected dose =  $218595 \times 10^3$  counts per minute (cpm)

time after administration (hr)	plasma + wash cpm/2 ml	RBC cpm/2 ml	whole blood cpm/2 ml
0.25	123984	2487	58794
0.50	99049	1846	47724
0.75	89075	1911	42339
1.0	81911	1630	39257
1.53	79070	1605	35894
2.15	65991	2386	30362
4.02	54763	1128	24445
6.07	43779	1100	20625
8.17	38315	1248	18276
12.0	30393	1020	14754
24.0	17654	1456	8610
47.9	10916	1101	5873
72.0	7114	818	3785
97.4	6422	552	3399
121	3647	678	2111
144	4684	686	2605
168	4401	732	2347
192	3499	962	2011
216	2523	940	1703



SUBJECT A.N.:  $^{67}\text{Ga}$ -transferrin Blood Data

Injected dose =  $304010 \times 10^3$  counts per minute (cpm)

time after administration (hr)	plasma + wash cpm/2 ml	RBC cpm/2 ml	whole blood cpm/2 ml
0.27	189404	6317	83955
0.52	154316	2848	72691
0.73	140083	2885	67007
0.98	127347	2281	61671
1.55	123946	2941	55179
1.97	113133	2654	50930
3.70	90698	2528	39772
6.35	65690	1471	30987
8.30	55022	1641	24930
10.3	46865	1550	20892
23.8	30071	1265	14021
48.7	15035	857	7572
71.4	11006	696	5609
97.7	9291	792	4710
120	6916	757	3721
150	7167	919	3502
167	5374	618	2773
191	4884	608	2576



**APPENDIX D**  
**BLOOD BIOCHEMISTRY DATA**



## APPENDIX D

## SUBJECT U.T.

Day of Experiment	Serum Iron ( $\mu\text{g/dl}$ )		TIBC ( $\mu\text{g/dl}$ )		Transferrin (mg/dl)		Ferritin (ng/ml)	
	A *	B †	A	B	A	B	A	B
0	98	100	380	418	275	288	68	60
1	98	106	400	398	288	363	70	65
2	94	106	400	420	288	363	72	63
3	128	100	384	388	264	363	69	67
4	114	92	406	392	324	311	72	63
5	96	81	404	392	288	324	65	55
6	110	126	408	392	264	311	69	61
7	112	100	430	396	299	275	69	49
8	101	86	408	408	264	324	69	59
9	114	88	406	400	275	311	73	62
Normal values	50–130		250–400		200–400		25–465	

\* A =  $^{67}\text{Ga}$ -Tf and  $^{59}\text{Fe}$ -citrate study  
† B =  $^{67}\text{Ga}$ -citrate study





SUBJECT C.W.

Day of Experiment	Serum Iron ( $\mu\text{g/dl}$ )		TIBC ( $\mu\text{g/dl}$ )		Transferrin (mg/dl)		Ferritin (ng/ml)	
	A *	B †	A	B	A	B	A	B
0	138	80	340	330	250	250	65	45
1	120	107	356	362	290	228	74	49
2	131	74	324	342	302	263	73	49
3	114	111	342	362	276	276	64	48
4	104	112	360	362	290	263	68	45
5	87	104	344	376	276	263	71	43
6	171	96	326	362	228	217	63	39
7	111	80	320	376	250	241	68	36
8	111	104	356	378	302	324	66	37
9	101	81	344	356	276	299	59	37
10	95		354		263		52	
Normal values	50–130		250–400		200–400		25–465	

\* A =  $^{67}\text{Ga}$ -Tf study  
† B =  $^{67}\text{Ga}$ -citrate and  $^{59}\text{Fe}$ -citrate study



SUBJECT B.L.

Day of Experiment	Serum Iron ( $\mu\text{g/dl}$ )		TIBC ( $\mu\text{g/dl}$ )		Transferrin (mg/dl)		Ferritin (ng/ml)	
	A *	B †	A	B	A	B	A	B
0	100	98	422	428	268	302	32	30
1 +	114	—	438	—	311	—	30	—
2	127	108	432	442	347	335	32	29
3	134	83	418	428	311	319	29	25
4	102	106	424	436	311	319	31	22
5	87	96	418	428	281	335	27	28
6	91	76	432	430	387	350	24	25
7	148	94	424	428	302	290	28	27
8	59	91	456	432	350	302	37	25
9	56	80	428	420	387	302	30	25
Normal values	50–130		250–400		200–400		25–465	

\* A =  $^{67}\text{Ga}$ -citrate study  
† B =  $^{67}\text{Ga}$ -Tf and  $^{59}\text{Fe}$ -citrate study  
+ Day 1 sample missed in study B



SUBJECT A.N.

Day of Experiment	Serum Iron ( $\mu\text{g/dl}$ )		TIBC ( $\mu\text{g/dl}$ )		Transferrin (mg/dl)		Ferritin (ng/ml)	
	A *	B †	A	B	A	B	A	B
0 +	—	70	—	306	218	229	451	513
1	142	106	316	328	240	218	366	492
2	72	140	302	316	229	229	451	452
3	120	89	308	306	195	240	492	449
4	68	82	320	336	218	297	575	332
5	89	127	298	312	186	268	451	406
6 ‡	—	105	—	354	—	311	—	542
7	85	83	316	322	218	268	616	520
8	85	57	328	320	229	235	542	603
9	110	—	320	—	240	—	502	—
Normal values	50–130		250–400		200–400		25–465	

\* A =  $^{67}\text{Ga}$ -citrate study

† B =  $^{67}\text{Ga}$ -Tf study

+ Study A, Day 0, samples for serum iron and TIBC determination lost.

‡ Study 1, Day 6, sample missed.



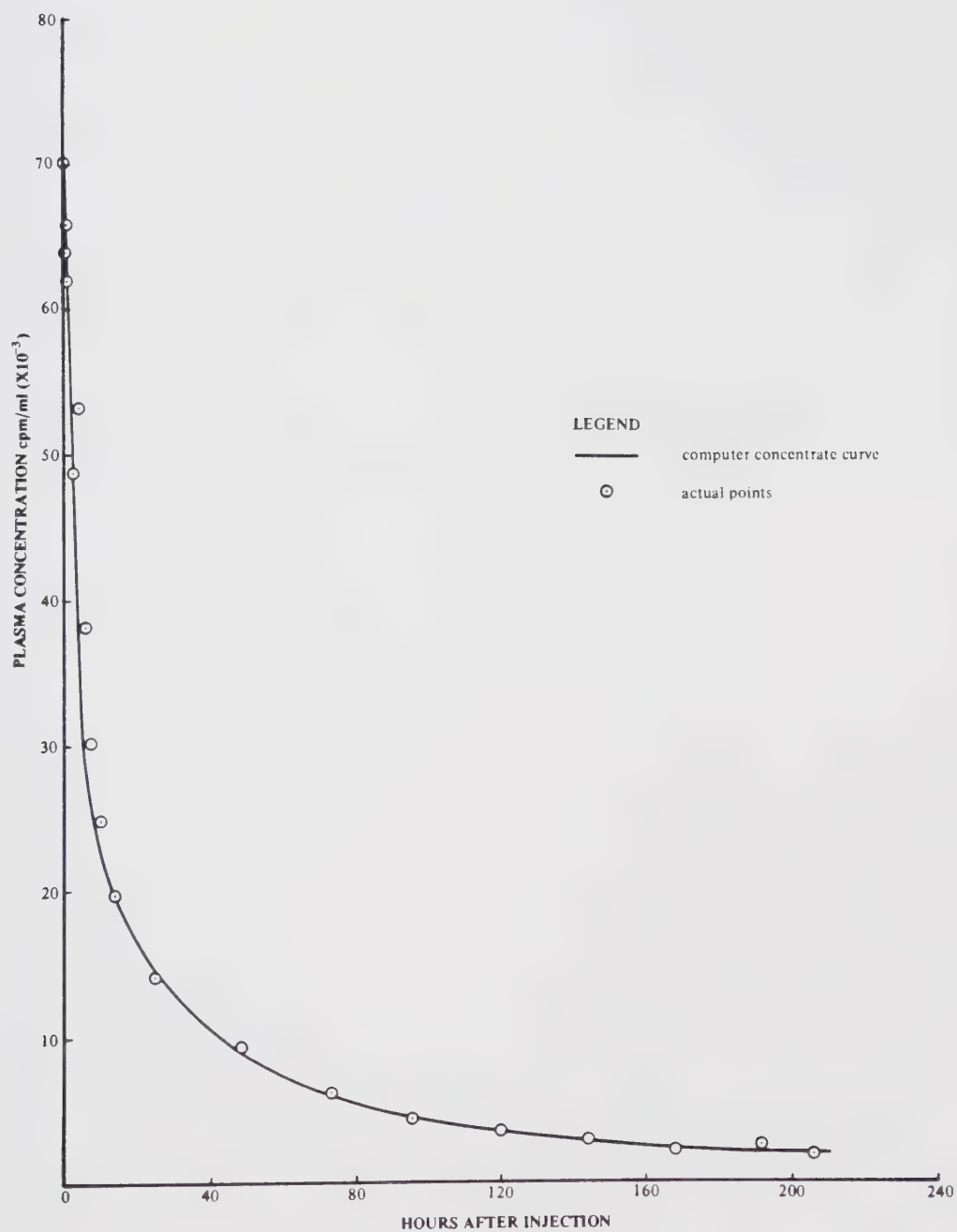
**APPENDIX E**

**PLASMA DISAPPEARANCE CURVES AND PERCENT DOSE IN  
COMPARTMENTS PLOTS**

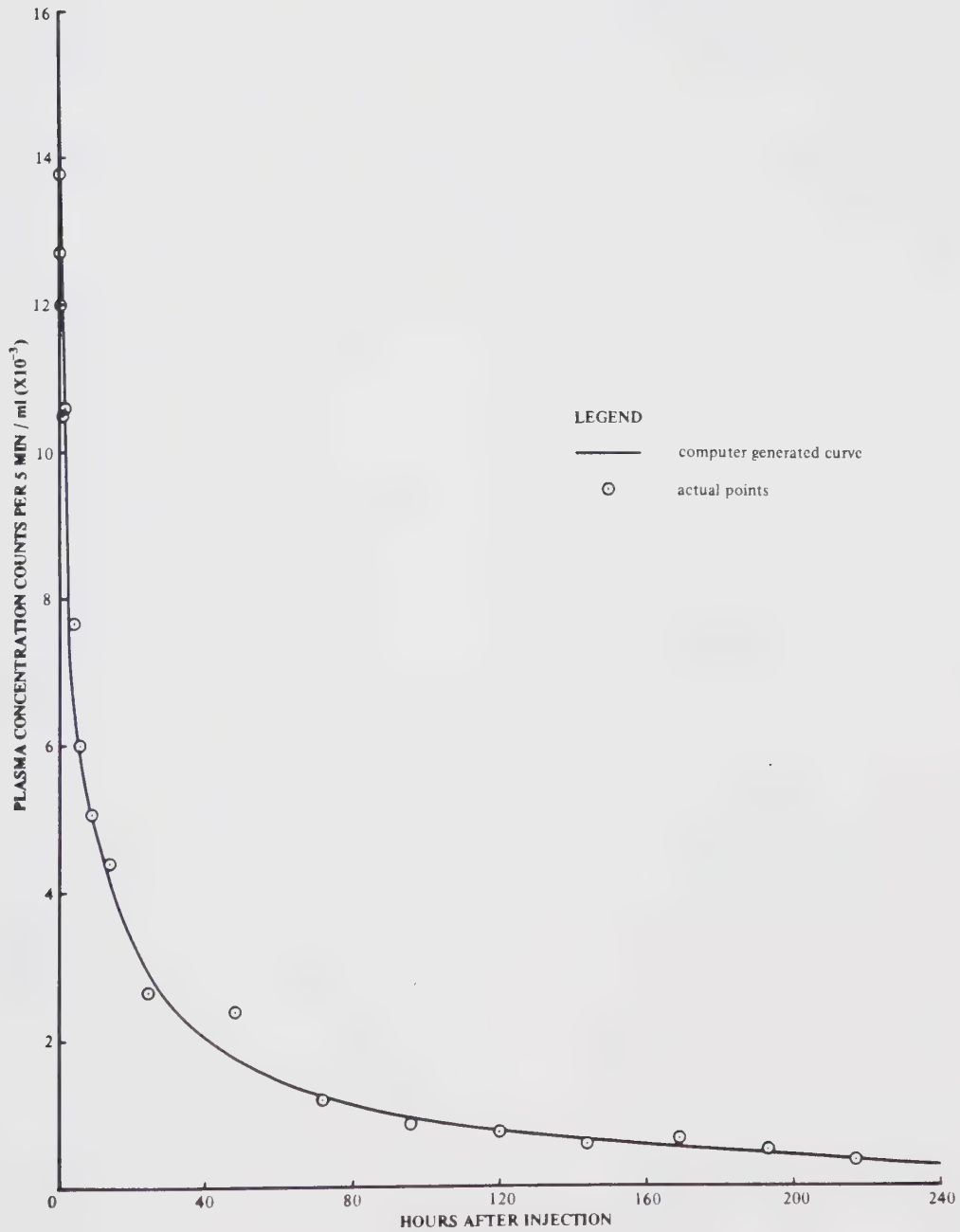




SUBJECT U.T.: Plasma disappearance of  $^{67}\text{Ga}$ -citrate

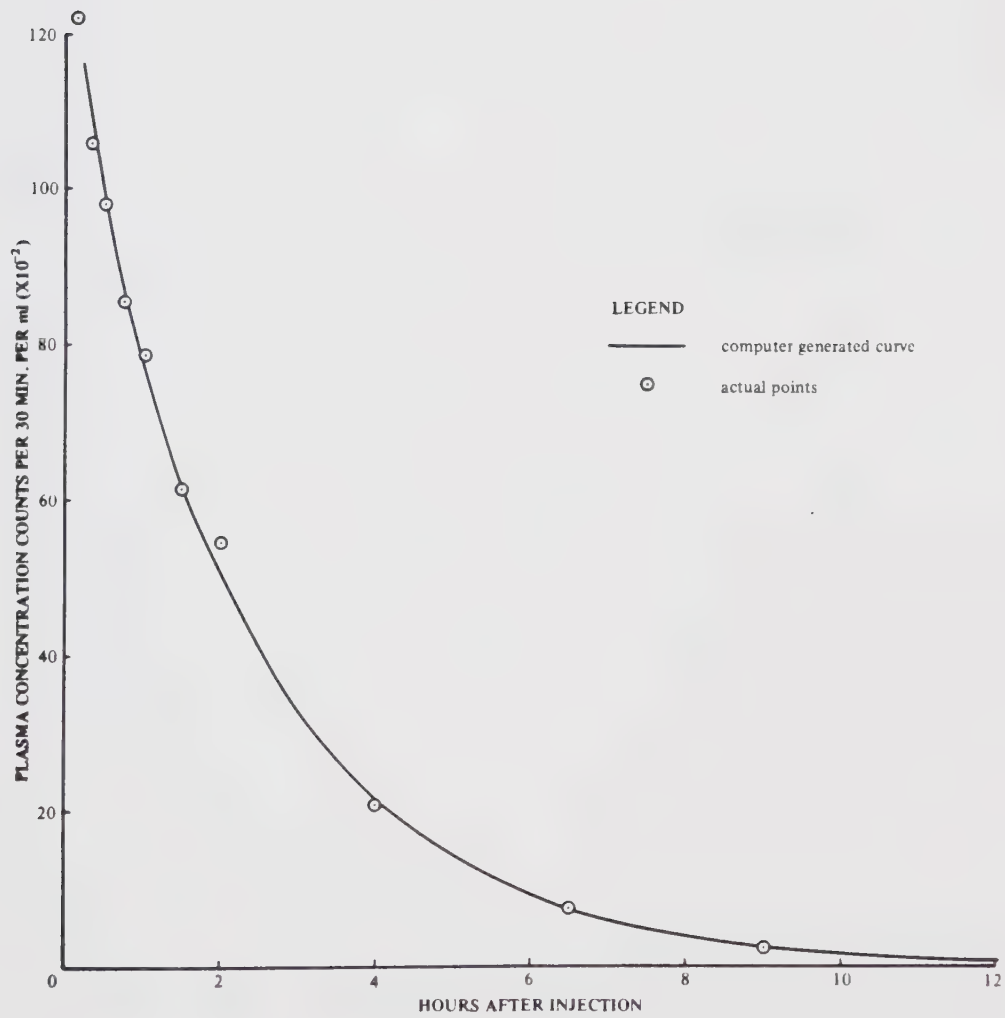




SUBJECT U.T.: Plasma disappearance of  $^{67}\text{Ga}$ -transferrin

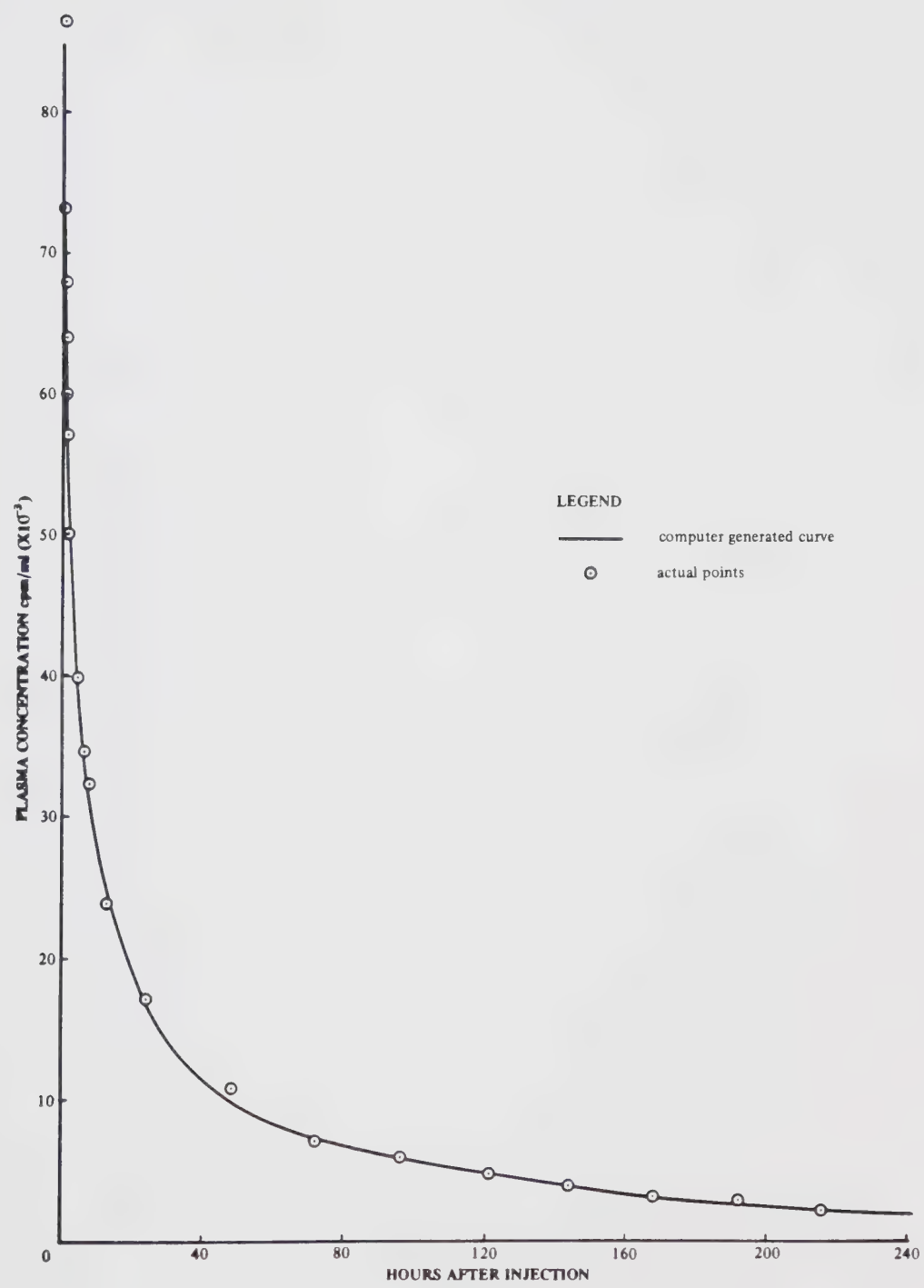


SUBJECT U.T.: Plasma disappearance of  $^{59}\text{Fe}$ -citrate





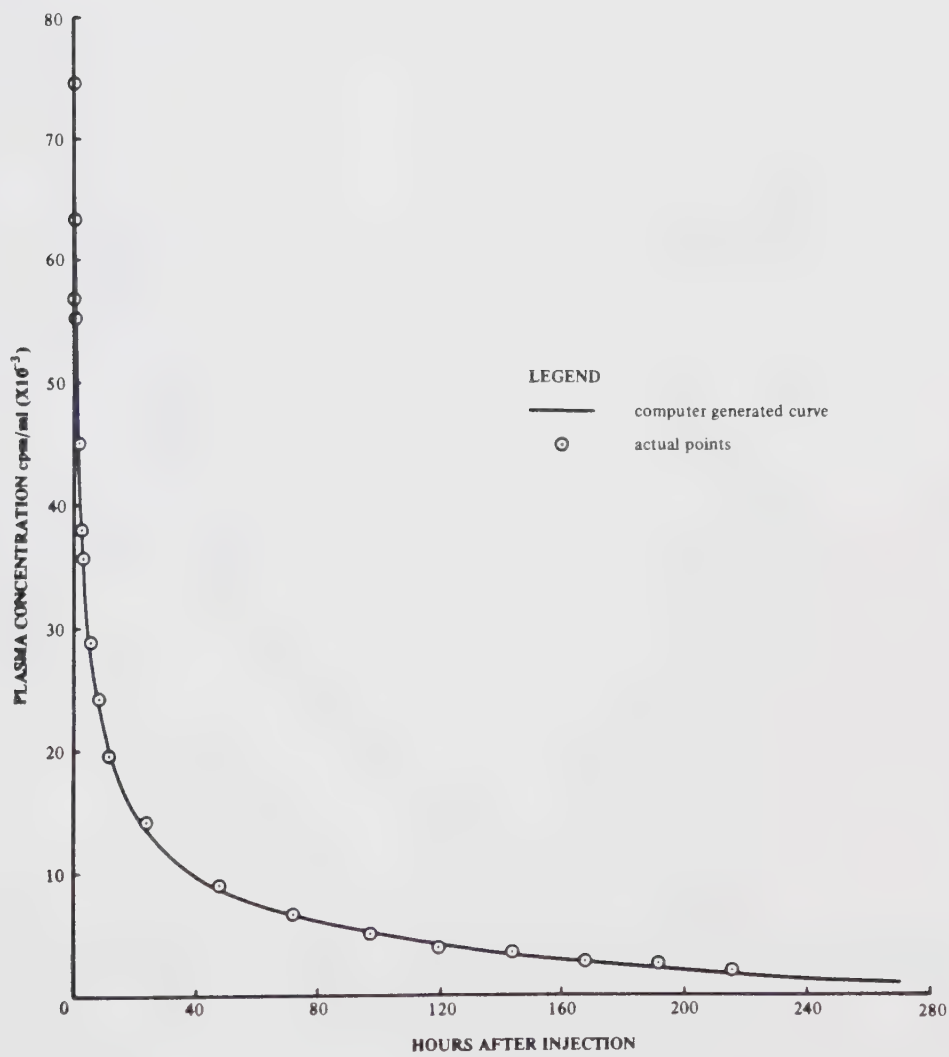
SUBJECT B.L.: Plasma clearance of <sup>67</sup>Ga-citrate



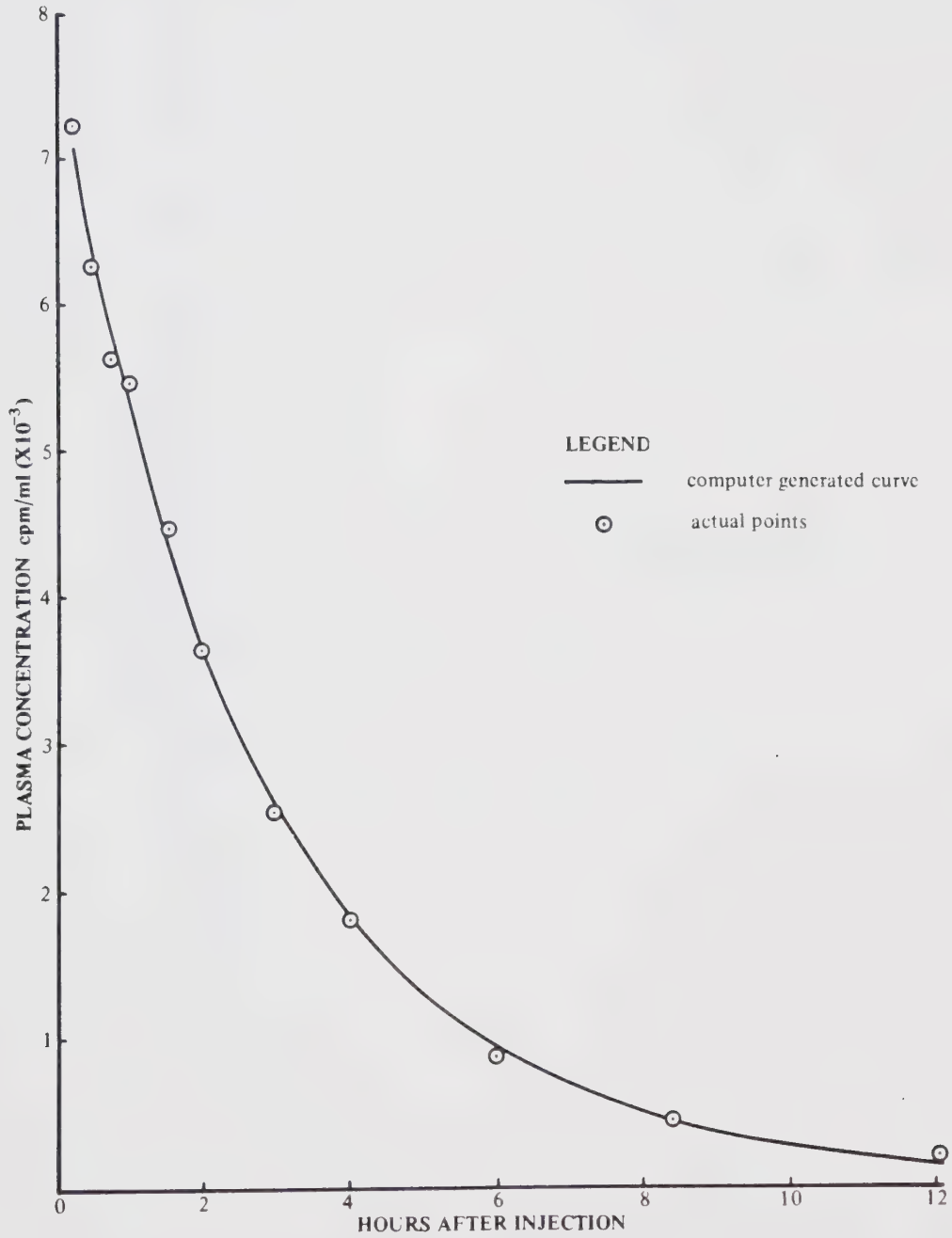




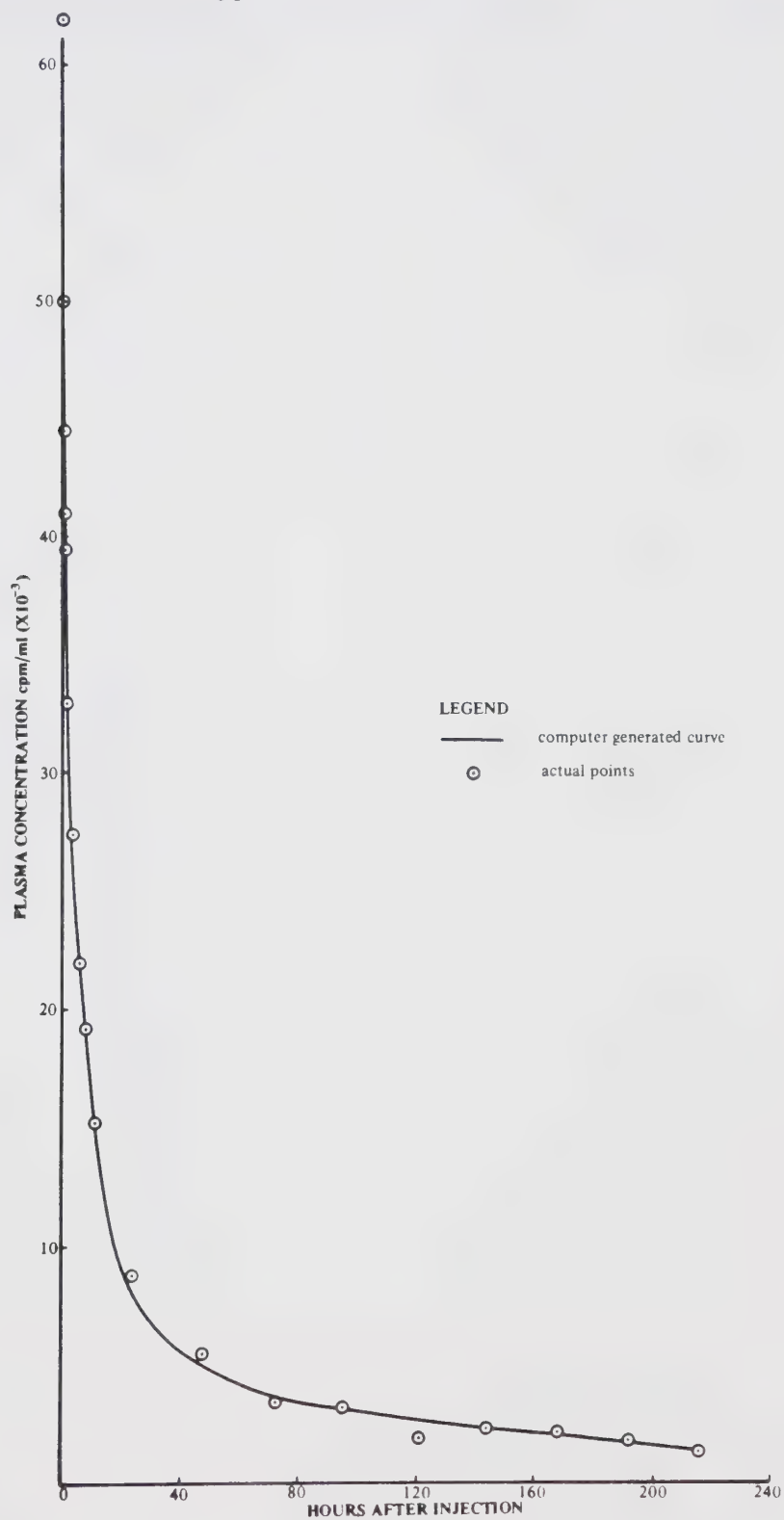
SUBJECT B.L.: Plasma disappearance of <sup>67</sup>Ga-transferrin



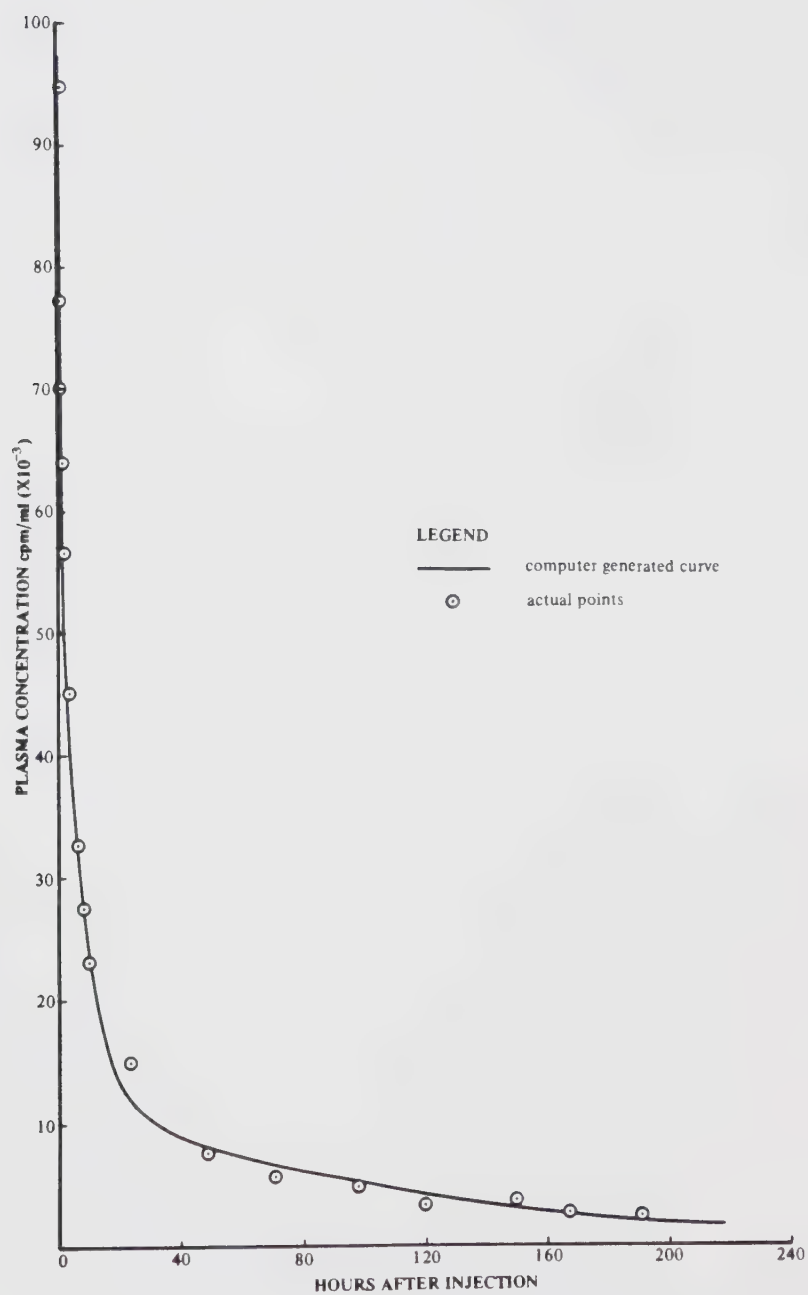


SUBJECT B.L.: Plasma disappearance of  $^{59}\text{Fe}$ -citrate



SUBJECT A.N.: Plasma disappearance of  $^{67}\text{Ga}$ -citrate

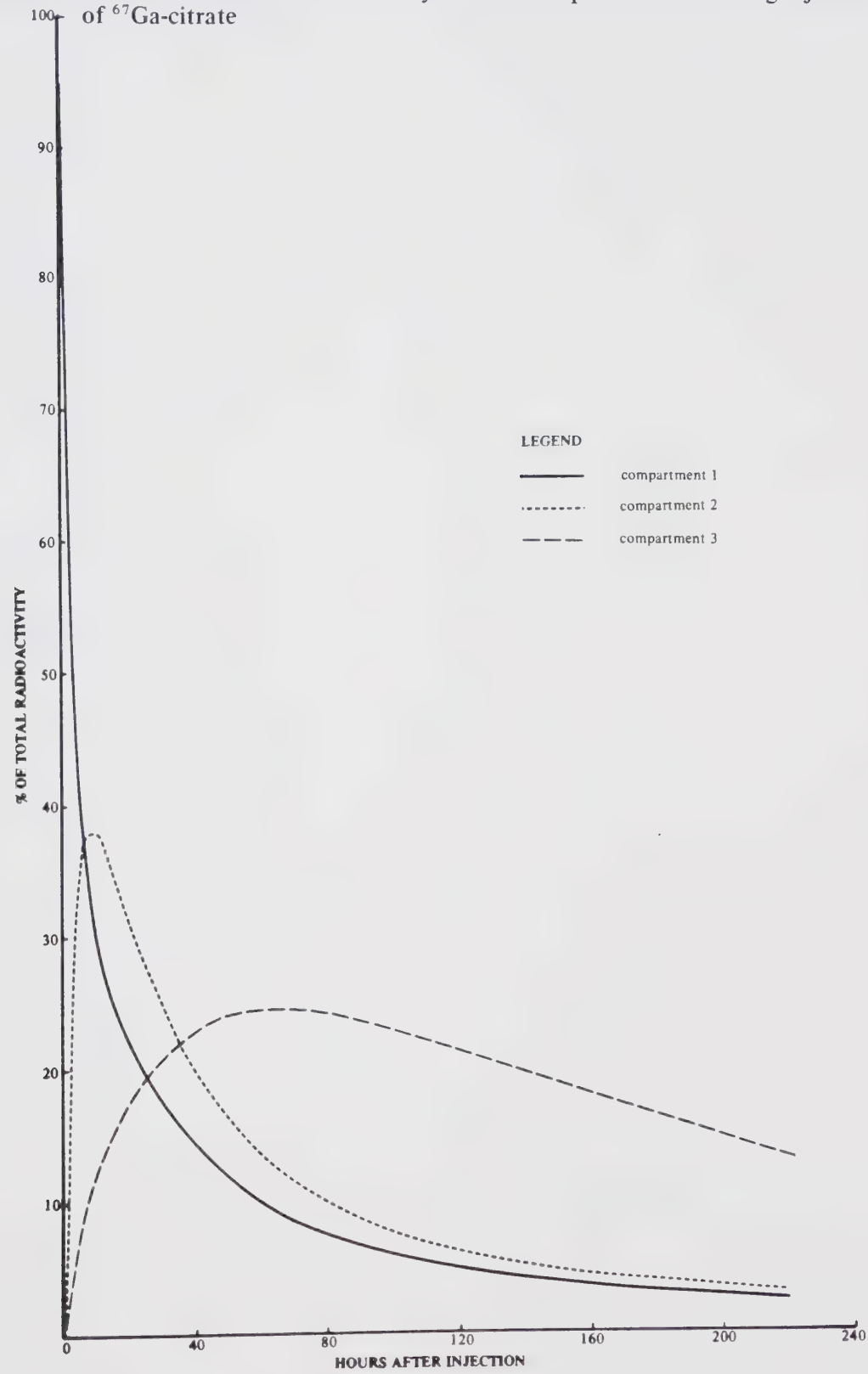


SUBJECT A.N.: Plasma disappearance of  $^{67}\text{Ga}$ -transferrin



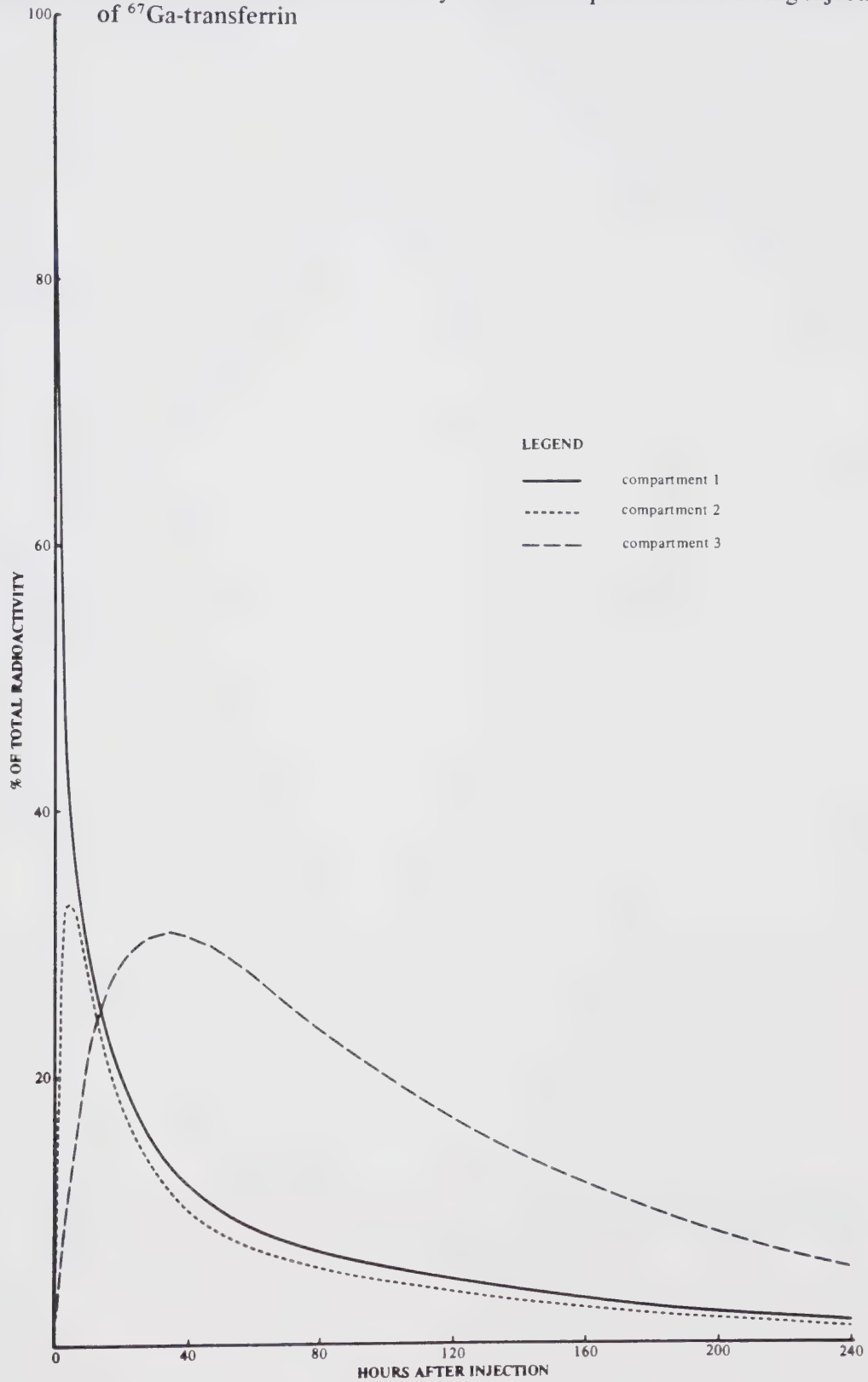


SUBJECT U.T.: Percent of total radioactivity in each compartment following injection of  $^{67}\text{Ga}$ -citrate



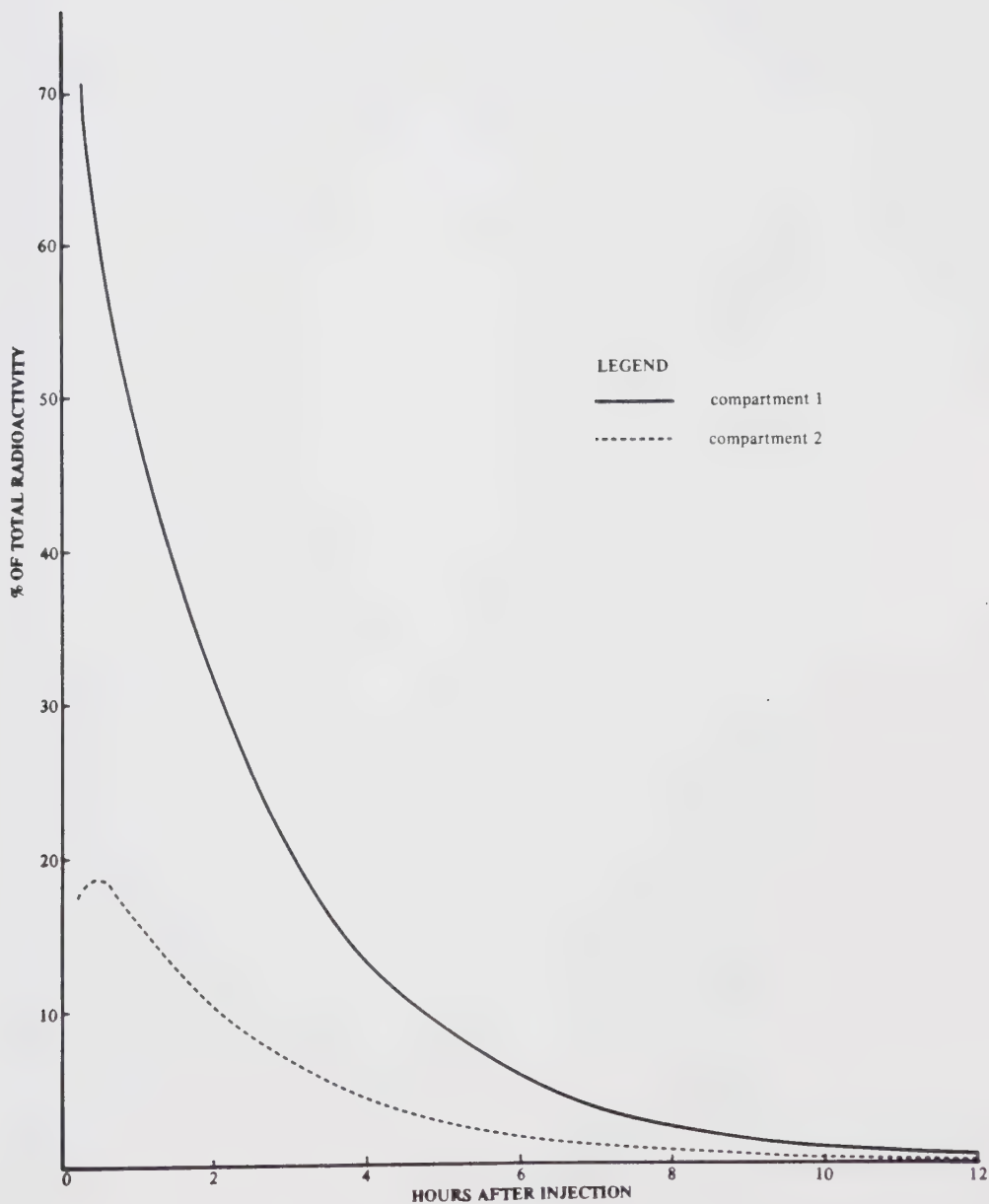


SUBJECT U.T.: Percent of total radioactivity in each compartment following injection of  $^{67}\text{Ga}$ -transferrin



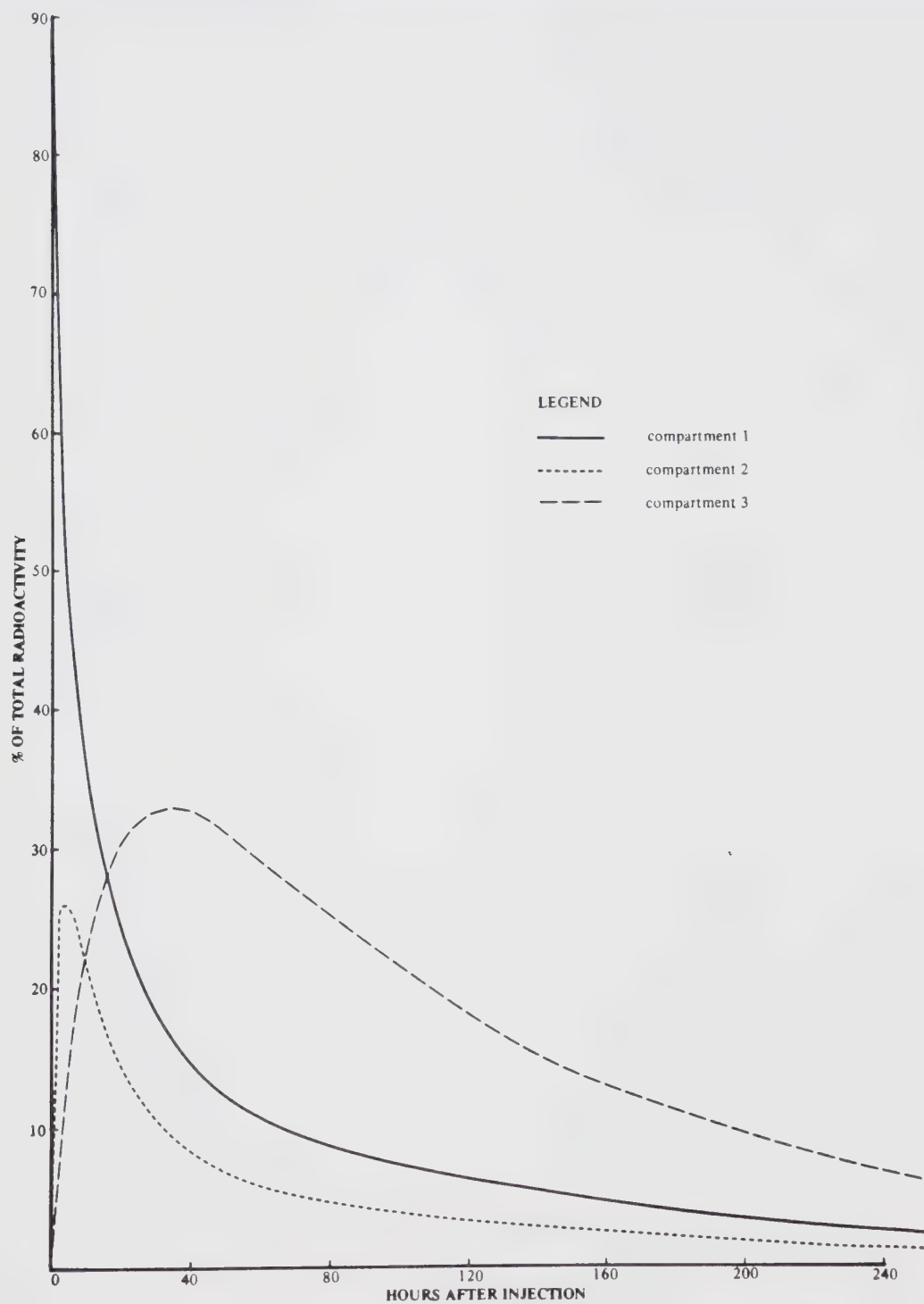


SUBJECT U.T.: Percent of total radioactivity in each compartment following injection of  $^{59}\text{Fe}$ -citrate





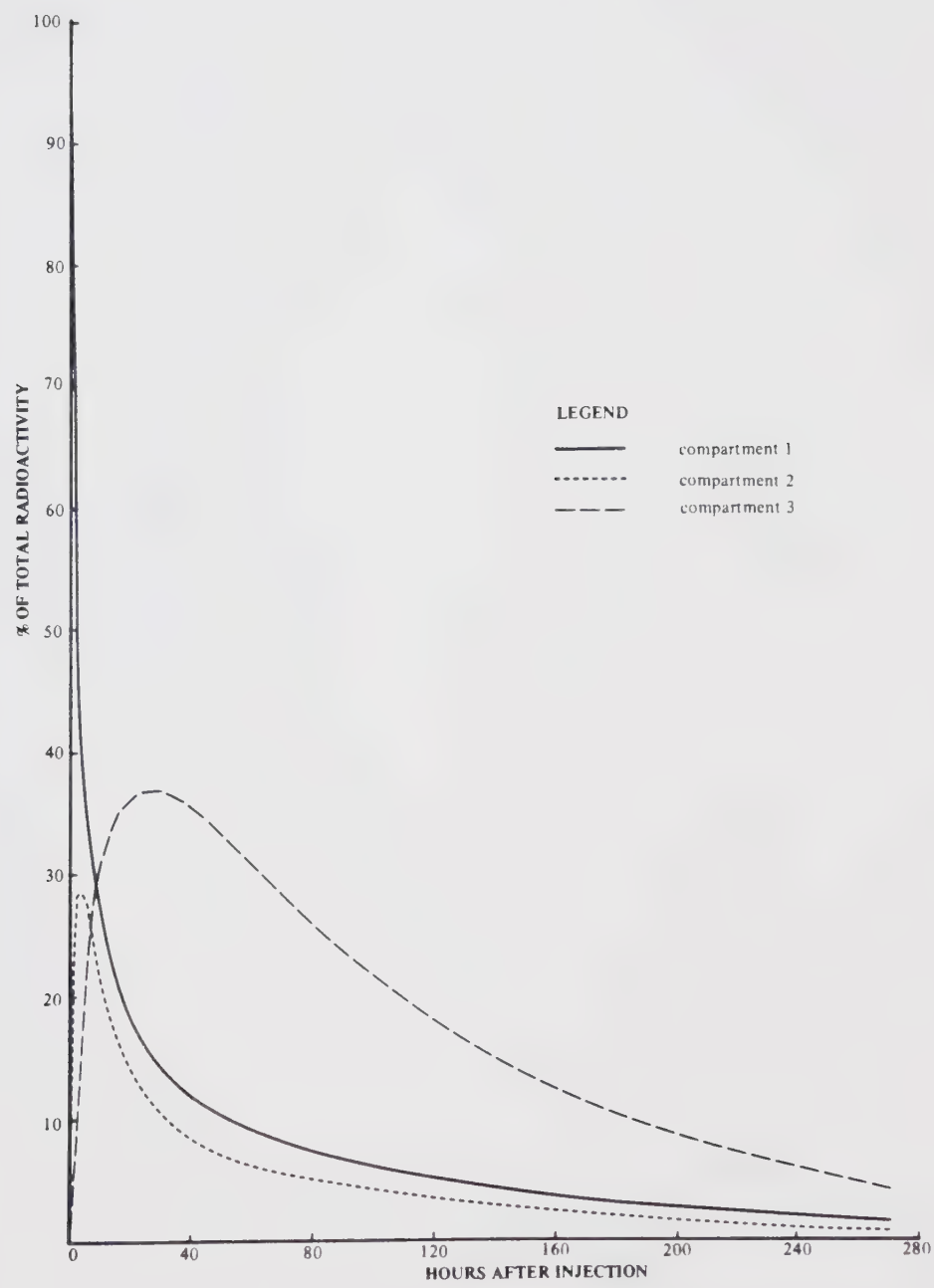
SUBJECT B.L.: Percent of total radioactivity in each compartment following injection of  $^{67}\text{Ga}$ -citrate





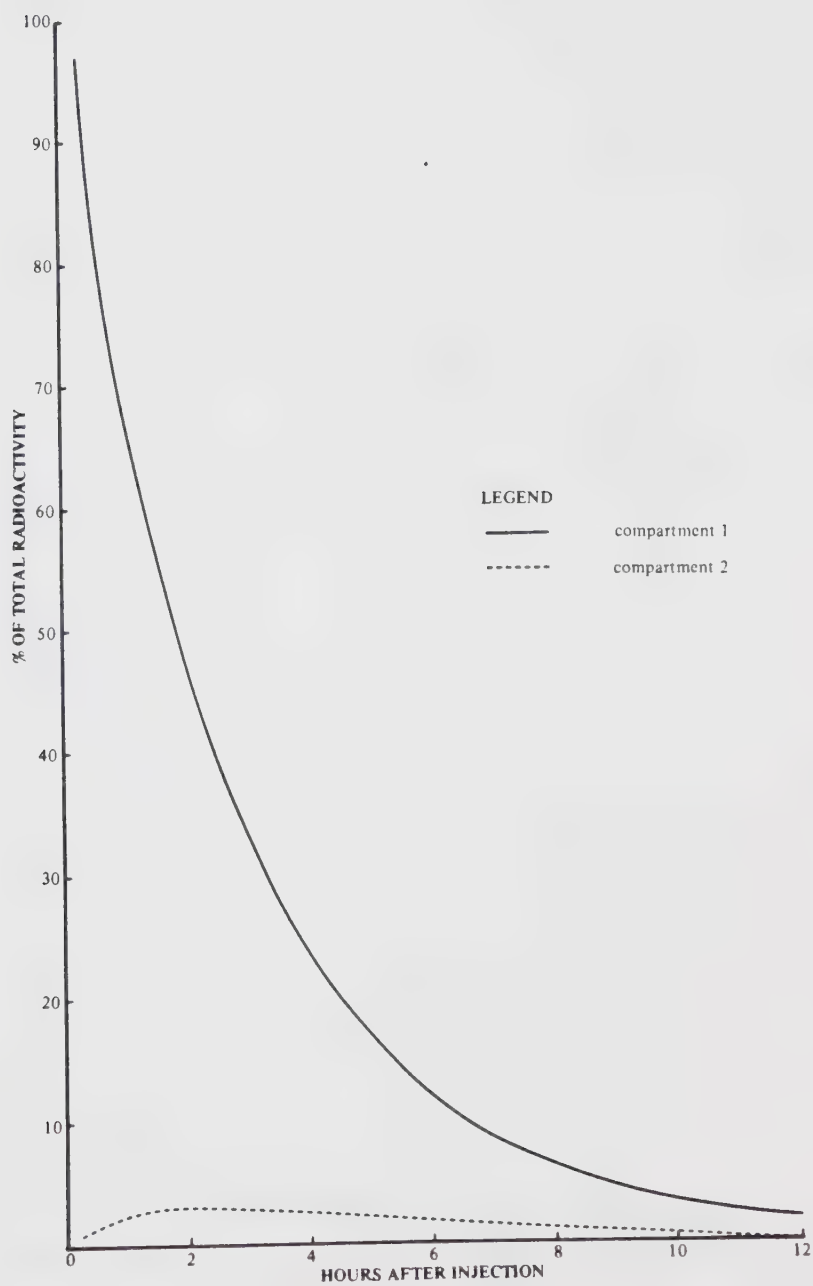


SUBJECT B.L.: Percent of total radioactivity in each compartment following injection of  $^{67}\text{Ga}$ -transferrin



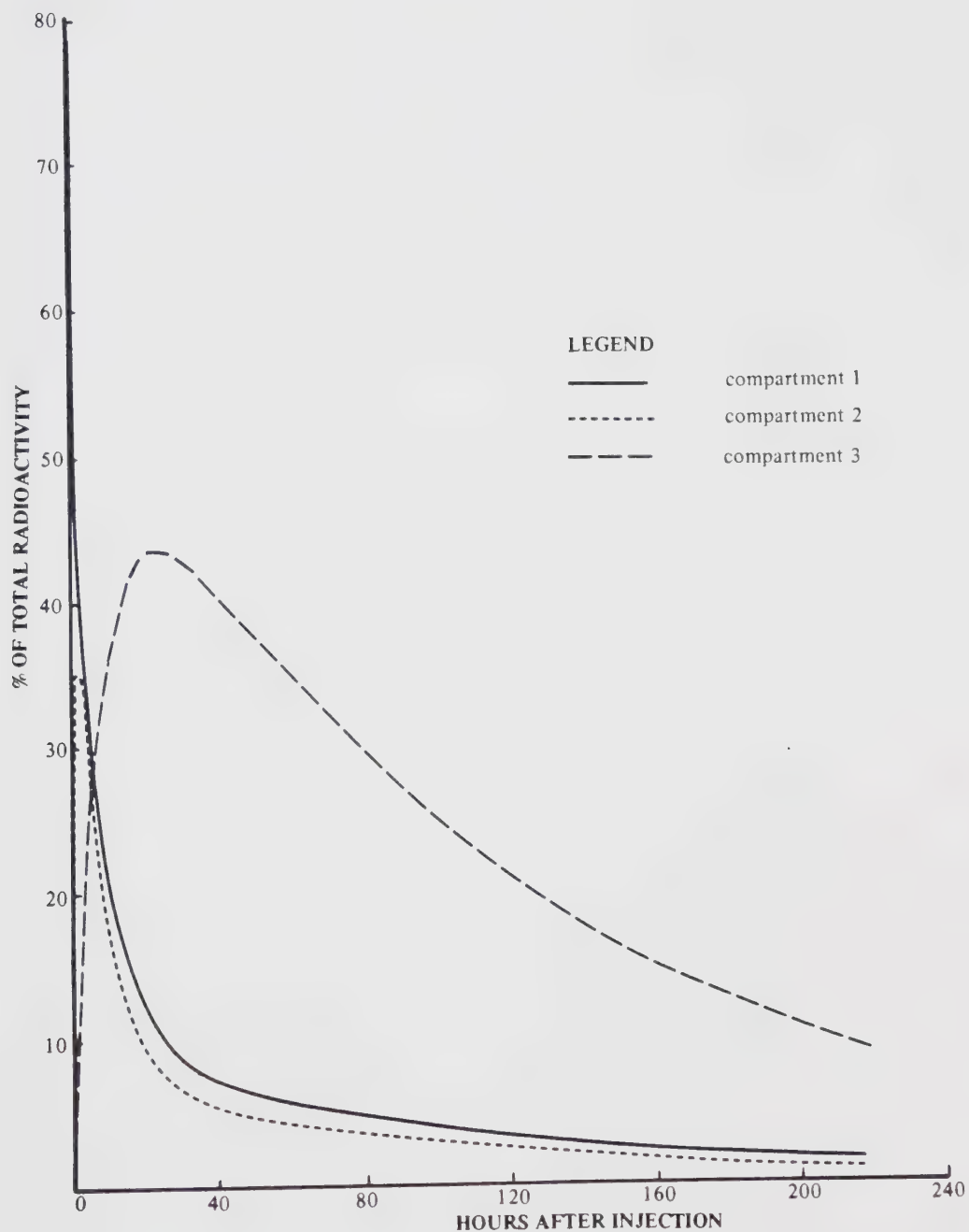


SUBJECT B.L.: Percent of total radioactivity in each compartment following injection of  $^{59}\text{Fe}$ -citrate



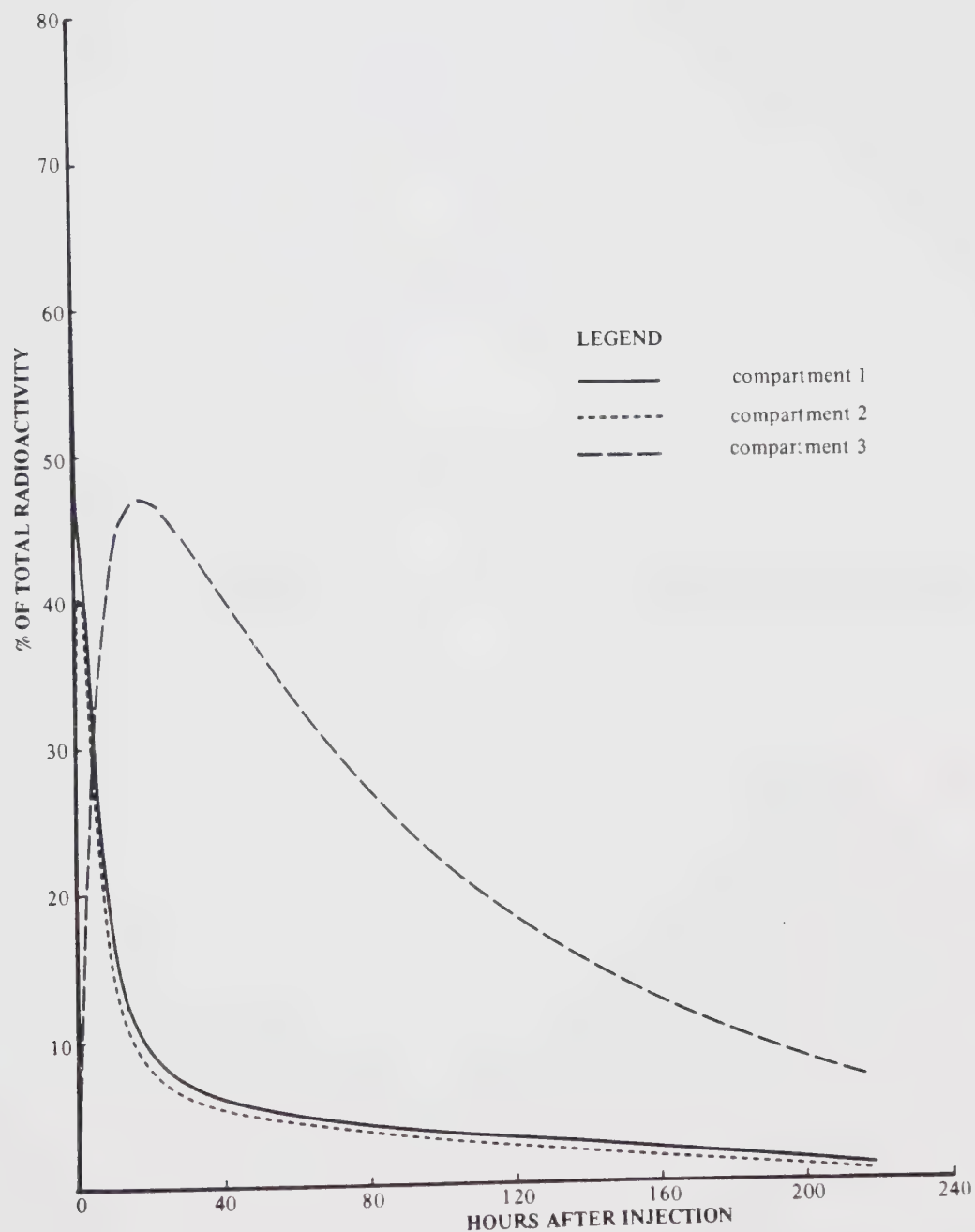


SUBJECT A.N.: Percent of total radioactivity remaining in each compartment following injection of  $^{67}\text{Ga}$ -citrate





SUBJECT A.N.: Percent of total radioactivity remaining in each compartment following injection of  $^{67}\text{Ga}$ -transferrin







**APPENDIX F**  
**PHARMACOKINETIC PARAMETERS FOR EACH SUBJECT**



# APPENDIX F

## Hybrid Rate Constants

Subject	<sup>67</sup> Ga-cit.	$\lambda_1$ <sup>67</sup> Ga-Tf	<sup>59</sup> Fe-cit.	<sup>67</sup> Ga-cit.	$\lambda_2$ <sup>67</sup> Ga-Tf	<sup>67</sup> Ga-cit.	$\lambda_3$ <sup>67</sup> Ga-Tf	<sup>59</sup> Fe-cit. *
U.T.	0.3299	0.645	7.47	0.0307	0.066	0.0050	0.0086	0.428
C.W.	0.4400	0.955	0.3907	0.0728	0.095	0.0053	0.0050	0.1748
B.L.	0.6246	0.6822	0.6027	0.0692	0.0888	0.0083	0.0090	0.3071
A.N.	2.137	4.018	—	0.1153	0.1578	0.0083	0.0099	—
$\bar{X}$	0.8829	1.575	2.8211	0.0720	0.1019	0.0067	0.0081	0.3033
s	0.8449	1.634	4.0274	0.0346	0.0393	0.0018	0.0022	0.1266

Values of “t” for <sup>67</sup>Ga-citrate and <sup>67</sup>Ga-Tf

$\lambda_1$ , t = 1.6999

$\lambda_2$ , t = 5.5105

$\lambda_3$ , t = 1.6875

At 3 DF, t at 0.05 = 3.182

0.01 = 5.841

Values of “t” for <sup>67</sup>Ga-citrate and <sup>59</sup>Fe-citrate

$\lambda_1$ , t = 0.9851

$\lambda_3$ , t = 4.0596

At 2 DF, t at 0.05 = 4.303

0.01 = 9.925

\* for <sup>59</sup>Fe-citrate, the elimination rate constant is  $\lambda_2$ ; however, it was included under  $\lambda_3$  for comparison with <sup>67</sup>Ga-citrate and <sup>67</sup>Ga-Tf.



Microscopic Rate Constants

Subject	k <sub>10</sub>		k <sub>12</sub>		k <sub>21</sub>		k <sub>13</sub>		k <sub>31</sub>	
	<sup>67</sup> Ga-cit.	<sup>67</sup> Ga-Tf	<sup>59</sup> Fe-cit.	<sup>67</sup> Ga-cit.	<sup>67</sup> Ga-Tf	<sup>59</sup> Fe-cit.	<sup>67</sup> Ga-cit.	<sup>67</sup> Ga-Tf	<sup>67</sup> Ga-cit.	<sup>67</sup> Ga-Tf
U.T.	0.038	0.046	0.566	0.156	0.264	1.68	0.135	0.331	5.65	0.026
C.W.	0.043	0.048	0.297	0.161	0.356	0.039	0.210	0.532	0.230	0.085
B.L.	0.037	0.045	0.358	0.204	0.251	0.035	0.386	0.374	0.517	0.049
A.N.	0.066	0.085	—	0.890	1.833	—	1.165	2.058	—	0.113
$\bar{X}$	0.046	0.056	0.407	0.353	0.676	0.585	0.474	0.824	2.13	0.068
s	0.014	0.019	0.141	0.359	0.773	0.949	0.473	0.827	3.05	0.038

Values of “t” for <sup>67</sup>Ga-citrate and <sup>67</sup>Ga-Tf; at 3 DF, t at 0.05 = 3.182  
0.01 = 5.841

k<sub>10</sub>, t = 3.244

k<sub>12</sub>, t = 1.548

k<sub>21</sub>, t = 1.805

k<sub>13</sub>, t = 3.478

k<sub>31</sub>, t = 2.324



Model Parameters

Subject	t <sup>1/2</sup> (hr)		Cl <sub>p</sub> (ml/hr)		V <sub>d</sub> area (l)		V <sub>p</sub> (l)	
	<sup>67</sup> Ga-cit.	<sup>67</sup> Ga-Tf	<sup>59</sup> Fe-cit.	<sup>67</sup> Ga-cit.	<sup>67</sup> Ga-Tf	<sup>59</sup> Fe-cit.	<sup>67</sup> Ga-cit.	<sup>67</sup> Ga-Tf
U.T.	138.6	80.6	1.62	132	235	1591	26.41	27.3
C.W.	130.8	138.6	3.96	152.8	148	867	28.83	29.5
B.L.	84.0	77.1	2.26	123.4	139.6	1008	14.95	15.53
A.N.	83.5	70.0	—	186.8	176.7	—	22.51	17.85
$\bar{X}$	109.2	91.57	2.613	148.8	174.8	1155	23.18	22.54
s	29.6	31.7	1.209	28.2	43.2	384	6.07	6.89

Values of “t” for <sup>67</sup>Ga-citrate and <sup>67</sup>Ga-Tf; at 3 DF, t at 0.05 = 3.182  
0.01 = 5.841

t<sup>1/2</sup>, t = 1.245  
Cl<sub>p</sub>, t = 0.993  
V<sub>d</sub> area, t = 0.468  
V<sub>p</sub>, t = 0.124

Values of “t” for <sup>67</sup>Ga-citrate and <sup>59</sup>Fe-citrate; at 2 DF, t at 0.05 = 4.303  
0.01 = 9.925

t<sup>1/2</sup>, t = 6.465  
Cl<sub>p</sub>, t = 4.588  
V<sub>d</sub> area, t = 4.080 (significant at 0.10)  
V<sub>p</sub>, t = 5.531





APPENDIX G  
*IN VIVO* DISTRIBUTION DATA



## APPENDIX G

## SUBJECT U.T.

<sup>67</sup>Ga-citrate

## Standards — Calculation of Correction Factors

Day of Experiment	Probe A counts per channel	Correction Factor	Probe B counts per channel	Correction Factor	Probe C counts per channel	Correction Factor
0	26678	1.00	23917	1.00	26448	1.00
1	21154	1.26	18841	1.27	20930	1.26
2	17794	1.50	15812	1.51	17549	1.51
3	14336	1.86	12768	1.87	14272	1.85
4	11599	2.30	10415	2.30	11498	2.30
5	9445	2.82	8418	2.84	9363	2.82
6	8150	3.27	7311	3.27	8127	3.25
7	6760	3.95	5991	3.99	6721	3.94
8	5455	4.89	4832	4.95	5414	4.89
9	4374	6.10	3846	6.22	4311	6.14



SUBJECT U.T.: Net Relative Organ Uptake of  $^{67}\text{Ga}$ -citrate

Day of Experiment	Net counts per channel	Corrected Counts	Relative Uptake	Radioactivity in whole blood	Net Relative Uptake
L I V E R					
0	19069	19069	1.00	1.00	0
1	14313	18034	0.95	0.27	0.68
2	11004	16506	0.87	0.20	0.67
3	9909	18431	0.93	0.14	0.79
4	7719	17754	0.97	0.11	0.86
5	7639	21542	1.13	0.10	1.03
6	6838	22360	1.17	0.10	1.07
7	5105	20165	1.06	0.09	0.97
8	4223	20650	1.08	0.08	1.00
9	3598	21948	1.15	0.08	1.07
S P L E E N					
0	15427	15427	1.00	1.00	0
1	11631	14655	0.95	0.27	0.68
2	9855	14782	0.96	0.20	0.76
3	6486	12064	0.78	0.14	0.64
4	5419	12464	0.81	0.11	0.70
5	2852	8043	0.52	0.10	0.42
6	3922	12825	0.83	0.10	0.73
7	3341	13197	0.86	0.09	0.77
8	3015	14743	0.96	0.08	0.88
9	2338	14262	0.92	0.08	0.84
H E A R T					
0	29684	29684	1.00	1.00	0
1	15575	19780	0.67	0.27	0.40
2	12481	18846	0.63	0.20	0.43
3	9391	17561	0.59	0.14	0.45
4	7817	17979	0.61	0.11	0.50
5	6335	17991	0.61	0.10	0.51
6	5261	17203	0.58	0.10	0.48
7	4467	17823	0.60	0.09	0.51
8	3869	19152	0.65	0.08	0.57
9	3111	19350	0.65	0.08	0.57

continued . . .



(U.T.,  $^{67}\text{Ga}$ -citrate)

Day of Experiment	Net counts per channel	Corrected Counts	Relative Uptake	Radioactivity in whole blood	Net Relative Uptake
S A C R U M					
0	14523	14523	1.00	1.00	0
1	11716	14879	1.02	0.27	0.75
2	8893	13428	0.92	0.20	0.72
3	7061	13204	0.91	0.14	0.77
4	5587	12850	0.88	0.11	0.77
5	4400	12496	0.86	0.10	0.76
6	3675	12017	0.83	0.10	0.73
7	2953	11782	0.81	0.09	0.72
8	2441	12083	0.83	0.08	0.75
9	1934	12029	0.83	0.08	0.75
K N E E					
0	3949	3949	1.00	1.00	0
1	4212	5307	1.34	0.27	1.07
2	3290	4968	1.26	0.20	1.06
3	2377	4397	1.11	0.14	0.97
4	1697	3903	0.99	0.11	0.88
5	1420	4004	1.01	0.10	0.91
6	1266	4114	1.04	0.10	0.94
7	985	3881	0.98	0.09	0.89
8	726	3550	0.90	0.08	0.82
9	593	3641	0.92	0.08	0.84





## SUBJECT U.T.

<sup>67</sup>Ga-transferrin

## Standards – Calculation of Correction Factors

Day of Experiment	Probe A counts per channel	Correction Factor	Probe B counts per channel	Correction Factor	Probe C counts per channel	Correction Factor
0	5222	1.00	4709	1.00	5288	1.00
1	4268	1.22	3906	1.21	4239	1.25
2	3465	1.51	3092	1.52	3462	1.53
3	2827	1.85	2489	1.89	2784	1.90
4	2296	2.27	2041	2.31	2270	2.33
5	1814	2.88	1602	2.94	1799	2.94
6	1467	3.56	1295	3.64	—	—
7	996	5.24	894	5.27	1475	3.59
8	848	6.16	733	6.42	1002	5.28
9	667	7.83	575	8.19	775	6.82



SUBJECT U.T.: Net Relative Organ Uptake of  $^{67}\text{Ga}$ -transferrin

Day of Experiment	Net counts per channel	Corrected Counts	Relative Uptake	Radioactivity in whole blood	Net Relative Uptake
L I V E R					
0	6498	6498	1.00	1.00	0
1	5158	6293	0.97	0.23	0.74
2	4019	6069	0.93	0.22	0.71
3	3437	6358	0.98	0.14	0.84
4	2434	5525	0.85	0.10	0.75
5	2156	6209	0.96	0.06	0.90
6	1827	6504	1.00	0.05	0.95
7	1136	5953	0.92	0.06	0.86
8	1020	6283	0.97	0.04	0.93
9	881	6898	1.06	0.05	1.01
S P L E E N					
0	6897	6897	1.00	1.00	0
1	4122	5029	0.73	0.23	0.50
2	3532	5333	0.77	0.22	0.55
3	1834	3393	0.49	0.14	0.35
4	2041	4633	0.67	0.10	0.57
5	995	2866	0.42	0.06	0.36
6	757	2695	0.39	0.05	0.34
7	471	2468	0.36	0.06	0.30
8	400	2464	0.36	0.04	0.32
9	359	2811	0.41	0.05	0.36
H E A R T					
0	12787	12787	1.00	1.00	0
1	6918	8371	0.65	0.23	0.42
2	5255	7988	0.62	0.22	0.40
3	4119	7785	0.61	0.14	0.47
4	3386	7822	0.61	0.10	0.51
5	2445	7188	0.56	0.06	0.50
6	2142	7797	0.61	0.05	0.56
7	1509	7952	0.62	0.06	0.56
8	1240	7961	0.62	0.04	0.58
9	1446	11843	0.93	0.05	0.88

continued . . .



## SUBJECT U.T.

 $^{59}\text{Fe}$ -citrate

## Standards — Calculation of Correction Factors

Day of Experiment	Probe A counts per channel	Correction Factor	Probe B counts per channel	Correction Factor	Probe C counts per channel	Correction Factor
0	83	1.00	71	1.00	50	1.00
1	73	1.14	62	1.15	28	1.79
2	65	1.28	67	1.06	34	1.47
3	69	1.20	61	1.16	36	1.39
4	68	1.22	54	1.31	32	1.56
5	69	1.20	47	1.51	29	1.72
6	62	1.34	46	1.54	—	—
7	48	1.73	41	1.73	50	1.00
8	49	1.69	40	1.78	23	2.17
9	45	1.84	40	1.78	23	2.17



SUBJECT U.T.: Net Relative Organ Uptake of  $^{59}\text{Fe}$ -citrate

Day of Experiment	Net counts per channel	Corrected Counts	Relative Uptake	Radioactivity in whole blood	Net Relative Uptake
L I V E R					
0	272	272	1.00	1.00	0
1	273	311	1.14	0.14	1.00
2	275	352	1.29	0.53	0.76
3	279	335	1.23	1.41	-0.18
4	252	307	1.13	1.37	-0.24
5	271	325	1.19	1.58	-0.39
6	271	363	1.33	1.76	-0.43
7	213	368	1.35	1.73	-0.38
8	222	375	1.38	1.71	-0.33
9	214	394	1.45	1.81	-0.36
S P L E E N					
0	292	292	1.00	1.00	0
1	265	302	1.03	0.14	0.89
2	288	369	1.26	0.53	0.73
3	219	263	0.90	1.41	-0.51
4	313	382	1.31	1.37	-0.06
5	187	224	0.77	1.58	-0.81
6	171	229	0.78	1.76	-0.98
7	154	266	0.91	1.73	-0.82
8	145	245	0.84	1.71	-0.87
9	137	252	0.86	1.81	-0.95
H E A R T					
0	485	485	1.00	1.00	0
1	427	491	1.01	0.14	0.87
2	464	492	1.01	0.53	0.48
3	489	567	1.17	1.41	-0.24
4	496	650	1.34	1.37	-0.03
5	461	696	1.44	1.58	-0.14
6	484	745	1.54	1.76	-0.22
7	414	716	1.48	1.73	-0.25
8	403	717	1.48	1.71	-0.23
9	413	735	1.52	1.81	-0.29

continued . . .





(U.T.,  $^{59}\text{Fe}$ -citrate)

Day of Experiment	Net counts per channel	Corrected Counts	Relative Uptake	Radioactivity in whole blood	Net Relative Uptake
S A C R U M					
0	323	323	1.00	1.00	0
1	487	560	1.73	0.14	1.59
2	412	437	1.35	0.53	0.82
3	330	383	1.19	1.41	-0.22
4	260	341	1.06	1.37	-0.31
5	229	346	1.07	1.58	-0.51
6	191	294	0.91	1.76	-0.85
7	162	280	0.87	1.73	-0.86
8	154	274	0.85	1.71	-0.86
9	149	265	0.82	1.81	-0.99
K N E E					
0	51	51	1.00	1.00	0
1	12	21	0.41	0.14	0.27
2	19	28	0.55	0.53	0.02
3	25	35	0.69	1.41	-0.72
4	30	47	0.92	1.37	-0.45
5	34	53	1.04	1.58	-0.54
6	—	—	—	1.76	—
7	29	29	0.57	1.73	-1.16
8	29	63	1.24	1.71	-0.47
9	30	65	1.27	1.81	-0.54



SUBJECT C.W.

$^{67}\text{Ga}$ -citrate

Standards – Calculation of Correction Factors

Day of Experiment	Probe A counts per channel	Correction Factor	Probe B counts per channel	Correction Factor
0	20127	1.00	17909	1.00
1	16320	1.23	14542	1.23
2	13183	1.53	11732	1.53
3	10602	1.90	9422	1.90
4	8301	2.42	7434	2.41
5	6705	3.00	6032	2.97
6	5438	3.70	4865	3.68
7	4273	4.71	4073	4.40
8	3324	6.05	2960	6.05
9	2659	7.57	2373	7.55



SUBJECT C.W.: Net Relative Organ Uptake of  $^{67}\text{Ga}$ -citrate

Day of Experiment	Net counts per channel	Corrected Counts	Relative Uptake	Radioactivity in whole blood	Net Relative Uptake
L I V E R					
0	150947	150947	1.00	1.00	0
1	108103	132967	0.88	0.18	0.70
2	93206	142605	0.94	0.12	0.82
3	77393	147047	0.97	0.09	0.88
4	66352	160572	1.06	0.08	0.98
5	54994	164982	1.09	0.07	1.02
6	49528	183254	1.21	0.06	1.15
7	41346	194740	1.29	0.05	1.24
8	32905	199404	1.32	0.05	1.27
9	28485	215631	1.43	0.04	1.39
S P L E E N					
0	113814	113814	1.00	1.00	0
1	95822	117861	1.04	0.18	0.86
2	79201	121178	1.06	0.12	0.94
3	64973	123449	1.08	0.09	0.99
4	50592	122433	1.08	0.08	1.00
5	34854	104562	0.92	0.07	0.85
6	26717	98853	0.87	0.06	0.81
7	28571	134569	1.18	0.05	1.13
8	19260	116716	1.03	0.05	0.98
9	18788	142225	1.25	0.04	1.21
H E A R T					
0	190492	190492	1.00	1.00	0
1	109257	134386	0.71	0.18	0.53
2	86579	132466	0.70	0.12	0.58
3	67250	127775	0.67	0.09	0.58
4	54978	132497	0.70	0.08	0.62
5	44503	132174	0.69	0.07	0.62
6	36852	135615	0.71	0.06	0.65
7	29827	131239	0.69	0.05	0.64
8	24815	150131	0.79	0.05	0.74
9	19540	147527	0.77	0.04	0.73

continued . . .



(C.W.,  $^{67}\text{Ga}$ -citrate)

Day of Experiment	Net counts per channel	Corrected Counts	Relative Uptake	Radioactivity in whole blood	Net Relative Uptake
S A C R U M					
0	116088	116088	1.00	1.00	0
1	96824	119094	1.03	0.18	0.85
2	77342	118333	1.02	0.12	0.91
3	62900	119510	0.03	0.09	0.94
4	50935	122753	1.06	0.08	0.98
5	40667	120781	1.04	0.07	0.97
6	32510	119637	1.03	0.06	0.97
7	26720	117568	1.01	0.05	0.96
8	21768	131696	1.13	0.05	1.08
9	17075	128916	1.11	0.04	1.07





SUBJECT C.W.

$^{67}\text{Ga}$ -transferrin

Standards – Calculation of Correction Factors

Day of Experiment	Probe A counts per channel	Correction Factor	Probe B counts per channel	Correction Factor
0	19700	1.00	17530	1.00
1	16489	1.19	14637	1.20
2	13386	1.47	11857	1.48
3	10822	1.82	9638	1.82
4	8712	2.26	7733	2.27
5	7067	2.79	6223	2.82
6	5718	3.45	5016	3.49
7	4628	4.26	4117	4.26
8	3743	5.26	3335	5.26
9	3020	6.52	2707	6.48



SUBJECT C.W.: Net Relative Organ Uptake of  $^{67}\text{Ga}$ -transferrin

Day of Experiment	Net counts per channel	Corrected Counts	Relative Uptake	Radioactivity in whole blood	Net Relative Uptake
L I V E R					
0	19248	19248	1.00	1.00	0
1	14322	17043	0.89	0.18	0.71
2	10213	15013	0.78	0.11	0.67
3	8671	15781	0.82	0.09	0.73
4	6169	13942	0.72	0.07	0.65
5	5070	14145	0.73	0.07	0.66
6	4136	14269	0.74	0.05	0.69
7	3530	15038	0.78	0.05	0.73
8	3130	16464	0.86	0.05	0.81
9	2305	15029	0.78	0.04	0.74
S P L E E N					
0	19324	19324	1.00	1.00	0
1	12461	14829	0.77	0.18	0.59
2	9320	13700	0.71	0.11	0.60
3	8056	14662	0.76	0.09	0.67
4	5817	13146	0.68	0.07	0.61
5	4514	12594	0.65	0.07	0.58
6	3386	11682	0.60	0.05	0.55
7	2922	12448	0.64	0.05	0.59
8	2369	12461	0.64	0.05	0.59
9	1272	8293	0.43	0.04	0.39
H E A R T					
0	33149	33149	1.00	1.00	0
1	15504	18605	0.56	0.18	0.38
2	11589	17152	0.52	0.11	0.41
3	8857	16120	0.49	0.09	0.40
4	7211	16369	0.49	0.07	0.42
5	5673	15998	0.48	0.07	0.41
6	4463	15620	0.47	0.05	0.42
7	3736	15915	0.48	0.05	0.43
8	2291	12051	0.36	0.05	0.31
9	2351	15234	0.46	0.04	0.42

continued . . .



(C.W.,  $^{67}\text{Ga}$ -Tf)

Day of Experiment	Net counts per channel	Corrected Counts	Relative Uptake	Radioactivity in whole blood	Net Relative Uptake
S A C R U M					
0	15911	15911	1.00	1.00	0
1	13748	16498	1.04	0.18	0.86
2	11594	17159	1.08	0.11	0.97
3	8200	14924	0.94	0.09	0.85
4	5891	13373	0.84	0.07	0.77
5	4571	12890	0.81	0.07	0.74
6	3680	12880	0.81	0.05	0.76
7	2894	12328	0.77	0.05	0.72
8	2824	14854	0.93	0.05	0.88
9	1822	11807	0.74	0.04	0.70



SUBJECT C.W.

<sup>59</sup>Fe-citrate

Standards – Calculation of Correction Factors

Day of Experiment	Probe A counts per channel	Correction Factor	Probe B counts per channel	Correction Factor
0	567	1.00	498	1.00
1	536	1.06	477	1.04
2	537	1.06	490	1.02
3	533	1.06	467	1.07
4	523	1.08	454	1.10
5	506	1.12	462	1.08
6	504	1.12	451	1.10
7	488	1.16	436	1.14
8	476	1.19	439	1.13
9	472	1.20	435	1.14





SUBJECT C.W.: Net Relative Organ Uptake of  $^{59}\text{Fe}$ -citrate

Day of Experiment	Net counts per channel	Corrected Counts	Relative Uptake	Radioactivity in whole blood	Net Relative Uptake
L I V E R					
0	632	632	1.00	1.00	0
1	623	660	1.04	0.07	0.97
2	654	693	1.10	0.22	0.88
3	664	704	1.11	0.47	0.64
4	698	754	1.19	0.74	0.45
5	728	815	1.29	0.98	0.31
6	764	856	1.35	1.06	0.29
7	749	869	1.38	1.13	0.25
8	709	844	1.34	1.15	0.19
9	770	924	1.46	1.15	0.31
S P L E E N					
0	498	498	1.00	1.00	0
1	540	572	1.15	0.07	1.08
2	581	616	1.24	0.22	1.02
3	606	642	1.29	0.47	0.82
4	612	661	1.33	0.74	0.59
5	543	608	1.22	0.98	0.24
6	560	627	1.26	1.06	0.20
7	615	713	1.43	1.13	0.30
8	515	613	1.23	1.15	0.08
9	603	724	1.45	1.15	0.30
H E A R T					
0	776	776	1.00	1.00	0
1	703	731	0.94	0.07	0.87
2	743	758	0.98	0.22	0.76
3	790	845	1.09	0.47	0.62
4	854	939	1.21	0.74	0.47
5	942	1017	1.31	0.98	0.33
6	883	971	1.25	1.06	0.19
7	906	1033	1.33	1.13	0.20
8	924	1044	1.35	1.15	0.20
9	906	1033	1.33	1.15	0.18

continued . . .



(C.W.,  $^{59}\text{Fe}$ -citrate)

Day of Experiment	Net counts per channel	Corrected Counts	Relative Uptake	Radioactivity of whole blood	Net Relative Uptake
S A C R U M					
0	607	607	1.00	1.00	0
1	882	917	1.51	0.07	1.47
2	841	858	1.41	0.22	1.19
3	705	754	1.24	0.47	0.77
4	637	701	1.15	0.74	0.41
5	573	619	1.02	0.98	0.04
6	515	567	0.93	1.06	-0.13
7	478	545	0.90	1.13	-0.23
8	484	547	0.90	1.15	-0.25
9	452	515	0.85	1.15	-0.30



SUBJECT B.L.

<sup>67</sup>Ga-citrate

Standards – Calculation of Correction Factors

Day of Experiment	Probe A counts per channel	Correction Factor	Probe B counts per channel	Correction Factor	Probe C counts per channel	Correction Factor
0	31842	1.00	28394	1.00	31517	1.00
1	26678	1.19	23917	1.19	26448	1.19
2	21154	1.51	18841	1.51	20930	1.51
3	17794	1.79	15812	1.80	17549	1.80
4	14336	2.22	12768	2.22	14272	2.21
5	11599	2.75	10415	2.73	11498	2.74
6	9445	3.37	8418	3.37	9363	3.37
7	8150	3.91	7311	3.88	8127	3.88
8	6760	4.71	5991	4.74	6721	4.69
9	5455	5.84	4832	5.88	5414	5.82



SUBJECT B.L. : Net Relative Organ Uptake of  $^{67}\text{Ga}$ -citrate

Day of Experiment	Net counts per channel	Corrected Counts	Relative Uptake	Radioactivity in whole blood	Net Relative Uptake
L I V E R					
0	29420	29420	1.00	1.00	0
1	22845	27186	0.92	0.28	0.64
2	20481	30926	1.05	0.17	0.88
3	16686	29868	1.02	0.12	0.90
4	14990	33278	1.13	0.10	1.03
5	11577	31837	1.08	0.08	1.00
6	10483	35328	1.20	0.07	1.13
7	9298	36355	1.24	0.06	1.18
8	7267	34228	1.16	0.05	1.11
9	5885	34368	1.17	0.04	1.13
S P L E E N					
0	20000	20000	1.00	1.00	0
1	11436	13609	0.68	0.28	0.40
2	9154	13823	0.69	0.17	0.52
3	8083	14469	0.72	0.12	0.60
4	6980	15496	0.77	0.10	0.67
5	5956	16379	0.82	0.08	0.74
6	4806	16196	0.81	0.07	0.74
7	3613	14127	0.71	0.06	0.65
8	3452	16259	0.81	0.05	0.76
9	2516	14693	0.73	0.04	0.69
H E A R T					
0	30449	30449	1.00	1.00	0
1	16944	20163	0.66	0.28	0.38
2	12394	18715	0.61	0.17	0.44
3	10232	18418	0.60	0.12	0.48
4	7502	16654	0.55	0.10	0.45
5	6822	18624	0.61	0.08	0.53
6	5028	16944	0.56	0.07	0.49
7	3856	14961	0.49	0.06	0.43
8	3287	15580	0.51	0.05	0.46
9	2791	16411	0.54	0.04	0.50

continued ...





(B.L.,  $^{67}\text{Ga}$ -citrate)

Day of Experiment	Net counts per channel	Corrected Counts	Relative Uptake	Radioactivity in whole blood	Net Relative Uptake
S A C R U M					
0	17893	17893	1.00	1.00	0
1	15252	18150	1.01	0.28	0.73
2	11128	16803	0.94	0.17	0.77
3	8929	16072	0.90	0.12	0.78
4	6277	13935	0.78	0.10	0.68
5	5491	14990	0.84	0.08	0.76
6	4470	15064	0.84	0.07	0.77
7	3651	14166	0.79	0.06	0.73
8	3016	14296	0.80	0.05	0.75
9	2355	13847	0.77	0.04	0.73
K N E E					
0	5318	5318	1.00	1.00	0
1	6499	7734	1.45	0.28	1.17
2	4700	7097	1.33	0.17	1.16
3	3735	6723	1.26	0.12	1.14
4	2641	5837	1.10	0.10	1.00
5	2179	5970	1.12	0.08	1.04
6	1619	5456	1.03	0.07	0.96
7	1222	4741	0.89	0.06	0.83
8	1011	4742	0.89	0.05	0.84
9	774	4505	0.85	0.04	0.81



## SUBJECT B.L.

<sup>67</sup>Ga-transferrin

## Standards – Calculation of Correction Factors

Day of Experiment	Probe A counts per channel	Correction Factor	Probe B counts per channel	Correction Factor
0	15630	1.00	13771	1.00
1	12767	1.22	11121	1.24
2	10161	1.54	8928	1.54
3	8058	1.94	6972	1.98
4	6348	2.46	5573	2.47
5	5149	3.03	4478	3.08
6	3979	3.93	3513	3.92
7	3116	5.02	2744	5.02
8	2442	6.40	2140	6.43
9	1822	8.58	1586	8.68



SUBJECT B.L.: Net Relative Organ Uptake of  $^{67}\text{Ga}$ -transferrin

Day of Experiment	Net counts per channel	Corrected Counts	Relative Uptake	Radioactivity in whole blood	Net Relative Uptake
L I V E R					
0	27853	27853	1.00	1.00	0
1	22880	27914	1.00	0.26	0.74
2	19593	30173	1.08	0.17	0.91
3	16637	32276	1.16	0.12	1.04
4	13509	33232	1.19	0.09	1.10
5	12448	37842	1.36	0.08	1.28
6	10076	39599	1.42	0.06	1.36
7	7887	39593	1.42	0.05	1.37
8	6369	40762	1.46	0.05	1.41
9	5541	47542	1.71	0.04	1.67
S P L E E N					
0	16396	16396	1.00	1.00	0
1	11433	13948	0.85	0.26	0.59
2	9431	14524	0.89	0.17	0.72
3	9209	17865	1.10	0.12	0.98
4	5223	12849	0.78	0.09	0.69
5	3004	9132	0.56	0.08	0.48
6	2765	10866	0.66	0.06	0.60
7	3474	17439	1.06	0.05	1.01
8	1694	10842	0.66	0.05	0.61
9	1855	15916	0.97	0.04	0.93
H E A R T					
0	33846	33846	1.00	1.00	0
1	17385	21557	0.64	0.26	0.38
2	12482	19222	0.57	0.17	0.40
3	10473	20737	0.61	0.12	0.49
4	7420	18327	0.54	0.09	0.45
5	5229	16105	0.48	0.08	0.40
6	4694	18400	0.54	0.06	0.48
7	3607	18107	0.53	0.05	0.48
8	2907	18721	0.55	0.05	0.50
9	1896	16457	0.49	0.04	0.45

continued . . .



## SUBJECT B.L.

<sup>59</sup>Fe-citrate

## Standards – Calculation of Correction Factors

Day of Experiment	Probe A counts per channel	Correction Factor	Probe B counts per channel	Correction Factor
0	880	1.00	790	1.00
1	872	1.01	778	1.01
2	865	1.02	765	1.03
3	849	1.04	759	1.04
4	837	1.05	749	1.05
5	833	1.06	746	1.06
6	808	1.09	733	1.08
7	797	1.10	720	1.10
8	782	1.13	706	1.12
9	776	1.13	697	1.13





SUBJECT B.L.: Net Relative Organ Uptake of  $^{59}\text{Fe}$ -citrate

Day of Experiment	Net counts per channel	Corrected Counts	Relative Uptake	Radioactivity in whole blood	Net Relative Uptake
L I V E R					
0	477	477	1.00	1.00	0
1	452	457	0.96	0.10	0.86
2	480	490	1.03	0.43	0.60
3	447	465	0.97	0.82	0.15
4	482	506	1.06	1.17	-0.11
5	500	530	1.11	1.40	-0.29
6	471	513	1.08	1.50	-0.42
7	456	502	1.05	1.49	-0.44
8	428	484	1.01	1.56	-0.55
9	463	523	1.10	1.52	-0.42
S P L E E N					
0	324	324	1.00	1.00	0
1	308	311	0.96	0.10	0.86
2	321	327	1.01	0.43	0.58
3	359	373	1.15	0.82	0.33
4	326	342	1.06	1.17	-0.11
5	282	299	0.92	1.40	-0.48
6	294	320	0.99	1.50	-0.51
7	332	365	1.13	1.49	-0.36
8	244	276	0.85	1.56	-0.71
9	280	316	0.98	1.52	-0.54
H E A R T					
0	528	528	1.00	1.00	0
1	511	521	0.99	0.10	0.89
2	505	520	0.98	0.43	0.55
3	538	560	1.06	0.82	0.24
4	521	547	1.04	1.17	-0.13
5	468	496	0.94	1.40	-0.46
6	499	539	1.02	1.50	-0.48
7	505	556	1.05	1.49	-0.44
8	486	544	1.03	1.56	-0.53
9	464	524	0.99	1.52	-0.53

continued . . .



(B.L.,  $^{59}\text{Fe}$ -citrate)

Day of Experiment	Net counts per channel	Corrected Counts	Relative Uptake	Radioactivity in whole blood	Net Relative Uptake
S A C R U M					
0	426	426	1.00	1.00	0
1	632	645	1.51	0.10	1.41
2	572	589	1.38	0.43	0.95
3	454	472	1.11	0.82	0.29
4	377	396	0.93	1.17	-0.24
5	330	350	0.82	1.40	-0.58
6	305	329	0.77	1.50	-0.73
7	259	285	0.67	1.49	-0.82
8	266	298	0.70	1.56	-0.86
9	252	285	0.67	1.52	-0.85
K N E E					
0	113	113	1.00	1.00	0
1	46	46	0.41	0.10	0.31
2	69	70	0.62	0.43	0.19
3	80	83	0.73	0.82	-0.09
4	95	100	0.88	1.17	-0.29
5	110	117	1.04	1.40	-0.36
6	104	113	1.00	1.50	-0.50
7	106	117	1.04	1.49	-0.45
8	103	116	1.03	1.56	-0.53
9	98	111	0.98	1.52	-0.54



## SUBJECT A.N.

<sup>67</sup>Ga-citrate

## Standards – Calculation of Correction Factors

Day of Experiment	Probe A counts per channel	Correction Factor	Probe B counts per channel	Correction Factor
0	52756	1.00	47457	1.00
1	46482	1.13	41868	1.13
2	37721	1.40	34033	1.39
3	30755	1.72	27729	1.71
4	24690	2.14	22254	2.13
5	20014	2.64	17991	2.64
6	16423	3.21	14768	3.21
7	13158	4.01	11745	4.04
8	10801	4.88	9726	4.88
9	8750	6.03	7895	6.01



SUBJECT A.N.: Net Relative Organ Uptake of  $^{67}\text{Ga}$ -citrate

Day of Experiment	Net counts per channel	Corrected Counts	Relative Uptake	Radioactivity in whole blood	Net Relative Uptake
L I V E R					
0	11700	11700	1.00	1.00	0
1	8595	9712	0.83	0.20	0.63
2	6892	9649	0.82	0.14	0.68
3	6021	10356	0.89	0.09	0.80
4	4743	10150	0.87	0.08	0.79
5	4003	10568	0.90	0.05	0.85
6	3199	10269	0.88	0.06	0.82
7	2608	10458	0.89	0.06	0.83
8	2256	11009	0.94	0.05	0.89
9	1963	11837	1.01	0.04	0.97
S P L E E N					
0	10781	10781	1.00	1.00	0
1	6802	7686	0.71	0.20	0.51
2	5054	7076	0.66	0.14	0.52
3	3649	6276	0.58	0.09	0.49
4	2746	5876	0.55	0.08	0.47
5	2268	5988	0.56	0.05	0.51
6	1909	6128	0.57	0.06	0.51
7	1400	5614	0.52	0.06	0.46
8	1239	6046	0.56	0.05	0.51
9	1033	6229	0.58	0.04	0.54
H E A R T					
0	13666	13666	1.00	1.00	0
1	6284	7101	0.52	0.20	0.32
2	5035	6999	0.51	0.14	0.37
3	3539	6052	0.44	0.09	0.35
4	2715	5783	0.42	0.08	0.34
5	2166	5718	0.42	0.05	0.37
6	1692	5431	0.40	0.06	0.34
7	1234	4985	0.36	0.06	0.30
8	1168	5700	0.42	0.05	0.37
9	840	5048	0.37	0.04	0.33

continued . . .





(A.N.,  $^{67}\text{Ga}$ -citrate)

Day of Experiment	Net counts per channel	Corrected Counts	Relative Uptake	Radioactivity in whole blood	Net Relative Uptake
S A C R U M					
0	7839	7839	1.00	1.00	0
1	5820	6577	0.84	0.20	0.64
2	4557	6334	0.81	0.14	0.67
3	3389	5795	0.74	0.09	0.65
4	2719	5791	0.74	0.08	0.64
5	2045	5399	0.69	0.05	0.64
6	1611	5171	0.66	0.06	0.60
7	1133	4577	0.58	0.06	0.52
8	1113	5431	0.69	0.05	0.64
9	891	5355	0.68	0.04	0.64
K N E E					
0	3195	3195	1.00	1.00	0
1	3280	3706	1.16	0.20	0.96
2	2371	3319	1.04	0.14	0.90
3	1741	2995	0.94	0.09	0.85
4	1265	2707	0.85	0.08	0.77
5	930	2455	0.77	0.05	0.72
6	752	2414	0.76	0.06	0.70
7	431	1728	0.54	0.06	0.48
8	460	2245	0.70	0.05	0.65
9	324	1954	0.61	0.04	0.57



SUBJECT A.N.

$^{67}\text{Ga}$ -transferrin

Standards – Calculation of Correction Factors

Day of Experiment	Probe A counts per channel	Correction Factor	Probe B counts per channel	Correction Factor
0	27033	1.00	24476	1.00
1	22018	1.23	20242	1.21
2	18420	1.47	16205	1.51
3	15090	1.79	13242	1.85
4	12008	2.25	10526	2.33
5	9816	2.75	8593	2.85
6	8304	3.26	6994	3.50
7	6461	4.18	5660	4.32
8	5035	5.37	4578	5.35



SUBJECT A.N.: Net Relative Organ Uptake of  $^{67}\text{Ga}$ -transferrin

Day of Experiment	Net counts per channel	Corrected Counts	Relative Uptake	Radioactivity in whole blood	Net Relative Uptake
L I V E R					
0	34421	34421	1.00	1.00	0
1	24376	29982	0.87	0.21	0.66
2	19083	28052	0.81	0.11	0.70
3	15992	28626	0.83	0.08	0.75
4	12622	28400	0.83	0.07	0.76
5	10873	29901	0.87	0.06	0.81
6	8753	28447	0.83	0.05	0.78
7	7167	29958	0.87	0.04	0.83
8	5598	30061	0.87	0.04	0.83
S P L E E N					
0	28522	28522	1.00	1.00	0
1	20029	24636	0.86	0.21	0.65
2	12379	18197	0.64	0.11	0.53
3	8597	15389	0.54	0.08	0.46
4	7523	16927	0.59	0.07	0.52
5	5389	14820	0.52	0.06	0.46
6	4267	13868	0.49	0.05	0.44
7	3716	15533	0.54	0.04	0.50
8	3464	18602	0.65	0.04	0.61
H E A R T					
0	34226	34226	1.00	1.00	0
1	15115	18289	0.53	0.21	0.32
2	10882	16432	0.48	0.11	0.37
3	9000	16650	0.49	0.08	0.41
4	6805	15856	0.46	0.07	0.39
5	4675	13324	0.39	0.06	0.36
6	3490	12215	0.36	0.05	0.31
7	2906	12554	0.37	0.04	0.33
8	2468	13204	0.39	0.04	0.35

continued . . .



(A.N.,  $^{67}\text{Ga-Tf}$ )

Day of Experiment	Net counts per channel	Corrected Counts	Relative Uptake	Radioactivity in whole blood	Net Relative Uptake
S A C R U M					
0	21862	21862	1.00	1.00	0
1	18721	22652	1.04	0.21	0.83
2	13275	20045	0.92	0.11	0.81
3	10443	19320	0.88	0.08	0.80
4	8283	19299	0.88	0.07	0.81
5	6113	17422	0.80	0.06	0.74
6	4442	15547	0.71	0.05	0.66
7	3779	16325	0.75	0.04	0.71
8	2918	15611	0.71	0.04	0.67
K N E E					
0	8048	8048	1.00	1.00	0
1	8693	10692	1.33	0.21	1.12
2	6585	9680	1.20	0.11	1.09
3	4817	8622	1.07	0.08	0.99
4	3460	7785	0.97	0.07	0.90
5	2794	7684	0.95	0.06	0.89
6	1917	6250	0.77	0.05	0.72
7	1554	6496	0.81	0.04	0.77
8	1161	6235	0.77	0.04	0.73

















**B30334**